University at Buffalo
The State University of New York

Development of Performance-based Testing Specifications for Seismic Isolators

by

Hyun-Myung Kim and Michael C. Constantinou

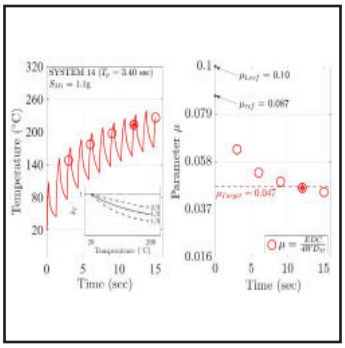
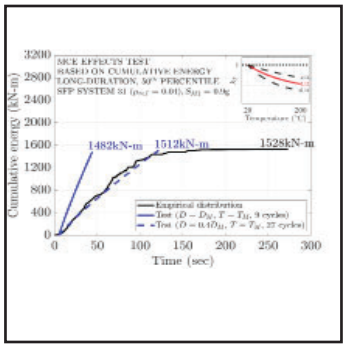
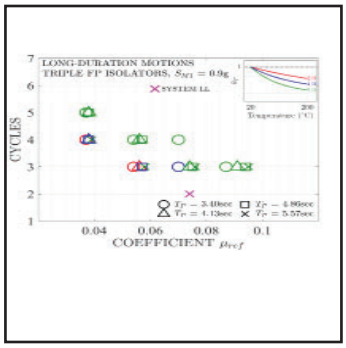
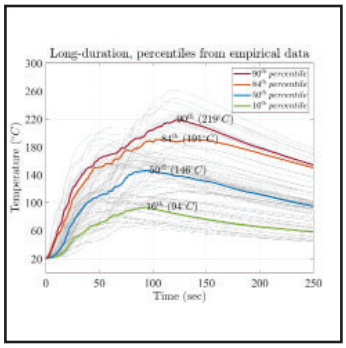

Technical Report MCEER-23-0002

August 18, 2023

NOTICE

This report was prepared by the University at Buffalo, State University of New York, as a result of research sponsored by MCEER. Neither MCEER, associates of MCEER, its sponsors, University at Buffalo, State University of New York, nor any person acting on their behalf:

a. makes any warranty, express or implied, with respect to the use of any information, apparatus, method, or process disclosed in this report or that such use may not infringe upon privately owned rights; or

b. assumes any liabilities of whatsoever kind with respect to the use of, or the damage resulting from the use of, any information, apparatus, method, or process disclosed in this report.

Any opinions, findings, and conclusions or recommendations expressed in this publication are those of the author(s) and do not necessarily reflect the views of MCEER or other sponsors.

University at Buffalo
The State University of New York

Development of Performance-based Testing Specifications for Seismic Isolators

by

Hyun-Myung Kim[1] and Michael C. Constantinou[2]

Publication Date: August 18, 2023
Submittal Date: May 2, 2023

Technical Report MCEER-23-0002

1. Graduate Student, Department of Civil, Structural and Environmental Engineering, University at Buffalo, The State University of New York
2 SUNY Distinguished Professor, Department of Civil, Structural and Environmental Engineering, University at Buffalo, The State University of New York

MCEER: Earthquake Engineering to Extreme Events
University at Buffalo, The State University of New York
212 Ketter Hall, Buffalo, NY 14260
buffalo.edu/mceer

Preface

MCEER was originally established by the National Science Foundation in 1986 at the University at Buffalo, The State University of New York, as the first National Center for Earthquake Engineering Research (NCEER). In 1998, it became known as the Multidisciplinary Center for Earthquake Engineering Research (MCEER), from which the current name, MCEER, evolved.

Comprising a consortium of researchers and industry partners from numerous disciplines and institutions throughout the United States, MCEER's mission expanded in the early 2000s from its original focus on earthquake engineering to one which addresses the technical and socioeconomic impacts of a variety of hazards, both natural and man-made, on critical infrastructure, facilities, and society.

This report presents a methodology and describes the testing conditions for (a) determining the bounding properties of isolators for use in analysis and design, and (b) interrogating the isolators to the effects of the maximum considered earthquake. Results are presented for single Friction Pendulum, triple Friction Pendulum and Lead-rubber isolators, for short- and long-duration motions. Information is also provided on how to test at specific probabilities of exceedance so that the test conditions are selected to be neither excessively conservative nor unconservative. Fundamental in this methodology is the use of analysis models in which the properties of the isolators (friction or characteristic strength) are dependent on the instantaneous temperature at the sliding interfaces or in the lead core.

ABSTRACT

Standard ASCE/SEI-7 regulates the use of seismic isolators in design practice and includes prototype testing specifications for isolators. Of these tests, important are tests to determine the bounding properties of the isolators, and tests to determine the adequacy of the isolators in the maximum considered earthquake. This report updates the conditions for testing isolators as specified in the standard to determine the bounding properties of isolators, and to determine the adequacy of the isolators in the maximum considered earthquake. The test conditions are determined by performing analyses with models that account for the time-variant properties of the isolators and computing the resultant isolator displacements. In performing the work, a large number of isolation systems (96 systems, comprising single friction pendulum, triple friction pendulum and lead-rubber), three different seismic hazards as measured by the spectral acceleration at the period of one second, and a large collection of bi-directional ground motions with short- and long-duration characteristics (71 pairs of each duration, 96 systems, three seismic hazards, for a total of 40896 ground motion pairs) were considered.

“This Page Intentionally Left Blank”

ACKNOWLEDGEMENTS

The lead author has been supported by a University at Buffalo Presidential Scholarship and by funds provided by the Samuel P. Capen Professorship.

“This Page Intentionally Left Blank”

TABLE OF CONTENTS

TABLE OF CONTENTS (CONT'D)

TABLE OF CONTENTS (CONT'D)

“This Page Intentionally Left Blank”

LIST OF FIGURES

LIST OF FIGURES (CONT'D)

LIST OF FIGURES (CONT'D)

LIST OF FIGURES (CONT'D)

LIST OF FIGURES (CONT'D)

LIST OF FIGURES (CONT'D)

LIST OF TABLES

LIST OF TABLES (CONT'D)

LIST OF TABLES (CONT'D)

LIST OF TABLES (CONT'D)

SECTION 1
INTRODUCTION

The testing of isolators is regulated by standards such as the ASCE/SEI-7 (2017), EN1998-1 (2004) and EN15129 (2009). Two important tests in these standards are:

1) A test to determine the properties of the isolators for analysis and design (specifically to determine factors $\lambda_{(test,\ max)}$ and $\lambda_{(test,\ min)}$ in ASCE/SEI-7). In ASCE/SEI-7, this test is prototype test Item 2(a) (also test Item 3) in section 17.8.2.2 in which the isolator is subjected to three cycles at various amplitudes of which most important is the one at amplitude of D_M, which is the maximum resultant displacement of the isolators computed either by simplified analysis or as the average of at least seven response history analyses (the actual value is the largest of 0.8 of the value computed by simplified analysis and the value computed in the response history analysis). The test is meant to be conducted dynamically at a period equal to the effective period T_M (per definition of ASCE/SEI-7) although the commentary of ASCE/SEI 7 (section C17.8) allows quasi-static testing depending on the availability of testing equipment. However, it has been common for most projects to conduct this test dynamically when it is used to determine the upper bound (from the recorded force-displacement loop in the first cycle) and the lower bound (in the third cycle) properties of the isolators for use in analysis and design (ASCE/SEI-7 makes clear how the properties are determined in the Commentary section C17.2.8.3. Also, McVitty and Constantinou (2015) provided a more detailed commentary and presented examples).

   Standard ASCE/SEI-7 allows for an alternate test (Item 2(b) in section 17.8.2.2) in which the prototype isolators are dynamically tested (at period T_M) in four cycles of varying amplitude in each cycle (at $0.25D_M$, $0.5D_M$, $0.67D_M$ and D_M).

2) A test to determine the adequacy of the isolators. In ASCE/SEI-7, this test is prototype test Item 4 in section 17.8.2.2, in which the isolator is subjected to at least 10 cycles of motion at amplitude of $0.75D_M$ and period of T_M (it is allowed to be performed in sets consisting of five continuous cycles followed by pause; thus, effectively this test is one of five cycles that is repeated).

The origin of these tests is in the tentative seismic isolation design requirements of the Structural Engineers Association of Northern California (1986), in which the amplitude of motion was specified as the "design displacement", which was then computed for a seismic input based on 500-year return period spectra.

Moreover, the requirements did not specify or even mention dynamic testing (it was meant that quasi-static testing was allowed). As codification of seismic isolation requirements became more formal, and standards such as ASCE/SEI-7 added requirements for seismically isolated structures, the specified tests increased, dynamic testing requirements were included and, when only the maximum earthquake was used in the analysis and design of seismically isolated buildings (with the 2016 version of ASCE/SEI-7), the amplitude of motion for the tests was specified as D_M for test Items 2(a) and 3, and $0.75D_M$ for test Item 4.

The number of cycles in these tests was based on studies of Kircher and Lashkari (1989), whereas a later, more advanced, study of Warn and Whittaker (2004) related the results to the properties of the isolation system, which were represented, in both studies, as bilinear hysteretic with time-invariant properties. In these studies, seismically isolated structures were subjected to bins of ground motions and the cumulative dissipated energy, or the cumulative displacement, of each isolator was computed. A test was then designed (isolator subjected to the average gravity load and one-directional motion of amplitude computed in the dynamic analysis and for number of cycles) so that the cumulative dissipated energy or the cumulative isolator displacement in the test and in the dynamic analysis were the same. As such, the tests represented the effects of the considered earthquake as computed in the response history analysis in terms of the cumulative energy or displacement (the two are exactly equivalent for systems that have time-invariant properties). That is, these studies established tests for the effects of the considered earthquake and not tests for determining the properties (particularly factors $\lambda_{(test,\ max)}$ and $\lambda_{(test,\ min)}$) for use in the analysis and design. At best they are suitable for test Item 4 but not for test Items 2(a) and 3. Moreover, the studies did not consider long-duration ground motions. A recent study of Kitayama and Constantinou (2021) demonstrated that (a) the duration of ground motion has important implications for test Items 2(a), 3 and 4 if they are based on the use of the cumulative energy, and (b) consideration of other criteria, such as the history of the temperature at the sliding interfaces of sliding bearings or the core of lead-rubber bearings, is a more appropriate criterion for establishing tests for the effects of the considered earthquake.

This report presents a study that determines the conditions of testing for:

1) Determining the bounding properties of isolators for use in analysis and design. The test conditions are determined by first performing analyses with models that account for the time-variant properties of the isolators and computing the resultant isolator displacements. Then the analyses are repeated using models with time-invariant isolator properties that result in the same isolator resultant displacement in an average sense. With the time-invariant isolator properties known and defined as those of the lower bound analysis, a test is designed to result in lower bound properties at the last cycle of the test, whereas the first cycle results in the upper bound properties. In this way, tests

are designed that correctly result in the properties for use in bounding analysis (specifically to determine factors $\lambda_{(test,\ max)}$ and $\lambda_{(test,\ min)}$ in ASCE/SEI-7; the lower and upper bound properties are then computed based on additional considerations of uncertainties in the properties and effects of aging). The lower bound properties are used to compute the isolation system resultant peak displacement in an average sense (quantity D_M as defined in ASCE/SEI-7). The test is meant to be a replacement for tests Items 2(a) and 3 of ASCE/SEI-7.

2) Determining the adequacy of the isolators in the maximum considered earthquake or equivalently a test to interrogate the isolators for the effects of the maximum considered earthquake, with consideration for the probability of exceedance of these effects (e.g., median effects, 90% percentile effects). The test is meant to be a replacement for test Item 4 of ASCE/SEI-7. The approach followed in determining the conditions of testing was based on the procedures in Fenz et al. (2011) using the histories of temperature computed at the sliding interfaces of sliding bearings or in the lead core of lead-rubber bearings. Moreover, conditions of testing were determined when using the cumulative dissipated energy histories instead of the temperature histories.

In performing the work, a large number of isolation systems (96 systems, comprising single friction pendulum, triple friction pendulum and lead-rubber), three different seismic hazards as measured by the spectral acceleration at the period of one second, and a large collection of bi-directional ground motions with short- and long-duration characteristics (71 pairs of each duration, 96 systems, and three seismic hazards, for a total of 40896 ground motion pairs) were considered. The short-duration motions had a geomean duration $Ds_{5\text{-}75}$ (Chandramohan et al., 2016; Kitayama and Constantinou, 2021) of less than 20 secs, whereas long-duration motions had a geomean duration $Ds_{5\text{-}75}$ between 15 and 80 sec. The ground motions were selected such that for each long-duration pair of ground motions there was a corresponding pair of short-duration motions that had response spectra in the two orthogonal directions that were essentially the same as the spectra of the corresponding long-duration pair. All ground motions were appropriate for far field conditions. In performing the analysis, isolator models with time-variant properties were needed. These models were based on validated theories for sliding isolators (Constantinou et al., 2007; Kumar et al., 2015; Kim and Constantinou, 2022, 2023) and lead-rubber isolators (Kalpakidis et al., 2010; Kumar et al., 2014). However, two enhancements in these models were made: (a) in the sliding bearings, the friction-temperature relationship was modified from a single case in Kim and Constantinou (2022, 2023) and Kumar et al. (2015) to three different cases so that other possible sliding interfaces are studied, and (b) the relationship between the effective yield stress of lead and temperature was extended beyond the model

of Kalpakidis et al. (2010) and Kumar et al. (2014) to be valid up to the melting temperature of lead. This was needed to better represent the behavior of lead-rubber bearing in some long-duration motions.

The results of this study show that:

1) For all seismic isolation systems and for short-duration motions, a test of three cycles at amplitude D_M and period T_M suffices to determine the lower bound properties for analysis. That is, test Items 2(a) and 3 of Section 17.8.2.2 of ASCE/SEI-7 are sufficient to determine factors $\lambda_{(test,\ max)}$ and $\lambda_{(test,\ min)}$ for short-duration motions. However, for long-duration motions, five cycles of motion at the same conditions of amplitude and period are needed to determine these factors.

2) For short-duration motions, a test to determine the adequacy of isolators in the maximum considered earthquake requires:
    a. For the 50th percentile effects, 8 cycles for single and triple FP isolators at amplitude $0.4D_M$ and period T_M, and 12 cycles for lead-rubber isolators at amplitude $0.5D_M$ and period T_M. This is consistent with but less onerous than the current requirements of test Item 4 of Section 17.8.2.2 of ASCE/SEI-7 in which the number of cycles is at least 10 with amplitude of $0.75D_M$ rather than $0.4D_M$ or $0.5D_M$.
    b. For the 90th percentile effects, 16 cycles for single and triple FP isolators at amplitude $0.4D_M$ and period T_M, and 24 cycles for lead-rubber isolators at amplitude $0.5D_M$ and period T_M.

3) For long-duration motions, a test to determine the adequacy of isolators in the maximum considered earthquake requires:
    a. For the 50th percentile effects, 18 cycles for single and triple FP isolators at amplitude $0.4D_M$ and period T_M, and 30 cycles for lead-rubber isolators at amplitude $0.5D_M$ and period T_M.
    b. For the 90th percentile effects, 36 cycles for single and triple FP isolators at amplitude $0.4D_M$ and period T_M, and 60 cycles for lead-rubber isolators at amplitude $0.5D_M$ and period T_M.

The difference between sliding and lead-rubber systems in the required number of cycles in the adequacy tests is related to the dependency of the strength of the isolators (friction force or characteristic strength) on temperature. For sliding isolators, the strength does not diminish but reaches a stable value as temperature

increases, whereas in lead-rubber isolators the strength may vanish as the temperature approaches the melting point of lead. While the number of cycles is less in the sliding isolators than in the lead-rubber isolators, the effects of the test may be more important due to wear of the materials of the sliding interface (Constantinou et al., 2007), whereas for the lead-rubber isolators, lead recovers its strength after many cycles of motion (e.g., see Fig. 8-25 in Constantinou et al., 2007).

“This Page Intentionally Left Blank”

SECTION 2
MODELING THE BEHAVIOR OF SEISMIC ISOLATORS

2.1 Introduction

The seismic isolators considered in this work are single and triple Friction Pendulum (FP) isolators and lead-rubber isolators. Figures 2-1 to 2-3 show cross sections of these isolators with their main geometric features and show idealized lateral force-displacement relationships for each isolator (W is the axial compressive load carried by the isolator).

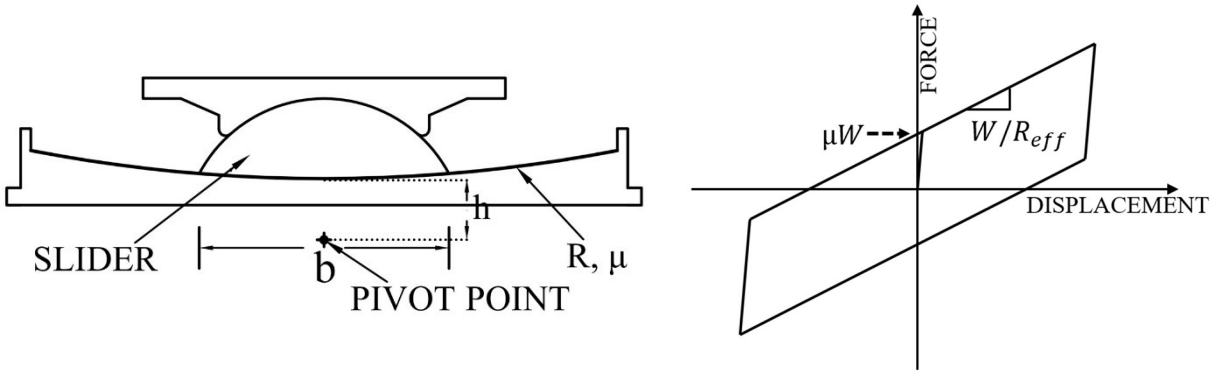

Figure 2-1 Geometry and Idealized Lateral Force-displacement Relationship of the Single FP

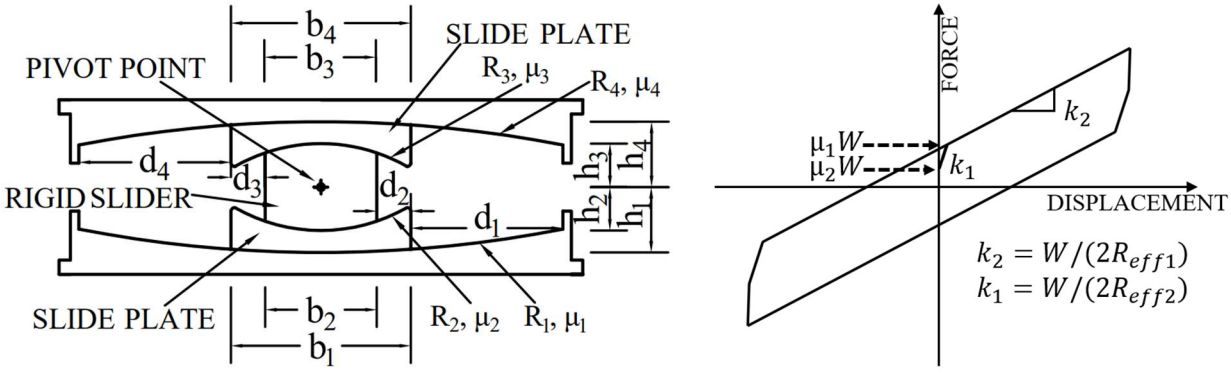

Figure 2-2 Geometry and Idealized Lateral Force-displacement Relationship of the Triple FP

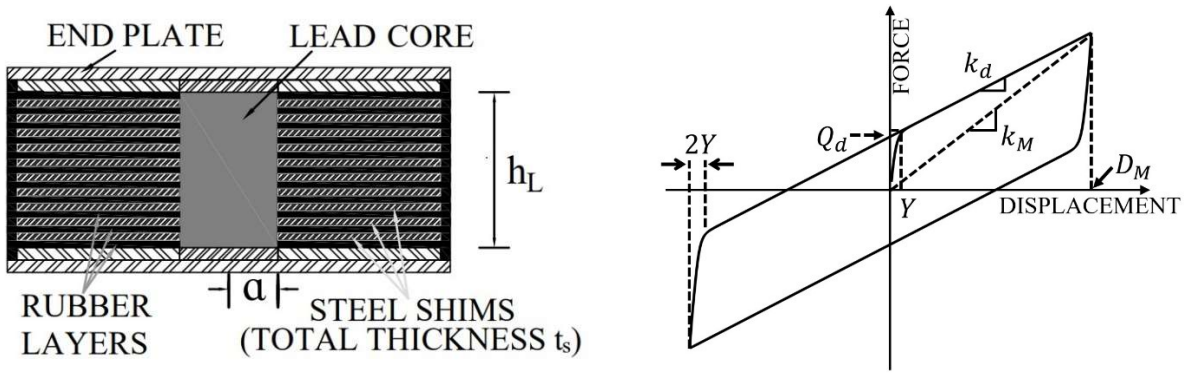

Figure 2-3 Geometry and Idealized Lateral Force-displacement Relationship of Lead-rubber Bearing

2.2 Modeling of Single and Triple FP Isolators

Single FP bearings has been described in Zayas et al., (1987), Mokha et al. (1990), Al-Hussaini et al (1994), Constantinou et al. (2011) and many others who described the behavior of the bearing as depicted in Figure 2-1 in terms of the lateral force F being a function of the displacement u, axial load W, friction coefficient μ and the effective radius R_{eff}, which is the distance of the center of curvature to the pivot point (as shown in Fig. 2-1 the pivot is outside the concave surface so that the effective radius is larger than the actual radius-otherwise is smaller)

$$R_{eff} = R + h \qquad (2-1)$$

The single FP model used in this work is the one implemented in element "FPBearingPTV" in program OpenSees (Kumar et al., 2015). In this model the coefficient of friction is dependent on the instantaneous pressure, velocity, and temperature. The main feature of the model utilized in this study is the dependency of the coefficient of friction on temperature at the center of the sliding interface. Constantinou et al. (2007) presented information on the dependency of the coefficient of friction at interfaces of sliding bearings on the velocity of sliding, pressure, and temperature. They also presented and validated by experimentation a theory on computing the change in temperature at a sliding interface as the result of frictional heating.

The computation of the temperature at the sliding interfaces requires knowledge of the instantaneous values of the coefficient of friction, the apparent bearing pressure (load divided by apparent contact area) and sliding velocity at each interface. The total temperature $T = T_0+\Delta T$ at time $t > 0$, consists of the starting

value T_0 at time zero and the rise ΔT at the sliding interface. The temperature rise ΔT at time t is given by (Constantinou et al., 2007):

$$\Delta T(t) = \frac{\sqrt{D}}{k\sqrt{\pi}} \int_0^t \frac{q(t-\tau)d\tau}{\sqrt{\tau}} \qquad (2-2)$$

where, D and k are the thermal diffusivity and conductivity of stainless steel, respectively, τ is a time parameter that varies between 0 and time t, and q(t) is the heat flux, which is calculated in accordance with the equation (2-3).

$$q(t) = \begin{cases} \mu(t)p(t)v(t), & d \le rContact \\ 0, & otherwise \end{cases} \qquad (2-3)$$

In equation (2-3), $\mu(t)$ is a friction coefficient, p(t) is the apparent bearing pressure at the sliding surface, and v(t) is the absolute value of the resultant velocity at the sliding surface. Also, d is the absolute value of the resultant displacement of the slider and rContact is the radius of the circular apparent contact area, which can be obtained by b/2 (see Figure 2-1). Equation (2-3) computes the temperature at the center of the bearing. Note that the heat flux may be intermittent depending on the motion of the slider over the contact area (Constantinou et al., 2007). Values of the thermal properties of stainless used in the analysis are presented in Table 2-1.

Table 2-1 Thermal Properties of Stainless Steel

Parameter	Unit	Value
Thermal Diffusivity	m^2/sec	$0.444 * 10^{-5}$
Thermal Conductivity	$Watt/(m°C)$	18

Important in this model is the dependency of the coefficient of friction on pressure, velocity and primarily temperature. In the model of Kumar et al. (2015) implemented in element "FPBearingPTV" of program OpenSees, the coefficient of friction is given by equations (2-4) to (2-7) in which μ_{ref} is the reference high speed coefficient of friction at the initial (time t = 0), temperature T_0 = 20°C and initial pressure p_0, α is velocity rate parameter (= 100s/m), p is the apparent pressure, and v is the amplitude of the velocity.

$$\mu(p, v, T) = \mu_{ref} k_p k_v k_T \qquad (2-4)$$

$$k_p = 0.7^{0.02(p-p_0)} \qquad (2-5)$$

$$k_v = (1 - 0.5e^{-av}) \qquad (2-6)$$

$$k_T = 0.79 \cdot (0.7^{0.02} + 0.40) \quad (2-7)$$

Function k_T accounts for the dependency of the coefficient of friction on the temperature and function k_P for the dependency of the coefficient of friction on instantaneous pressure. These functions have been calibrated using general data that apply for FP bearings. Also, function k_v for the dependency of the coefficient of friction on velocity assumes that the ratio of the very low speed to high-speed coefficient of friction equals to 0.5 (supported by data in Constantinou et al., 2007).

In this study, the dependency of the coefficient of friction was expanded to account for additional cases beyond the single case described by equation (2-7). Specifically, two additional cases were added, described by equations (2-8) and (2-9). Figure 2-4 presents graphs of coefficient k_T vs. the temperature in the three cases. Note that the three cases were selected so that the friction coefficient reduces from the starting value at temperature of 20°C to 2/3, 1/2 and 1/3 of the starting value at a temperature of about 200°C.

$$k_T = 0.84 \cdot (0.7^{0.0085} + 0.25) \quad (2-8)$$

$$k_T = 0.97 \cdot (0.7^{0.029T} + 0.22) \quad (2-9)$$

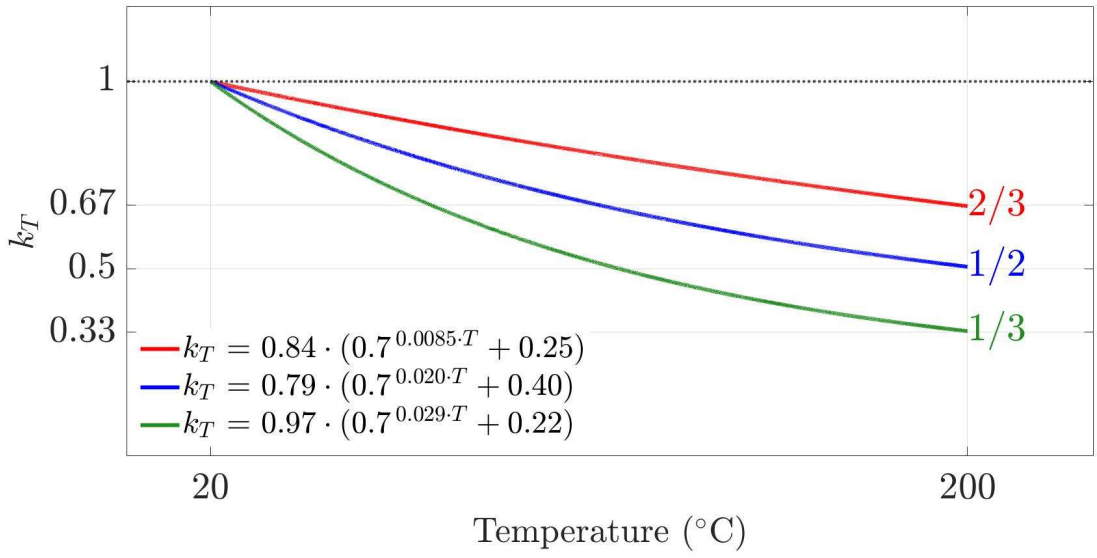

Figure 2-4 Friction Coefficient-Temperature Relationships Considered in Analysis

Element "FPBearingPTV" of program OpenSees was modified to include the additional cases of coefficient k_T for the analyses of structures with single FP isolators for this study.

The behavior of the Triple FP bearing has been described in Fenz and Constantinou (2008a to 2008d, 2009) and summarized in Constantinou et al. (2011). The following parameters determine the response of Triple FP bearing: friction coefficients at its four sliding interfaces, μ_i, nominal displacement capacities, d_i, radii of curvature R_i, and heights h_i, where i = 1 to 4. The effective radii of curvature are defined as $R_{eff\,i} = R_i - h_i$, and the actual displacement capacities are given by $d_i^* = \frac{R_{effi}}{R_i} d_i$. When the inner ring is absent, the actual total displacement is increased by $b_2/2$, at which point the isolator becomes unstable (Sarlis and Constantinou, 2013). In the Fenz and Constantinou (2008a, c) model, the following conditions need to apply: 1) $R_{eff\,1} = R_{eff\,4} \gg R_{eff\,2} = R_{eff\,3}$, 2) $\mu_2 = \mu_3 < \mu_1 < \mu_4$, 3) $d_1^* > (\mu_4 - \mu_1) \cdot R_{eff\,1}$, 4) $d_2^* > (\mu_1 - \mu_2) \cdot R_{eff\,2}$, 5) $d_3^* > (\mu_4 - \mu_3) \cdot R_{eff\,3}$. These conditions typically apply for practical Triple FP bearings.

A computational model for the Triple FP element was developed initially by Fenz and Constantinou (2008d, 2009), and later Sarlis and Constantinou (2010) presented details of modeling the bearing in program SAP2000 (CSI, 2011) in a report to the engineering community. Dao et al. (2013) implemented the model in the program OpenSees (McKenna et al., 2010), having improved on the use of multi-directional gap elements, whereas the model in SAP2000 required the use of several one-directional gap elements. The element, named "TripleFrictionPendulum", cannot account for the dependency of the coefficient of friction on temperature as the actual displacements and sliding velocities at each of the four sliding interfaces of the isolator are not computed.

Recently, Kim and Constantinou (2022, 2023) expanded the Fenz theory to obtain estimates of the displacements and velocities at all four sliding interfaces of the triple FP isolator and modified the Dao element in OpenSees to account for the temperature dependency of the coefficient of friction. The new element is called "TripleFrictionPendulumX". The model has been verified by comparison to the validated, more advanced but unidirectional model, of Sarlis and Constantinou (2013, 2016). The report of Kim and Constantinou (2022) provides details on how to use the revised triple FP element "TripleFrictionPendulumX" in OpenSees for accounting for the triaxial behavior of the triple FP bearing with due consideration for the dependency of friction on the temperature, in addition to velocity and pressure, at each sliding interface. For the study of this report, the dependency of the friction coefficient on temperature was modelled using the three laws described by equations, (2-7), (2-8) and (2-9).

2.3 Modeling Lead-rubber Isolators

Kalpakidis et al. (2008, 2009a, 2009b, 2010) developed and validated a theory that can predict the degradation of the characteristic strength (quantity Q_d in Figure 2-3) because of heating of the lead core. In general, the isolator is characterized by the characteristic strength Q_d, the post-elastic stiffness k_d, and the effective yield displacement Y. The yield displacement is not known but observations from tests of lead-rubber isolators (Kalpakidis and Constantinou, 2008) suggest values of about 10mm to 30mm. The characteristic strength and post-elastic stiffness are related to the properties of lead and rubber, and the geometry:

$$K_d = \frac{GA_r}{T_r} \qquad (2-10)$$

$$Q_d = A_L \sigma_{YL} \qquad (2-11)$$

In these equations, G is the shear modulus of rubber, A_r is the bonded rubber area, T_r is the total rubber thickness, A_L is the area of lead (= $\pi\alpha^2$ per Fig. 2-3) and σ_{YL} is the effective yield stress of lead. The effective yield stress of lead is dependent on temperature and an equation relating the two based on tests of Kalpakidis and Constantinou (2008, 2009a, 2009b) is the following, where σ_{YL0} is the effective yield strength of lead at the start of motion (at temperature of 20°C), T_L is the rise in temperature and E_2 is a parameter equal to 0.0069/°C.

$$\sigma_{YL} = \sigma_{YL} \cdot e^{(-E_2 \cdot T_L)} \qquad (2-12)$$

The computation of the temperature rise in the lead core was based on partially solving the complex three-dimensional heat conduction problem of the heat generated in the body of the lead and conducted through the steel end plates and the reinforcing shim plates. The temperature rise T_L in the lead core is governed by the following ordinary differential equation, in which t is the time, τ is a dimensionless time, ρ_L is the density of lead (=11300kg/m^3), c_L is the specific heat of lead (=130J/kg·°C), α_s is the thermal diffusivity of the steel end and shim plates (=1.4×10^{-5}m^2/sec), and k_s is the thermal conductivity of the steel end and shim plates (=50Watt/m·°C), h_L is the height of the lead core, t_s is the total thickness of the steel shim plates, α is the radius of the lead core (see Figure 2-3), and $\dot{U}$ is the resultant velocity of the top of the lead core with respect to its bottom.

$$\frac{dT_L}{dt} = \frac{\sigma_{YL}(T_L) \cdot |\dot{U}|}{\rho_L \cdot c_L \cdot h_L} - \frac{k_s \cdot T_L}{a \cdot \rho_L \cdot c_L \cdot h_L}\left[\frac{1}{F} + 1.274\left(\frac{t_s}{a}\right)\left(\tau^{-\frac{1}{3}}\right)\right] \quad (2-13)$$

$$F = \begin{cases} 2\left(\frac{\tau}{\pi}\right)^{\frac{1}{2}} - \left(\frac{\tau}{\pi}\right) \cdot \left[2 - \left(\frac{\tau}{4}\right) - \left(\frac{\tau}{4}\right)^2 - \frac{15}{4} \cdot \left(\frac{\tau}{4}\right)^3\right], & \tau < 0.6 \\ \frac{8}{3\pi} - \frac{1}{2(\pi \cdot \tau)^{\frac{1}{2}}} \cdot \left[1 - \left(\frac{1}{3 \cdot (4\tau)}\right) - \frac{1}{6 \cdot (4\tau)^2} - \frac{1}{12 \cdot (4\tau)^3}\right], & \tau \geq 0.6 \end{cases} \quad (2-14)$$

$$\tau = \frac{\alpha_s \cdot t}{a^2} \quad (2-15)$$

This model, including additional features of elastomeric bearings, was implemented in element "LeadRubberX" in program OpenSees by Kumar et al. (2014). This element was used in this study after a modification to expand the range of validity of the relationship between the effective yield stress of lead and temperature up to the melding point of lead as this was needed in analyses with long-duration motions. The revised relationship between the yield strength and temperature ($T = T_0 + T_L$) is

$$\sigma_{YL} = \begin{cases} \sigma_{YL0} \cdot e^{(-E_2 \cdot T_L)}, & T = T_L + T_o \leq 250°C \\ \sigma_{YL0} \cdot e^{(-E_2 \cdot 250)} \cdot \left(\frac{327 - T_L}{327 - 250}\right), & 250°C < T = T_L + T_o \leq 327°C \\ 0, & T = T_L + T_o > 327°C \end{cases} \quad (2-16)$$

Figure 2-5 shows the variation of the normalized effective yield strength of lead (σ_{YL}/σ_{YL0}) with temperature per equation (2-16). It should be noted that the original model for the effective yield strength per equation (2-12), would have predicted, instead of zero, a ratio σ_{YL}/σ_{YL0}=0.12 at the melting temperature of lead, as seen in Figure 2-5. This difference appeared important in some analyses with long-duration motions when the temperature of the lead core approached the melting point.

Moreover, an error in coding of the element that resulted in an ever-increasing temperature in the lead core was corrected. Also, a modification was made in the calculation of the initial value of the effective yield strength of lead, σ_{YL0}, from the user-supplied initial value of the yield strength (force) of the bearing, F_y in element LeadRubberX. The effective yield strength of lead was computed based on equation (2-17) using the user supplied data in element LeadRubberX: the yield strength F_y (see Figure 2-3) and parameter α (alpha), which is the ratio of the post-elastic stiffness to the elastic stiffness.

$$\sigma_{YL0} = \frac{Q_d}{A_L} = \frac{1-\alpha}{A_L} F_y \qquad (2-17)$$

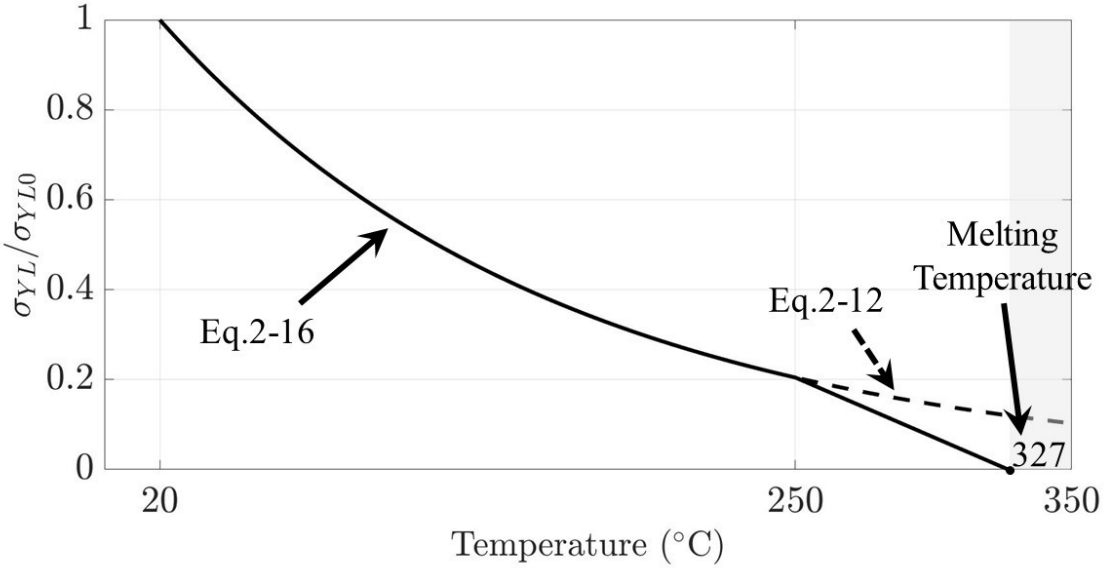

Figure 2-5 Normalized Effective Yield Strength of Lead as Function of Temperature

A new element was created called "LeadRubberX2", which is described in more detail in Appendix A, where examples are also presented that demonstrate the importance of the modifications.

SECTION 3
GROUND MOTIONS USED FOR RESPONSE HISTORY ANALYSIS

3.1 Long- and Short-Duration Ground Motions Used in Analysis

The ground motions used for response history analysis consisted of 71 pairs of horizontal orthogonal components with long-duration characteristics and another 71 pairs of horizontal orthogonal components with short-duration characteristics that were spectrally equivalent to the 71 pairs of long-duration motions. The long-duration motions were obtained from a set identified by Chandramohan et al. (2016) except for two record sets (Infiernillo Media Cortina and Villita Corona Centro, both from the 1985 Michoacan, Mexico events). The spectrally equivalent short-duration motions were obtained from Kitayama and Constantinou (2021) who identified the motions from the PEER NGA-West2 database that included about 20000 records. The methodology of selection of the motions has been described in Kitayama and Constantinou (2021) who also provided a digital appendix with information on each motion. All motions were baseline-corrected and filtered using the procedures of Boore and Bommer (2005) and Boore (2005). The selection procedure maintained the long-duration motions as originally recorded and then selected and scaled only in amplitude the short-duration motions such that for each long-duration pair of ground motions there is a corresponding pair of short-duration motions that has response spectra in the two orthogonal directions that are essentially the same as the spectra of the corresponding long-duration pair. An example of spectrally equivalent long- and short-duration motions is provided in Figure 3-1 where the spectra of the two sets of pairs are compared.

The duration of the ground motions was identified using the $Ds_{5\text{-}75}$ measure (Chandramohan et al., 2016), which is defined as the time interval over which 5% to 75% of the integral I of Equation (3-1) is accumulated. In this equation, a(t) is the ground motion acceleration history and t_{max} is the duration of the record:

$$I = \int_{o}^{t_{max}} a^2 dt \qquad (3-1)$$

The short-duration motions had the $Ds_{5\text{-}75}$ duration less than 25 second, and the long-duration motions had the $Ds_{5\text{-}75}$ duration of at least one of the horizontal components greater than 25 second. Figure 3-2 presents the distribution of the geometric mean of the durations of the two orthogonal components of the 71 pairs of short-duration and the 71 pairs of long-duration motions of this study. Kitayama and Constantinou (2021) presented complete information on the two sets of spectrally equivalent ground motions.

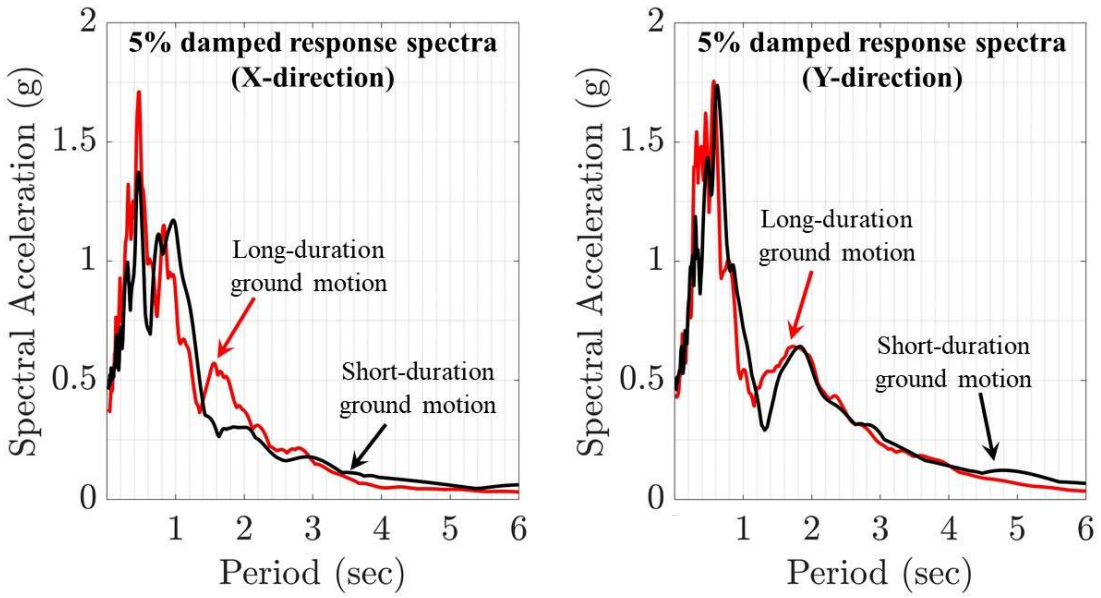

Figure 3-1 Acceleration Response Spectra of Spectrally Equivalent Pair of Long- and Short-duration Motions (long-duration: 2011 Tohoku Iwanuma, Japan; short-duration: 1999 Chi-Chi CHY006, Taiwan)

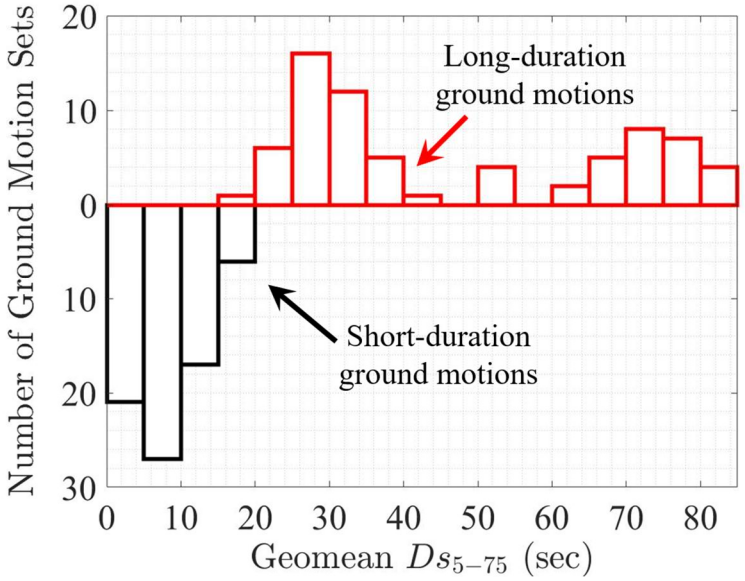

Figure 3-2 Geometric Mean of Ds_{5-75} Duration of Ground Motions used in Analysis

The 142 pairs of ground motions used in the analysis were recorded in the far-field. The vertical ground motion component was not considered in the analysis because (a) its effects on the isolator displacement

are known from analysis and shake table testing to be minor for sliding isolation systems (Sarlis et al., 2013; Cilsalar and Constantinou, 2017), (b) its effects are known from analysis to be insignificant on the histories of temperature computed for the sliding surfaces of triple FP isolators (Kim and Constantinou, 2022), and (c) the effects on the isolator displacements are known from shake table testing to be insignificant to minor (less than 10% difference) for lead-rubber systems even for near-fault seismic excitation (Hwang and Hsu, 2000).

Important for this study is the effect of, or lack of, the vertical ground motion on the computed histories of temperature at the sliding surfaces of FP isolators. An example from the data in Kim and Constantinou (2022) is presented below. A structure was analyzed with triple FP isolators having friction coefficient values (initial values at the starting temperature of 20^{o}C and at high velocity) of 0.04 and 0.08 for the two main surfaces (surfaces 1 and 4, respectively), and 0.01 for the two secondary surfaces (from examples in Section 6 of Kim and Constantinou, 2022). Analysis was performed with one-directional fault-normal (FN) and the vertical (V) components of the long-duration ground motion recorded at the Kaminoyama station in the 2011 Tohoku earthquake, scaled in amplitude by factor of 8.0 (Section 6.1.1 of Kim and Constantinou, 2022 presents results for only FN, and Section 6.1.3 presents results for both FN and V components). The analysis was performed in program OpenSees and only considered the effect of temperature on friction as described by equation (2-7). Results on the computed histories of temperature at the sliding interfaces and normalized isolators force-displacement loops are compared in Figure 3-3, where it is apparent the vertical ground motion has insignificant effects on the temperature and on the isolator displacement.

3.2 Scaling of Ground Motions for Response History Analysis

Each pair of the spectrally equivalent long-duration and short-duration ground motions suites was scaled in amplitude only to represent, individually and in an average sense, target response spectra for the maximum considered earthquake (MCE_R). The target spectra were represented by the spectral response acceleration parameter at the period of 1 second, S_{M1}, with values of 0.7g, 0.9g and 1.1g. The short period spectral acceleration parameter was not used as it did not affect the scaling process when based on amplitude scaling with a long effective period. In the scaling process, (a) the components of each pair were scaled by the same factor, which differed from pair to pair, and (b) the difference between the SRSS spectra of each pair of motions and the target spectrum (in terms of the sum of the square errors) was minimized in the range of $0.75T_M$ to $1.25T_M$, where T_M is the effective period as defined in ASCE/SEI-7 for the lower bound conditions that result in the largest mean resultant isolator displacement D_M.

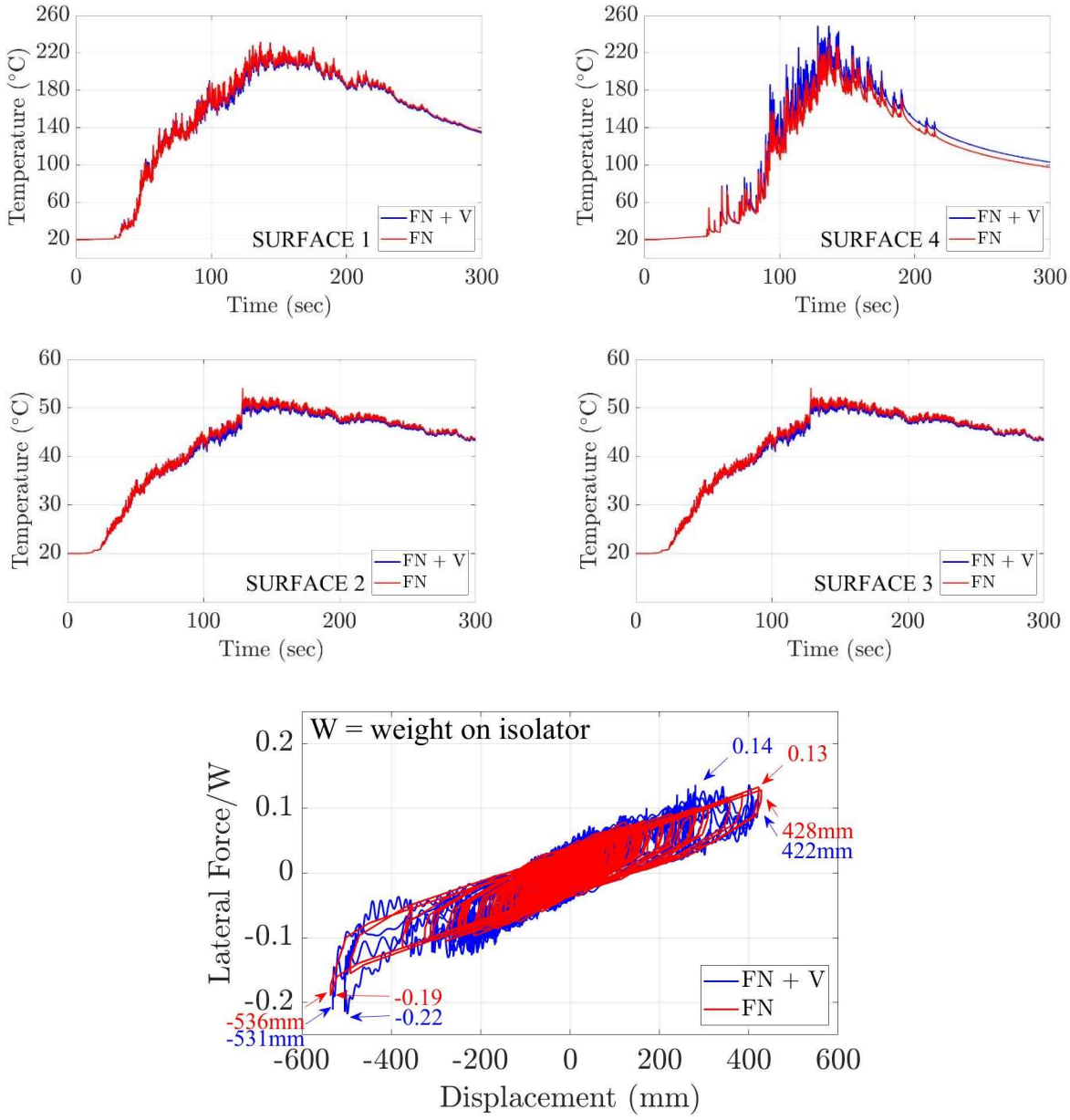

Figure 3-3 Example of Effect of Vertical Ground Motion on Force-displacement Loop and Histories of Temperature at the Sliding Interfaces of Triple FP Isolators

Period T_M is defined as the effective period in the lower bound conditions. In this study the lower bound conditions are defined only when considering heating effects without consideration of manufacturing variability. Period T_M is not known until the response history analysis using the lower bound time-invariant properties is completed and displacement D_M is computed. This required a multistep analysis process as follows:

1) The system to be analyzed is defined in terms of its characteristic strength or friction coefficients under dynamic conditions and at the starting temperature of the isolators (assumed 20°C in this study).
2) An estimate of the lower bound properties of characteristic strength or friction coefficient is obtained by dividing the starting values of properties by a factor, say 1.5.
3) Using the lower bound time-invariant properties computed in step 2, simplified ELF analysis per ASCE/SEI-7 is performed to compute displacement D_M.
4) Using this estimate of displacement D_M and the lower bound properties calculated in step 2, the effective period T_M is computed.
5) Using this value of effective period T_M, scaling of the ground motions is performed.
6) Response history analysis of the system with time-variant properties is performed using all 71 pairs of ground motion and the mean resultant isolator displacement is computed. This displacement is compared to the value computed by the ELF procedure in step 3.
7) The process in steps 2 to 6 is repeated by assuming a different value of the factor in step 2 (say 1.4 or 1.6) until the displacement computed in step 2 is essentially the same as the one computed in step 6.
8) When completing step 7, the period T_M has been properly calculated. The ground motions are then properly scaled using this value of the period and response history analysis is performed.

This procedure requires several dynamic analyses for each system and seismic hazard (in terms of S_{M1}) considered (96 systems and 3 hazards, total of 288 cases). There is a different period T_M for each of these 288 cases, so that the ground motions in the analysis differ depending on the system and hazard analyzed. An example of the spectra of the scaled motions is presented in Figures 3-4 and 3-5 for the triple FP isolation system 33 and the lead-rubber isolation system 322 (see Section 4 for details). The triple FP system 33 has period based on the post-elastic stiffness (pendulum period) T_P equal to 4.86sec and ratio of the zero-displacement force intercept at normal temperature (20°C) and high-speed motion to the weight μ equal to 0.075. Moreover, the friction-temperature relationship is the one given by equation (2-7). The lead-rubber system 322 has period based on the post-elastic stiffness T_d equal 4.00sec a ratio of the zero-displacement force intercept (or characteristic strength) at normal temperature (20°C) to the weight Q_d/W equal to 0.16 and a ratio of the lead core radius to its height a/h_L equal to 0.6. The target spectrum is described by S_{M1}=0.9g. The values of displacement D_M computed in the response history analysis, and the corresponding values of period T_M are shown in the figures. The figures show the SRSS spectra of each of the 71 scaled pairs of the short and of the long-duration, the average SRSS spectrum, and the target spectrum for the two isolation systems. The scaled ground motions represent well the target spectrum in an average sense within

the bounds of period range $0.75T_M$ to $1.25T_M$ while maintaining significant variability in the individual motions to be able to obtain statistical measures of the response of the analyzed structures beyond just the median or the mean. Appendix B presents graphs like those of Figures 3-4 and 3-5 for each of the 288 cases analyzed.

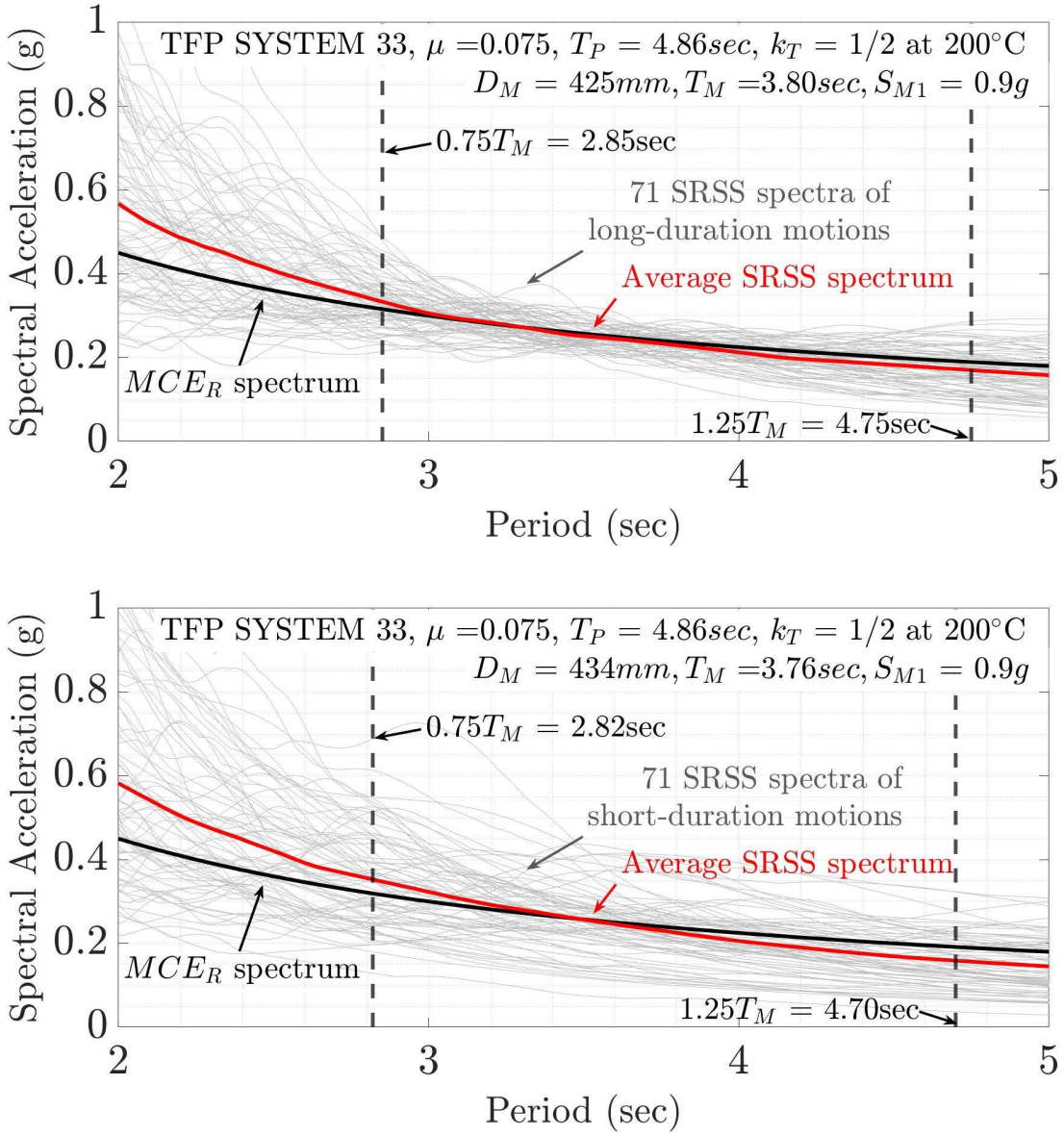

Figure 3-4 Comparison of Individual and Average SRSS Response Spectra of Scaled Ground Motions to Target Spectrum for System 33 (top: long-duration motions; bottom: short-duration motions)

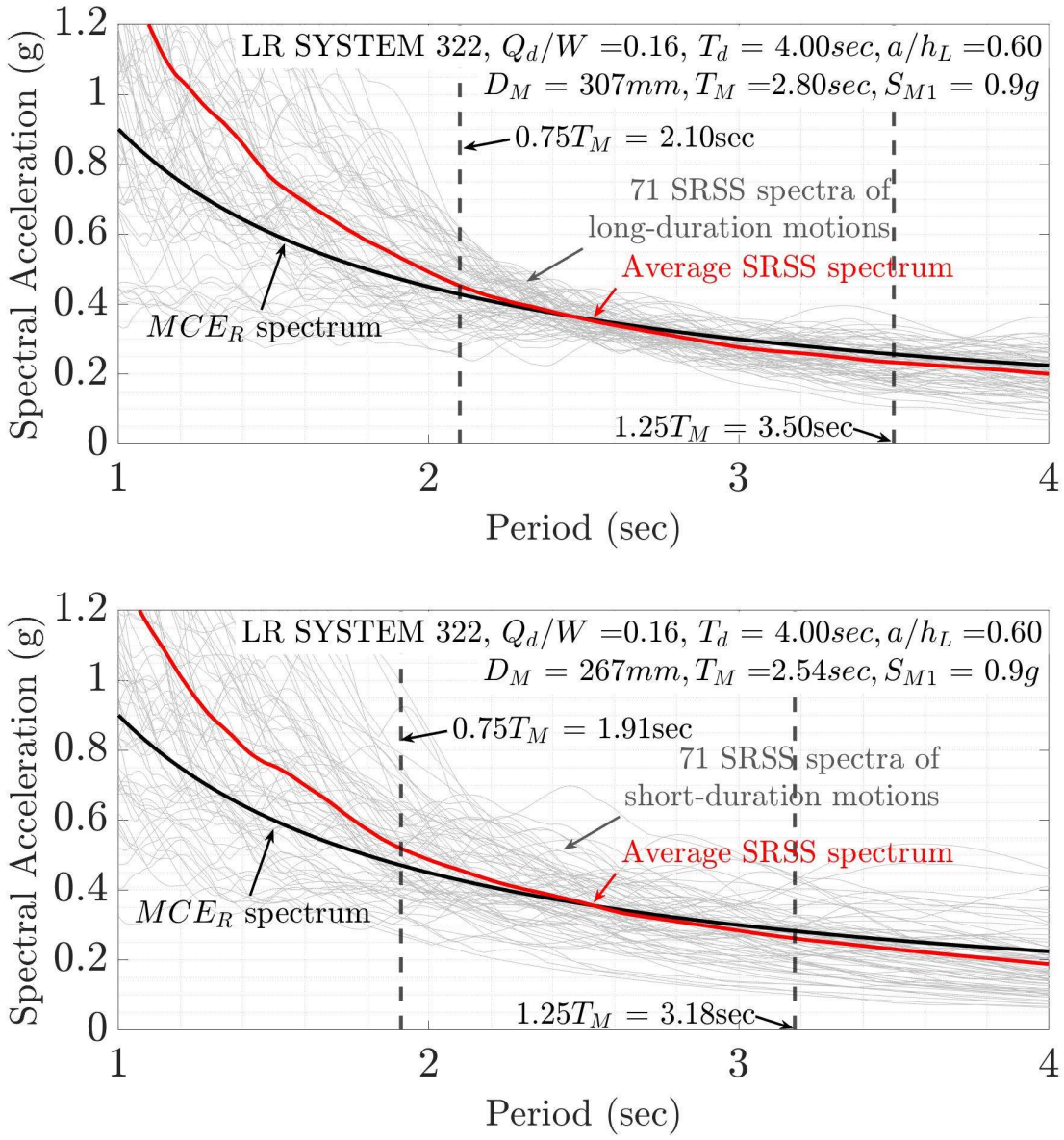

Figure 3-5 Comparison of Individual and Average SRSS Response Spectra of Scaled Ground Motions to Target Spectrum for System 322 (top: long-duration motions; bottom: short-duration motions)

It may be noted that for the triple FP system 33 in Figure 3-4, the computed displacement D_M is slightly smaller, and the effective period T_M is slightly larger in the long-duration than in the short-duration motions. This occurs because the strength of the isolation system (friction force) is slightly smaller in the long-duration motions due to more heating effects leading to a smaller effective stiffness for the calculation of the effective period.

“This Page Intentionally Left Blank”

SECTION 4
ANALYZED SEISMIC ISOLATION SYSTEMS

4.1 Seismically Isolated Structure

The study requires the analysis of isolated structures with a wide range of properties to describe the behavior of most systems of practical significance for many bi-directional ground motions in the far field. The vertical component of the ground motion is not included as it does not have any important effects on either the isolator displacement response or the temperature histories in sliding interfaces or the lead core of isolators. Also, overturning moment effects, and uplift is any, and torsion do not affect the global performance of isolation systems and are not considered in this study. These effects do affect the loads and displacements for individual isolators but that is determined in project-specific analyses and considered in the testing of isolators by requiring testing for a range of axial loads (in addition to the gravity load) and displacements that include the additional displacement due to torsion.

Accordingly, the study analyzed a rigid mass model with the center of mass located at the isolation system level so that there are no overturning moment effects. A single isolator carrying a representative gravity load was sufficient for the analysis the systems considered. The gravity load assumed carried by a single isolator is W=2558kN for 92 cases, and for four additional cases with actual triple FP and lead-rubber isolators, the gravity load was approximately as in the actual application. It is generally accepted that considering flexibility or inelastic action in the superstructure of an isolated building results in reduced isolation system displacements (ASCE/SEI-7 recognizes this in Section 17.6.4.1 by introducing equation 17.6-1).

All isolation systems were assumed to have sufficient displacement capacity to accommodate the demand without any displacement restrainers. Failure of the isolators was not considered.

4.2 Single FP Isolation Systems

The single FP isolators had the geometry and lateral force-displacement relationship shown in Figure 2-1. Table 4-1 lists the common parameters used for all analyzed single FP systems. Note that the contact diameter of the slider is based on standardized designs (11inch or 279.4mm). The displacement capacity of the isolator was considered unlimited.

Table 4-1 Common Parameters of Single FP Systems

Parameter	Unit	Value
Weight on one isolator, W	kN	2558
Diameters of rigid slider, b	mm (in)	279.4 (11.0)
Velocity rate parameter, *a*	sec/m	100
Thermal diffusivity of the stainless steel, D	m^2/sec	0.444×10^{-5}
Thermal conductivity of the stainless steel, k	Watt/(m·°C)	18
Initial temperature, T_0	°C	20

A total of eight different systems were studied, numbered 11, 12, 13, 14, 31, 32, 33 and 34. Table 4-2 presents information on the properties of the eight systems. The value of the friction coefficient μ is value at the start of motion prior to any heating effects and for high-speed conditions. The effective radius is based on standardized isolators that have been utilized. Smaller radius isolators were not considered as they would be too stiff for the seismic hazard considered. Period T_P is the pendulum period, given by the following equation, where g is the acceleration of gravity.

$$T_P = 2\pi\sqrt{\frac{R_{eff}}{g}} \qquad (4-1)$$

Table 4-2 Single FP Geometric and Frictional Parameters

System	11	31	12	32	13	33	14	34
R_{eff} mm (inch)	3048 (120)	6045 (238)	3048 (120)	6045 (238)	3048 (120)	6045 (238)	3048 (120)	6045 (238)
μ	0.04	0.04	0.06	0.06	0.08	0.08	0.10	0.10
T_P (sec)	3.50	4.93	3.50	4.93	3.50	4.93	3.50	4.93

Moreover, three different friction coefficient vs temperature relationships were utilized as described by equations (2-4) to (2-9). Specifically, equation (2-4) described the behavior of the coefficient of friction, with μ_{ref} having the value of μ in Table 4-2, parameter k_P=1 (there is no variation in contact pressure), parameter k_V per equation (2-6) with *a*=100sec/m, and parameter k_T as given by equation (2-7) or (2-8) or (2-9) (three different cases as depicted in Figure 2-4). For the complete description of the single FP element "FPBearingPTV" in program OpenSees (Kumar et al., 2015), a yield displacement is needed. It was specified as Y=0.25mm.

4.3 Triple FP Isolation Systems

The triple FP isolators had the geometry and lateral force-displacement relationship shown in Figure 2-2. Table 4-3 lists the common parameters used for all analyzed triple FP systems. Note that the geometry of the inner the slider (rigid slider and inner plates) is based on a standardized design. The displacement capacity of the isolator is considered unlimited.

Table 4-3 Common Parameters of Triple FP Systems

Parameter	Unit	Value
Weight on the isolator, W	kN	2558
Nominal displacement capacities (outer surface), d_1=d_4		Unlimited
Nominal displacement capacities (inner surface), d_2=d_3	mm (in)	38.1 (1.5)
Diameters of slide plates, b_1=b_4	mm (in)	279.4 (11.0)
Diameters of rigid slider, b_2=b_3	mm (in)	203.2 (8.0)
Distance of concave plate to pivot point, h_1=h_4	mm (in)	114.0 (4.5)
Distance of slide plate to pivot point, h_2=h_3	mm (in)	76.0 (3.0)
Velocity rate parameter, *a*	sec/m	100
Thermal diffusivity of the stainless steel, D	m^2/sec	$0.444x10^{-5}$
Thermal conductivity of the stainless steel, k	Watt/(m·°C)	18
Initial temperature, T_0	°C	20

A total of sixteen different systems were studied, with their parameters presented in Tables 4-4 to 4-7, grouped based on the friction properties. The friction coefficient values listed in these tables are at the start of motion prior to any heating effects and for high-speed conditions. The radii are based on standardized isolators that have been utilized. The friction coefficients at the two main sliding interfaces are considered equal, as this has been the most common case in applications. Period T_P is the pendulum period when motion occurs on the two main sliding interfaces, given by the following equation, where g is the acceleration of gravity.

$$T_P = 2\pi\sqrt{\frac{2R_{eff}}{g}} \qquad (4-2)$$

Also, parameter μ is the zero-displacement force intercept at start of motion divided by the weight and is used as a single parameter to describe the frictional behavior rather than the four friction coefficient values at the four sliding interfaces. This parameter is calculated using the following equation (Fenz and Constantinou, 2008a, c).

$$\mu = \mu_1 - \frac{(\mu_1 - \mu_2)R_{eff2}}{R_{eff1}} \qquad (4-3)$$

Distances d_i^* are the actual displacement capacities at each sliding interface (which lesser than the nominal capacities d_i, i=1, 2, 3 or 4) given by

$$d_i^* = \frac{R_{effi}}{R_i} d_i \qquad (4-4)$$

Moreover, three different friction coefficient vs temperature relationships were utilized as described by equations (2-4) to (2-9). Specifically, equation (2-4) described the behavior of the coefficient of friction, with μ_{ref} having the values of $\mu_1=\mu_4$ and $\mu_2=\mu_3$ per Tables 4-4 to 4-7 (that is, heating effects on friction were considered for all four sliding interfaces), parameter k_P=1 (there is no variation in contact pressure), parameter k_V per equation (2-6) with a =100sec/m, and parameter k_T as given by equation (2-7) or (2-8) or (2-9) (three different cases as depicted in Figure 2-4).

Table 4-4 Triple FP Geometric and Frictional Parameters for Systems 11 to 41

	System 11	**System 21**	**System 31**	**System 41**
$R_1=R_4$, mm (in)	1549.4 (61.0)	2235.2 (88.0)	3048.0 (120.0)	3962.4 (156.0)
$R_2=R_3$, mm (in)	304.8 (12.0)	304.8 (12.0)	304.8 (12.0)	304.8 (12.0)
$R_{eff1}=R_{eff4}$, mm	1435.4	2121.2	2934.0	3848.4
$R_{eff2}=R_{eff3}$, mm	228.8	228.8	228.8	228.8
$d_1^*=d_4^*$	Unlimited	Unlimited	Unlimited	Unlimited
$d_2^*=d_3^*$, mm	28.6	28.6	28.6	28.6
$\mu_1=\mu_4$	0.04	0.04	0.04	0.04
$\mu_2=\mu_3$	0.02	0.02	0.02	0.02
μ	0.037	0.038	0.038	0.039
T_P, sec	3.40	4.13	4.86	5.57

Table 4-5 Triple FP Geometric and Frictional Parameters for Systems 12 to 42

	System 12	**System 22**	**System 32**	**System 42**
$R_1=R_4$, mm (in)	1549.4 (61.0)	2235.2 (88.0)	3048.0 (120.0)	3962.4 (156.0)
$R_2=R_3$, mm (in)	304.8 (12.0)	304.8 (12.0)	304.8 (12.0)	304.8 (12.0)
$R_{eff1}=R_{eff4}$, mm	1435.4	2121.2	2934.0	3848.4
$R_{eff2}=R_{eff3}$, mm	228.8	228.8	228.8	228.8
$d_1^*=d_4^*$	Unlimited	Unlimited	Unlimited	Unlimited
$d_2^*=d_3^*$, mm	28.6	28.6	28.6	28.6
$\mu_1=\mu_4$	0.06	0.06	0.06	0.06
$\mu_2=\mu_3$	0.02	0.02	0.02	0.02
μ	0.054	0.056	0.057	0.058
T_P, sec	3.40	4.13	4.86	5.57

Table 4-6 Triple FP Geometric and Frictional Parameters for Systems 13 to 43

	System 13	System 23	System 33	System 43
R_1=R_4, mm (in)	1549.4 (61.0)	2235.2 (88.0)	3048.0 (120.0)	3962.4 (156.0)
R_2=R_3, mm (in)	304.8 (12.0)	304.8 (12.0)	304.8 (12.0)	304.8 (12.0)
R_{eff1}=R_{eff4}, mm	1435.4	2121.2	2934.0	3848.4
R_{eff2}=R_{eff3}, mm	228.8	228.8	228.8	228.8
d_1^*=d_4^*	Unlimited	Unlimited	Unlimited	Unlimited
d_2^*=d_3^*, mm	28.6	28.6	28.6	28.6
μ_1=μ_4	0.08	0.08	0.08	0.08
μ_2=μ_3	0.02	0.02	0.02	0.02
μ	0.070	0.074	0.075	0.076
T_P, sec	3.40	4.13	4.86	5.57

Table 4-7 Triple FP Geometric and Frictional Parameters for Systems 14 to 44

	System 14	System 24	System 34	System 44
R_1=R_4, mm (in)	1549.4 (61.0)	2235.2 (88.0)	3048.0 (120.0)	3962.4 (156.0)
R_2=R_3, mm (in)	304.8 (12.0)	304.8 (12.0)	304.8 (12.0)	304.8 (12.0)
R_{eff1}=R_{eff4}, mm	1435.4	2121.2	2934.0	3848.4
R_{eff2}=R_{eff3}, mm	228.8	228.8	228.8	228.8
d_1^*=d_4^*	Unlimited	Unlimited	Unlimited	Unlimited
d_2^*=d_3^*, mm	28.6	28.6	28.6	28.6
μ_1=μ_4	0.10	0.10	0.10	0.10
μ_2=μ_3	0.02	0.02	0.02	0.02
μ	0.087	0.091	0.094	0.095
T_P, sec	3.40	4.13	4.86	5.57

For the complete description of the triple FP element in program OpenSees (Kim and Constantinou, 2022, 2023), a yield displacement Y=0.4mm was used. This is slightly larger than that for the single FP isolators (=0.25mm) due to the larger total thickness of the deformable materials used in the four sliding interfaces.

4.4 Lead-rubber Isolation Systems

The lead-rubber isolators had the geometry and lateral force-displacement relationship shown in Figure 2-3 and described by equations (2-10) to (2-16). Table 4-8 lists the common parameters used for all analyzed lead-rubber systems. The displacement capacity of the isolator is considered unlimited. Sixteen different systems with the total steel thickness t_s set equal to 0.30 times the lead core height h_L ($t_s = 0.3h_L$) were studied. The parameters of these 18 systems are presented in Tables 4-9 and 4-10, grouped based on two values of the ratio of the lead core radius to its height a/h_L.

Table 4-8 Common Parameters of Lead-rubber Systems

Parameter	Unit	Value
Weight on the isolator, W	kN	2558
Initial effective yield stress of lead, σ_{YL0}	MPa	13
Yield displacement, Y	mm	20
Density of lead, ρ_L	kg/m^3	11300
Specific heat of lead, c_L	Joule/(kg·°C)	130
Thermal conductivity of steel, k_S	Watt/(m·°C)	50
Thermal diffusivity of steel, α_S	m^2/s	1.41×10^{-5}
Parameter E_2	1/°C	0.0069
Initial temperature, T_0	°C	20

Table 4-9 Lead Rubber System Parameters for Case α/h_L =0.3

	System 111	System 211	System 311	System 121	System 221	System 321	System 131	System 231	System 331
Post-elastic stiffness, k_d (kN/mm)	2.575	1.144	0.644	2.575	1.144	0.644	2.575	1.144	0.644
Lead core radius, *a* (mm)	71	71	71	100	100	100	123	123	123
Lead core height, h_L (mm)	236.7	236.7	236.7	333.3	333.3	333.3	410	410	410
Steel shim total thickness, t_s (mm)	71	71	71	100	100	100	123	123	123
Viscous damping parameter, C_d (N·sec/m)	32774.8	21845.6	16390.6	32774.8	21845.6	16390.6	32774.8	21845.6	16390.6
Post-elastic period, T_d (sec)	2	3	4	2	3	4	2	3	4
Initial Strength/Weight Q_d/W	0.08	0.08	0.08	0.16	0.16	0.16	0.24	0.24	0.24

Table 4-10 Lead Rubber System Parameters for Case α/h_L =0.6

	System 112	System 212	System 312	System 122	System 222	System 322	System 132	System 232	System 332
Post-elastic stiffness, k_d (kN/mm)	2.575	1.144	0.644	2.575	1.144	0.644	2.575	1.144	0.644
Lead core radius, *a* (mm)	71	71	71	100	100	100	123	123	123
Lead core height, h_L (mm)	118.3	118.3	118.3	166.7	166.7	166.7	205	205	205
Steel shim total thickness, t_s (mm)	35.5	35.5	35.5	50	50	50	61.5	61.5	61.5
Viscous damping parameter, C_d (N·sec/m)	32774.8	21845.6	16390.6	32774.8	21845.6	16390.6	32774.8	21845.6	16390.6
Post-elastic period, T_d (sec)	2	3	4	2	3	4	2	3	4
Initial Strength/Weight Q_d/W	0.08	0.08	0.08	0.16	0.16	0.16	0.24	0.24	0.24

Moreover, the lead-rubber isolator model included an additional force to account for the inherent ability of rubber to dissipate energy. This force was modeled as a linear viscous force in each of the two orthogonal horizontal directions, $F=C_dV$, where V is the relative velocity in the considered direction (isolated structure with respect to the ground) and C_d is the damping constant computed as follows using an effective damping for rubber β=0.02.

$$C_d = 2\beta\left(\frac{2\pi}{T_d}\right)\left(\frac{W}{g}\right) \qquad (4-5)$$

4.5 Additional Lead-rubber and Triple FP Systems

The choice of geometric parameters of the systems of Tables 4-9 and 4-10, radius *a*, lead core height h_L and steel shim total thickness t_s, is arbitrary but follows certain rules based on actual lead-rubber isolators. Six very different full-size lead-rubber isolators described in Kalpakidis and Constantinou (2008), had the following geometric relationships: a/t_s~1 for five cases and a/t_s~*1.5* for one case, a/h_L=0.13 to 0.46, and t_s/h_L=0.16 to 0.56. The range of these dimensional quantities in Tables 4-9 and 4-10 is: a/t_s=1 or 2, a/h_L=0.3 or 0.6 and t_s/h_L=0.3, which covers well the range of these parameters in actual lead-rubber isolators. However, the following require clarification:

1) The values of the lead core height in Tables 4-9 and 4-10 indicate that the rubber total height (which always is less than the lead core height) could have been small for the computed isolator displacements (e.g., in the most extreme case, see Table 4-10, system 312 which has total rubber thickness less than 118mm, whereas the computed value of the average displacement is reported later in Section 5 to exceed 1000mm for some analyses). This inconsistency does not affect the results as the rubber height is not used in any calculation and the failure of the isolators is not considered. Rather, the stiffness is k_d is computed based on the assumed value of period T_d, which is parametrically varies. The values of the lead core radius, lead core height and steel shim total thickness are only used in the solution of the heat conduction problem in accordance with equations (2-13) to (2-16).
2) To investigate the possible effects that the geometric parameters on the computed response, three additional cases were considered using actual lead-rubber bearings based on the geometry of bearings reported in Kalpakidis and Constantinou (2008). Table 4-11 lists the properties of these three systems. System 5 represents isolators used in the Erzurum Hospital in Turkey (Constantinou et al., 2007). System 4 represents the same isolators as those of system 5 but with a lower modulus

rubber so that the period is longer. System 6 represents isolators used in Coronado Bridge in San Diego, California.

Table 4-11 Parameters of Additional Lead Rubber Systems (all other parameters per Table 4-8)

	System 4	System 5	System 6
Weight on the isolator, W (kN)	10266	10266	2483
Initial effective yield stress of lead, σ_{YL0} (MPa)	16.9	16.9	9.7
Post-elastic stiffness, k_d (kN/mm)	2.582	4.590	2.498
Lead core radius, *a* (mm)	153	153	140
Lead core height, h_L (mm)	333	333	400
Steel shim total thickness, t_s (mm)	125	125	95
Viscous damping parameter, C_d (N·sec/m)	65752.5	87670.0	31806.6
Post-elastic period, T_d (sec)	4	3	2
Initial Strength/Weight Q_d/W	0.121	0.121	0.241

Also, the geometric parameters of the single and triple FP systems in sections 4.2 and 4.3, and particularly the contact diameter or slide plate diameter (=279.4mm), affects the heating process of the sliding interfaces resulting in many cases where the heat flux is intermittent, which occurs when the displacement exceeds half the diameter of the contact area (=139.7mm) per equation (2-3). The difference in the heating process between intermittent and continuous heat fluxes may be appreciated in the test results and model predictions presented in Constantinou et al. (2007). Accordingly, one more triple FP system was selected from an actual application with large gravity load so that the slide plate diameter is large to generate continuous heat flux conditions in most analyses. It is termed system LL and is representative in geometry and load of isolators used in the Loma Linda University Medical Center in California. The frictional properties of the LL isolator are differently specified than those of the Loma Linda University Medical Center. The geometric and frictional properties of the LL isolator, and other parameters of the isolator used in the analysis are presented in Table 4-12. The friction coefficient-temperature relationships of equations (2-7) to (2-9) were considered. The model of triple FP isolator LL in the analysis included its stiffening, which was engaged only in a small number of ground motions. The ultimate displacement capacity of the isolator was considered unlimited. The computed average isolator displacement D_M for the 9 analyzed cases were less than the displacement at which stiffening occurs. System LL has very similar characteristics with triple

FP system 43 but for the large contact area which results more often in continuous heat flux, and the contact pressure on the main sliding interfaces which is 33.6MPa for system LL and 41.7MPa for system 43. The higher pressure affects heating through a proportional increase in the heat flux as shown in equation (2-3).

Table 4-12 Parameters of Additional Triple FP System LL

Parameter	Unit	Value
Weight on the isolator, W	kN	13350
Nominal displacement capacities (outer surface), $d_1=d_4$	mm (in)	533.4 (21.0)
Nominal displacement capacities (inner surface), $d_2=d_3$	mm (in)	101.6 (4.0)
Diameters of slide plates, $b_1=b_4$	mm (in)	711.2 (28.0)
Diameters of rigid slider, $b_2=b_3$	mm (in)	508.0 (20.0)
Distance of concave plate to pivot point, $h_1=h_4$	mm (in)	215.9 (8.5)
Distance of slide plate to pivot point, $h_2=h_3$	mm (in)	165.1 (6.5)
Radii of curvature $R_1=R_4$	mm (in)	3962.4 (156.0)
Radii of curvature $R_2=R_3$	mm (in)	558.8 (22)
Effective radii of curvature $R_{eff1}=R_{eff4}$	mm	3746.5
Effective radii of curvature $R_{eff2}=R_{eff3}$	mm	393.7
Actual displacement capacity $d_1^*=d_4^*$	mm	504.3
Actual displacement capacity $d_2^*=d_3^*$, mm	mm	71.6
Reference coefficient of friction $\mu_1=\mu_4$	-	0.08
Reference coefficient of friction $\mu_2=\mu_3$	-	0.02
Reference parameter per eq. (4-3) μ	-	0.074
Pendulum period T_P	sec	5.49
Velocity rate parameter, *a*	sec/m	100
Thermal diffusivity of the stainless steel, D	m^2/sec	$0.444x10^{-5}$
Thermal conductivity of the stainless steel, k	Watt/(m·°C)	18
Initial temperature, T_0	°C	20
Reference values are values at the start of motion prior to any heating effects		

“This Page Intentionally Left Blank”

SECTION 5
RESULTS FOR TEST TO OBTAIN LOWER BOUND PROPERTIES

5.1 Procedure for Test Design

The procedure for designing a test to determine the lower bound properties of an isolation system follows the procedures of ASCE/SEI 7 for determining the bounding values of the isolation system properties (characteristic strength and post-elastic stiffness) for use in analysis and design. These procedures require to determine by testing of prototype isolators values of factors $\lambda_{(test,\ max)}$ and $\lambda_{(test,\ min)}$ which when multiplied by nominal values of the isolator properties result in the upper bound and the lower bound properties after additional adjustments to account for manufacturing variability and aging (McVitty and Constantinou, 2015 provide detailed examples). The upper bound properties are based on results obtained in the first cycle of test, whereas the lower bound properties are based on results on some later cycle. In ASCE/SEI-7 standard the lower bound properties are based on the third cycle (test Items 2(a) and 3 in section 17.8.2.2) where the isolator is subjected to three cycles at amplitude D_M and period T_M. The interest in this work is to determine the number of cycles needed in a test at amplitude D_M and period T_M so that the properties obtained in the last cycle of test and used in analysis with time-invariant properties (without heating effects on the characteristic strength or friction) result in the same average isolator resultant displacement as analysis with time-variant properties (with heating effects considered). The procedure follows these steps:

1) For each of the 96 seismic isolation systems described in Section 4, and for each of the three ground motion intensities considered (total of 288 cases), the short- and long-duration ground motion suites are scaled as described in Section 3.2.

2) Each system is analyzed for each of the scaled suites (short- and long-duration) of ground motions using the time-variant properties (i.e., with heating effects considered) of the isolators as described in Section 4. The average resultant isolator displacement D_M is calculated. Tables 5-1 to 5-11 present the results of the analysis in terms of the average resultant displacement, the effective period and the strength reduction factor computed in step 3 below.

3) Each system is repeatedly analyzed for each of the scaled suites (short- and long-duration) of ground motions using time-invariant properties (i.e., without considering heating effects) of the isolators until the computed average resultant isolator displacement D_M is essentially the same as

that computed in step 2 when using time-variant properties. This iterative process starts with an assumed value of constant characteristic strength for lead-rubber isolators or friction coefficient μ for single FP isolators or friction coefficients $\mu_1 = \mu_4$ for triple FP isolators that is less than the initial value (at the start of motion when the isolator temperature is normal) in the time-variant model of step 2. The friction coefficients $\mu_2 = \mu_3$ at the two inner sliding surfaces of triple FP isolators are assumed to be constant (that is, not affected by heating which is much less than that at the two main sliding interfaces) and are not reduced. A strength reduction factor for reducing the initial value of the characteristic strength or friction coefficients to obtain the time-invariant characteristic strength or friction coefficients is determined. Values of this reduction factor are reported in Tables 5-1 to 5-11.

4) The isolator of the analyzed system is then again analyzed using time-variant properties when subject to the axial load used in the analysis of steps 2 and 3, and several cycles of imposed motion at amplitude D_M and period T_M as they have been computed in step 1 and reported in Tables 5-1 to 5-11. At the end of each cycle, the characteristic strength over the weight ratio for lead-rubber isolators Q_d/W or a parameter μ for FP isolators is computed as typically done in testing of isolators using equation (5-1), where EDC is the energy dissipated per cycle normalized by the weight (in actual testing, the instantaneous shear force is normalized by the instantaneous vertical force before computing the EDC as the vertical force is not constant but varies due to test machine performance limitations).

$$\mu \; or \; \frac{Q_d}{W} = \frac{EDC}{4WD} \qquad (5-1)$$

D in equation (5-1) is the amplitude of motion in the cycle considered, which is equal to D_M for the tests of section 5-2. However, it is different than D_M for other tests evaluated in section 5-3 later in this report.

Note that parameter μ in equation (5-1) is an average per cycle representation of the coefficient of friction of single FP isolators (it would have been the same as parameter μ of equation 4-3 when friction is unaffected by temperature). The same applies for the zero-displacement force intercept divided by the weight ratio for triple FP isolators, and the characteristic strength to weight ratio for lead-rubber isolators.

Figures 5-1 to 5-4 present examples of the calculations for the following four cases, where S_{M1}=1.1g. Appendix C presents results like those of Figures 5-1 to 5-4 for each of the 288 systems cases analyzed.

a) Lead-rubber system 332, for which W=2558kN, T_d=4sec, $(Q_d/W)_{ref}$ = 0.24. The computed response parameters in steps 2 and 3 for long-duration motions were D_M=314mm, T_M=2.48sec, and the strength reduction factor=1.90.

b) Triple FP system 44, for which W=2558kN, T_P=5.57sec, μ_{ref} =0.095, μ_{1ref} =μ_{4ref} = 0.10, the friction coefficient-temperature relationship followed the law of equation 2-9 for which parameter k_T reduces to 1/3 of the starting value at the temperature of 200°C. The computed response parameters in steps 2 and 3 for long-duration motions were D_M=637mm, T_M=4.51sec, strength reduction factor=2.23.

c) Triple FP system 43, for which W=2558kN, T_P=5.57sec, μ_{ref} =0.076, μ_{1ref} =μ_{4ref}=0.08, the friction coefficient-temperature relationship followed the law of equation 2-7 for which parameter k_T reduces to 1/2 of the starting value at the temperature of 200°C. The computed response parameters in steps 2 and 3 for long-duration motions were D_M=607mm, T_M=4.42sec, strength reduction factor=1.67.

d) Triple FP system LL, for which W=13350kN, T_P=5.49sec, μ_{ref} = 0.074, μ_{1ref} = μ_{4ref} = 0.08, the friction coefficient-temperature relationship followed the law of equation 2-7 for which parameter k_T reduces to 1/2 of the starting value at the temperature of 200°C. The computed response parameters in steps 2 and 3 for long-duration motions were D_M=632mm, T_M=4.44sec, strength reduction factor=1.72.

   Note that triple FP system LL is effectively the same as triple FP system 43 in terms of pendulum period and initial (reference) values of coefficients μ_{ref} and μ_{1ref}, and has very similar response parameters D_M, T_M and strength reduction factor. System LL has different heating effects than system 43 as seen in the force-displacement loops and the history of temperature because the heat flux is intermittent for system 43 but continuous for system LL.

5) The number of cycles needed is that for which the computed values of parameters Q_d/W or μ per equation (5-1) is equal or very close to the value determined by dividing the starting value of the ratio of the characteristic strength for lead-rubber isolators or the zero-displacement force intercept for FP isolators to the weight by the computed strength reduction factor. For the case of the lead-rubber system 332 of Figure 5-1, the starting value of the normalized strength is 0.24, the strength reduction factor is 1.90, so the target value of normalized strength is 0.24/1.90=0.1263. This value of normalized strength computed using equation (5-1) is reached following three complete cycles of motions as shown in Figure 5-1. This is the required number of cycles for a test to determine the lower bound properties.

For the case of the Triple FP system 44 of Figure 5-2, the starting value of friction coefficients μ_{1ref} $=\mu_{4ref}$ is 0.10, the starting value of the zero-displacement force intercept over the weight ratio μ_{ref}=0.095 and reduction factor is 2.23. The reduction factor applies to the friction coefficients μ_{1ref} $=\mu_{4ref}$ (the corresponding reduction factor for the zero-displacement force intercept over the weight ratio μ_{ref} is slightly different than 2.23 since the two inner sliding interfaces with lesser values of friction coefficients were assumed constant and heating effects were neglected in the analysis of step 4). The target value of friction coefficients $\mu_1=\mu_4$=0.10/2.23=0.0448, and the target value of the zero-displacement force intercept over the weight ratio μ is 0.0434 computed using equation 4-3 with R_{eff1}=3848.4mm, R_{eff2}=228.8mm, μ_1 =0.10/2.23=0.0448 and μ_2 =0.02 (without reduction). This value of parameter μ computed per equation (5-1) is reached following four complete cycles of motions as shown in Figure 5-2. This is the required number of cycles for a test to determine the lower bound properties.

While triple FP systems 43 and LL have essentially the same pendulum period, initial values of coefficients μ_{ref} and μ_{1ref}, and response parameters D_M, T_M and strength reduction factor, they require different number of cycles to obtain the lower bound properties- four and two cycles, respectively. This is due to the heating effects which are more in the LL system that experiences continuous heat flux versus the intermittent head flux of system 43.

Table 5-1 Average Resultant Isolator Displacements, Effective Periods, Reduction Factors and Required Number of Test Cycles for Single FP Systems Computed when S_{M1} = 0.7g

	k_T = 2/3 at 200°C								k_T = 1/2 at 200°C								k_T = 1/3 at 200°C							
	Short-duration				Long-duration				Short-duration				Long-duration				Short-duration				Long-duration			
	D_M (mm)	T_M (sec)	Factor	Cycles	D_M (mm)	T_M (sec)	Factor	Cycles	D_M (mm)	T_M (sec)	Factor	Cycles	D_M (mm)	T_M (sec)	Factor	Cycles	D_M (mm)	T_M (sec)	Factor	Cycles	D_M (mm)	T_M (sec)	Factor	Cycles
System 11 T_P = 3.50 sec μ_{ref} = 0.040	310	3.03	1.17	**2**	293	3.03	1.25	**4**	331	3.09	1.31	**2**	318	3.11	1.45	**4**	359	3.16	1.49	**2**	346	3.18	1.67	**4**
System 31 T_P = 4.93 sec μ_{ref} = 0.040	338	3.87	1.14	**2**	335	3.91	1.22	**4**	356	3.97	1.25	**2**	366	4.07	1.41	**4**	381	4.09	1.40	**2**	404	4.21	1.62	**4**
System 12 T_P = 3.50 sec μ_{ref} = 0.060	267	2.81	1.24	**2**	269	2.85	1.34	**3**	290	2.91	1.41	**2**	298	2.97	1.57	**3**	327	3.03	1.66	**2**	336	3.08	1.88	**3**
System 32 T_P = 4.93 sec μ_{ref} = 0.060	275	3.39	1.18	**1**	269	3.46	1.31	**3**	293	3.56	1.34	**2**	298	3.68	1.53	**3**	320	3.75	1.56	**2**	336	3.91	1.82	**3**
System 13 T_P = 3.50 sec μ_{ref} = 0.080	240	2.61	1.27	**1**	240	2.67	1.40	**3**	260	2.73	1.44	**1**	269	2.82	1.68	**3**	295	2.89	1.77	**2**	306	2.97	2.02	**3**
System 33 T_P = 4.93 sec μ_{ref} = 0.080	240	3.05	1.25	**1**	238	3.13	1.37	**3**	258	3.23	1.41	**1**	264	3.39	1.64	**3**	284	3.48	1.68	**2**	298	3.66	1.98	**3**
System 14 T_P = 3.50 sec μ_{ref} = 0.100	220	2.43	1.29	**1**	220	2.50	1.44	**2**	241	2.57	1.48	**1**	249	2.69	1.76	**3**	273	2.76	1.82	**2**	287	2.87	2.18	**3**
System 34 T_P = 4.93 sec μ_{ref} = 0.100	221	2.78	1.28	**1**	218	2.86	1.41	**2**	239	2.98	1.46	**1**	243	3.15	1.71	**2**	266	3.26	1.76	**2**	278	3.48	2.16	**3**

μ_{ref} is the starting value of the coefficient of friction prior to any heating effects, Factor=friction coefficient reduction factor

Table 5-2 Average Resultant Isolator Displacements, Effective Periods, Reduction Factors and Required Number of Test Cycles for Single FP Systems Computed when S_{M1} = 0.9g

	k_T = 2/3 at 200°C								k_T = 1/2 at 200°C								k_T = 1/3 at 200°C							
	Short-duration				Long-duration				Short-duration				Long-duration				Short-duration				Long-duration			
	D_M (mm)	T_M (sec)	Factor	Cycles	D_M (mm)	T_M (sec)	Factor	Cycles	D_M (mm)	T_M (sec)	Factor	Cycles	D_M (mm)	T_M (sec)	Factor	Cycles	D_M (mm)	T_M (sec)	Factor	Cycles	D_M (mm)	T_M (sec)	Factor	Cycles
System 11 T_P = 3.50 sec μ_{ref} = 0.040	464	3.16	1.17	**2**	439	3.17	1.26	**4**	493	3.21	1.31	**2**	473	3.23	1.47	**5**	526	3.26	1.47	**2**	512	3.28	1.70	**5**
System 31 T_P = 4.93 sec μ_{ref} = 0.040	506	4.14	1.14	**2**	515	4.20	1.23	**4**	529	4.21	1.23	**2**	558	4.32	1.42	**5**	561	4.31	1.38	**2**	605	4.42	1.62	**5**
System 12 T_P = 3.50 sec μ_{ref} = 0.060	412	3.01	1.26	**2**	412	3.04	1.36	**4**	446	3.08	1.41	**2**	464	3.14	1.63	**5**	493	3.16	1.64	**2**	522	3.22	1.95	**5**
System 32 T_P = 4.93 sec μ_{ref} = 0.060	410	3.74	1.20	**2**	414	3.83	1.33	**4**	439	3.88	1.35	**2**	462	4.04	1.59	**5**	477	4.04	1.55	**2**	518	4.21	1.87	**5**
System 13 T_P = 3.50 sec μ_{ref} = 0.080	366	2.84	1.29	**2**	369	2.90	1.43	**3**	400	2.95	1.49	**2**	418	3.02	1.71	**4**	447	3.06	1.77	**2**	473	3.14	2.08	**4**
System 33 T_P = 4.93 sec μ_{ref} = 0.080	359	3.43	1.26	**2**	363	3.53	1.40	**3**	385	3.60	1.43	**2**	405	3.77	1.67	**4**	423	3.81	1.69	**2**	462	4.02	2.06	**4**
System 14 T_P = 3.50 sec μ_{ref} = 0.100	339	2.71	1.33	**2**	342	2.78	1.51	**3**	367	2.82	1.54	**2**	387	2.93	1.83	**4**	415	2.97	1.89	**2**	443	3.06	2.24	**4**
System 34 T_P = 4.93 sec μ_{ref} = 0.100	333	3.19	1.30	**2**	334	3.32	1.50	**3**	357	3.38	1.50	**2**	372	3.58	1.80	**4**	392	3.62	1.79	**2**	424	3.85	2.21	**4**

μ_{ref} is the starting value of the coefficient of friction prior to any heating effects, Factor=friction coefficient reduction factor

Table 5-3 Average Resultant Isolator Displacements, Effective Periods, Reduction Factors and Required Number of Test Cycles for Single FP Systems Computed when S_{M1} = 1.1g

	k_T = 2/3 at 200°C								k_T = 1/2 at 200°C								k_T = 1/3 at 200°C							
	Short-duration				Long-duration				Short-duration				Long-duration				Short-duration				Long-duration			
	D_M (mm)	T_M (sec)	Factor	Cycles	D_M (mm)	T_M (sec)	Factor	Cycles	D_M (mm)	T_M (sec)	Factor	Cycles	D_M (mm)	T_M (sec)	Factor	Cycles	D_M (mm)	T_M (sec)	Factor	Cycles	D_M (mm)	T_M (sec)	Factor	Cycles
System 11 T_P = 3.50 sec μ_{ref} = 0.040	630	3.24	1.15	**2**	598	3.25	1.27	**5**	662	3.27	1.27	**2**	637	3.29	1.46	**5**	696	3.30	1.41	**2**	681	3.33	1.68	**5**
System 31 T_P = 4.93 sec μ_{ref} = 0.040	689	4.31	1.13	**2**	712	4.37	1.23	**5**	717	4.36	1.21	**2**	762	4.46	1.41	**5**	754	4.43	1.35	**2**	816	4.53	1.60	**5**
System 12 T_P = 3.50 sec μ_{ref} = 0.060	574	3.12	1.24	**2**	587	3.17	1.39	**5**	614	3.18	1.38	**2**	649	3.24	1.64	**5**	673	3.24	1.61	**2**	717	3.29	1.91	**5**
System 32 T_P = 4.93 sec μ_{ref} = 0.060	563	3.97	1.19	**2**	586	4.08	1.35	**5**	600	4.08	1.32	**2**	647	4.24	1.59	**5**	647	4.21	1.51	**2**	714	4.37	1.85	**5**
System 13 T_P = 3.50 sec μ_{ref} = 0.080	509	2.99	1.30	**2**	528	3.06	1.47	**4**	551	3.07	1.46	**2**	586	3.14	1.73	**4**	610	3.15	1.71	**2**	663	3.23	2.13	**5**
System 33 T_P = 4.93 sec μ_{ref} = 0.080	492	3.70	1.27	**2**	512	3.83	1.43	**4**	528	3.85	1.43	**2**	571	4.03	1.69	**4**	578	4.03	1.67	**2**	647	4.23	2.07	**5**
System 14 T_P = 3.50 sec μ_{ref} = 0.100	466	2.87	1.34	**2**	488	2.96	1.55	**4**	508	2.98	1.56	**2**	543	3.07	1.84	**4**	568	3.08	1.83	**2**	616	3.17	2.26	**4**
System 34 T_P = 4.93 sec μ_{ref} = 0.100	452	3.47	1.31	**2**	466	3.62	1.52	**4**	486	3.65	1.51	**2**	518	3.85	1.81	**4**	536	3.86	1.78	**2**	594	4.08	2.22	**4**

μ_{ref} is the starting value of the coefficient of friction prior to any heating effects, Factor=friction coefficient reduction factor

Table 5-4 Average Resultant Isolator Displacements, Effective Periods, Reduction Factors and Required Number of Test Cycles for Triple FP Systems Computed when S_{M1} = 0.7g

	k_T = 2/3 at 200°C								k_T = 1/2 at 200°C								k_T = 1/3 at 200°C							
	Short-duration				Long-duration				Short-duration				Long-duration				Short-duration				Long-duration			
	D_M (mm)	T_M (sec)	Factor	Cycles	D_M (mm)	T_M (sec)	Factor	Cycles	D_M (mm)	T_M (sec)	Factor	Cycles	D_M (mm)	T_M (sec)	Factor	Cycles	D_M (mm)	T_M (sec)	Factor	Cycles	D_M (mm)	T_M (sec)	Factor	Cycles
System 11 T_P = 3.40 sec μ_{ref} = 0.037	341	3.02	1.19	**2**	308	2.99	1.20	**2**	366	3.08	1.39	**2**	331	3.06	1.42	**3**	397	3.13	1.59	**2**	360	3.12	1.70	**3**
System 21 T_P = 4.13 sec μ_{ref} = 0.038	356	3.51	1.17	**2**	338	3.49	1.19	**2**	381	3.60	1.35	**2**	366	3.59	1.39	**3**	410	3.68	1.55	**2**	400	3.68	1.61	**3**
System 31 T_P = 4.86 sec μ_{ref} = 0.038	364	3.91	1.15	**2**	352	3.91	1.18	**2**	387	4.03	1.31	**2**	381	4.06	1.38	**3**	413	4.15	1.49	**2**	419	4.18	1.58	**3**
System 41 T_P = 5.57 sec μ_{ref} = 0.039	377	4.28	1.15	**2**	358	4.25	1.17	**2**	403	4.44	1.31	**2**	388	4.44	1.36	**3**	430	4.61	1.54	**3**	429	4.62	1.56	**3**
System 12 T_P = 3.40 sec μ_{ref} = 0.054	286	2.84	1.25	**2**	257	2.80	1.28	**2**	307	2.92	1.46	**2**	279	2.89	1.50	**2**	336	3.01	1.73	**2**	307	2.99	1.79	**2**
System 22 T_P = 4.13 sec μ_{ref} = 0.056	296	3.22	1.24	**2**	279	3.19	1.27	**2**	317	3.34	1.43	**2**	302	3.33	1.48	**2**	347	3.47	1.68	**2**	334	3.47	1.75	**2**
System 32 T_P = 4.86 sec μ_{ref} = 0.057	307	3.54	1.23	**2**	288	3.51	1.27	**2**	327	3.70	1.42	**2**	314	3.70	1.48	**2**	351	3.85	1.64	**2**	348	3.89	1.75	**2**
System 42 T_P = 5.57 sec μ_{ref} = 0.058	316	3.81	1.24	**2**	295	3.77	1.28	**2**	336	3.99	1.41	**2**	318	3.98	1.47	**2**	359	4.17	1.60	**2**	350	4.20	1.71	**2**
System 13 T_P = 3.40 sec μ_{ref} = 0.070	257	2.68	1.30	**2**	229	2.62	1.32	**2**	276	2.79	1.54	**2**	248	2.75	1.59	**2**	303	2.91	1.89	**2**	278	2.89	1.99	**2**
System 23 T_P = 4.13 sec μ_{ref} = 0.074	268	3.00	1.31	**2**	247	2.95	1.33	**2**	286	3.15	1.53	**2**	268	3.12	1.57	**2**	312	3.31	1.84	**2**	300	3.32	1.95	**2**
System 33 T_P = 4.86 sec μ_{ref} = 0.075	277	3.25	1.30	**2**	256	3.21	1.35	**2**	295	3.43	1.50	**2**	277	3.41	1.57	**2**	322	3.65	1.80	**2**	310	3.67	1.92	**2**
System 43 T_P = 5.57 sec μ_{ref} = 0.076	285	3.45	1.30	**2**	264	3.41	1.35	**2**	304	3.68	1.51	**2**	283	3.64	1.57	**2**	330	3.93	1.80	**2**	315	3.95	1.93	**2**
System 14 T_P = 3.40 sec μ_{ref} = 0.087	241	2.56	1.37	**2**	214	2.50	1.39	**2**	258	2.68	1.64	**2**	229	2.63	1.67	**2**	283	2.82	2.05	**2**	258	2.80	2.15	**2**
System 24 T_P = 4.13 sec μ_{ref} = 0.091	253	2.84	1.39	**2**	228	2.76	1.39	**2**	269	3.01	1.65	**2**	248	2.97	1.69	**2**	292	3.19	2.00	**2**	279	3.20	2.13	**2**
System 34 T_P = 4.86 sec μ_{ref} = 0.094	262	3.07	1.40	**2**	238	2.99	1.42	**2**	278	3.26	1.64	**2**	257	3.22	1.70	**2**	302	3.49	1.98	**2**	288	3.51	2.12	**2**
System 44 T_P = 5.57 sec μ_{ref} = 0.095	270	3.26	1.43	**2**	248	3.17	1.43	**2**	287	3.48	1.65	**2**	266	3.42	1.69	**2**	311	3.76	2.00	**2**	295	3.77	2.14	**2**

μ_{ref} is the starting value of the ratio of zero-displacement force intercept and weight prior to any heating effects, Factor=friction coefficient reduction factor

Table 5-5 Average Resultant Isolator Displacements, Effective Periods, Reduction Factors and Required Number of Test Cycles for Triple FP Systems Computed when S_{M1} = 0.9g

	k_T = 2/3 at 200°C								k_T = 1/2 at 200°C								k_T = 1/3 at 200°C							
	Short-duration				Long-duration				Short-duration				Long-duration				Short-duration				Long-duration			
	D_M (mm)	T_M (sec)	Factor	Cycles	D_M (mm)	T_M (sec)	Factor	Cycles	D_M (mm)	T_M (sec)	Factor	Cycles	D_M (mm)	T_M (sec)	Factor	Cycles	D_M (mm)	T_M (sec)	Factor	Cycles	D_M (mm)	T_M (sec)	Factor	Cycles
System 11 T_P = 3.40 sec μ_{ref} = 0.037	510	3.14	1.23	**3**	462	3.12	1.28	**4**	543	3.18	1.45	**3**	498	3.17	1.52	**5**	580	3.22	1.70	**3**	546	3.22	1.85	**5**
System 21 T_P = 4.13 sec μ_{ref} = 0.038	532	3.69	1.19	**2**	515	3.69	1.24	**4**	567	3.76	1.40	**3**	556	3.77	1.46	**4**	604	3.81	1.58	**3**	605	3.84	1.74	**5**
System 31 T_P = 4.86 sec μ_{ref} = 0.038	543	4.17	1.17	**2**	541	4.19	1.23	**4**	579	4.27	1.34	**3**	586	4.30	1.42	**4**	615	4.36	1.53	**3**	637	4.41	1.69	**5**
System 41 T_P = 5.57 sec μ_{ref} = 0.039	570	4.62	1.16	**2**	559	4.64	1.22	**4**	612	4.75	1.33	**3**	608	4.78	1.41	**4**	650	4.86	1.49	**3**	667	4.92	1.62	**4**
System 12 T_P = 3.40 sec μ_{ref} = 0.054	428	3.00	1.30	**2**	390	2.98	1.35	**3**	467	3.08	1.56	**3**	428	3.07	1.64	**4**	517	3.15	1.92	**3**	477	3.15	2.08	**4**
System 22 T_P = 4.13 sec μ_{ref} = 0.056	444	3.46	1.27	**2**	422	3.46	1.32	**3**	482	3.58	1.49	**3**	467	3.59	1.58	**4**	530	3.68	1.78	**3**	521	3.70	1.92	**4**
System 32 T_P = 4.86 sec μ_{ref} = 0.057	453	3.85	1.25	**2**	438	3.86	1.31	**3**	488	4.01	1.48	**3**	484	4.03	1.55	**3**	530	4.14	1.71	**3**	545	4.21	1.89	**4**
System 42 T_P = 5.57 sec μ_{ref} = 0.058	466	4.17	1.23	**2**	444	4.17	1.29	**3**	501	4.37	1.44	**2**	492	4.40	1.52	**3**	551	4.56	1.66	**2**	555	4.62	1.80	**3**
System 13 T_P = 3.40 sec μ_{ref} = 0.070	379	2.87	1.36	**2**	347	2.85	1.42	**3**	414	2.97	1.62	**2**	381	2.96	1.71	**3**	468	3.08	2.07	**3**	432	3.07	2.21	**4**
System 23 T_P = 4.13 sec μ_{ref} = 0.074	391	3.27	1.34	**2**	374	3.27	1.41	**3**	427	3.41	1.58	**2**	410	3.42	1.68	**3**	477	3.56	1.95	**3**	468	3.58	2.09	**3**
System 33 T_P = 4.86 sec μ_{ref} = 0.075	404	3.59	1.32	**2**	386	3.59	1.39	**3**	434	3.76	1.53	**2**	425	3.80	1.65	**3**	480	3.96	1.85	**2**	482	4.02	2.04	**3**
System 43 T_P = 5.57 sec μ_{ref} = 0.076	414	3.86	1.32	**2**	393	3.86	1.40	**3**	443	4.05	1.50	**2**	429	4.09	1.63	**3**	488	4.29	1.78	**2**	487	4.38	1.99	**3**
System 14 T_P = 3.40 sec μ_{ref} = 0.087	353	2.77	1.43	**2**	320	2.75	1.51	**3**	383	2.88	1.73	**2**	350	2.87	1.83	**3**	431	3.01	2.19	**3**	399	3.00	2.34	**3**
System 24 T_P = 4.13 sec μ_{ref} = 0.091	365	3.12	1.42	**2**	345	3.12	1.51	**3**	394	3.28	1.70	**2**	376	3.28	1.80	**3**	443	3.47	2.13	**3**	429	3.47	2.24	**3**
System 34 T_P = 4.86 sec μ_{ref} = 0.094	377	3.39	1.40	**2**	355	3.40	1.50	**3**	405	3.59	1.66	**2**	387	3.60	1.76	**3**	446	3.82	2.03	**2**	444	3.88	2.21	**3**
System 44 T_P = 5.57 sec μ_{ref} = 0.095	386	3.61	1.39	**2**	364	3.63	1.50	**3**	416	3.87	1.67	**2**	392	3.86	1.75	**3**	454	4.11	1.97	**2**	448	4.19	2.18	**3**

μ_{ref} is the starting value of the coefficient of friction prior to any heating effects, Factor=friction coefficient reduction factor

Table 5-6 Average Resultant Isolator Displacements, Effective Periods, Reduction Factors and Required Number of Test Cycles for Triple FP Systems Computed when S_{M1} = 1.1g

	k_T = 2/3 at 200°C								k_T = 1/2 at 200°C								k_T = 1/3 at 200°C							
	Short-duration				Long-duration				Short-duration				Long-duration				Short-duration				Long-duration			
	D_M (mm)	T_M (sec)	Factor	Cycles	D_M (mm)	T_M (sec)	Factor	Cycles	D_M (mm)	T_M (sec)	Factor	Cycles	D_M (mm)	T_M (sec)	Factor	Cycles	D_M (mm)	T_M (sec)	Factor	Cycles	D_M (mm)	T_M (sec)	Factor	Cycles
System 11 T_P = 3.40 sec μ_{ref} = 0.037	685	3.20	1.24	**3**	631	3.20	1.33	**6**	725	3.23	1.45	**4**	678	3.23	1.57	**6**	768	3.26	1.71	**4**	739	3.27	1.91	**6**
System 21 T_P = 4.13 sec μ_{ref} = 0.038	718	3.79	1.19	**3**	708	3.80	1.27	**5**	757	3.84	1.38	**3**	759	3.86	1.49	**5**	798	3.88	1.56	**3**	818	3.91	1.79	**6**
System 31 T_P = 4.86 sec μ_{ref} = 0.038	737	4.32	1.17	**2**	750	4.36	1.26	**5**	780	4.40	1.34	**3**	804	4.45	1.47	**5**	824	4.47	1.52	**3**	872	4.52	1.73	**6**
System 41 T_P = 5.57 sec μ_{ref} = 0.039	782	4.82	1.16	**2**	784	4.86	1.23	**4**	836	4.94	1.33	**3**	847	4.98	1.43	**5**	884	5.01	1.48	**3**	921	5.08	1.65	**5**
System 12 T_P = 3.40 sec μ_{ref} = 0.054	590	3.10	1.33	**3**	540	3.09	1.39	**4**	640	3.16	1.60	**4**	592	3.16	1.71	**5**	693	3.21	1.94	**4**	659	3.22	2.18	**6**
System 22 T_P = 4.13 sec μ_{ref} = 0.056	611	3.62	1.29	**3**	592	3.62	1.35	**4**	659	3.71	1.51	**3**	650	3.73	1.63	**5**	715	3.78	1.77	**3**	724	3.82	2.00	**5**
System 32 T_P = 4.86 sec μ_{ref} = 0.057	621	4.06	1.26	**2**	616	4.09	1.33	**4**	666	4.18	1.44	**2**	681	4.24	1.60	**5**	721	4.29	1.68	**3**	758	4.38	1.94	**5**
System 42 T_P = 5.57 sec μ_{ref} = 0.058	645	4.47	1.25	**2**	626	4.48	1.31	**4**	697	4.62	1.42	**2**	701	4.69	1.57	**5**	758	4.77	1.65	**3**	789	4.88	1.89	**5**
System 13 T_P = 3.40 sec μ_{ref} = 0.070	525	3.00	1.38	**3**	483	2.99	1.48	**4**	578	3.09	1.70	**3**	534	3.08	1.81	**4**	643	3.16	2.12	**3**	604	3.17	2.39	**5**
System 23 T_P = 4.13 sec μ_{ref} = 0.074	542	3.46	1.36	**3**	520	3.46	1.43	**4**	593	3.58	1.63	**3**	580	3.60	1.74	**4**	655	3.70	1.98	**3**	656	3.73	2.17	**4**
System 33 T_P = 4.86 sec μ_{ref} = 0.075	551	3.83	1.33	**2**	537	3.86	1.41	**4**	597	3.99	1.55	**2**	599	4.05	1.70	**4**	653	4.15	1.85	**3**	684	4.24	2.12	**4**
System 43 T_P = 5.57 sec μ_{ref} = 0.076	567	4.16	1.32	**2**	544	4.18	1.41	**4**	612	4.34	1.51	**2**	607	4.42	1.67	**4**	676	4.56	1.79	**2**	699	4.68	2.07	**4**
System 14 T_P = 3.40 sec μ_{ref} = 0.087	480	2.91	1.47	**3**	444	2.91	1.59	**4**	528	3.01	1.79	**3**	490	3.01	1.92	**4**	603	3.12	2.29	**3**	564	3.13	2.58	**5**
System 24 T_P = 4.13 sec μ_{ref} = 0.091	495	3.32	1.45	**3**	476	3.34	1.55	**4**	541	3.46	1.71	**3**	526	3.49	1.86	**4**	612	3.62	2.16	**3**	608	3.66	2.38	**4**
System 34 T_P = 4.86 sec μ_{ref} = 0.094	508	3.64	1.40	**2**	490	3.68	1.52	**4**	549	3.83	1.66	**2**	542	3.88	1.82	**4**	609	4.03	2.02	**3**	629	4.12	2.29	**4**
System 44 T_P = 5.57 sec μ_{ref} = 0.095	519	3.91	1.39	**2**	498	3.96	1.52	**4**	557	4.13	1.62	**2**	547	4.19	1.78	**4**	622	4.39	1.96	**2**	637	4.51	2.23	**4**

μ_{ref} is the starting value of the coefficient of friction prior to any heating effects, Factor=friction coefficient reduction factor

Table 5-7 Average Resultant Isolator Displacements, Effective Periods, Reduction Factors and Required Number of Test Cycles for Additional Triple FP System LL

	S_{M1} = 0.7g							
	Short-duration				Long-duration			
	D_M (mm)	T_M (sec)	Factor	Cycles	D_M (mm)	T_M (sec)	Factor	Cycles
k_T = 2/3 at 200°C	301	3.49	1.30	**2**	272	3.40	1.31	**2**
k_T = 1/2 at 200°C	319	3.71	1.52	**2**	288	3.61	1.53	**2**
k_T = 1/3 at 200°C	346	3.99	1.87	**2**	317	3.91	1.88	**2**

T_P = 5.49 sec, μ_{ref} = 0.074, μ_{1ref} = 0.08
μ_{ref} is the starting value of the ratio of zero-displacement force intercept and weight prior to any heating effects, Factor=friction coefficient reduction factor

	S_{M1} = 0.9g							
	Short-duration				Long-duration			
	D_M (mm)	T_M (sec)	Factor	Cycles	D_M (mm)	T_M (sec)	Factor	Cycles
k_T = 2/3 at 200°C	439	3.92	1.36	**2**	402	3.85	1.38	**2**
k_T = 1/2 at 200°C	470	4.12	1.59	**2**	437	4.07	1.61	**2**
k_T = 1/3 at 200°C	528	4.41	1.99	**2**	497	4.36	1.99	**2**

T_P = 5.49 sec, μ_{ref} = 0.074, μ_{1ref} = 0.08
μ_{ref} is the starting value of the ratio of zero-displacement force intercept and weight prior to any heating effects, Factor=friction coefficient reduction factor

	S_{M1} = 1.1g							
	Short-duration				Long-duration			
	D_M (mm)	T_M (sec)	Factor	Cycles	D_M (mm)	T_M (sec)	Factor	Cycles
k_T = 2/3 at 200°C	598	4.24	1.42	**2**	564	4.19	1.42	**2**
k_T = 1/2 at 200°C	666	4.48	1.72	**2**	632	4.44	1.72	**2**
k_T = 1/3 at 200°C	749	4.71	2.16	**2**	741	4.72	2.21	**2**

T_P = 5.49 sec, μ_{ref} = 0.074, μ_{1ref} = 0.08
μ_{ref} is the starting value of the ratio of zero-displacement force intercept and weight prior to any heating effects, Factor=friction coefficient reduction factor

Table 5-8 Average Resultant Isolator Displacements, Effective Periods, Reduction Factors and Required Number of Test Cycles for Lead-rubber Systems Computed when S_{M1} = 0.7g

		Short-duration				Long-duration			
		D_M (mm)	T_M (sec)	Factor	Cycles	D_M (mm)	T_M (sec)	Factor	Cycles
a/h_L =0.3	**System 111** (T_d = 2 sec, $(Q_d/W)_{ref}$ = 0.08)	180	1.73	1.30	**2**	170	1.77	1.70	**5**
	System 211 (T_d = 3 sec, $(Q_d/W)_{ref}$ = 0.08)	223	2.36	1.30	**2**	221	2.47	1.70	**4**
	System 311 (T_d = 4 sec, $(Q_d/W)_{ref}$ = 0.08)	251	2.84	1.30	**2**	271	3.07	1.70	**4**
	System 121 (T_d = 2 sec, $(Q_d/W)_{ref}$ = 0.16)	121	1.35	1.10	**2**	108	1.37	1.30	**5**
	System 221 (T_d = 3 sec, $(Q_d/W)_{ref}$ = 0.16)	137	1.63	1.10	**2**	130	1.70	1.30	**4**
	System 321 (T_d = 4 sec, $(Q_d/W)_{ref}$ = 0.16)	151	1.82	1.10	**1**	149	1.93	1.30	**4**
	System 131 (T_d = 2 sec, $(Q_d/W)_{ref}$ = 0.24)	91	1.07	1.05	**2**	79	1.03	1.10	**3**
	System 231 (T_d = 3 sec, $(Q_d/W)_{ref}$ = 0.24)	105	1.24	1.05	**1**	96	1.21	1.10	**3**
	System 331 (T_d = 4 sec, $(Q_d/W)_{ref}$ = 0.24)	109	1.31	1.05	**1**	105	1.31	1.10	**2**
a/h_L =0.6	**System 112** (T_d = 2 sec, $(Q_d/W)_{ref}$ = 0.08)	200	1.80	1.70	**3**	199	1.85	2.40	**5**
	System 212 (T_d = 3 sec, $(Q_d/W)_{ref}$ = 0.08)	258	2.53	1.70	**2**	258	2.64	2.40	**4**
	System 312 (T_d = 4 sec, $(Q_d/W)_{ref}$ = 0.08)	293	3.12	1.70	**2**	325	3.37	2.40	**3**
	System 122 (T_d = 2 sec, $(Q_d/W)_{ref}$ = 0.16)	128	1.43	1.30	**2**	120	1.46	1.50	**4**
	System 222 (T_d = 3 sec, $(Q_d/W)_{ref}$ = 0.16)	150	1.78	1.30	**2**	146	1.85	1.50	**3**
	System 322 (T_d = 4 sec, $(Q_d/W)_{ref}$ = 0.16)	162	2.00	1.30	**2**	170	2.14	1.50	**3**
	System 132 (T_d = 2 sec, $(Q_d/W)_{ref}$ = 0.24)	94	1.10	1.10	**2**	87	1.13	1.30	**4**
	System 232 (T_d = 3 sec, $(Q_d/W)_{ref}$ = 0.24)	108	1.27	1.10	**1**	105	1.35	1.30	**3**
	System 332 (T_d = 4 sec, $(Q_d/W)_{ref}$ = 0.24)	114	1.36	1.10	**1**	116	1.47	1.30	**3**

$(Q_d/W)_{ref}$ is the starting value of the characteristic strength divided by weight prior to any heating effects, Factor=strength reduction factor

Table 5-9 Average Resultant Isolator Displacements, Effective Periods, Reduction Factors and Required Number of Test Cycles for Lead-rubber Systems Computed when S_{M1} = 0.9g

		Short-duration				Long-duration			
		D_M (mm)	T_M (sec)	Factor	Cycles	D_M (mm)	T_M (sec)	Factor	Cycles
a/h_L =0.3	**System 111** (T_d = 2 sec, $(Q_d/W)_{ref}$ = 0.08)	272	1.85	1.80	**4**	268	1.88	2.20	**6**
	System 211 (T_d = 3 sec, $(Q_d/W)_{ref}$ = 0.08)	357	2.65	1.80	**3**	347	2.70	2.20	**5**
	System 311 (T_d = 4 sec, $(Q_d/W)_{ref}$ = 0.08)	404	3.33	1.80	**3**	435	3.46	2.20	**4**
	System 121 (T_d = 2 sec, $(Q_d/W)_{ref}$ = 0.16)	175	1.51	1.20	**2**	163	1.56	1.50	**5**
	System 221 (T_d = 3 sec, $(Q_d/W)_{ref}$ = 0.16)	208	1.92	1.20	**2**	202	2.03	1.50	**4**
	System 321 (T_d = 4 sec, $(Q_d/W)_{ref}$ = 0.16)	227	2.19	1.20	**2**	241	2.41	1.50	**4**
	System 131 (T_d = 2 sec, $(Q_d/W)_{ref}$ = 0.24)	135	1.24	1.10	**2**	121	1.23	1.20	**4**
	System 231 (T_d = 3 sec, $(Q_d/W)_{ref}$ = 0.24)	157	1.48	1.10	**2**	145	1.48	1.20	**3**
	System 331 (T_d = 4 sec, $(Q_d/W)_{ref}$ = 0.24)	168	1.61	1.10	**2**	161	1.64	1.20	**3**
a/h_L =0.6	**System 112** (T_d = 2 sec, $(Q_d/W)_{ref}$ = 0.08)	313	1.91	2.60	**4**	325	1.93	3.20	**5**
	System 212 (T_d = 3 sec, $(Q_d/W)_{ref}$ = 0.08)	435	2.79	2.60	**3**	419	2.82	3.20	**4**
	System 312 (T_d = 4 sec, $(Q_d/W)_{ref}$ = 0.08)	490	3.57	2.60	**3**	529	3.67	3.20	**3**
	System 122 (T_d = 2 sec, $(Q_d/W)_{ref}$ = 0.16)	195	1.63	1.60	**3**	192	1.68	2.00	**5**
	System 222 (T_d = 3 sec, $(Q_d/W)_{ref}$ = 0.16)	236	2.15	1.60	**2**	247	2.29	2.00	**4**
	System 322 (T_d = 4 sec, $(Q_d/W)_{ref}$ = 0.16)	267	2.54	1.60	**2**	307	2.80	2.00	**3**
	System 132 (T_d = 2 sec, $(Q_d/W)_{ref}$ = 0.24)	143	1.29	1.20	**2**	140	1.39	1.60	**5**
	System 232 (T_d = 3 sec, $(Q_d/W)_{ref}$ = 0.24)	169	1.57	1.20	**2**	171	1.74	1.60	**4**
	System 332 (T_d = 4 sec, $(Q_d/W)_{ref}$ = 0.24)	185	1.73	1.20	**2**	194	1.98	1.60	**3**

$(Q_d/W)_{ref}$ is the starting value of the characteristic strength divided by weight prior to any heating effects, Factor=strength reduction factor

Table 5-10 Average Resultant Isolator Displacements, Effective Periods, Reduction Factors and Required Number of Test Cycles for Lead-rubber Systems Computed when S_{M1} = 1.1g

		Short-duration				Long-duration			
		D_M (mm)	T_M (sec)	Factor	Cycles	D_M (mm)	T_M (sec)	Factor	Cycles
a/h_L =0.3	**System 111** (T_d = 2 sec, $(Q_d/W)_{ref}$ = 0.08)	381	1.91	2.20	**4**	388	1.93	2.70	**6**
	System 211 (T_d = 3 sec, $(Q_d/W)_{ref}$ = 0.08)	527	2.79	2.20	**3**	501	2.82	2.70	**5**
	System 311 (T_d = 4 sec, $(Q_d/W)_{ref}$ = 0.08)	595	3.58	2.20	**3**	632	3.67	2.70	**4**
	System 121 (T_d = 2 sec, $(Q_d/W)_{ref}$ = 0.16)	244	1.63	1.30	**2**	235	1.69	1.70	**5**
	System 221 (T_d = 3 sec, $(Q_d/W)_{ref}$ = 0.16)	295	2.16	1.30	**2**	303	2.31	1.70	**4**
	System 321 (T_d = 4 sec, $(Q_d/W)_{ref}$ = 0.16)	332	2.54	1.30	**2**	372	2.82	1.70	**4**
	System 131 (T_d = 2 sec, $(Q_d/W)_{ref}$ = 0.24)	186	1.37	1.15	**2**	173	1.42	1.40	**5**
	System 231 (T_d = 3 sec, $(Q_d/W)_{ref}$ = 0.24)	219	1.69	1.15	**2**	213	1.79	1.40	**4**
	System 331 (T_d = 4 sec, $(Q_d/W)_{ref}$ = 0.24)	236	1.88	1.15	**2**	241	2.04	1.40	**4**
a/h_L =0.6	**System 112** (T_d = 2 sec, $(Q_d/W)_{ref}$ = 0.08)	427	1.94	3.10	**4**	461	1.96	4.60	**6**
	System 212 (T_d = 3 sec, $(Q_d/W)_{ref}$ = 0.08)	632	2.87	3.10	**3**	614	2.91	4.60	**5**
	System 312 (T_d = 4 sec, $(Q_d/W)_{ref}$ = 0.08)	707	3.73	3.10	**3**	785	3.83	4.60	**4**
	System 122 (T_d = 2 sec, $(Q_d/W)_{ref}$ = 0.16)	277	1.74	1.80	**3**	288	1.81	2.50	**5**
	System 222 (T_d = 3 sec, $(Q_d/W)_{ref}$ = 0.16)	354	2.40	1.80	**2**	374	2.55	2.50	**4**
	System 322 (T_d = 4 sec, $(Q_d/W)_{ref}$ = 0.16)	405	2.92	1.80	**2**	477	3.23	2.50	**3**
	System 132 (T_d = 2 sec, $(Q_d/W)_{ref}$ = 0.24)	201	1.44	1.30	**2**	202	1.57	1.90	**5**
	System 232 (T_d = 3 sec, $(Q_d/W)_{ref}$ = 0.24)	244	1.82	1.30	**2**	259	2.07	1.90	**4**
	System 332 (T_d = 4 sec, $(Q_d/W)_{ref}$ = 0.24)	258	2.03	1.30	**2**	314	2.48	1.90	**3**

$(Q_d/W)_{ref}$ is the starting value of the characteristic strength divided by weight prior to any heating effects, Factor=strength reduction factor

Table 5-11 Average Resultant Isolator Displacements, Effective Periods, Reduction Factors and Required Number of Test Cycles for Additional Lead-rubber Systems

	S_{M1} = 0.7g							
	Short-duration				Long-duration			
	D_M (mm)	T_M (sec)	Factor	Cycles	D_M (mm)	T_M (sec)	Factor	Cycles
System 4 (T_d = 4 sec, $(Q_d/W)_{ref}$ = 0.121)	190	2.31	1.26	**2**	201	2.52	1.57	**4**
System 5 (T_d = 3 sec, $(Q_d/W)_{ref}$ = 0.121)	172	1.99	1.24	**2**	169	2.09	1.50	**4**
System 6 (T_d = 2 sec, $(Q_d/W)_{ref}$ = 0.241)	90	1.06	1.05	**2**	79	1.04	1.12	**4**

	S_{M1} = 0.9g							
	Short-duration				Long-duration			
	D_M (mm)	T_M (sec)	Factor	Cycles	D_M (mm)	T_M (sec)	Factor	Cycles
System 4 (T_d = 4 sec, $(Q_d/W)_{ref}$ = 0.121)	300	2.73	1.40	**2**	341	3.08	2.07	**4**
System 5 (T_d = 3 sec, $(Q_d/W)_{ref}$ = 0.121)	267	2.28	1.40	**2**	272	2.42	1.87	**4**
System 6 (T_d = 2 sec, $(Q_d/W)_{ref}$ = 0.241)	132	1.22	1.07	**2**	119	1.23	1.22	**5**

	S_{M1} = 1.1g							
	Short-duration				Long-duration			
	D_M (mm)	T_M (sec)	Factor	Cycles	D_M (mm)	T_M (sec)	Factor	Cycles
System 4 (T_d = 4 sec, $(Q_d/W)_{ref}$ = 0.121)	445	3.13	1.71	**2**	506	3.40	2.48	**4**
System 5 (T_d = 3 sec, $(Q_d/W)_{ref}$ = 0.121)	391	2.52	1.66	**2**	399	2.63	2.25	**4**
System 6 (T_d = 2 sec, $(Q_d/W)_{ref}$ = 0.241)	184	1.36	1.12	**2**	166	1.39	1.33	**5**

$(Q_d/W)_{ref}$ is the starting value of the characteristic strength divided by weight prior to any heating effects, Factor=strength reduction factor

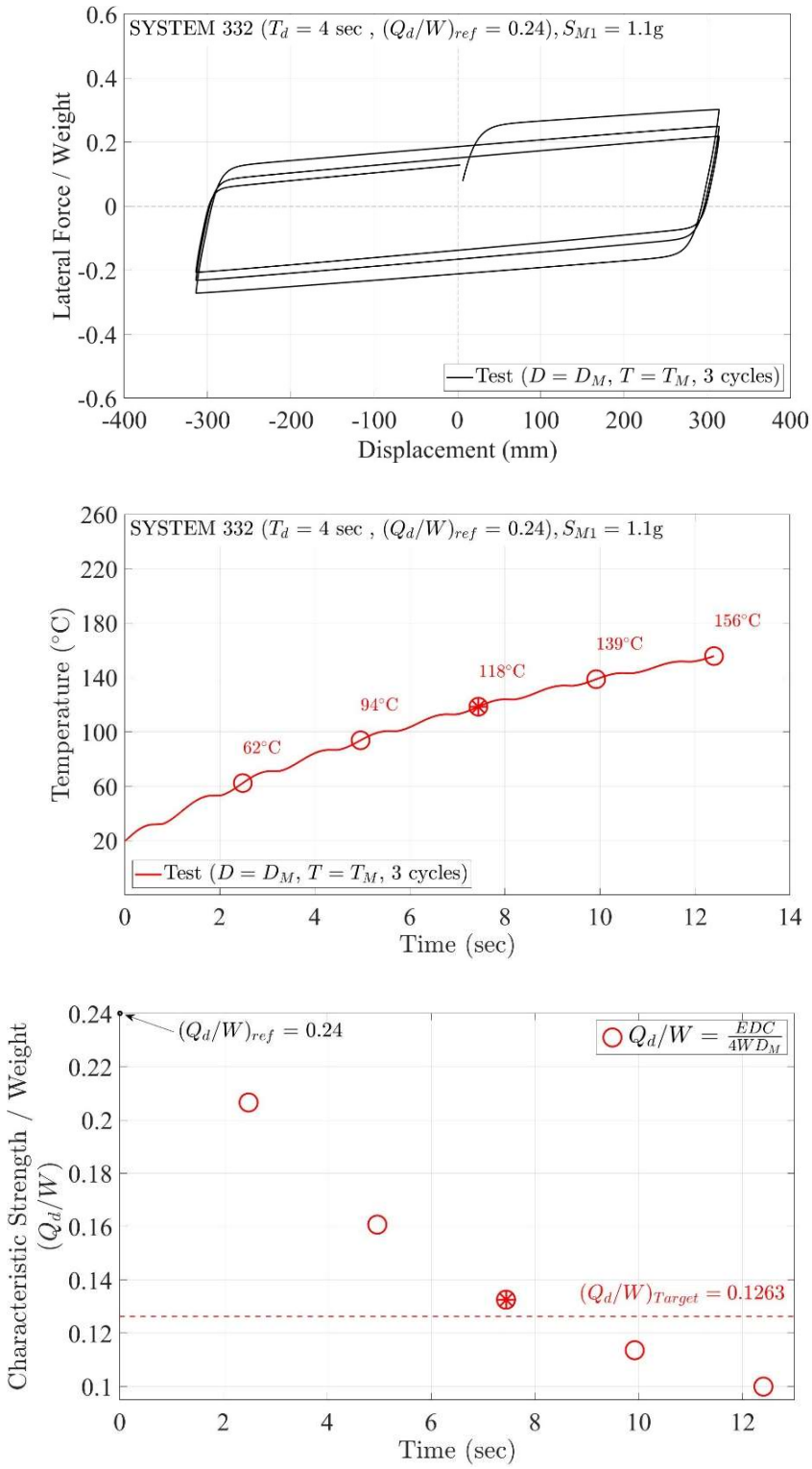

Figure 5-1 Computed Force-displacement Loop and Histories of Temperature in Lead Core and Characteristic Strength over Weight per Cycle of Lead-rubber System 332 in Test to Determine Number of Cycles for Lower Bound Properties in Long-duration Motions when S_{M1}=1.1g

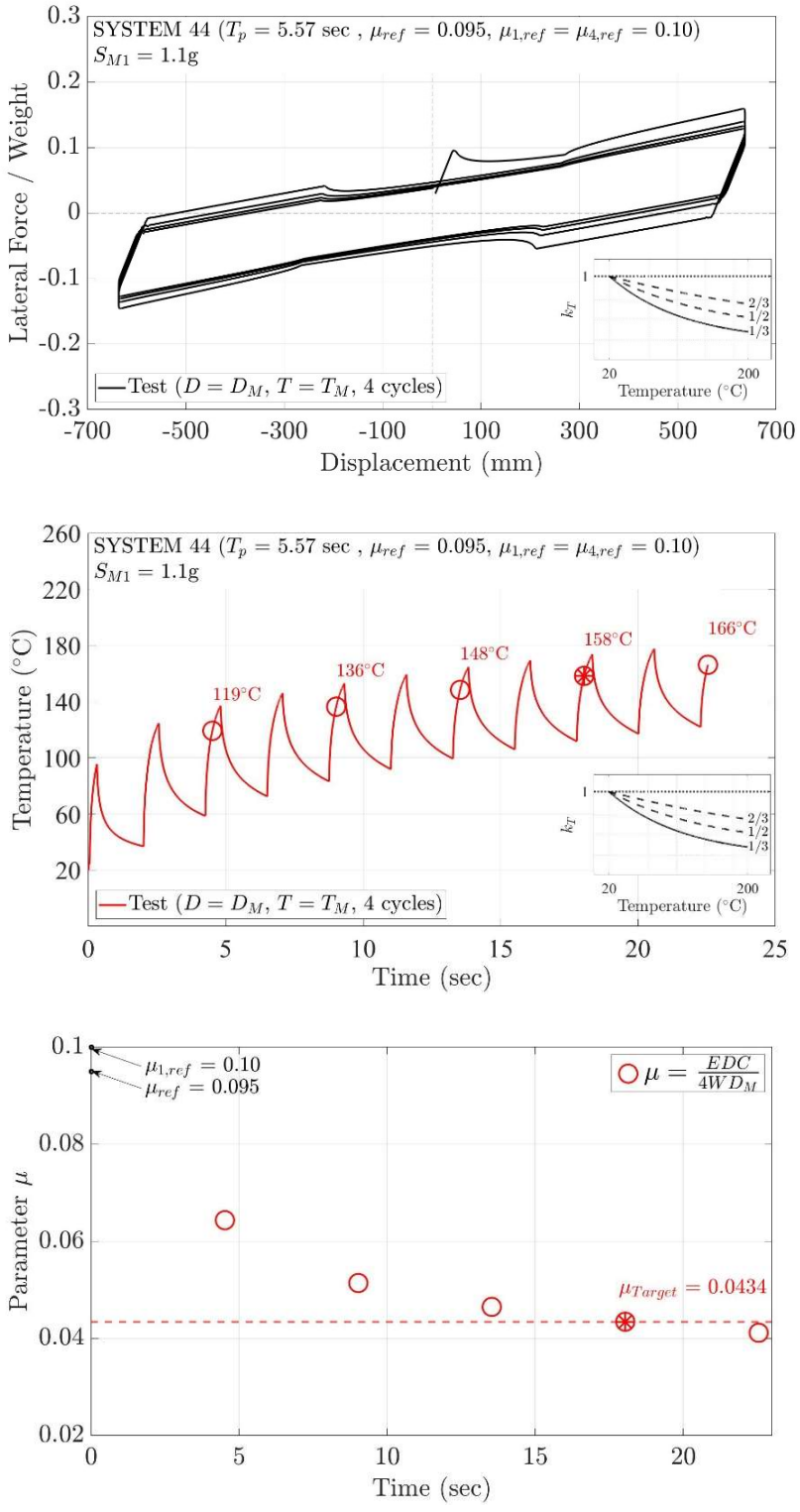

Figure 5-2 Computed Force-displacement Loop and Histories of Temperature at Sliding Interface and Parameter μ per Cycle of Triple FP System 44 in Test to Determine Number of Cycles for Lower Bound Properties in Long-duration Motions when S_{M1}=1.1g

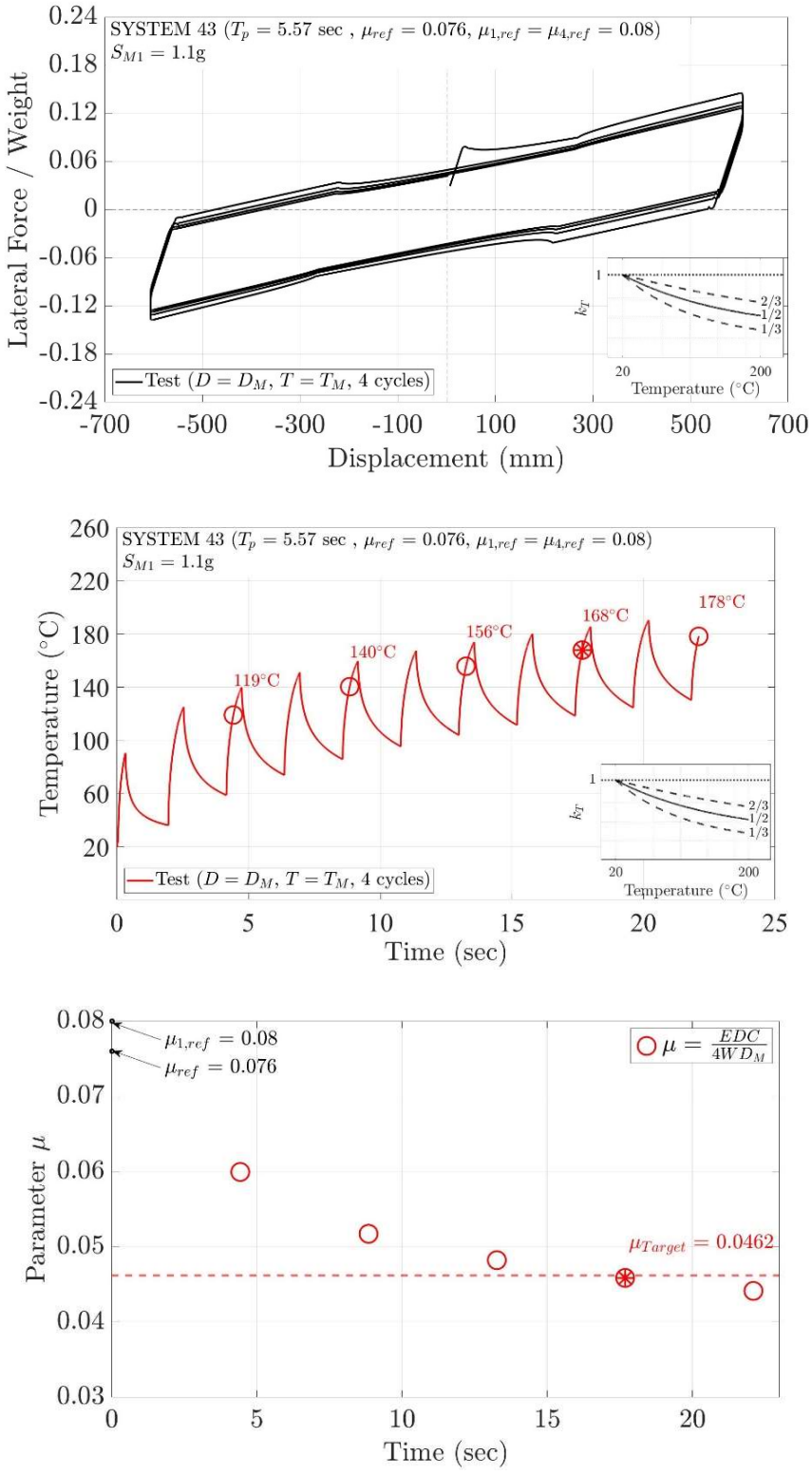

Figure 5-3 Computed Force-displacement Loop and Histories of Temperature at Sliding Interface and Parameter μ per Cycle of Triple FP System 43 in Test to Determine Number of Cycles for Lower Bound Properties in Long-duration Motions when S_{M1}=1.1g

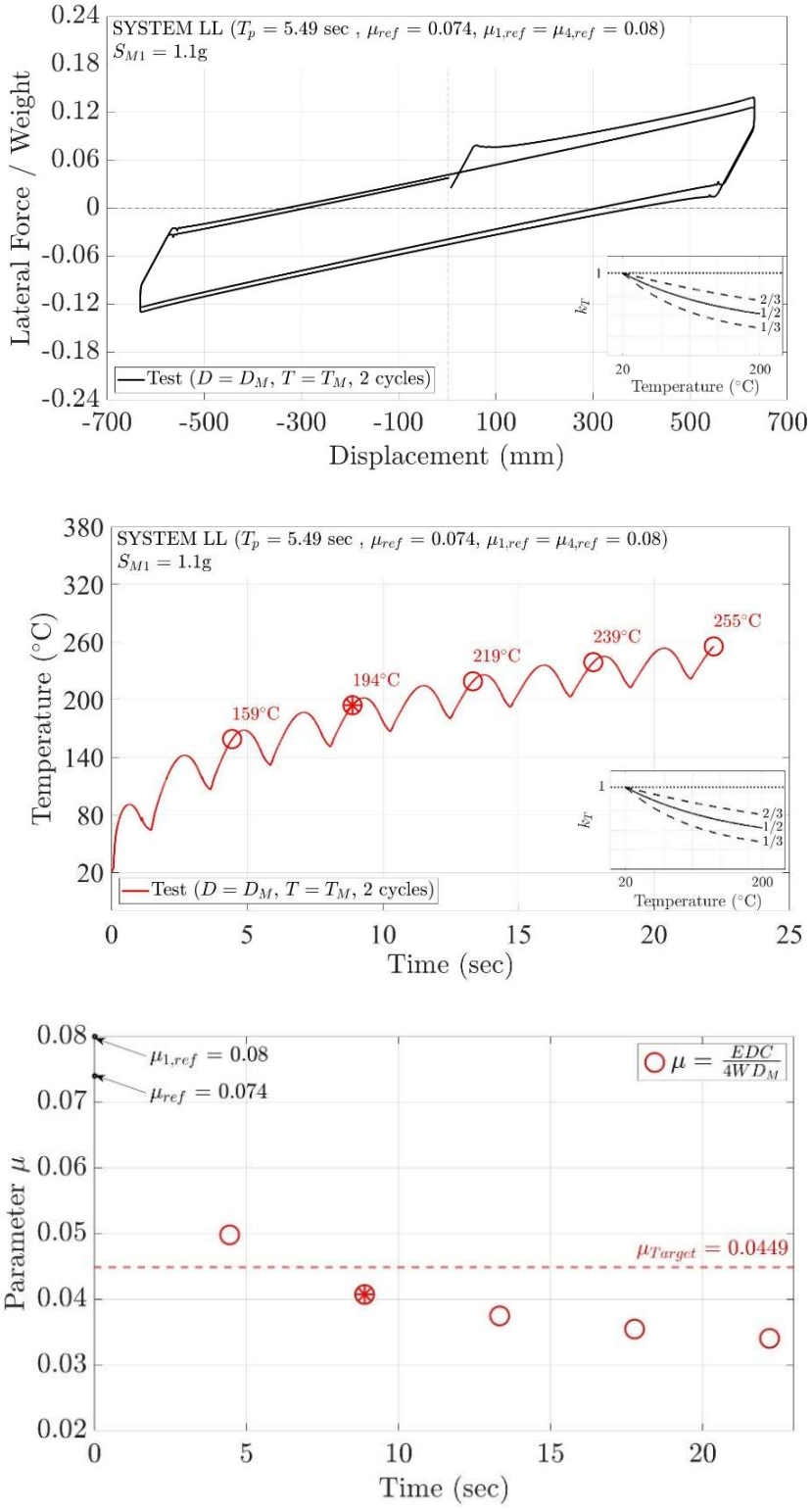

Figure 5-4 Computed Force-displacement Loop and Histories of Temperature at Sliding Interface and Parameter μ per Cycle of Triple FP System LL in Test to Determine Number of Cycles for Lower Bound Properties in Long-duration Motions when S_{M1}=1.1

5.2 Results for Required Number of Cycles to Obtain Lower Bound Properties

The procedure described in Section 5.1 was applied for the 288 cases (96 systems and three seismic intensities) considered in this work. Appendix C presents figures like Figures 5-1 and 5-4, and additional data, for each of these cases. Figures 5-5 to 5-13 present results on the required number of cycles for all cases when the ground motion duration is short, and Figures 5-14 to 5-22 present results on the required number of cycles for all cases when the ground motion duration is long. Note that each figure contains many data which overlap. For example, in Figure 5-5 there are 21 cases but only 7 data points appear as there is significant overlap of the data. Tables 5-1 to 5-11 include detailed information on the number of cycles for each of the 288 cases.

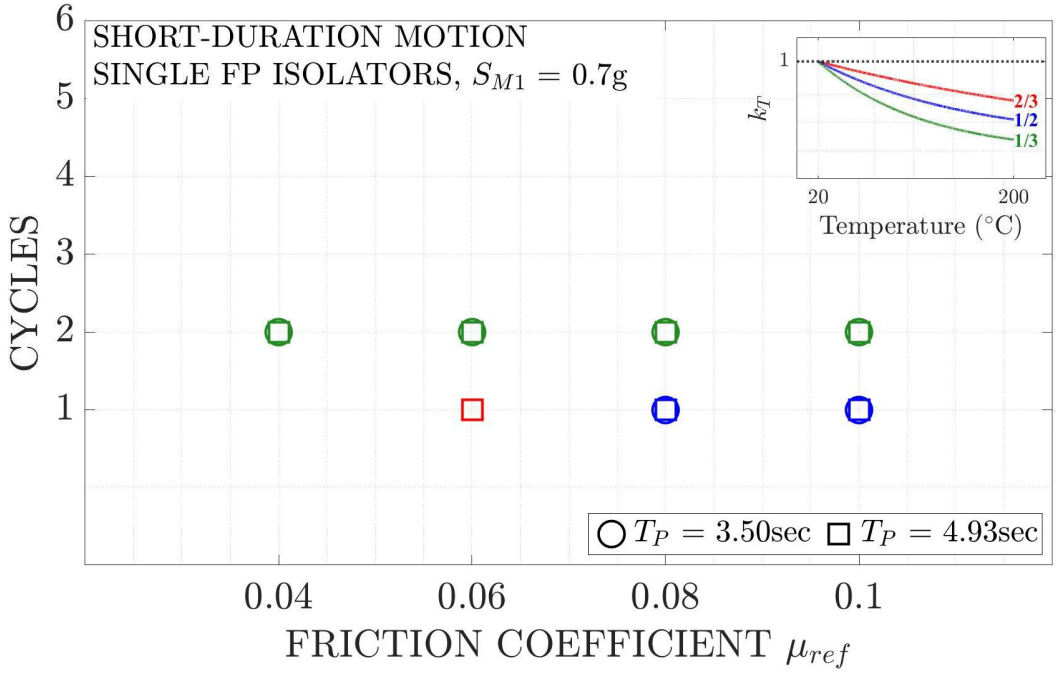

Figure 5-5 Required Number of Cycles for Lower Bound Test of Single FP Isolators in Short-duration Ground Motions with S_{M1}=0.7g

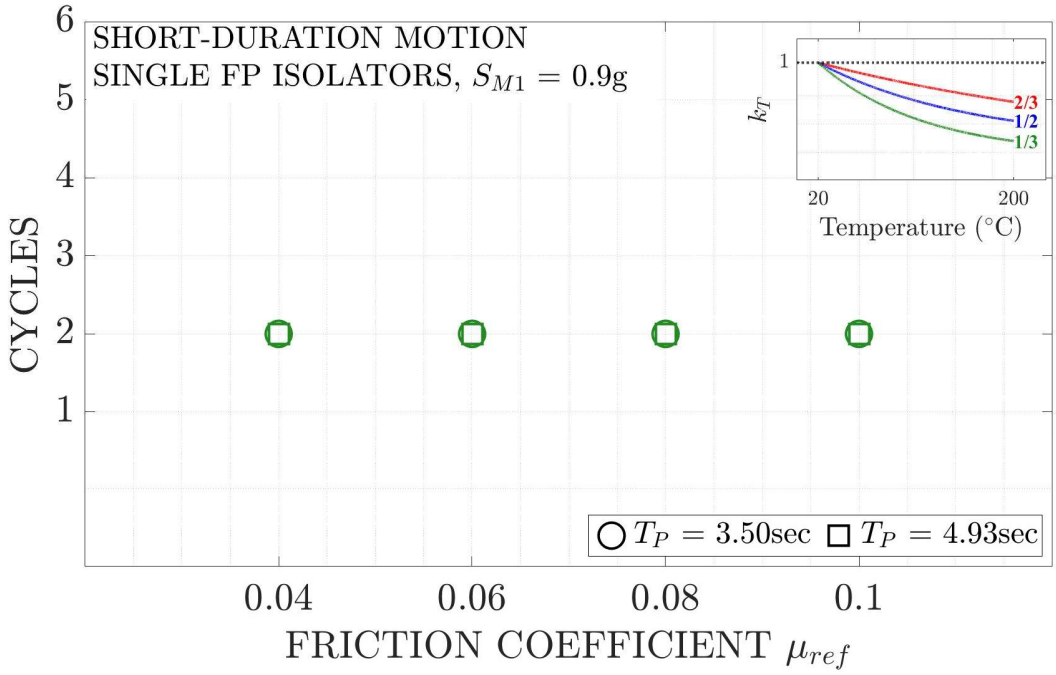

Figure 5-6 Required Number of Cycles for Lower Bound Test of Single FP Isolators in Short-duration Ground Motions with S_{M1}=0.9g

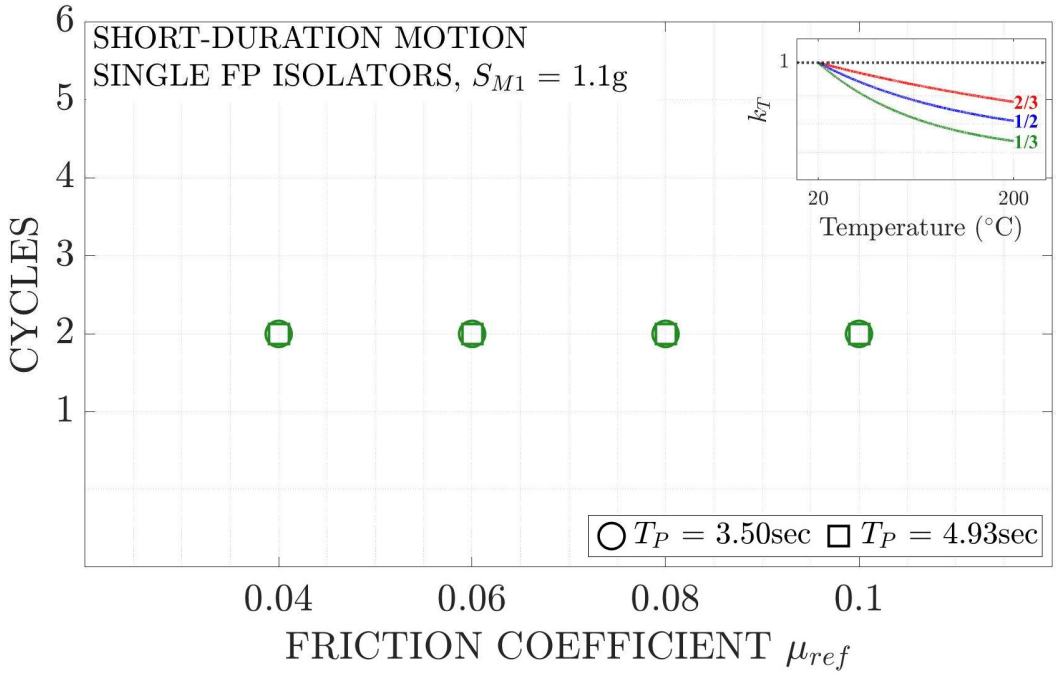

Figure 5-7 Required Number of Cycles for Lower Bound Test of Single FP Isolators in Short-duration Ground Motions with S_{M1}=1.1g

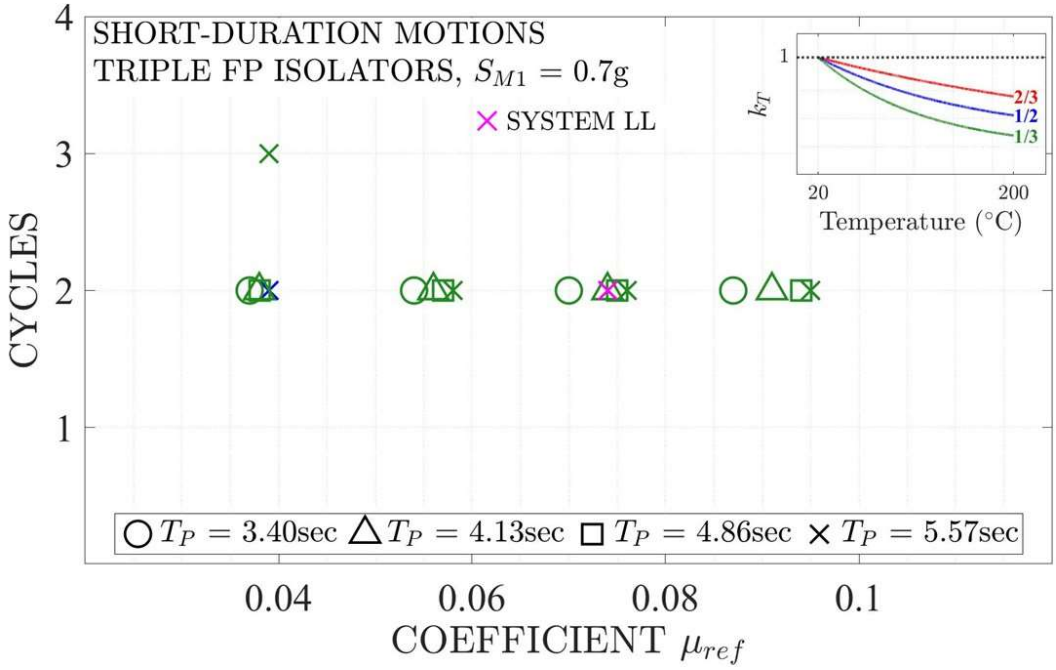

Figure 5-8 Required Number of Cycles for Lower Bound Test of Triple FP Isolators in Short-duration Ground Motions with S_{M1}=0.7g

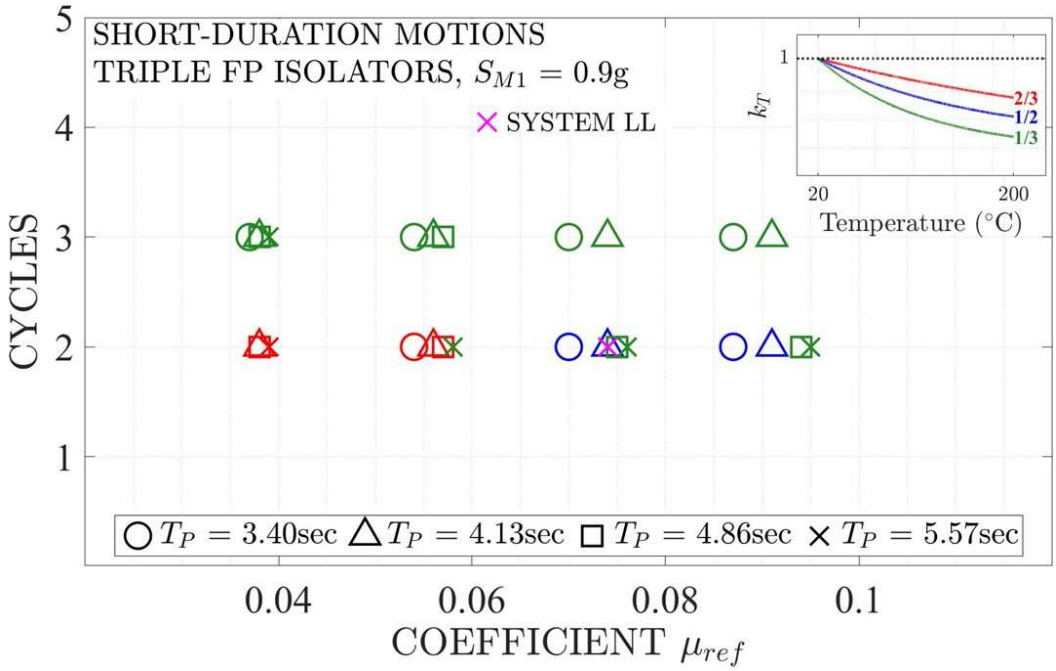

Figure 5-9 Required Number of Cycles for Lower Bound Test of Triple FP Isolators in Short-duration Ground Motions with S_{M1}=0.9g

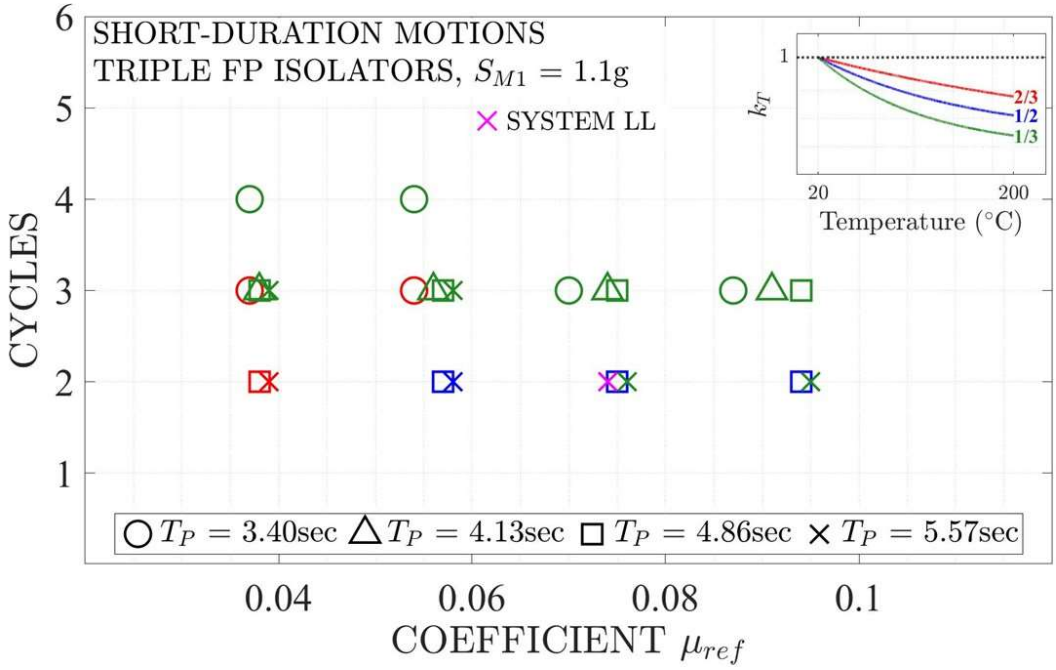

Figure 5-10 Required Number of Cycles for Lower Bound Test of Triple FP Isolators in Short-duration Ground Motions with S_{M1}=1.1g

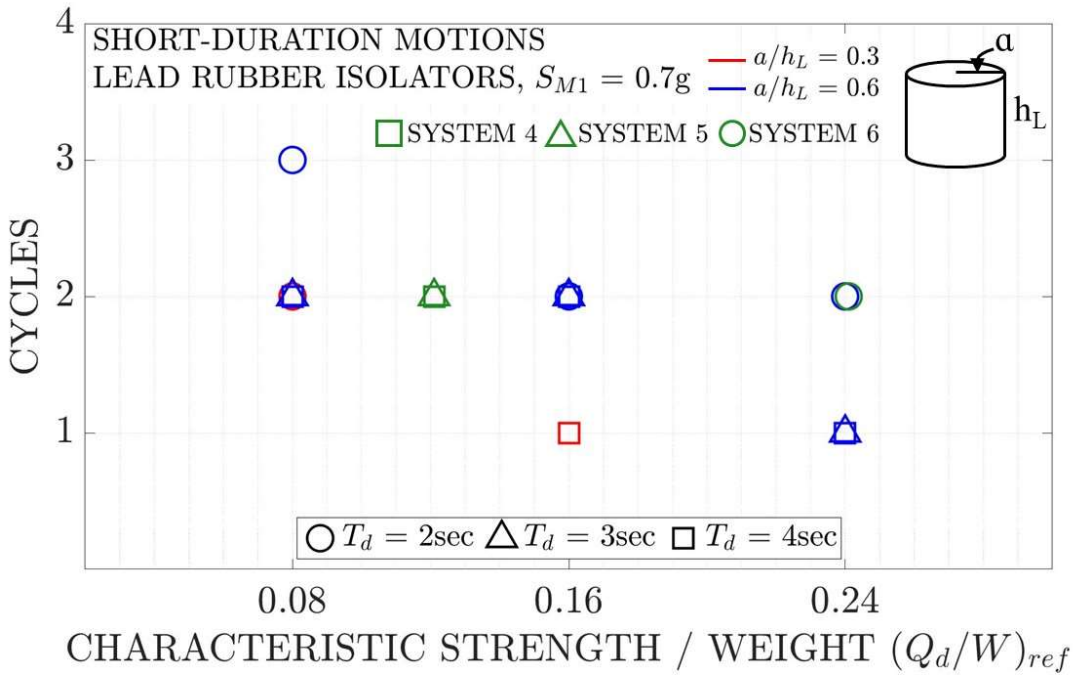

Figure 5-11 Required Number of Cycles for Lower Bound Test of Lead-rubber Isolators in Short-duration Ground Motions with S_{M1}=0.7g

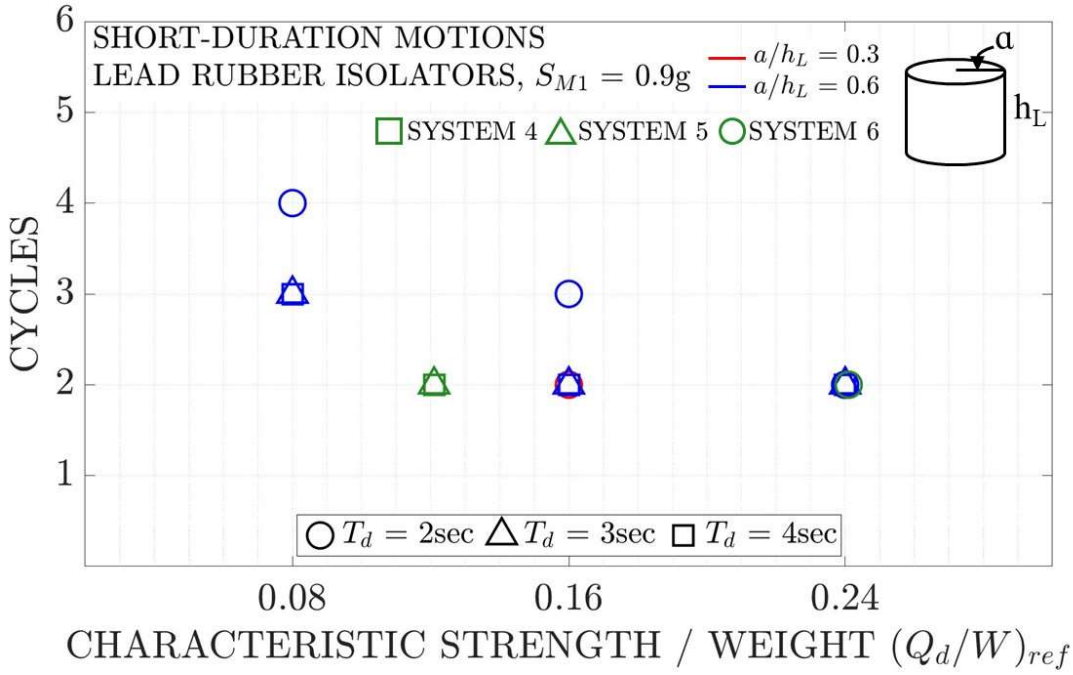

Figure 5-12 Required Number of Cycles for Lower Bound Test of Lead-rubber Isolators in Short-duration Ground Motions with S_{M1}=0.9g

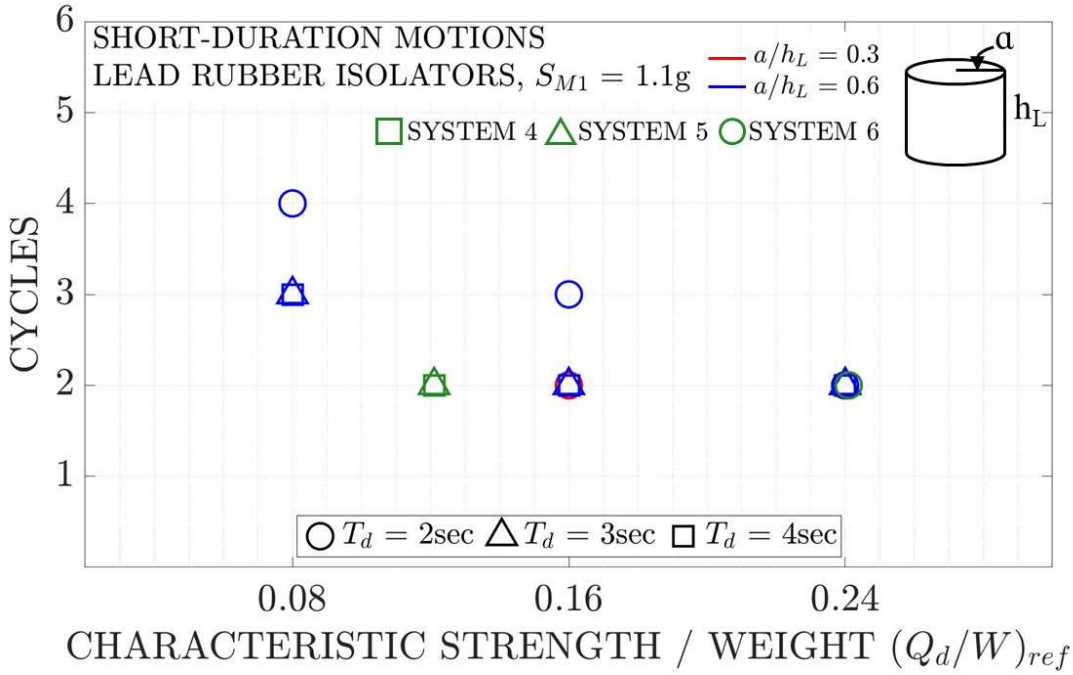

Figure 5-13 Required Number of Cycles for Lower Bound Test of Lead-rubber Isolators in Short-duration Ground Motions with S_{M1}=1.1g

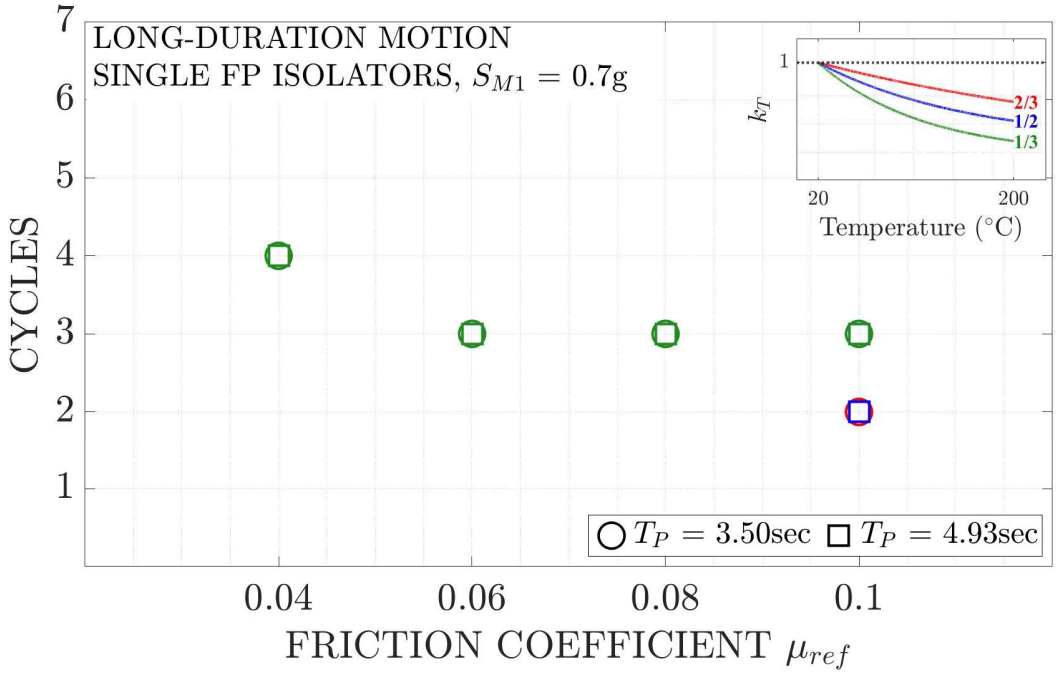

Figure 5-14 Required Number of Cycles for Lower Bound Test of Single FP Isolators in Long-duration Ground Motions with S_{M1}=0.7g

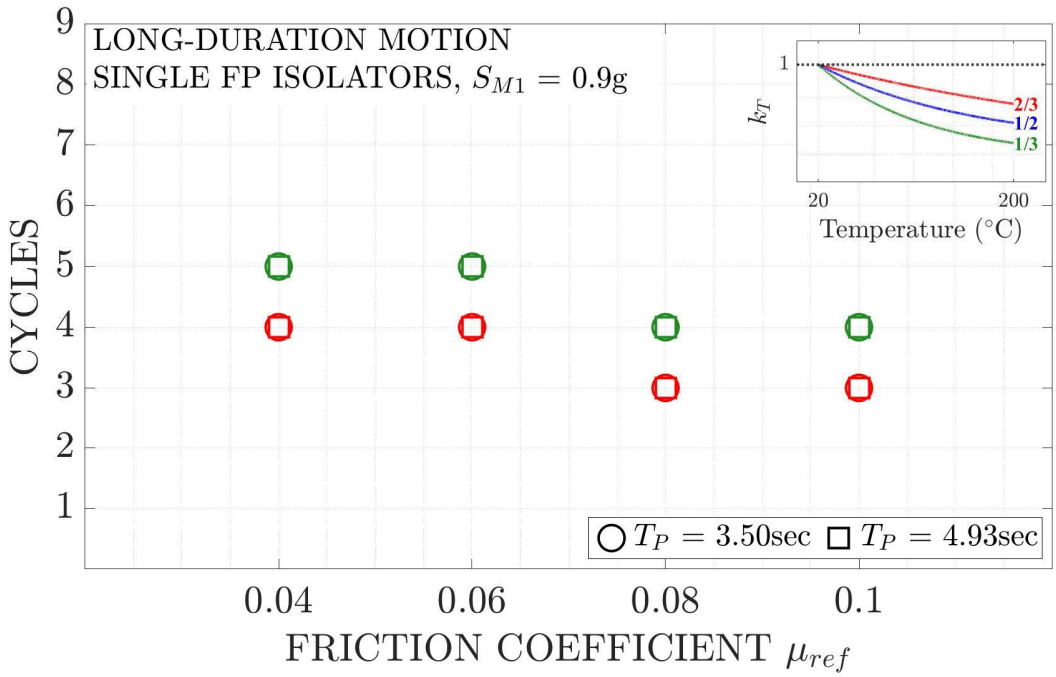

Figure 5-15 Required Number of Cycles for Lower Bound Test of Single FP Isolators in Long-duration Ground Motions with S_{M1}=0.9g

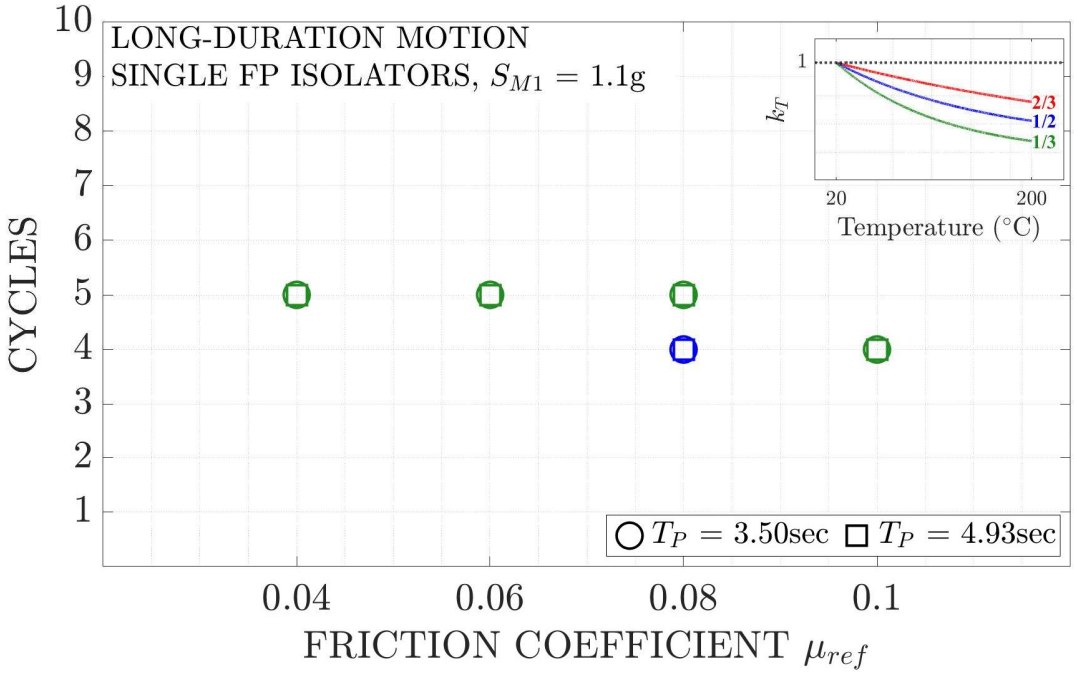

Figure 5-16 Required Number of Cycles for Lower Bound Test of Single FP Isolators in Long-duration Ground Motions with S_{M1}=1.1g

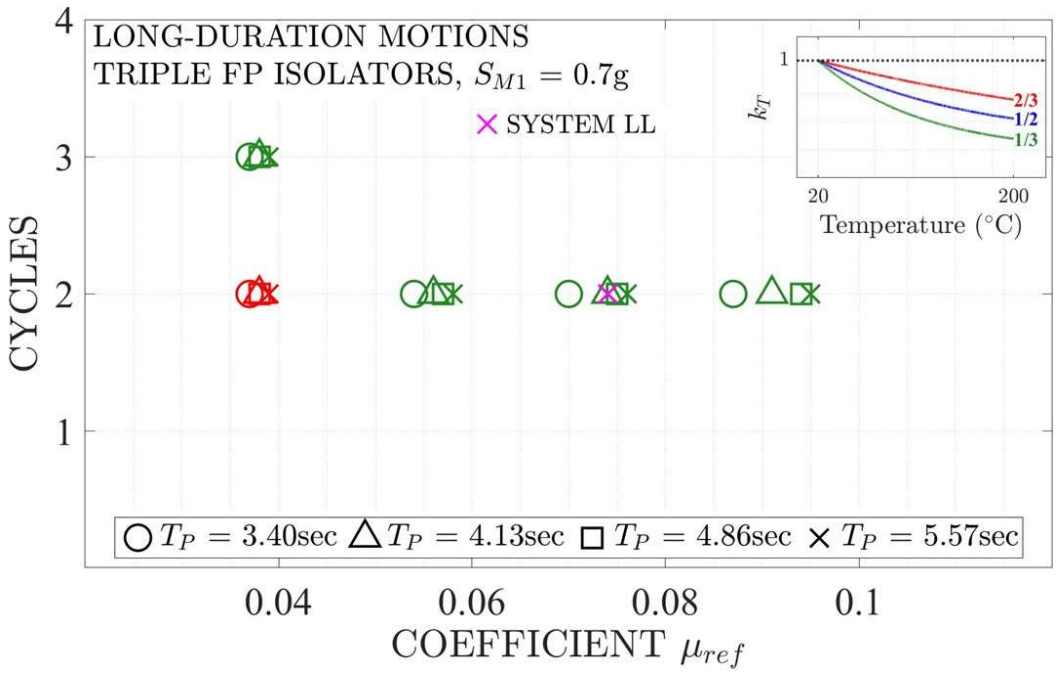

Figure 5-17 Required Number of Cycles for Lower Bound Test of Triple FP Isolators in Long-duration Ground Motions with S_{M1}=0.7g

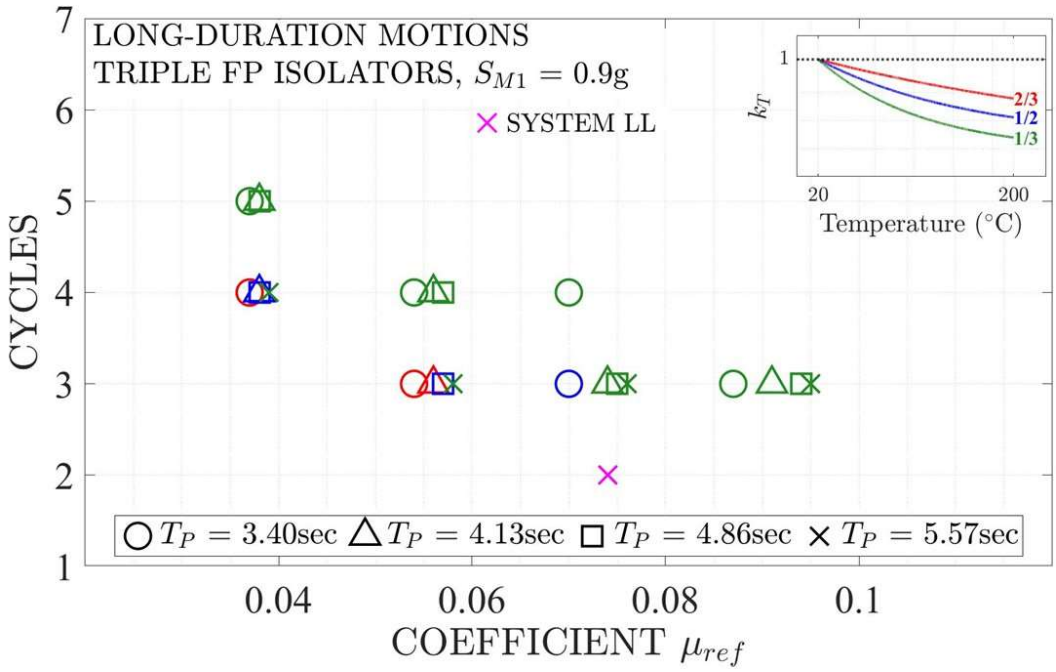

Figure 5-18 Required Number of Cycles for Lower Bound Test of Triple FP Isolators in Long-duration Ground Motions with S_{M1}=0.9g

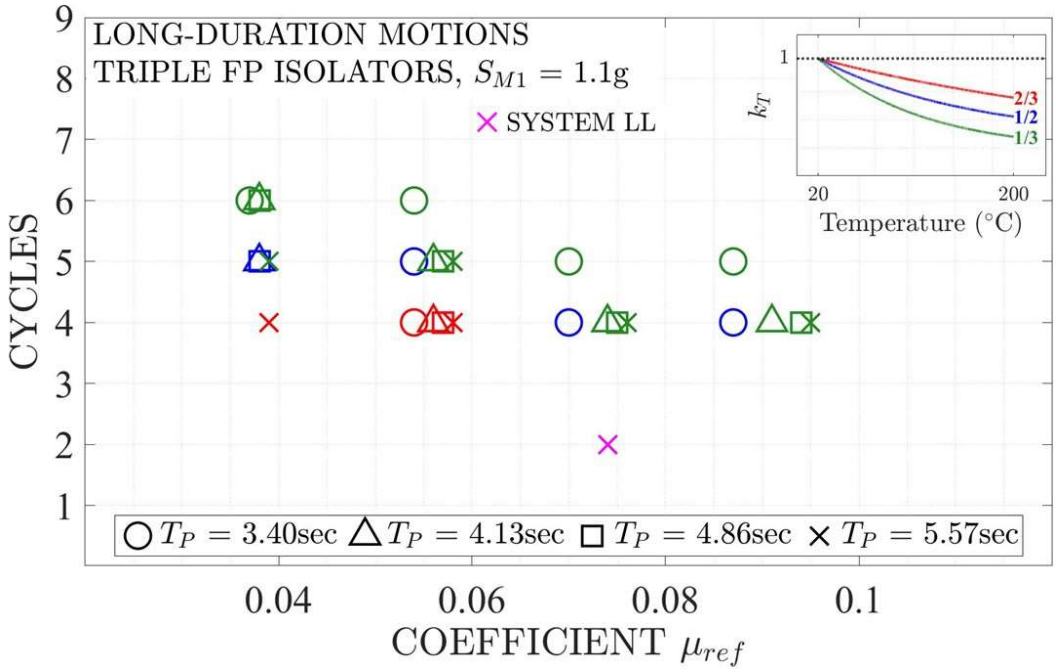

Figure 5-19 Required Number of Cycles for Lower Bound Test of Triple FP Isolators in Long-duration Ground Motions with S_{M1}=1.1g

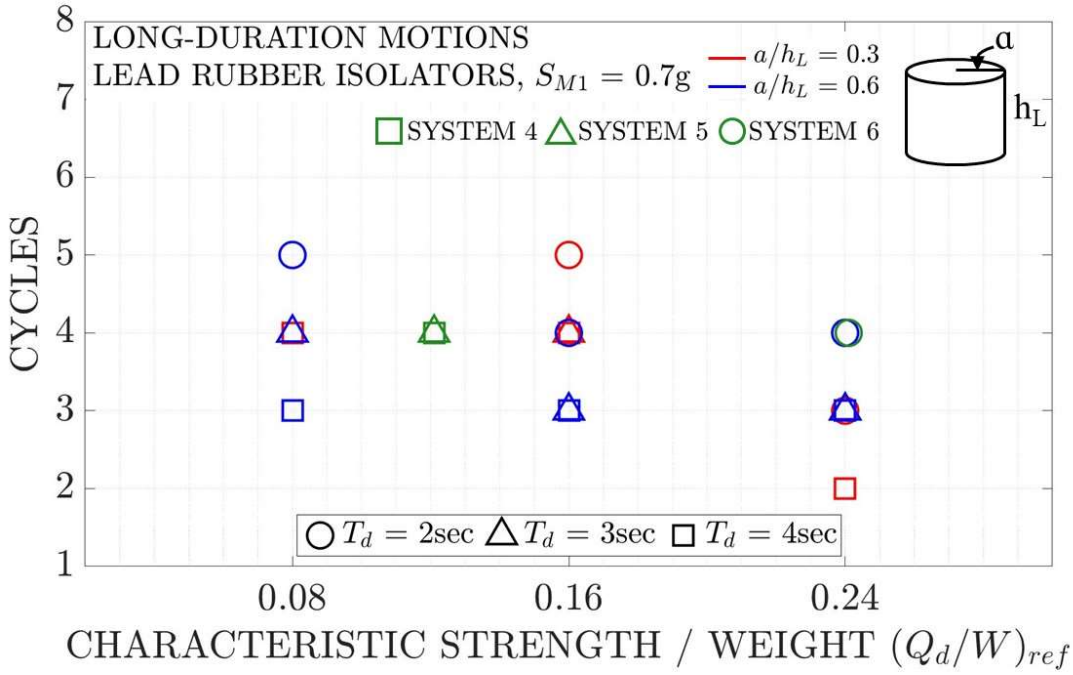

Figure 5-20 Required Number of Cycles for Lower Bound Test of Lead-rubber Isolators in Long-duration Ground Motions with S_{M1}=0.7g

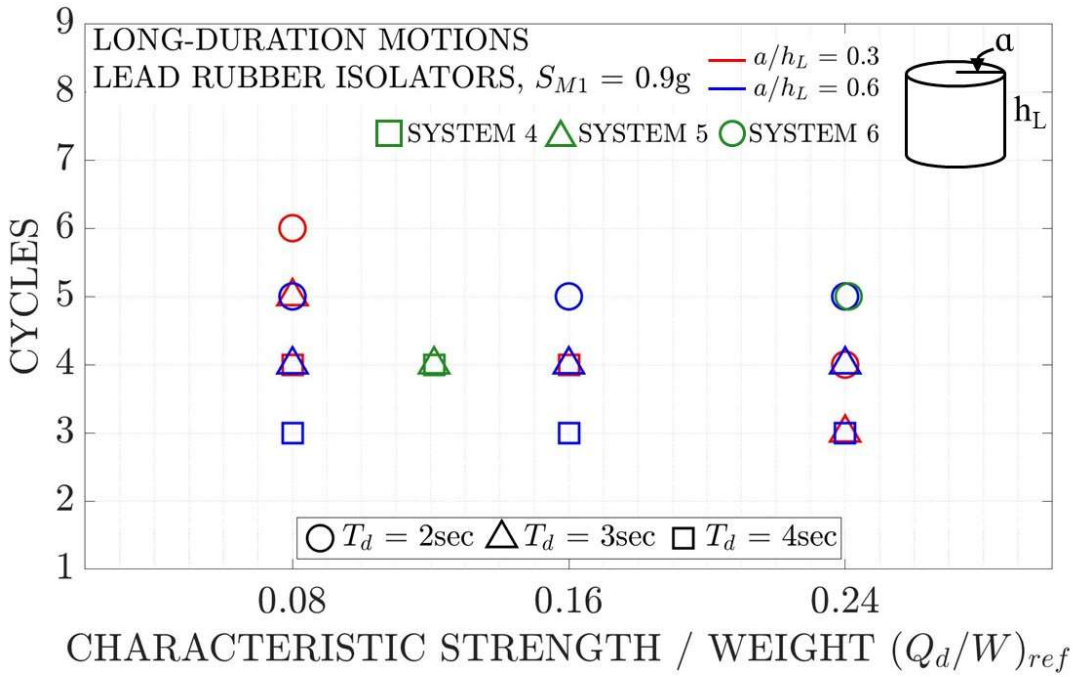

Figure 5-21 Required Number of Cycles for Lower Bound Test of Lead-rubber Isolators in Long-duration Ground Motions with S_{M1}=0.9g

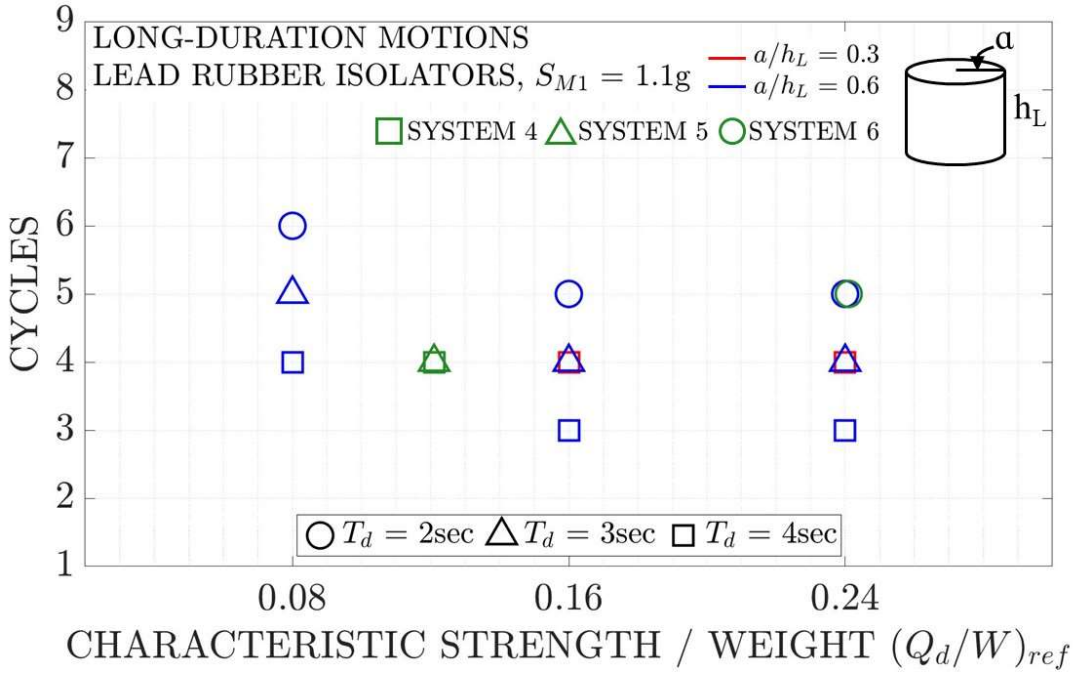

Figure 5-22 Required Number of Cycles for Lower Bound Test of Lead-rubber Isolators in Long-duration Ground Motions with S_{M1}=1.1g

The results show that the required number of cycles at amplitude D_M and period T_M varies from one to four for short-duration ground motions and from two to six for long-duration ground motions, with the largest number of cycles required for systems with the lowest considered starting value of friction coefficient or of the ratio of characteristic strength to weight, which are uncommon in practice. The results also show that the required number of cycles is smaller for single FP and lead-rubber systems than for triple FP systems, except for the special case of the triple FP system LL. Smaller number of cycles are needed for systems with more heating as in the case of the single FP versus the triple FP, and for systems in which heating is continuous rather than intermittent as in the lead-rubber systems and triple FP system LL rather than all other triple FP systems studied.

It is evident in the results that for all seismic isolation systems considered and for short-duration motions, a test of three cycles at amplitude D_M and period T_M suffices or is conservative to determine the lower bound properties for analysis. That is, test Items 2(a) and 3 of Section 17.8.2.2 of ASCE/SEI-7 are sufficient to determine factors $\lambda_{(test,\ max)}$ and $\lambda_{(test,\ min)}$ for short-duration motions. However, generally for long-duration motions, five cycles of motion at the same conditions of amplitude and period are needed, and could be conservative, to determine these factors. Triple FP system LL is a special case in which heating of the sliding interfaces is continuous due to the very large contact area, leading to requirement for only two cycles

of test at amplitude D_M and period T_M, even for long-duration ground motions. For such cases use of three cycles in testing per test Items 2(a) and 3 of Section 17.8.2.2 of ASCE/SEI-7, or five cycle under the same conditions for long-duration ground motions, is conservative. To avoid overdue conservatism for such special cases, the engineer may choose to perform project-specific analyses along the lines of this report, and of a related work by Fenz et al. (2011) for the single FP isolators of the Arkutun-Dagi Offshore Platform, to determine the most appropriate testing conditions.

5.3 Evaluation of Alternative Test

Standard ASCE/SEI-7 allows for an alternate test (Item 2(b) in section 17.8.2.2) in lieu of test item 2(a), in which the prototype isolators are dynamically tested at period T_M in four cycles of varying amplitude in each cycle (single cycle at D_M, followed by single cycles at $0.67D_M$, $0.5\ D_M$ and $0.25\ D_M$), instead of three cycles at amplitude D_M and period T_M. We investigated the equivalency of the tests 2(a) and 2(b) utilizing the results of Section 5.2 for short-duration motions as test 2(a) has been shown to be valid only for short-duration motions. Specifically, we selected several systems from the 288 cases analyzed in Section 5.2 and analyzed the systems for the conditions of the two tests using the computed values of displacement D_M and period T_M in Table 5-1 to 5-11. We used two cases of seismic intensity measured by the value parameter S_{M1}, 0.9g and 1.1g. For the case of sliding isolation systems, we only considered the case in which the friction coefficient-temperature relationship is given by equation (2-7), in which friction drops from the starting value at 20ºC to a value equal to half that at temperature of about 200ºC.

Results are presented in Figures 5-23 to 5-30 for eight cases when S_{M1}=0.9g and in Figures 5-31 to 5-38 for the same eight cases when S_{M1}=1.1g. Each of figures includes force-displacement loops and temperature histories at the center of the main sliding interfaces or the bulk of the lead core for the two tests. The force-displacement loops were then used to calculate the energy dissipated per cycle (EDC), which was then used to compute parameter μ for FP isolators or parameter Q_d/W for lead-rubber isolators using equation (5-1). Values of EDC and of parameters μ and Q_d/W for each cycle are presented in each figure. Parameters μ and Q_d/W are the same for the first cycle as both tests have identical conditions for that cycle (amplitude D_M at period T_M). The values of these parameters in the third and fourth cycles are important for the comparison of the two tests. The results in Figures 5-23 to 5-38 show that for the single and triple FP systems, except for the special triple FP system LL, the 4-cycle test provides the same or conservative results (lower values of lower bound properties) than the 3-cycle test. For the case of lead-rubber systems, the 4-cycle test provides the same or unconservative results (higher values of lower bound properties) than the 3-cycle test. For the special triple FP system LL, the 4-cycle test provides unconservative results (higher

values of lower bound properties) than the 3-cycle test. The behavior observed for the triple FP system LL resembles that of the lead-rubber systems. The similarity in behavior of triple FP system LL and the lead-rubber systems is related to the heating process, which is continuous for the triple FP system LL, like for the lead-rubber systems, in both the 3-cycle and the 4-cycle tests. For all other single and triple FP systems studied, the heating process is intermittent for the 3-cycle test but is partially intermittent and partially continuous for the 4-cycle test. The continuous heating in the last cycle of the 4-cycle test may lead to lower value of the friction parameter μ obtained over the last cycle, which results in conservative estimation of the lower bound properties.

It is apparent in the temperature histories at the sliding interfaces or the lead core of Figures 5-23 to 5-38 that systematically the 4-cycle test results in lower peak temperature than the 3-cycle test. Had we evaluated the instantaneous values of friction coefficient or characteristic strength at the end of each test we would have found the values to be less for the 3-cycle than the 4-cycle test as the temperature is higher. However, what is compared in the two tests are values of parameter μ for FP isolators and parameter Q_d/W for lead-rubber isolators computed using equation (5-1) with data obtained over the entire last cycle of motion, as done in the testing of isolators. This has an averaging effect. Moreover, in the case of sliding isolators there an additional effect of the amplitude of motion affecting heating when the amplitude of motion is small by comparison to the slider dimension so that the heat flux is continuous rather than intermittent.

It has been shown that a test per ASCE/SEI-7 Item 2(b) in section 17.8.2.2 (one cycle at D_M, followed by single cycles at $0.67D_M$, $0.5D_M$ and $0.25D_M$, all at period T_M) will result in values of properties in the fourth cycle that are essentially the same or conservative by comparison to those obtained in the third cycle of a test per ASCE/SEI-7 Items 2(a) and 3 in section 17.8.2.2 (three cycles at D_M and period T_M) for single and triple FP systems provided that the amplitude D_M is large by comparison to the diameter of the contact area so that the heat flux conditions are intermittent. This is not generally valid for lead-rubber systems, in which the 4-cycle test may overestimate the lower bound properties by comparison to the 3-cycle test, although the overestimation is not significant.

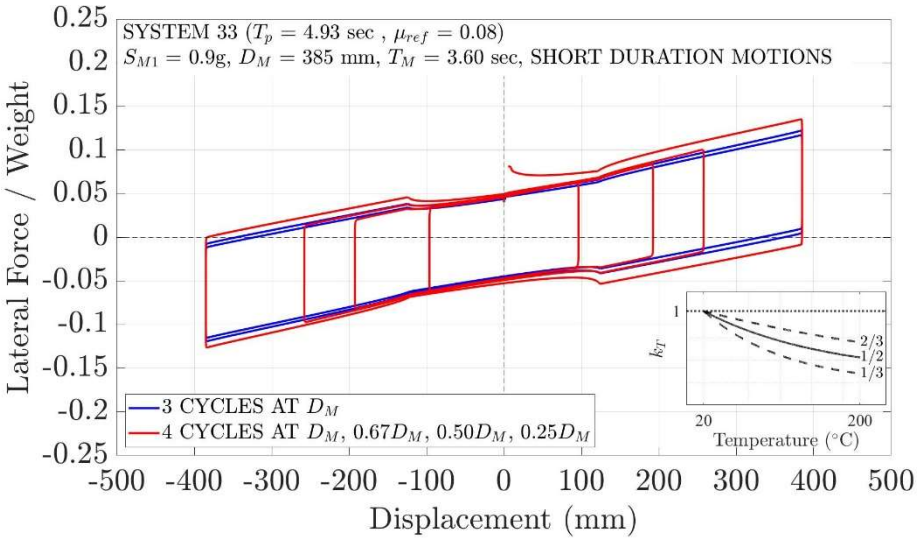

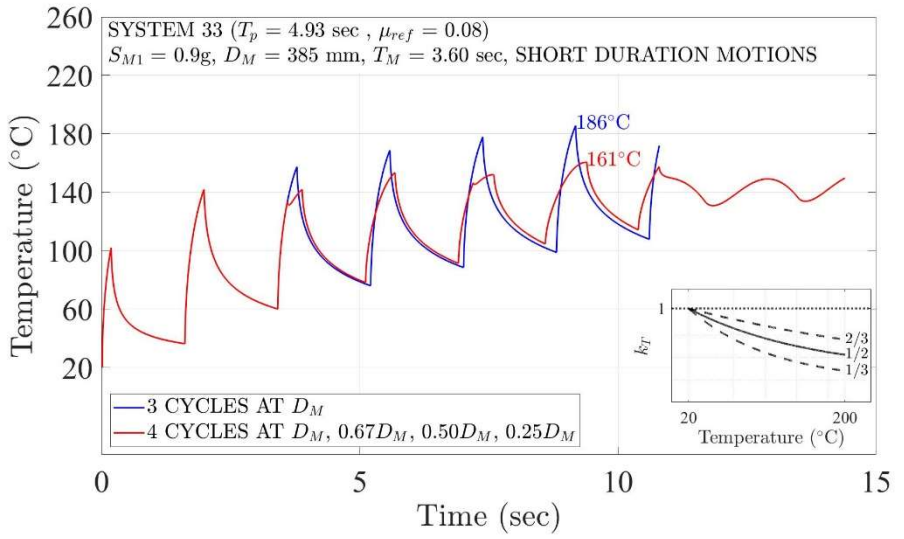

	Cycles	EDC (kN-m)	Parameter μ	μ^{1st}/μ^{3rd}
3-Cycle Test at D_M	**1**	**245**	**0.0623**	**1.26**
	2	210	0.0533	
	3	**195**	**0.0495**	
	Cycles	EDC (kN-m)	Parameter μ	μ^{1st}/μ^{4th}
4-Cycle Test at D_M to 0.25D_M	**1**	**245**	**0.0623**	**1.34**
	2	139	0.0526	
	3	95	0.0483	
	4	**46**	**0.0466**	

Figure 5-23 Results of 3-Cycle and 4-Cycle Tests for Single FP System 33 when S_{M1} = 0.9g

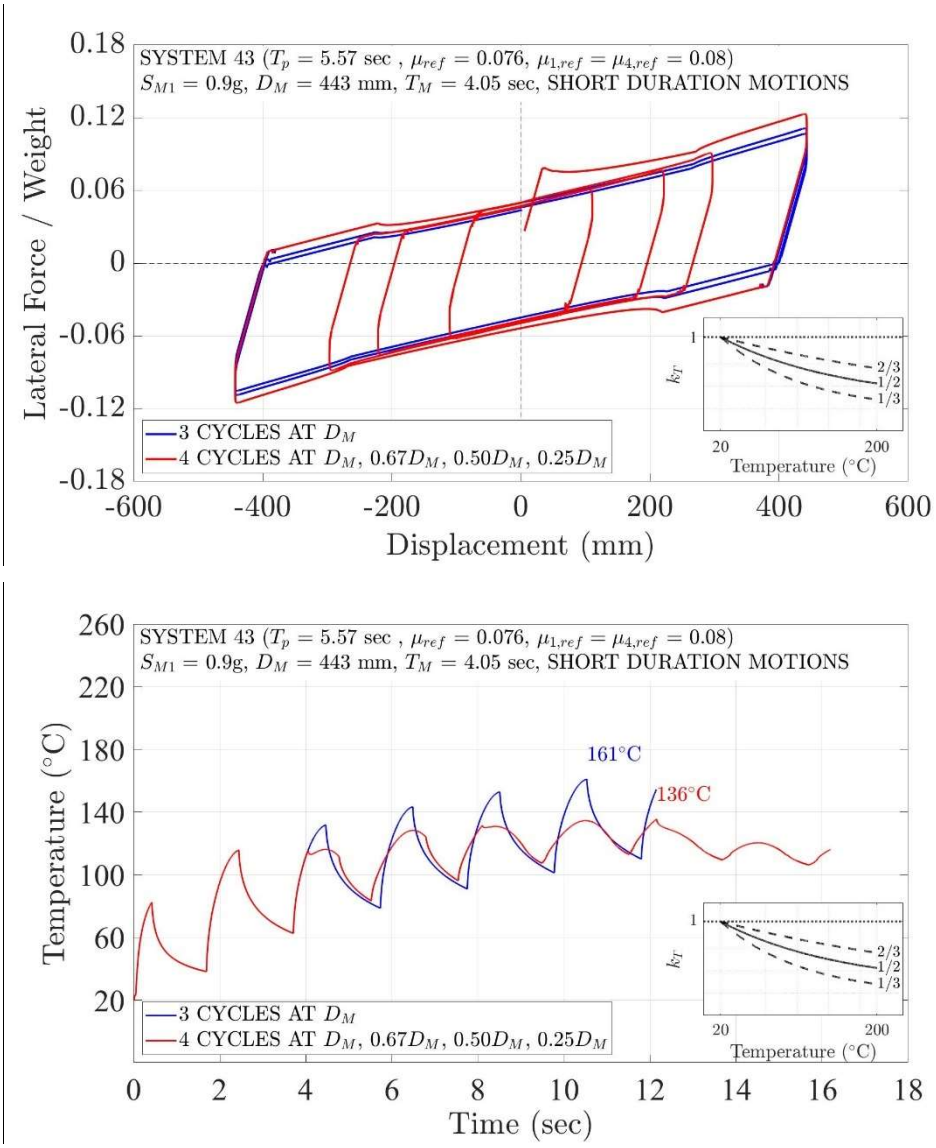

	Cycles	EDC (kN-m)	Parameter μ	μ^{1st}/μ^{3rd}
3-Cycle Test at D_M	**1**	**267**	**0.0589**	**1.25**
	2	230	0.0506	
	3	**213**	**0.0471**	
	Cycles	EDC (kN-m)	Parameter μ	μ^{1st}/μ^{4th}
4-Cycle Test at D_M to 0.25D_M	**1**	**267**	**0.0589**	**1.26**
	2	152	0.0500	
	3	107	0.0472	
	4	**53**	**0.0467**	

Figure 5-24 Results of 3-Cycle and 4-Cycle Tests for Triple FP System 43 when S_{M1} = 0.9g

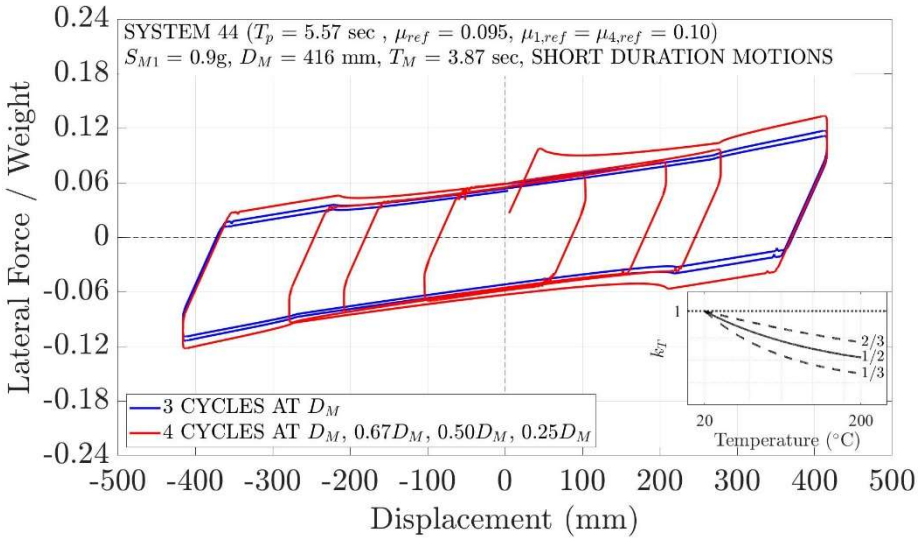

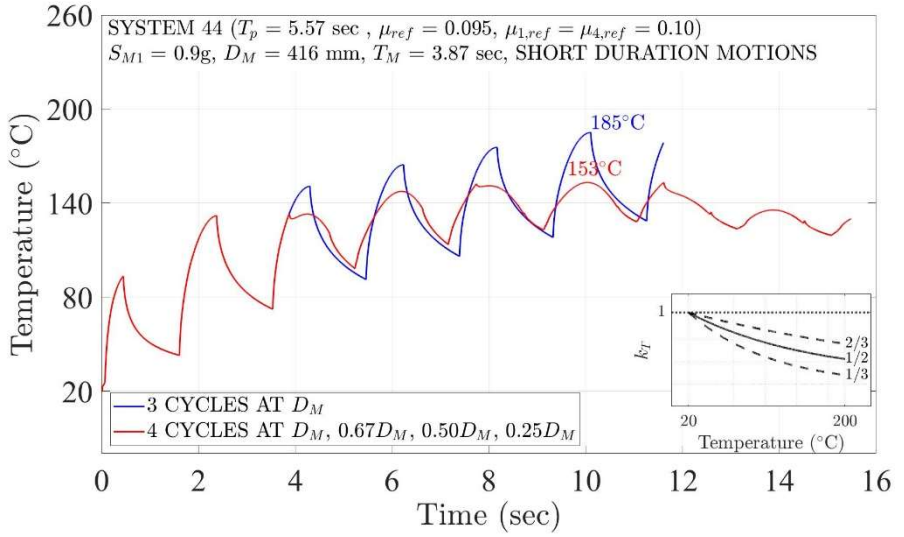

	Cycles	EDC (kN-m)	Parameter μ	μ^{1st}/μ^{3rd}
3-Cycle Test at D_M	**1**	**299**	**0.0702**	**1.29**
	2	250	0.0589	
	3	**232**	**0.0545**	
	Cycles	EDC (kN-m)	Parameter μ	μ^{1st}/μ^{4th}
4-Cycle Test at D_M to 0.25D_M	**1**	**299**	**0.0702**	**1.29**
	2	165	0.0580	
	3	117	0.0551	
	4	**58**	**0.0545**	

Figure 5-25 Results of 3-Cycle and 4-Cycle Tests for Triple FP System 44 when S_{M1} = 0.9g

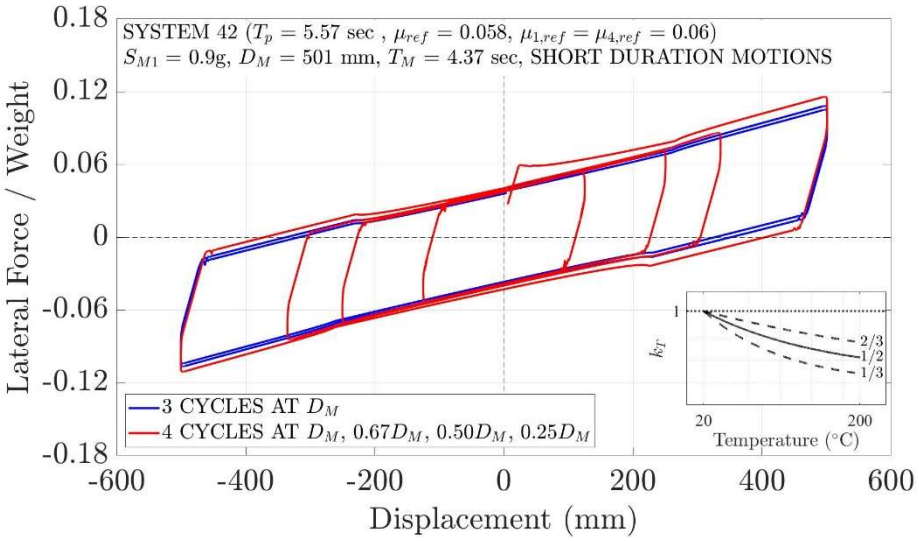

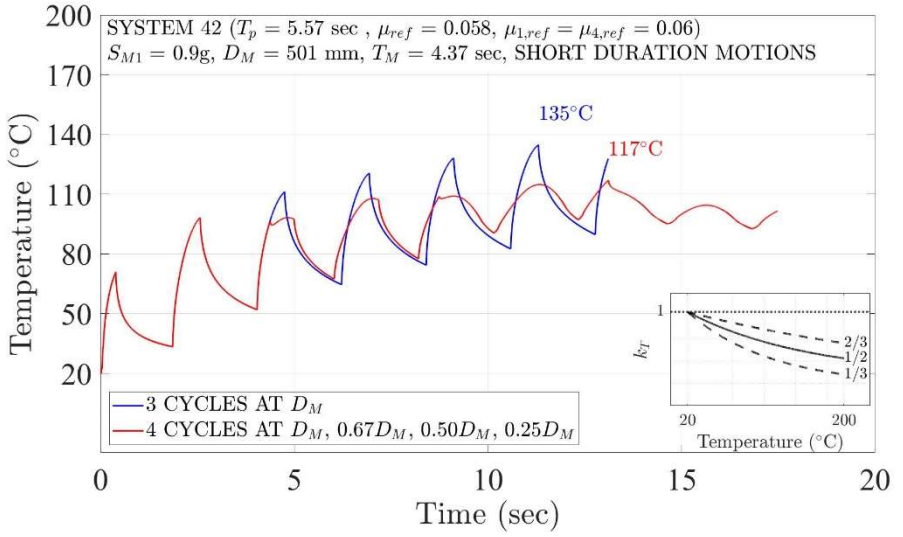

	Cycles	EDC (kN-m)	Parameter μ	μ^{1st}/μ^{3rd}
3-Cycle Test at D_M	**1**	**240**	**0.0469**	**1.21**
	2	212	0.0414	
	3	**199**	**0.0389**	
	Cycles	EDC (kN-m)	Parameter μ	μ^{1st}/μ^{4th}
4-Cycle Test at D_M to 0.25D_M	**1**	**240**	**0.0469**	**1.24**
	2	140	0.0409	
	3	98	0.0384	
	4	**48**	**0.0378**	

Figure 5-26 Results of 3-Cycle and 4-Cycle Tests for Triple FP System 42 when S_{M1} = 0.9g

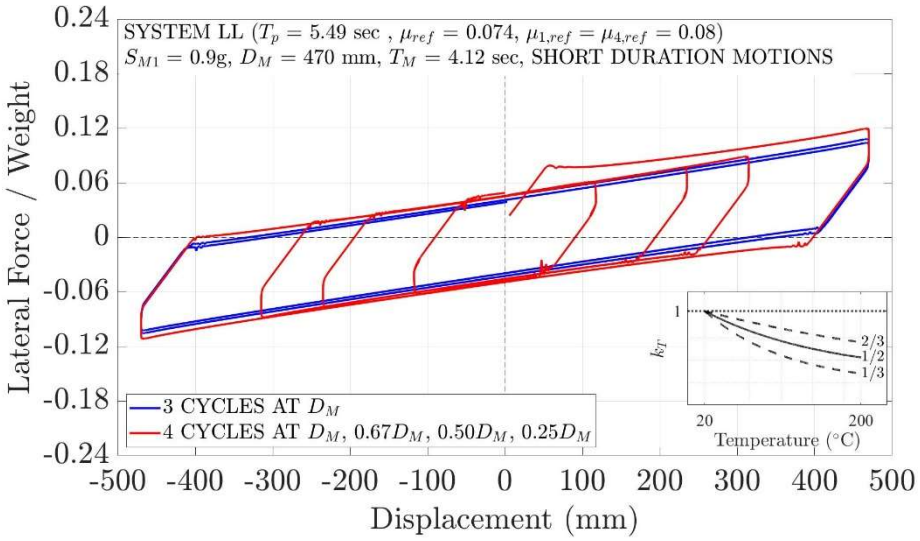

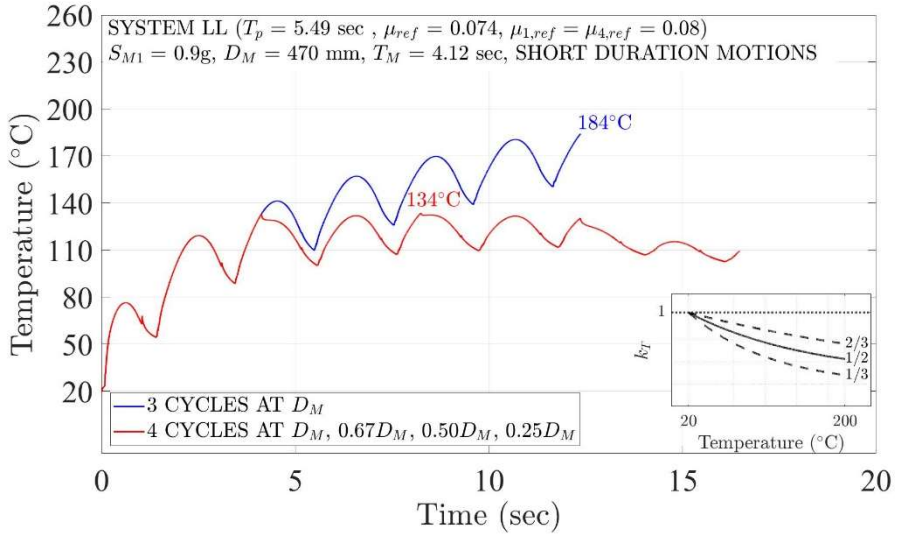

	Cycles	EDC (kN-m)	Parameter μ	μ^{1st}/μ^{3rd}
3-Cycle Test at D_M	**1**	**1328**	**0.0529**	**1.30**
	2	1106	0.0441	
	3	**1022**	**0.0407**	
	Cycles	EDC (kN-m)	Parameter μ	μ^{1st}/μ^{4th}
4-Cycle Test at D_M to 0.25D_M	**1**	**1328**	**0.0529**	**1.18**
	2	782	0.0465	
	3	571	0.0455	
	4	**281**	**0.0448**	

Figure 5-27 Results of 3-Cycle and 4-Cycle Tests for Triple FP System LL when S_{M1} = 0.9g

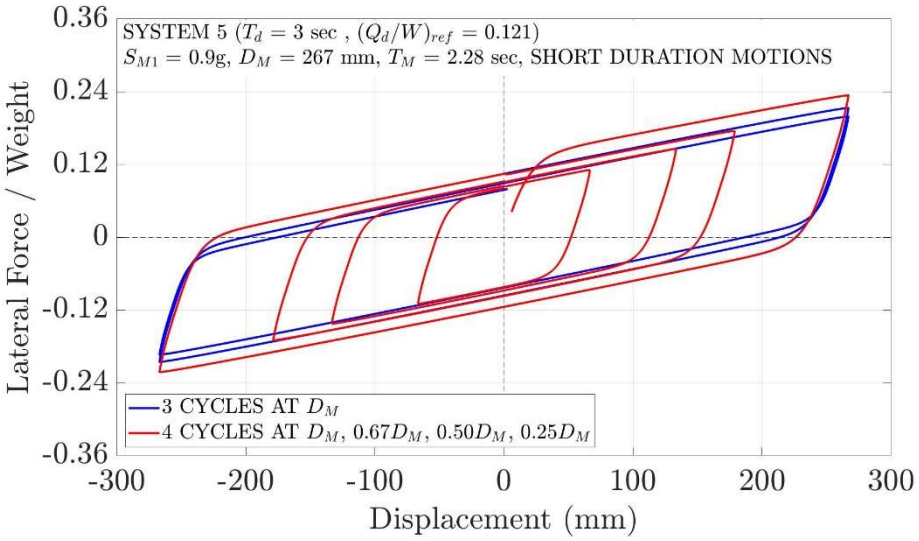

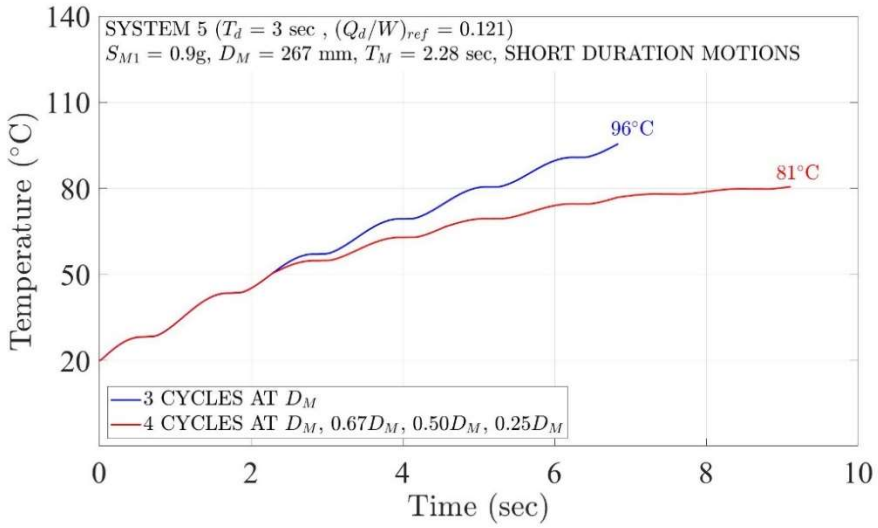

3-Cycle Test at D_M	Cycles	EDC (kN-m)	Parameter (Q_d/W)	$(Q_d/W)^{1st}$ / $(Q_d/W)^{3rd}$
	1	**1184**	**0.1080**	**1.41**
	2	982	0.0896	
	3	**840**	**0.0767**	
4-Cycle Test at D_M to $0.25D_M$	Cycles	EDC (kN-m)	Parameter (Q_d/W)	$(Q_d/W)^{1st}$ / $(Q_d/W)^{4th}$
	1	**1184**	**0.1080**	**1.37**
	2	676	0.0920	
	3	459	0.0836	
	4	**216**	**0.0787**	

Figure 5-28 Results of 3-Cycle and 4-Cycle Tests for Lead-rubber System 5 when S_{M1} = 0.9g

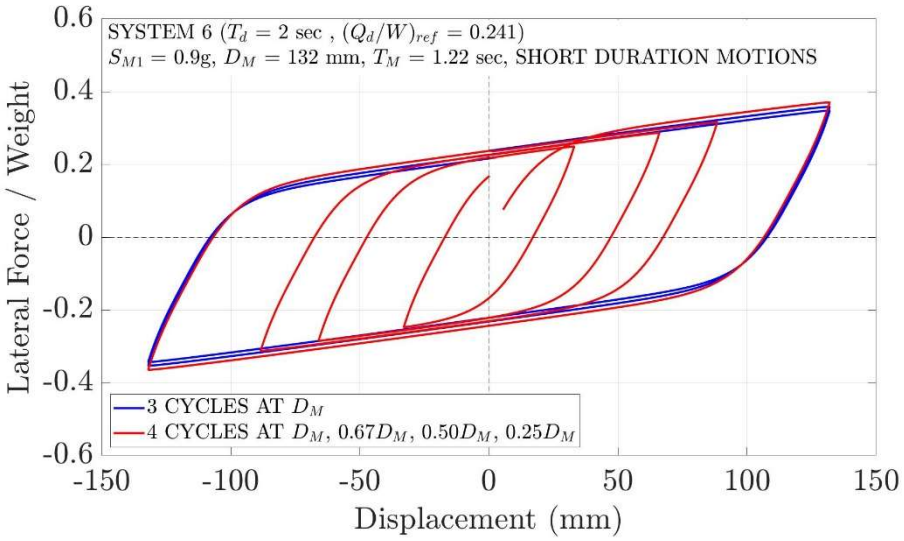

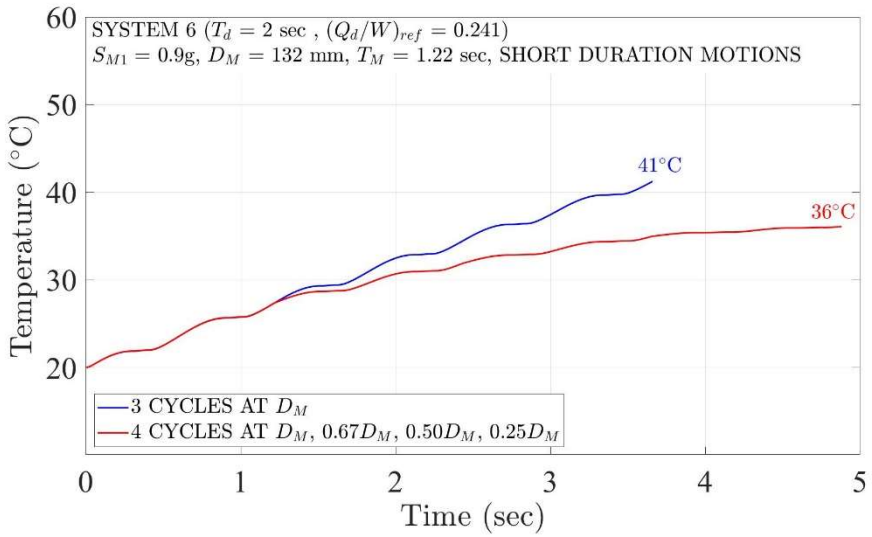

3-Cycle Test at D_M	Cycles	EDC (kN-m)	Parameter (Q_d/W)	$(Q_d/W)^{1st}$ / $(Q_d/W)^{3rd}$
	1	**304**	**0.232**	**1.10**
	2	291	0.222	
	3	**277**	**0.211**	
4-Cycle Test at D_M to $0.25D_M$	Cycles	EDC (kN-m)	Parameter (Q_d/W)	$(Q_d/W)^{1st}$ / $(Q_d/W)^{4th}$
	1	**304**	**0.232**	**1.10**
	2	196	0.223	
	3	142	0.216	
	4	**69**	**0.210**	

Figure 5-29 Results of 3-Cycle and 4-Cycle Tests for Lead-rubber System 6 when S_{M1} = 0.9g

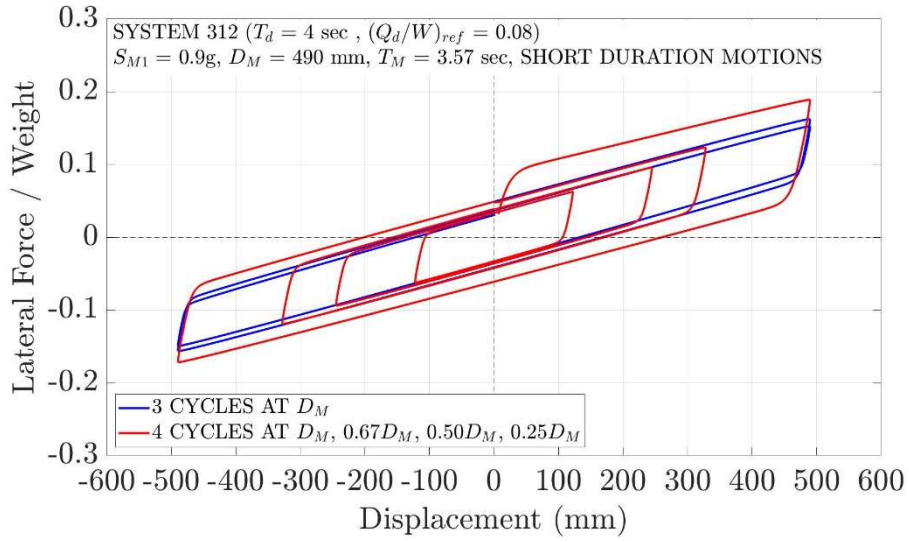

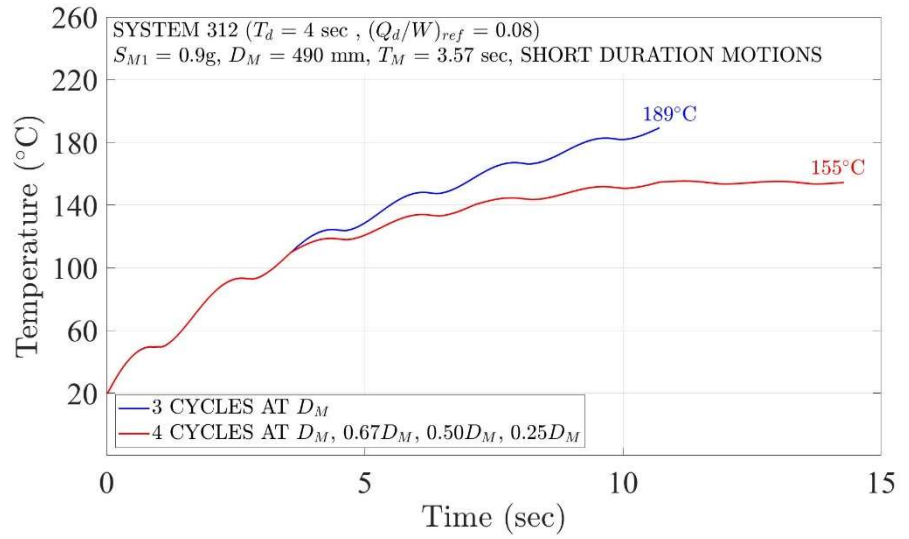

	Cycles	EDC (kN-m)	Parameter (Q_d/W)	$(Q_d/W)^{1st} / (Q_d/W)^{3rd}$
3-Cycle Test at D_M	**1**	**287**	**0.0572**	**2.07**
	2	181	0.0362	
	3	**138**	**0.0276**	
	Cycles	EDC (kN-m)	Parameter (Q_d/W)	$(Q_d/W)^{1st} / (Q_d/W)^{4th}$
4-Cycle Test at D_M to $0.25D_M$	**1**	**287**	**0.0572**	**1.83**
	2	130	0.0386	
	3	83	0.0330	
	4	**39**	**0.0312**	

Figure 5-30 Results of 3-Cycle and 4-Cycle Tests for Lead-rubber System 312 when $S_{M1} = 0.9$g

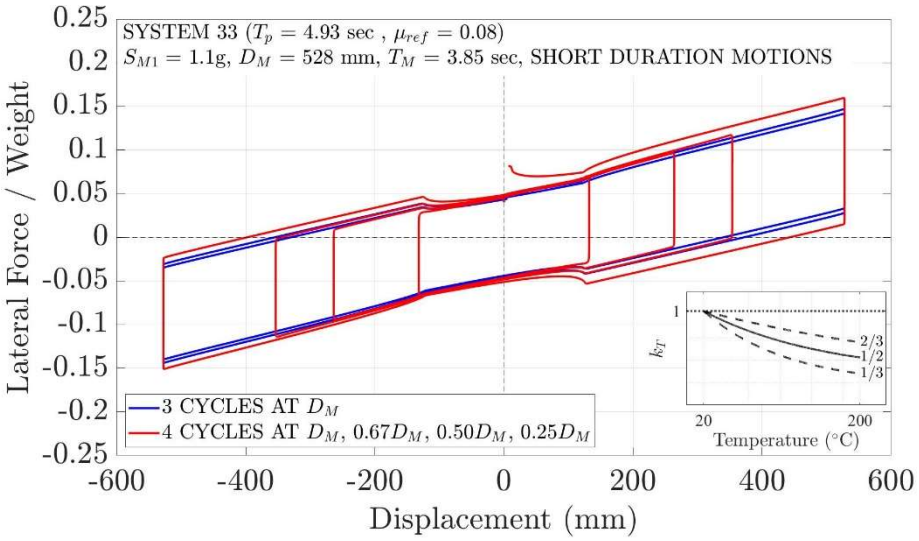

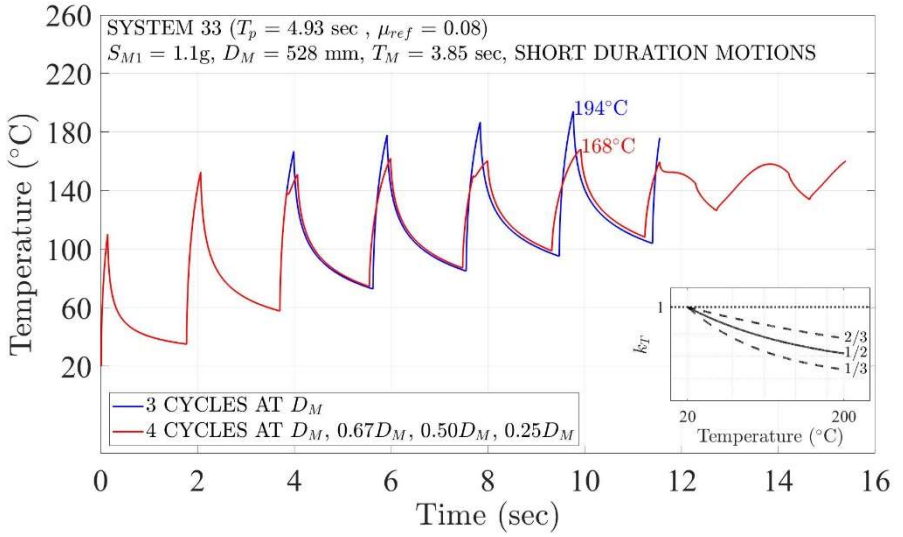

	Cycles	EDC (kN-m)	Parameter μ	μ^{1st}/μ^{3rd}
3-Cycle Test at D_M	**1**	**341**	**0.0632**	**1.25**
	2	293	0.0542	
	3	**272**	**0.0504**	
	Cycles	EDC (kN-m)	Parameter μ	μ^{1st}/μ^{4th}
4-Cycle Test at D_M to 0.25D_M	**1**	**341**	**0.0632**	**1.37**
	2	194	0.0535	
	3	133	0.0493	
	4	**62**	**0.0460**	

Figure 5-31 Results of 3-Cycle and 4-Cycle Tests for Single FP System 33 when S_{M1} = 1.1g

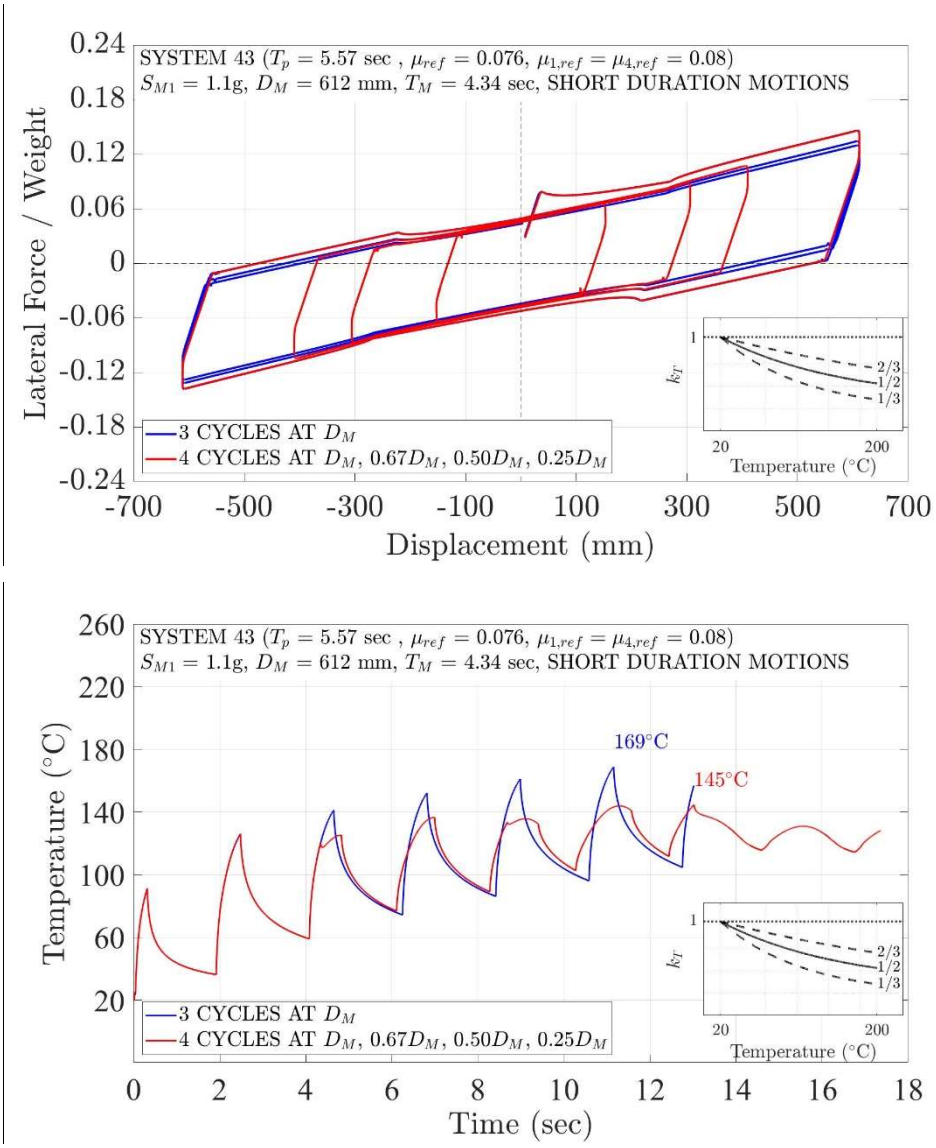

	Cycles	EDC (kN-m)	Parameter μ	μ^{1st}/μ^{3rd}
3-Cycle Test at D_M	**1**	**375**	**0.0599**	**1.25**
	2	323	0.0516	
	3	**301**	**0.0481**	
	Cycles	EDC (kN-m)	Parameter μ	μ^{1st}/μ^{4th}
4-Cycle Test at D_M to 0.25D_M	**1**	**375**	**0.0599**	**1.29**
	2	214	0.0511	
	3	148	0.0471	
	4	**72**	**0.0463**	

Figure 5-32 Results of 3-Cycle and 4-Cycle Tests for Triple FP System 43 when S_{M1} = 1.1g

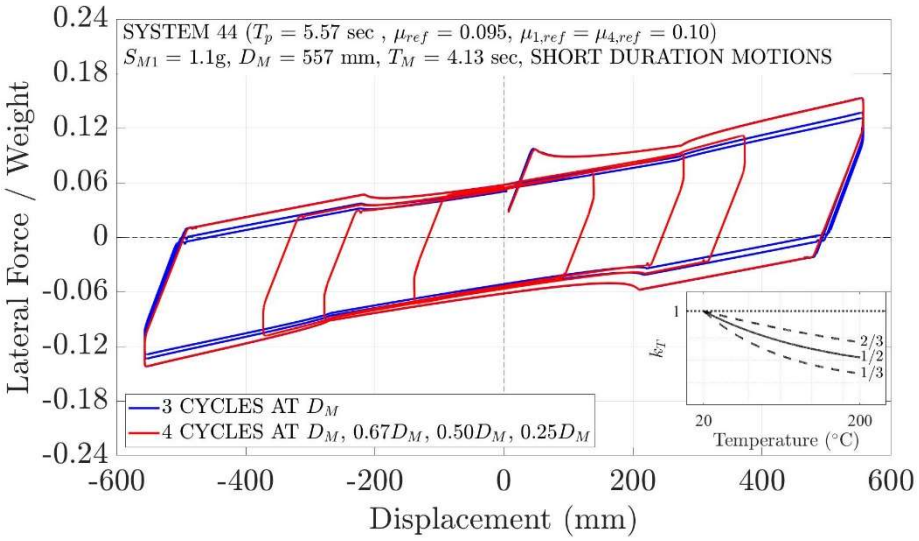

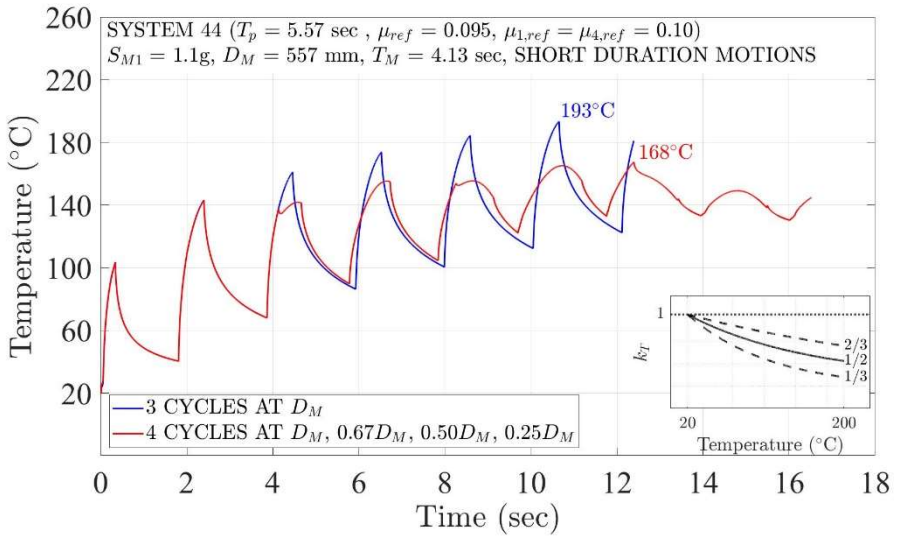

	Cycles	EDC (kN-m)	Parameter μ	μ^{1st}/μ^{3rd}
3-Cycle Test at D_M	**1**	**407**	**0.0714**	**1.28**
	2	342	0.0601	
	3	**317**	**0.0556**	
	Cycles	EDC (kN-m)	Parameter μ	μ^{1st}/μ^{4th}
4-Cycle Test at D_M to 0.25D_M	**1**	**407**	**0.0714**	**1.33**
	2	227	0.0594	
	3	155	0.0545	
	4	**77**	**0.0538**	

Figure 5-33 Results of 3-Cycle and 4-Cycle Tests for Triple FP System 44 when S_{M1} = 1.1g

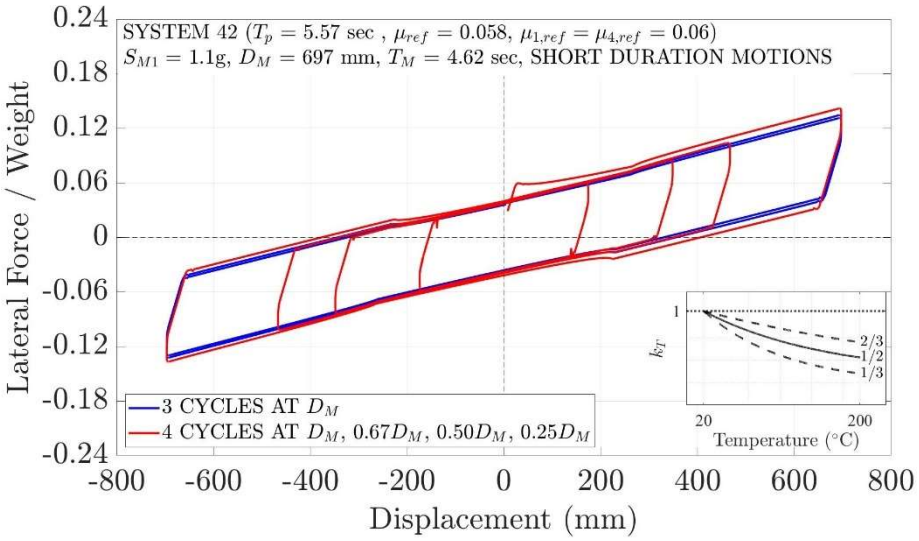

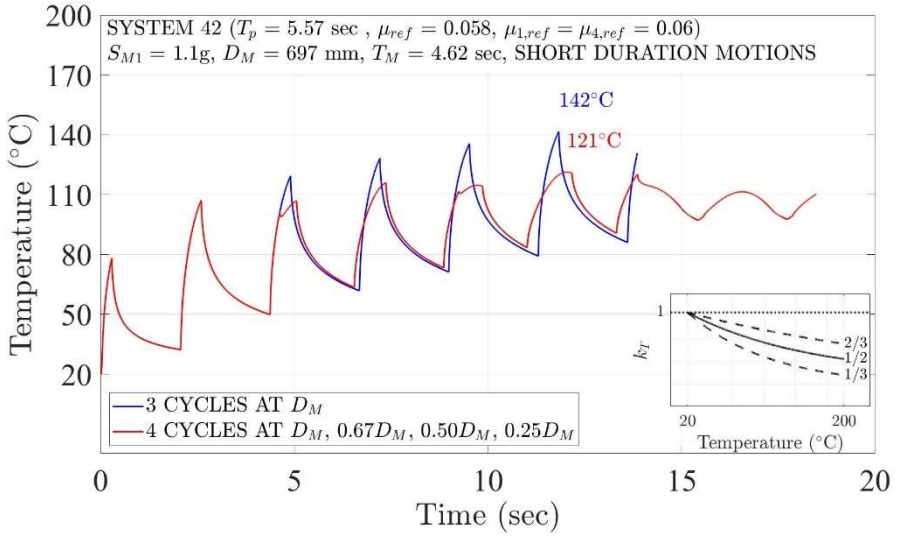

	Cycles	EDC (kN-m)	Parameter μ	μ^{1st}/μ^{3rd}
3-Cycle Test at D_M	**1**	**338**	**0.0474**	**1.20**
	2	300	0.0421	
	3	**282**	**0.0396**	
	Cycles	EDC (kN-m)	Parameter μ	μ^{1st}/μ^{4th}
4-Cycle Test at D_M to 0.25D_M	**1**	**338**	**0.0474**	**1.25**
	2	199	0.0416	
	3	138	0.0388	
	4	**67**	**0.0378**	

Figure 5-34 Results of 3-Cycle and 4-Cycle Tests for Triple FP System 42 when S_{M1} = 1.1g

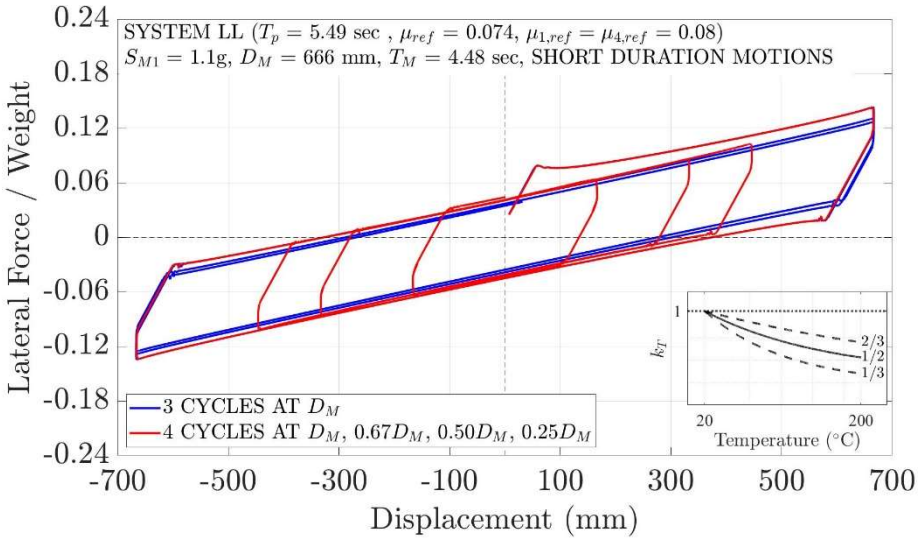

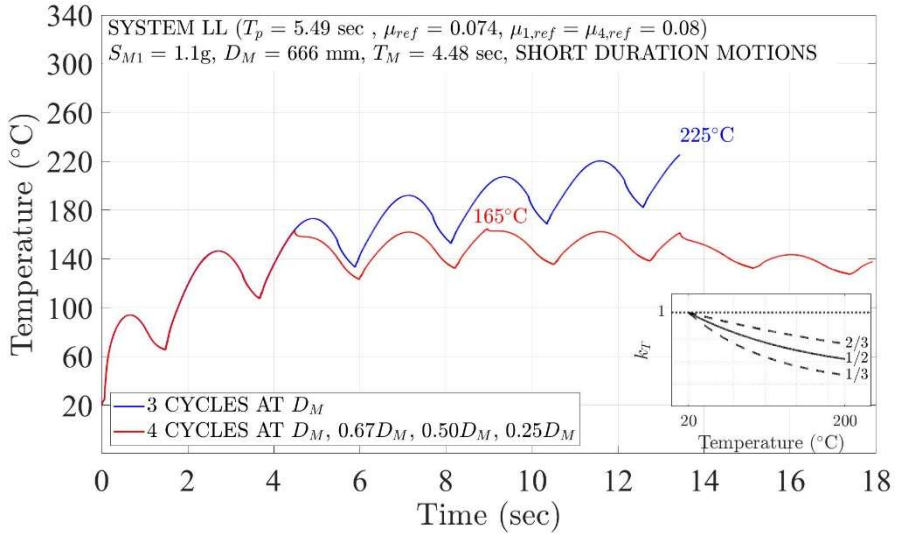

	Cycles	EDC (kN-m)	Parameter μ	μ^{1st}/μ^{3rd}
3-Cycle Test at D_M	**1**	**1759**	**0.0495**	**1.33**
	2	1436	0.0404	
	3	**1322**	**0.0372**	
	Cycles	EDC (kN-m)	Parameter μ	μ^{1st}/μ^{4th}
4-Cycle Test at D_M to 0.25D_M	**1**	**1759**	**0.0495**	**1.17**
	2	1020	0.0428	
	3	747	0.0420	
	4	**376**	**0.0423**	

Figure 5-35 Results of 3-Cycle and 4-Cycle Tests for Triple FP System LL when S_{M1} = 1.1g

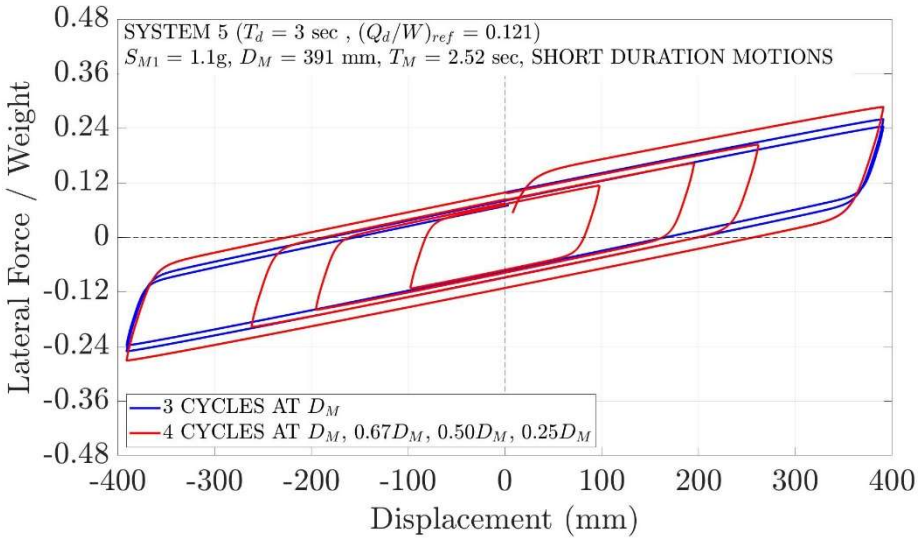

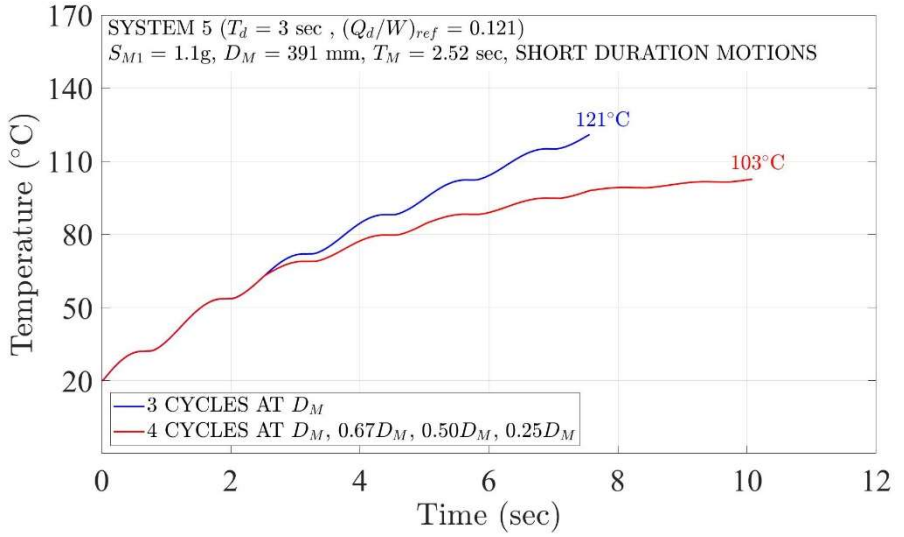

	Cycles	EDC (kN-m)	Parameter (Q_d/W)	$(Q_d/W)^{1st}$ / $(Q_d/W)^{3rd}$
3-Cycle Test at D_M	**1**	**1657**	**0.1032**	**1.58**
	2	1282	0.0799	
	3	**1051**	**0.0654**	
	Cycles	EDC (kN-m)	Parameter (Q_d/W)	$(Q_d/W)^{1st}$ / $(Q_d/W)^{4th}$
4-Cycle Test at D_M to 0.25D_M	**1**	**1657**	**0.1032**	**1.51**
	2	890	0.0828	
	3	588	0.0733	
	4	**274**	**0.0682**	

Figure 5-36 Results of 3-Cycle and 4-Cycle Tests for Lead-rubber System 5 when S_{M1} = 1.1g

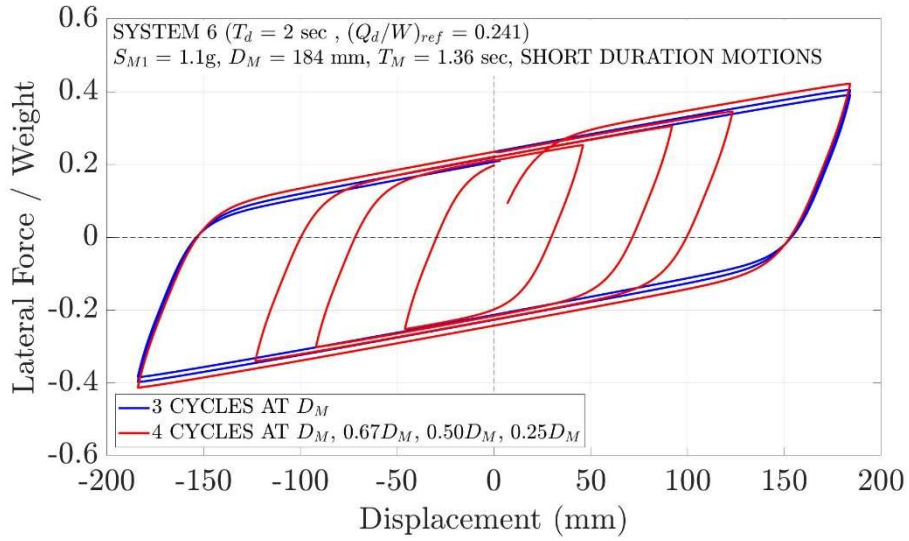

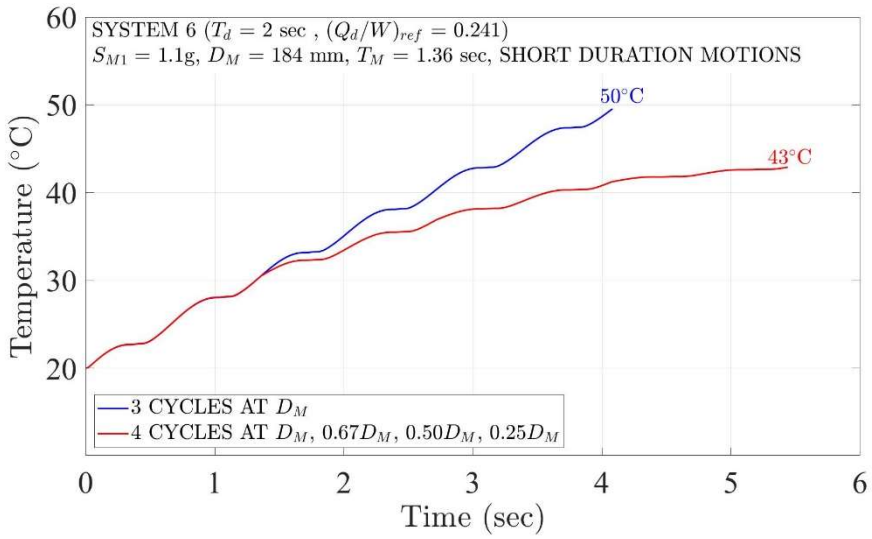

3-Cycle Test at D_M	Cycles	EDC (kN-m)	Parameter (Q_d/W)	$(Q_d/W)^{1st}$ / $(Q_d/W)^{3rd}$
	1	**420**	**0.230**	**1.14**
	2	393	0.215	
	3	**368**	**0.202**	
4-Cycle Test at D_M to 0.25D_M	Cycles	EDC (kN-m)	Parameter (Q_d/W)	$(Q_d/W)^{1st}$ / $(Q_d/W)^{4th}$
	1	**420**	**0.230**	**1.14**
	2	266	0.217	
	3	190	0.208	
	4	**92**	**0.202**	

Figure 5-37 Results of 3-Cycle and 4-Cycle Tests for Lead-rubber System 6 when S_{M1} = 1.1g

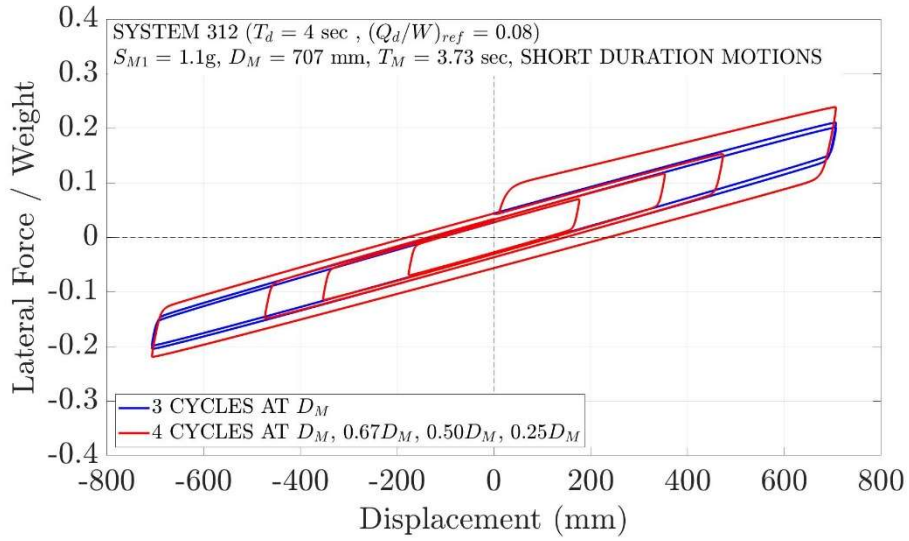

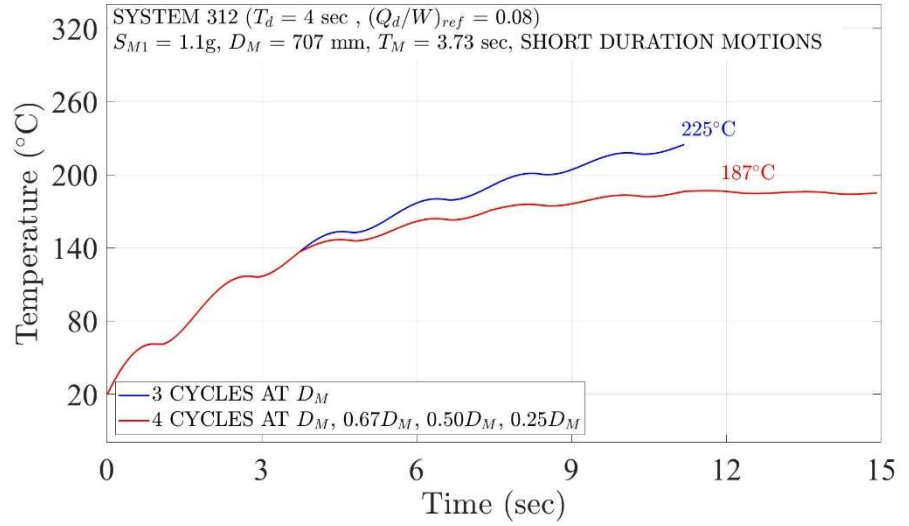

	Cycles	EDC (kN-m)	Parameter (Q_d/W)	$(Q_d/W)^{1st}$ / $(Q_d/W)^{3rd}$
3-Cycle Test at D_M	**1**	**373**	**0.0519**	**2.36**
	2	212	0.0296	
	3	**158**	**0.0220**	
	Cycles	EDC (kN-m)	Parameter (Q_d/W)	$(Q_d/W)^{1st}$ / $(Q_d/W)^{4th}$
4-Cycle Test at D_M to $0.25D_M$	**1**	**373**	**0.0519**	**2.05**
	2	153	0.0316	
	3	97	0.0267	
	4	**46**	**0.0253**	

Figure 5-38 Results of 3-Cycle and 4-Cycle Tests for Lead-rubber System 312 when S_{M1} = 1.1g

“This Page Intentionally Left Blank”

SECTION 6
DETAILED RESULTS OF RESPONSE HISTORY ANALYSIS

6.1 Introduction

Section 4 of this report described 96 seismic isolation systems that were analyzed for three cases of seismic intensity, measured by the value of S_{M1} being 0.7g, 0.9g or 1.1g, and for suites of short-duration and long-duration ground motions, each consisting of 71 pairs of horizontal components. Results obtained in the analyses were used in Section 5 to design experiments for obtaining the lower bound properties of isolators.

This section presents detailed results of the analyses as they are useful to better understand the behavior of seismic isolation systems, and to design experiments for determining the adequacy of isolators, a topic to be covered in Section 7. Results presented include the following:

1) Tabulated values of mean, median, 84th percentile and 90th percentile values of the peak resultant isolator displacement and of the resultant residual displacement. The values are counted values based on the empirical data. To be able to compute residual displacements, the ground motion durations were increased by adding zero acceleration data to 250 seconds for short-duration ground motions, and to 365 seconds for long-duration motions.

2) Graphs of probability distributions of the empirical data and lognormal representations for the probability of non-exceedance vs the maximum displacement and vs the residual displacement. Also, plotted counted values (empirical data) of the resultant isolator displacement and of the resultant residual displacement for 16%, 50% (median), 84% and 90% probabilities of being exceeded.

3) 16th, 50th (median), 84th and 90th percentile histories of cumulative energy as obtained from the empirical data (counted) and again from the lognormal distributions (fitted). Comparisons of histories of the cumulative energy obtained using the empirical data and the lognormal distributions are also presented to demonstrate differences.

4) 16th, 50th (median), 84th and 90th percentile histories of temperature at the main sliding interface or the bulk of the lead core as obtained from the empirical data (counted) and again from the lognormal

distributions (fitted). Comparisons of histories of the temperature obtained using the empirical data and the lognormal distributions are also presented to demonstrate differences.

6.2 Results for Single FP Isolation Systems

Tables 6-1 to 6-6 present results on the resultant maximum displacements and residual displacements for the single FP systems. The results include values of mean, median, 84th and 90th percentile counted values from the empirical data. Higher percentile values could not be obtained from the empirical data due to the sample size of 71 values. Higher percentile values can be computed from the lognormal distributions fitted to the empirical data. Also, the tables present values of the ratio of the 90th percentile isolator maximum resultant displacement to the mean value, which can be utilized in the design of isolators. Typically, analysis involves the use of seven (or 11) ground motions in response history analysis of seismically isolated buildings (ASCE/SEI-7) from which the mean maximum resultant isolator displacement can be computed. The isolator displacement capacity should be larger than the mean, and the 90th percentile/mean ratio provides a simple scale factor for computing a value that has an acceptable probability of exceedance. For example, Huang et al. (2009) computed many scale factors for seismically isolated nuclear structures of which the 99th/mean scale factor was 2.2. Kammerer et al. (2019) recommended the use of a scale factor of 1.6 for obtaining the 90th percentile isolator displacement from the mean value. The results in Tables 6-1 to 6-6 show that a value of for the 90th/mean scale factor for the isolator displacement is 1.4 to 1.6, thus providing additional verification for the value recommended in Kammerer et al. (2019) for single FP isolation systems. The 84th/mean scale factor for the isolator displacement is 1.3 to 1.4. The values of the scale factor for long-duration ground motions are slightly smaller than those for short-duration motions. This is due to a smaller variability in the long-duration ground motions that in the short-duration ground motions as seen in the spectra of Figure 3-4 and 3-5, and in Appendix B.

The results in Tables 6-1 to 6-6, and others to be presented for triple FP and lead-rubber systems, provide information to obtain scale factors for the 90th/mean or the 84th/mean isolators displacements so that an isolator displacement demand with an acceptable probability of exceedance is computed. Note that the approach of obtaining a higher percentile estimate of displacement from the mean value (Huang et al. 2009, Kammerer et al., 2019), and other direct procedures (O'Reilly et al., 2022) do not account for the effect of the superstructure failure characteristics when computing the probability of collapse (e.g., Kitayama et al., 2018, 2019). Specifically, inelastic action in the superstructure results in reduction of isolator displacements by comparison to elastic superstructure response, or rigid superstructure response as assumed in this study.

Table 6-1 Mean and Median Resultant Maximum Displacements and Residual Displacements of Single FP Systems for S_{M1}=0.7g

	k_T = 2/3 at 200°C								k_T = 1/2 at 200°C								k_T = 1/3 at 200°C							
	Maximum Resultant Displacement (mm)				Residual Resultant Displacement (mm)				Maximum Resultant Displacement (mm)				Residual Resultant Displacement (mm)				Maximum Resultant Displacement (mm)				Residual Resultant Displacement (mm)			
	Short-duration		Long-duration		Short-duration		Long-duration		Short-duration		Long-duration		Short-duration		Long-duration		Short-duration		Long-duration		Short-duration		Long-duration	
	Median	Mean	Median	Mean	Median	Mean	Median	Mean	Median	Mean	Median	Mean	Median	Mean	Median	Mean	Median	Mean	Median	Mean	Median	Mean	Median	Mean
System 11 T_P = 3.50 sec μ_{ref} = 0.040	297	310	308	293	5	9	2	3	313	331	333	318	5	9	2	3	330	359	354	346	5	10	1	2
System 31 T_P = 4.93 sec μ_{ref} = 0.040	321	338	340	335	8	16	3	6	331	356	379	366	8	14	3	5	365	381	404	404	8	13	2	5
System 12 T_P = 3.50 sec μ_{ref} = 0.060	264	267	270	269	7	11	3	3	279	290	314	298	7	11	2	3	319	327	355	336	5	10	2	3
System 32 T_P = 4.93 sec μ_{ref} = 0.060	275	275	277	269	14	19	4	6	291	293	300	298	13	18	4	6	310	320	344	336	12	18	3	6
System 13 T_P = 3.50 sec μ_{ref} = 0.080	234	240	238	240	9	12	3	4	253	260	277	269	8	12	3	4	299	295	323	306	7	11	2	3
System 33 T_P = 4.93 sec μ_{ref} = 0.080	229	240	240	238	16	20	5	7	261	258	272	264	14	19	5	6	286	284	312	298	13	19	4	6
System 14 T_P = 3.50 sec μ_{ref} = 0.100	212	220	221	220	9	12	3	4	244	241	251	249	10	12	3	4	271	273	305	287	9	13	3	4
System 34 T_P = 4.93 sec μ_{ref} = 0.100	212	221	231	218	20	23	5	7	244	239	246	243	16	21	5	7	277	266	289	278	17	20	5	6

μ_{ref} is the starting value of the coefficient of friction prior to any heating effects, Factor=friction coefficient reduction factor; all results are counted values

Table 6-2 Mean, 84th Percentile and 90th Percentile Resultant Maximum Displacements of Single FP Systems for S_{M1}=0.7g

	k_T = 2/3 at 200°C								k_T = 1/2 at 200°C								k_T = 1/3 at 200°C							
	Short-duration				Long-duration				Short-duration				Long-duration				Short-duration				Long-duration			
	Mean	84th	90th	90th / Mean	Mean	84th	90th	90th / Mean	Mean	84th	90th	90th / Mean	Mean	84th	90th	90th / Mean	Mean	84th	90th	90th / Mean	Mean	84th	90th	90th / Mean
System 11 T_P = 3.50 sec μ_{ref} = 0.040	310	423	489	**1.58**	293	406	424	**1.45**	331	456	505	**1.53**	318	434	457	**1.44**	359	480	533	**1.48**	346	458	492	**1.42**
System 31 T_P = 4.93 sec μ_{ref} = 0.040	338	457	490	**1.45**	335	452	474	**1.41**	356	484	492	**1.38**	366	485	530	**1.45**	381	516	553	**1.45**	404	536	557	**1.38**
System 12 T_P = 3.50 sec μ_{ref} = 0.060	267	391	448	**1.68**	269	400	442	**1.64**	290	417	464	**1.60**	298	446	486	**1.63**	327	476	493	**1.51**	336	488	514	**1.53**
System 32 T_P = 4.93 sec μ_{ref} = 0.060	275	404	467	**1.70**	269	395	421	**1.57**	293	421	488	**1.67**	298	427	449	**1.51**	320	455	491	**1.53**	336	460	505	**1.50**
System 13 T_P = 3.50 sec μ_{ref} = 0.080	240	368	407	**1.70**	240	375	418	**1.74**	260	395	440	**1.69**	269	412	454	**1.69**	295	440	468	**1.59**	306	469	503	**1.64**
System 33 T_P = 4.93 sec μ_{ref} = 0.080	240	332	412	**1.72**	238	361	387	**1.63**	258	372	435	**1.69**	264	395	427	**1.62**	284	424	475	**1.67**	298	436	451	**1.51**
System 14 T_P = 3.50 sec μ_{ref} = 0.100	220	342	399	**1.81**	220	354	399	**1.81**	241	382	418	**1.73**	249	386	436	**1.75**	273	422	454	**1.66**	287	451	494	**1.72**
System 34 T_P = 4.93 sec μ_{ref} = 0.100	221	316	391	**1.77**	218	349	368	**1.69**	239	346	405	**1.69**	243	370	392	**1.61**	266	398	440	**1.65**	278	415	438	**1.58**
Average 90th / Mean				**1.67**				**1.62**				**1.62**				**1.59**				**1.57**				**1.54**

μ_{ref} is the starting value of the coefficient of friction prior to any heating effects, Factor=friction coefficient reduction factor

Table 6-3 Mean and Median Resultant Maximum Displacements and Residual Displacements of Single FP Systems for S_{M1}=0.9g

	k_T = 2/3 at 200°C								k_T = 1/2 at 200°C								k_T = 1/3 at 200°C							
	Maximum Resultant Displacement (mm)				Residual Resultant Displacement (mm)				Maximum Resultant Displacement (mm)				Residual Resultant Displacement (mm)				Maximum Resultant Displacement (mm)				Residual Resultant Displacement (mm)			
	Short-duration		Long-duration		Short-duration		Long-duration		Short-duration		Long-duration		Short-duration		Long-duration		Short-duration		Long-duration		Short-duration		Long-duration	
	Median	Mean	Median	Mean	Median	Mean	Median	Mean	Median	Mean	Median	Mean	Median	Mean	Median	Mean	Median	Mean	Median	Mean	Median	Mean	Median	Mean
System 11 T_P = 3.50 sec μ_{ref} = 0.040	432	464	443	439	7	11	2	3	455	493	464	473	6	11	1	3	490	526	517	512	6	10	1	2
System 31 T_P = 4.93 sec μ_{ref} = 0.040	485	506	524	515	11	16	3	6	514	529	552	558	9	17	3	6	552	561	602	605	9	15	2	6
System 12 T_P = 3.50 sec μ_{ref} = 0.060	396	412	423	412	6	12	2	4	435	446	471	464	7	12	2	4	481	493	514	522	7	13	2	4
System 32 T_P = 4.93 sec μ_{ref} = 0.060	386	410	424	414	15	23	4	8	417	439	469	462	12	20	4	8	462	477	509	518	12	18	3	7
System 13 T_P = 3.50 sec μ_{ref} = 0.080	366	366	386	369	10	15	3	4	386	400	427	418	8	13	2	4	430	447	475	473	8	14	2	4
System 33 T_P = 4.93 sec μ_{ref} = 0.080	356	359	373	363	20	25	5	8	380	385	422	405	17	25	4	8	395	423	474	462	14	23	4	8
System 14 T_P = 3.50 sec μ_{ref} = 0.100	320	339	351	342	12	17	3	5	377	367	404	387	10	16	3	4	417	415	452	443	7	12	2	4
System 34 T_P = 4.93 sec μ_{ref} = 0.100	342	333	342	334	19	26	7	9	365	357	394	372	20	26	6	8	389	392	445	424	15	26	4	8

μ_{ref} is the starting value of the coefficient of friction prior to any heating effects, Factor=friction coefficient reduction factor; all results are counted values

Table 6-4 Mean, 84th Percentile and 90th Percentile Resultant Maximum Displacements of Single FP Systems for S_{M1}=0.9g

	k_T = 2/3 at 200°C								k_T = 1/2 at 200°C								k_T = 1/3 at 200°C							
	Short-duration				Long-duration				Short-duration				Long-duration				Short-duration				Long-duration			
	Mean	84th	90th	90th / Mean	Mean	84th	90th	90th / Mean	Mean	84th	90th	90th / Mean	Mean	84th	90th	90th / Mean	Mean	84th	90th	90th / Mean	Mean	84th	90th	90th / Mean
System 11 T_P = 3.50 sec μ_{ref} = 0.040	464	639	686	**1.48**	439	579	610	**1.39**	493	660	709	**1.44**	473	605	645	**1.36**	526	697	745	**1.42**	512	621	681	**1.33**
System 31 T_P = 4.93 sec μ_{ref} = 0.040	506	681	739	**1.46**	515	672	709	**1.38**	529	710	770	**1.46**	558	721	762	**1.37**	561	772	842	**1.50**	605	750	834	**1.38**
System 12 T_P = 3.50 sec μ_{ref} = 0.060	412	596	627	**1.52**	412	607	644	**1.56**	446	632	652	**1.46**	464	669	704	**1.52**	493	674	706	**1.43**	522	731	781	**1.50**
System 32 T_P = 4.93 sec μ_{ref} = 0.060	410	562	633	**1.54**	414	575	604	**1.46**	439	590	629	**1.43**	462	612	666	**1.44**	477	645	691	**1.45**	518	680	730	**1.41**
System 13 T_P = 3.50 sec μ_{ref} = 0.080	366	565	613	**1.67**	369	561	610	**1.65**	400	580	629	**1.57**	418	636	658	**1.57**	447	627	661	**1.48**	473	700	736	**1.56**
System 33 T_P = 4.93 sec μ_{ref} = 0.080	359	527	606	**1.69**	363	523	566	**1.56**	385	546	626	**1.63**	405	570	601	**1.48**	423	591	630	**1.49**	462	631	679	**1.47**
System 14 T_P = 3.50 sec μ_{ref} = 0.100	339	532	578	**1.71**	342	530	580	**1.70**	367	558	598	**1.63**	387	606	642	**1.66**	415	598	640	**1.54**	443	679	715	**1.61**
System 34 T_P = 4.93 sec μ_{ref} = 0.100	333	502	563	**1.69**	334	497	523	**1.57**	357	535	600	**1.68**	372	541	586	**1.58**	392	573	622	**1.59**	424	605	626	**1.48**
Average 90th / Mean				**1.60**				**1.53**				**1.54**				**1.50**				**1.49**				**1.47**

μ_{ref} is the starting value of the coefficient of friction prior to any heating effects, Factor=friction coefficient reduction factor

Table 6-5 Mean and Median Resultant Maximum Displacements and Residual Displacements of Single FP Systems for S_{M1}=1.1g

	k_T = 2/3 at 200°C								k_T = 1/2 at 200°C								k_T = 1/3 at 200°C							
	Maximum Resultant Displacement (mm)				Residual Resultant Displacement (mm)				Maximum Resultant Displacement (mm)				Residual Resultant Displacement (mm)				Maximum Resultant Displacement (mm)				Residual Resultant Displacement (mm)			
	Short-duration		Long-duration		Short-duration		Long-duration		Short-duration		Long-duration		Short-duration		Long-duration		Short-duration		Long-duration		Short-duration		Long-duration	
	Median	Mean	Median	Mean	Median	Mean	Median	Mean	Median	Mean	Median	Mean	Median	Mean	Median	Mean	Median	Mean	Median	Mean	Median	Mean	Median	Mean
System 11 T_P = 3.50 sec μ_{ref} = 0.040	586	630	608	598	7	13	2	3	615	662	654	637	7	12	1	3	653	696	684	681	7	12	1	4
System 31 T_P = 4.93 sec μ_{ref} = 0.040	670	689	707	712	11	20	3	7	700	717	746	762	12	20	3	7	727	754	804	816	13	20	2	5
System 12 T_P = 3.50 sec μ_{ref} = 0.060	541	574	571	587	9	16	2	4	580	614	632	649	9	15	2	4	622	673	668	717	9	13	2	4
System 32 T_P = 4.93 sec μ_{ref} = 0.060	524	563	597	586	14	24	4	9	588	600	637	647	14	20	4	7	632	647	707	714	12	22	3	8
System 13 T_P = 3.50 sec μ_{ref} = 0.080	479	509	527	528	8	16	3	5	542	551	571	586	9	16	2	4	595	610	630	663	10	16	2	5
System 33 T_P = 4.93 sec μ_{ref} = 0.080	477	492	526	512	20	30	5	10	490	528	591	571	17	28	4	10	554	578	645	647	14	22	4	8
System 14 T_P = 3.50 sec μ_{ref} = 0.100	452	466	506	488	12	20	3	5	494	508	540	543	9	16	3	5	549	568	598	616	10	18	2	4
System 34 T_P = 4.93 sec μ_{ref} = 0.100	468	452	487	466	24	32	7	10	485	486	536	518	19	32	5	9	505	536	605	594	18	29	4	9

μ_{ref} is the starting value of the coefficient of friction prior to any heating effects, Factor=friction coefficient reduction factor; all results are counted values

Table 6-6 Mean, 84th Percentile and 90th Percentile Resultant Maximum Displacements of Single FP Systems for S_{M1}=1.1g

	k_T = 2/3 at 200°C								k_T = 1/2 at 200°C								k_T = 1/3 at 200°C							
	Short-duration				Long-duration				Short-duration				Long-duration				Short-duration				Long-duration			
	Mean	84th	90th	90th / Mean	Mean	84th	90th	90th / Mean	Mean	84th	90th	90th / Mean	Mean	84th	90th	90th / Mean	Mean	84th	90th	90th / Mean	Mean	84th	90th	90th / Mean
System 11 T_P = 3.50 sec μ_{ref} = 0.040	630	875	900	**1.43**	598	753	796	**1.33**	662	892	957	**1.45**	637	771	829	**1.30**	696	923	1003	**1.44**	681	815	880	**1.29**
System 31 T_P = 4.93 sec μ_{ref} = 0.040	689	938	1036	**1.50**	712	897	952	**1.34**	717	959	1063	**1.48**	762	945	1013	**1.33**	754	1010	1139	**1.51**	816	1003	1058	**1.30**
System 12 T_P = 3.50 sec μ_{ref} = 0.060	574	794	822	**1.43**	587	839	874	**1.49**	614	840	872	**1.42**	649	912	965	**1.49**	673	943	967	**1.44**	717	984	1037	**1.45**
System 32 T_P = 4.93 sec μ_{ref} = 0.060	563	758	771	**1.37**	586	774	842	**1.44**	600	816	846	**1.41**	647	837	882	**1.36**	647	880	973	**1.50**	714	901	980	**1.37**
System 13 T_P = 3.50 sec μ_{ref} = 0.080	509	748	793	**1.56**	528	796	838	**1.59**	551	776	806	**1.46**	586	870	904	**1.54**	610	856	906	**1.49**	663	942	989	**1.49**
System 33 T_P = 4.93 sec μ_{ref} = 0.080	492	684	770	**1.57**	512	714	754	**1.47**	528	710	769	**1.46**	571	775	821	**1.44**	578	772	837	**1.45**	647	834	903	**1.40**
System 14 T_P = 3.50 sec μ_{ref} = 0.100	466	707	763	**1.64**	488	760	805	**1.65**	508	741	797	**1.57**	543	825	879	**1.62**	568	801	867	**1.53**	616	905	963	**1.56**
System 34 T_P = 4.93 sec μ_{ref} = 0.100	452	672	762	**1.69**	466	671	726	**1.56**	486	686	762	**1.57**	518	729	766	**1.48**	536	743	770	**1.44**	594	812	857	**1.44**
Average 90th / Mean				**1.52**				**1.48**				**1.48**				**1.44**				**1.47**				**1.41**

μ_{ref} is the starting value of the coefficient of friction prior to any heating effects, Factor=friction coefficient reduction factor

Figures 6-1 and 6-2 present a sample of results on the distribution of the maximum resultant displacement and of the residual resultant displacement for the single FP system 31 (T_P=4.93s, μ_{ref}=0.04) when S_{M1}=0.9g. The results are for the case in which the friction coefficient-temperature relationship is given by equation (2-7), in which friction drops from the starting value at 20°C to a value equal to half that at temperature of about 200°C. Appendix D contains detailed results for all studied single FP systems.

Median and dispersion values shown in Figures 6-1 and 6-2 may be used to construct the lognormal distributions which were fitted to the empirical data. The percentile values listed in each figure are based on the fitted lognormal distributions.

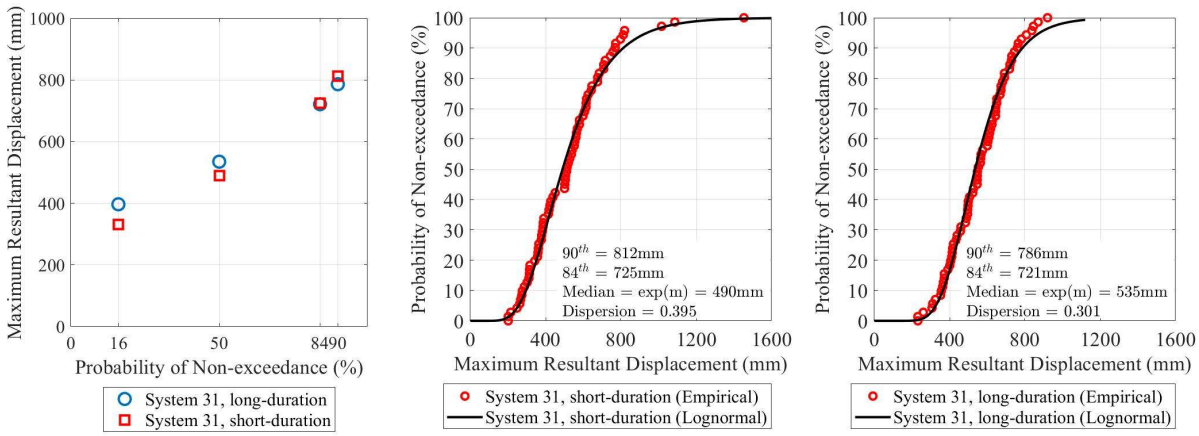

Figure 6-1 Distributions of Maximum Resultant Displacement for Single FP System 31 (T_P = 4.93s, μ_{ref} = 0.04) when S_{M1} = 0.9g (friction case when k_T=0.5 at 200°C)

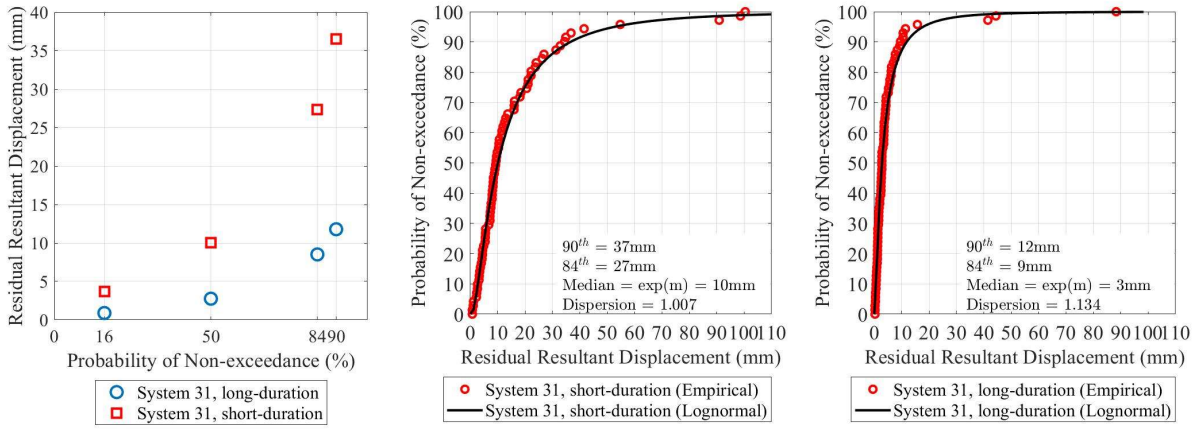

Figure 6-2 Distributions of Residual Resultant Displacement for Single FP System 31 (T_P = 4.93s, μ_{ref} = 0.04) when S_{M1} = 0.9g (friction case when k_T=0.5 at 200°C)

In the lognormal model, the probability of non-exceedance (or cumulative distribution function CDF) is described by the following equation:

$$CDF(x) = \int_{-\infty}^{x} \frac{1}{\sigma s\sqrt{2\pi}} \exp\left[-\frac{(\ln(s) - \mathrm{m})^2}{2\sigma^2}\right] ds \qquad (6-1)$$

In equation (6-1), x is the random variable (in this study the value of peak displacement or other response parameter), m and σ are, respectively, the mean and standard deviation of the natural logarithm of the empirical data. Parameter σ is called the dispersion factor. Figures 6-1 and 6-2 (and all similar figures in Appendices D, E and F) report the value of the dispersion and the value of the median of the lognormal distribution, which is equal to exp(m). The figures also include values of the 84th and 90th percentile value of response parameters that were calculated using equation (6-1). For example, for the computation of the 90th percentile value of the maximum resultant displacement for short-duration motions (see Figure 6-1), equation (6-1) is used with m=ln(median)=ln(490)=6.194, σ=0.395, CDF=0.9 and the value of x is the 90th percentile maximum resultant displacement. The fitting of the empirical data with a lognormal distribution was performed in program MATLAB (Mathworks, 2020) using the "fitdist" function.

The results in Tables 6-1 to 6-6, Figures 6-1 and 6-2, and many more in Appendix D show that the median, other percentile values and the mean values of residual displacement for the case of long-duration motions are systematically smaller than the corresponding ones for short-duration motions. This is explained by the duration and by the low intensity tail of long-duration motions that tend to assist the systems in reducing the residual displacements.

Results in Appendix D also show that in some cases there are notable differences between the distributions based on the empirical data and the fitted lognormal distributions of maximum resultant displacements. This is mostly observed in cases where friction is high, and the seismic intensity is low. An example is provided in Figure 6-3 for the single FP system 34 (T_P=4.93s, μ_{ref}=0.10), when S_{M1}=0.7g, in long-duration ground motions and when the friction coefficient-temperature relationship is given by equation (2-7), in which friction drops from the starting value at 20^{o}C to a value equal to half that at temperature of about 200^{o}C. In this case, the fitted lognormal distribution does not properly represent the empirical data.

Four types of goodness-of-fit statistical tests were performed to check whether the data could be represented with lognormal distributions: a) The One-sample Kolmogorov-Smirnov test (Massey, 1951), b) the Chi-square test (Pearson, 1900), c) the Lilliefors test (Lilliefors, 1969) and d) the Jarque-Bera test (Jarque and

Bera, 1987). Kumar et al. (2015) have used the same goodness-of-fit tests. Computations were performed using functions "kstest", "Chi2gof", "lillietest" and "jbtest" for the four tests, respectively, in program MATLAB (Mathworks, 2020). The results are in terms of a test parameter, h, having either a value of 1 (failed to fit) or zero (fitted). For the case of the single FP system 34 of Figure 6-3, the One-sample Kolmogorov-Smirnov goodness-of-fit test showed acceptable fit of the empirical data with a lognormal distribution, whereas the other three tests did not. Appendix D, and Appendices E and F for the triple FP and the lead-rubber systems report results of the four goodness-of-fit tests for each of the 288 systems studied. The differences between empirical results and fitted lognormal distributions are important only for some of the single FP systems, but not for the triple FP and the lead-rubber systems. The interested reader may use the results in the appendices to decide on the use of the lognormally fitted distributions.

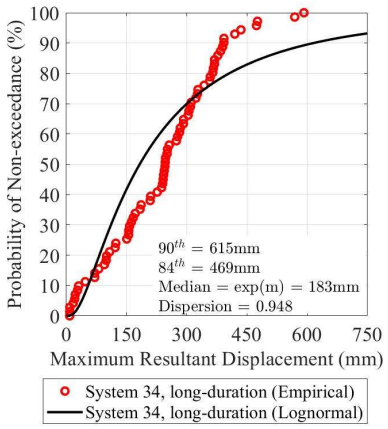

Figure 6-3 Empirical and Fitted Distributions of Maximum Resultant Displacement for Single FP System 34 (T_P = 4.93s, μ_{ref} = 0.10) when S_{M1} = 0.7g (friction case when k_T=0.5 at 200°C) in Long-Duration Ground Motions

Figure 6-4 presents results on the computed histories of cumulative energy, and Figure 6-5 presents results on the computed histories of temperature at the sliding interface for the single FP system 31 (T_P=4.93s, μ_{ref} =0.04) when S_{M1}=0.9g and the friction coefficient-temperature relationship is given by equation (2-7), in which friction drops from the starting value at 20°C to a value equal to half that at temperature of about 200°C.

The computation of the "empirical" percentile histories of these quantities was performed by counting of the empirical data from 71 analyses at each time step after shifting in time as explained below. The computation for the "lognormal" percentile histories of these quantities was performed by first fitting the

data of the 71 analyses at each time step, after shifting in time, with a lognormal distribution, and then using the fitted distributions to compute the median and 90th percentile values at each time step. Prior to any statistical calculations, the calculated histories of cumulative energy and temperature had to be shifted in time due to significant differences in the duration of the ground motions, including a portion at the start where the response was negligible. The starting point in time was selected to be when the total temperature was 20.5^{o}C (the rise in temperature above the starting temperature was 0.5^{o}C) and when the cumulative energy reached 5kN-m.

The results in Figures 6-4 and 6-5 show small differences between the empirical and the fitted lognormal distribution results-something that was systematically observed for low friction systems. Another example is provided in Figure 6-6 for the high friction single FP system 34 (T_P =4.93s, μ_{ref} =0.10), when S_{M1} =0.7g, long-duration ground motions and the friction coefficient-temperature relationship is given by equation (2-7), where the median (50th percentile) and 90th percentile cumulative energy and temperature histories are compared. In this case the empirical and lognormal histories of cumulative energy differ significantly, but the histories of temperature do not.

Goodness-of-fit tests were also performed for the lognormally fitted cumulative energy and temperature histories at each time step. Results are presented for the test parameter h as function of time and as percent passing rate for each of the 288 studied systems in Appendices D, E and F. Tables 6-7 and 6-8 present results of the goodness-of-fit tests for the Single FP System 31 (T_P =4.93s, μ_{ref} =0.04) when S_{M1} =0.9g (friction case when k_T =0.5 at 200^{o}C), for which the histories of cumulative energy and temperature are presented in Figures 6-4 and 6-5. The test passing rates are never equal to 100% as for some times the fitting fails. The reader may decide on which passing rate is acceptable-we consider that the lognormal distributions properly fit the empirical data when the passing rate is larger than 80% in at least two of the fitness tests.

The cumulative energy was computed by numerical integration of the force-displacement in each of the two principal directions and then calculating the sum of the two as done in past studies of Warn and Whittaker (2004) and Kitayama and Constantinou (2021).

The histories of cumulative energy and temperature at the sliding interface will be used in Section 7 for the development of tests that assess the adequacy of isolators in the maximum considered earthquake. In this report, and for the purpose of designing experiments to represent the effects of the maximum earthquake in Section 7, only the empirical distributions are used.

Of interest is to note in Figures 6-5 and 6-5, and many more similar figures in Appendix D, the significant differences in the final values of the cumulative energy and the peak values of temperature between the long- and short-duration motions.

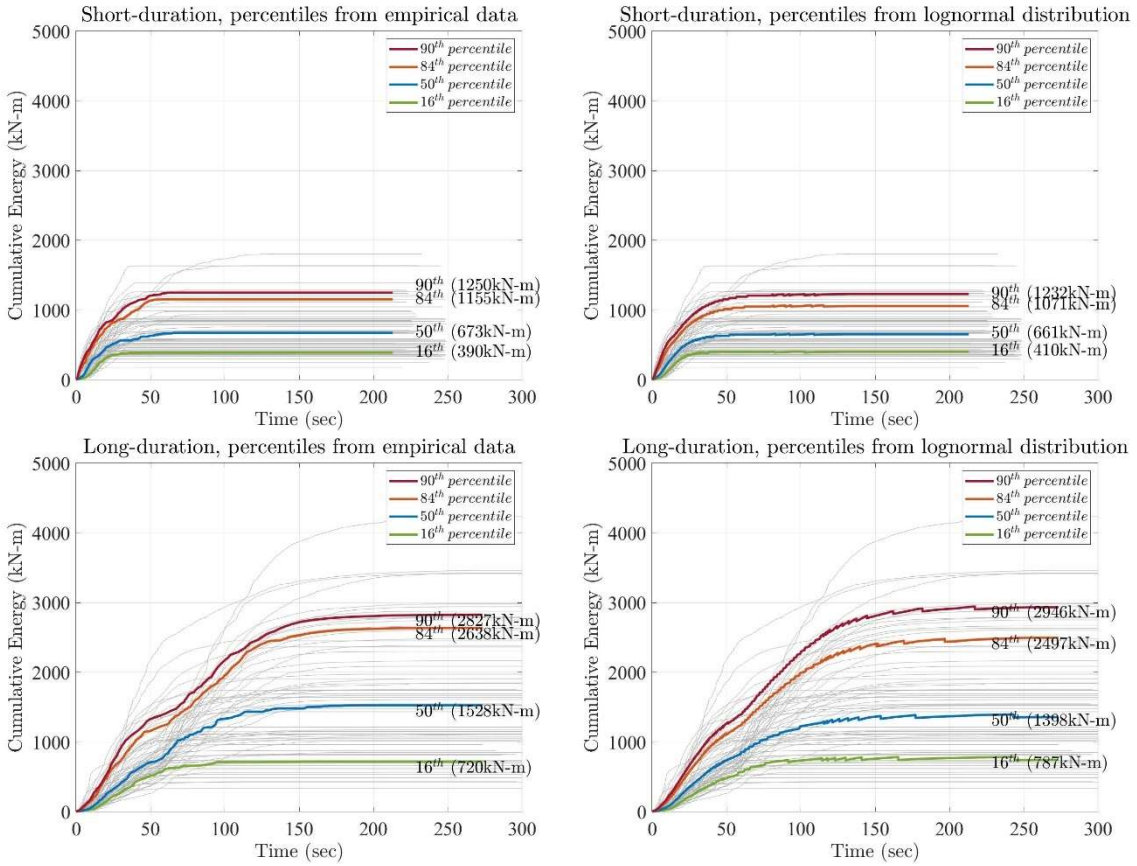

Figure 6-4 Cumulative Energy Histories for Single FP System 31

(T_P = 4.93s, μ_{ref} = 0.04) when S_{M1} = 0.9g (friction case when k_T=0.5 at 200°C)

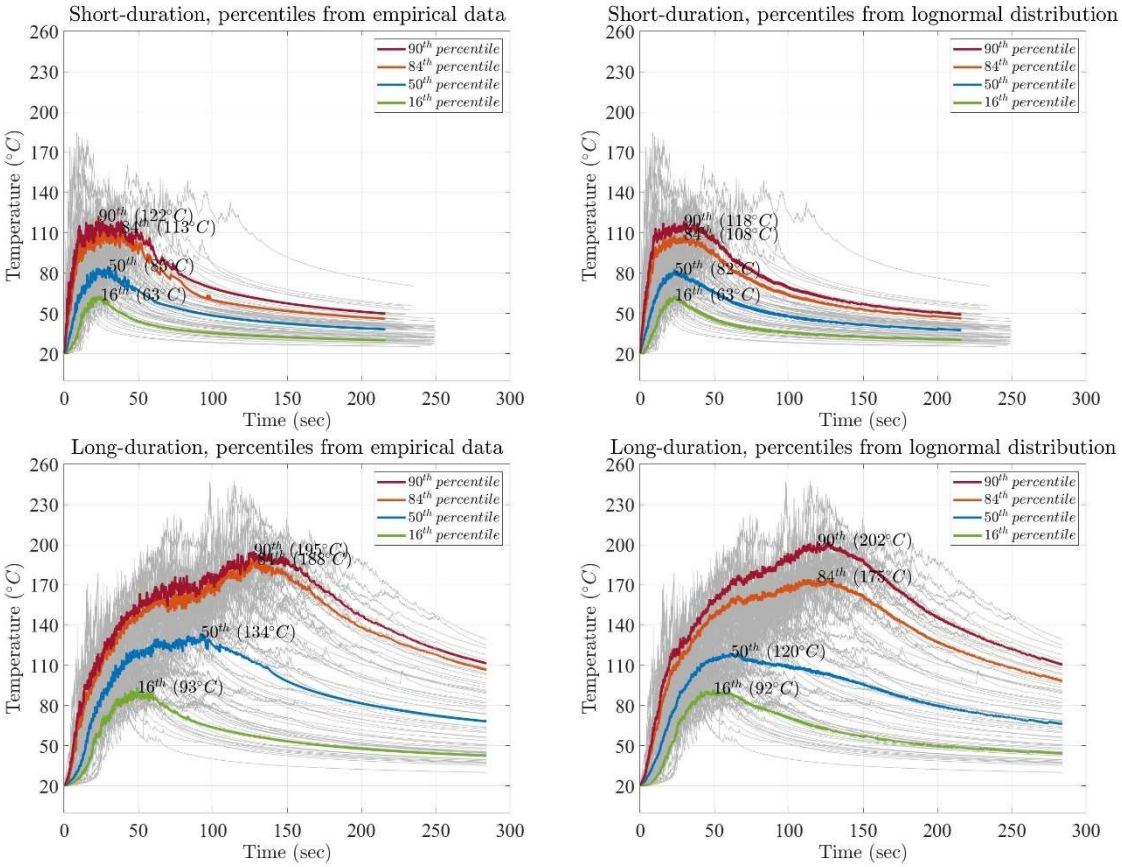

Figure 6-5 Histories of Temperature at the Sliding Interface for Single FP System 31 (T_P = 4.93s, μ_{ref} = 0.04) when S_{M1} = 0.9g (friction case when k_T=0.5 at 200°C)

Table 6-7 Goodness-of-Fit Results for Lognormal Distributions of Cumulative Energy Histories for Single FP System 31 (T_P = 4.93s, μ_{ref} = 0.04) when S_{M1} = 0.9g (friction case when k_T=0.5 at 200°C)

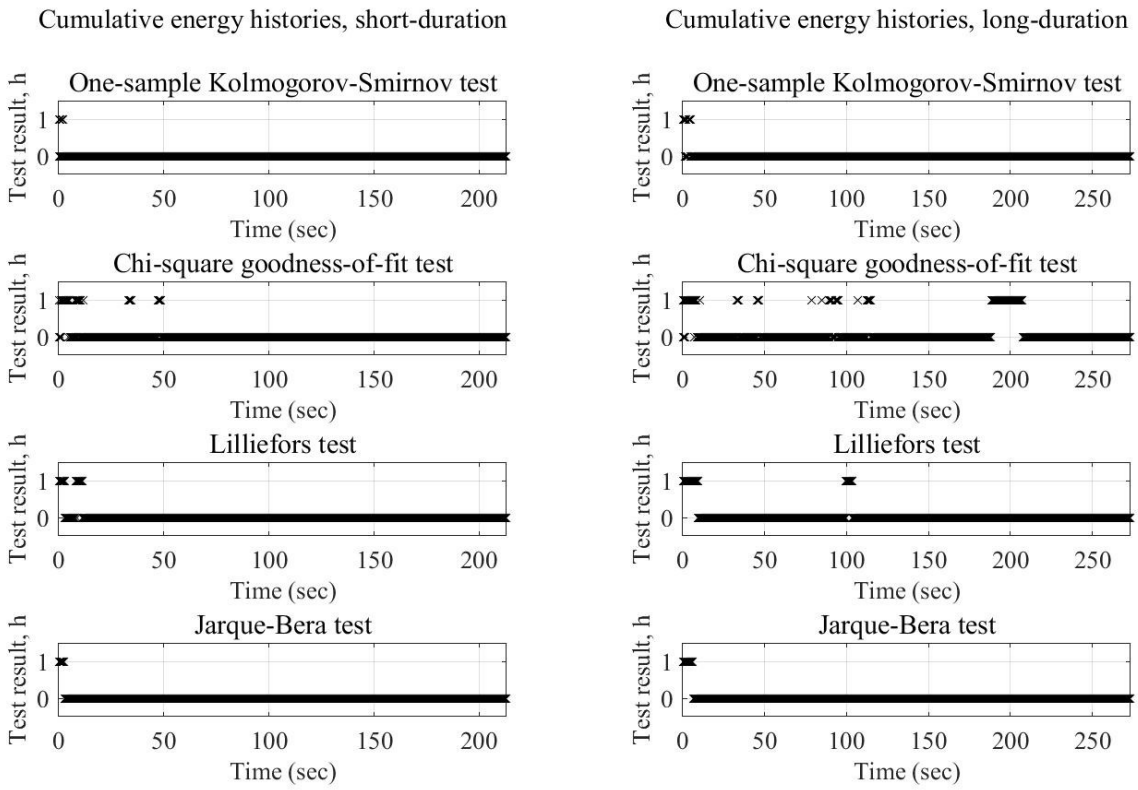

Goodness-of-fit test	Test Passing Rate (%)	
	Short-duration	Long-duration
One-sample Kolmogorov-Smirnov	99.8	99.0
Chi-square	95.7	86.8
Lilliefors	97.2	95.0
Jarque-Bera	98.7	97.7

Table 6-8 Goodness-of-Fit Results for Lognormal Distributions of Temperature Histories for Single FP System 31 (T_P = 4.93s, μ_{ref} = 0.04) when S_{M1} = 0.9g (friction case when k_T=0.5 at 200°C)

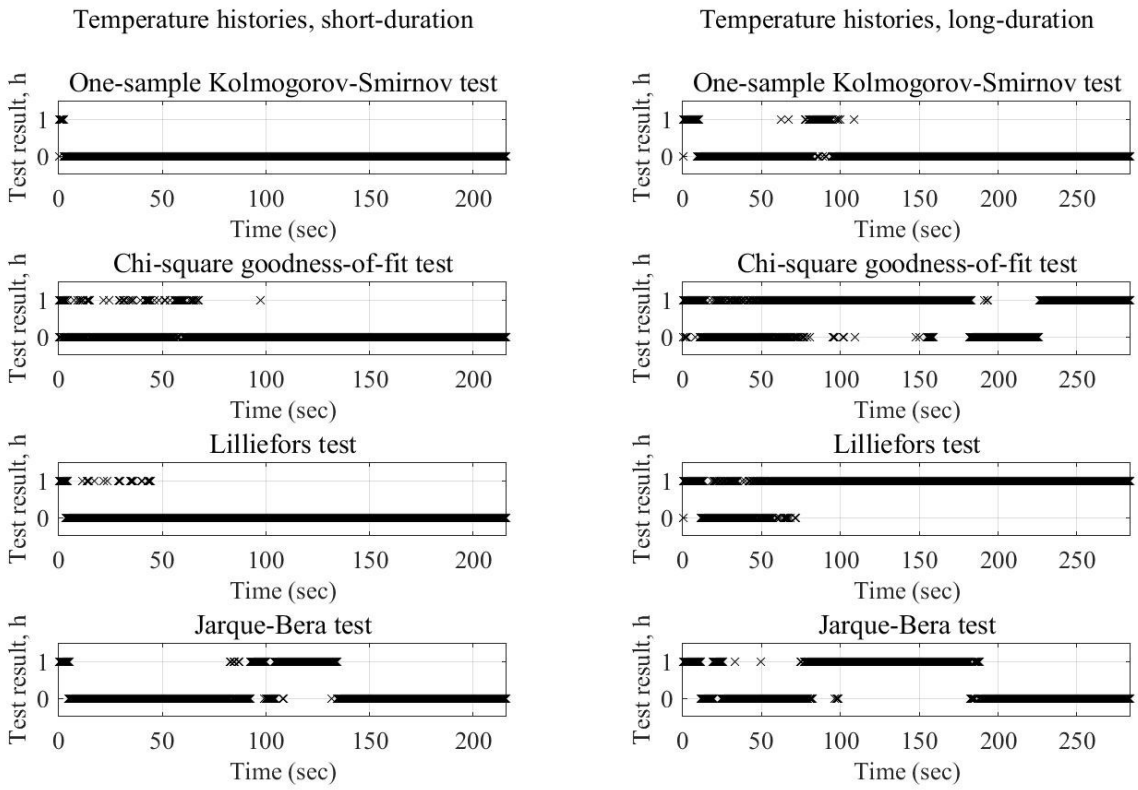

Goodness-of-fit test	Test Passing Rate (%)	
	Short-duration	Long-duration
One-sample Kolmogorov-Smirnov	98.8	91.9
Chi-square	95.5	31.0
Lilliefors	97.2	12.9
Jarque-Bera	80.1	56.9

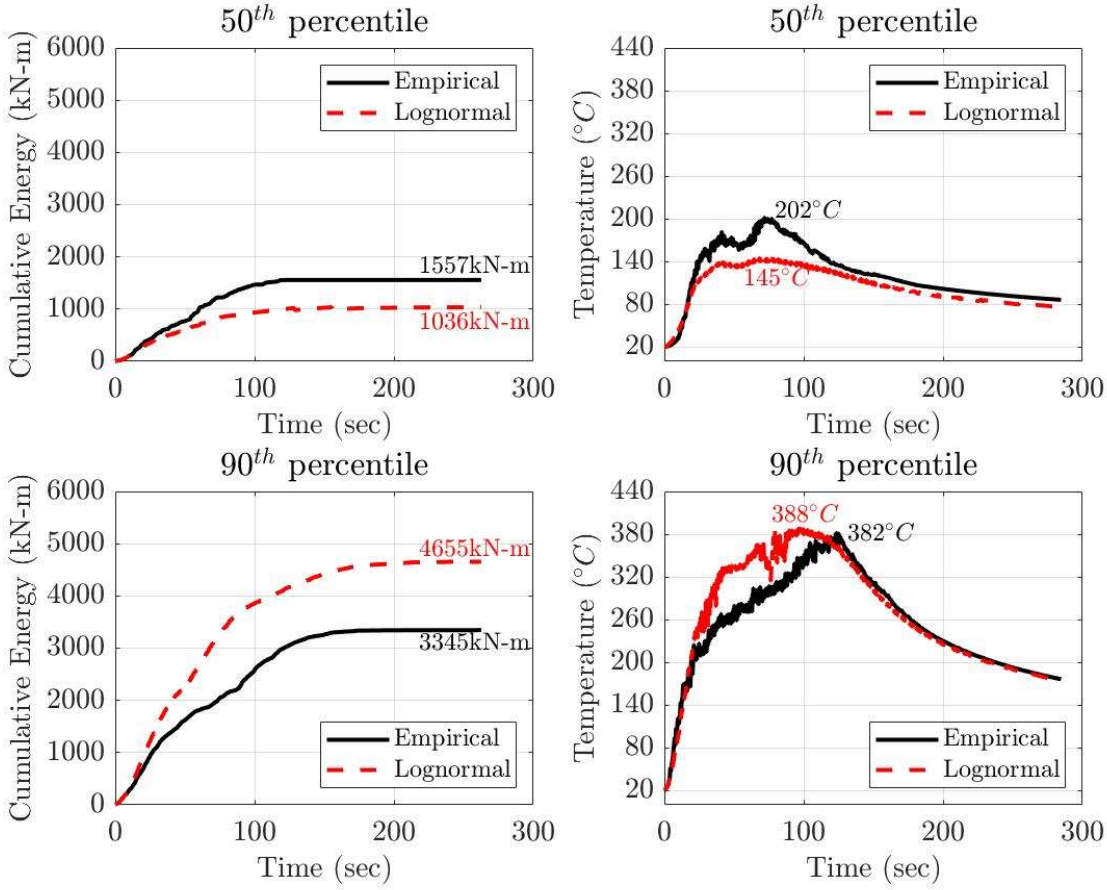

Figure 6-6 Empirical and Fitted Lognormal Distributions of Cumulative Energy and Temperature Histories for Single FP System 34 (T_P = 4.93s, μ_{ref} = 0.10) when S_{M1} = 0.7g (friction case when k_T=0.5 at 200ºC) in Long-Duration Ground Motions

6.3 Results for Triple FP Isolation Systems

Tables 6-9 to 6-16 present results on the resultant maximum displacements and residual displacements for the triple FP systems. The results include values of mean, median, 84^{th} and 90^{th} percentile counted values from the empirical data. Also, the tables present values of the 90^{th} percentile isolator maximum resultant displacement to the mean value, which can be utilized in the design of isolators. The results in Tables 6-9 to 6-16 show that a value of for the 90^{th}/mean scale factor for the isolator displacement of triple FP systems is 1.3 to 1.5, which a little smaller than the values of 1.4 to 1.6 computed for the single FP isolation systems in Section 6.2. The special triple FP system LL has a larger scale factor that is close to that for the single FP system, due likely to the heating effects that are continuous rather than intermittent as in all other cases of studied triple FP systems.

As in the case of the single FP systems, the values of the scale factor for long-duration ground motions are a little smaller than those for the short-duration motions.

Table 6-9 Mean and Median Resultant Maximum Displacements and Residual Displacements of Triple FP Systems for S_{M1}=0.7g

	k_T = 2/3 at 200°C								k_T = 1/2 at 200°C								k_T = 1/3 at 200°C							
	Maximum Resultant Displacement (mm)				Residual Resultant Displacement (mm)				Maximum Resultant Displacement (mm)				Residual Resultant Displacement (mm)				Maximum Resultant Displacement (mm)				Residual Resultant Displacement (mm)			
	Short-duration		Long-duration		Short-duration		Long-duration		Short-duration		Long-duration		Short-duration		Long-duration		Short-duration		Long-duration		Short-duration		Long-duration	
	Median	Mean	Median	Mean	Median	Mean	Median	Mean	Median	Mean	Median	Mean	Median	Mean	Median	Mean	Median	Mean	Median	Mean	Median	Mean	Median	Mean
System 11 T_P = 3.40 sec μ_{ref} = 0.037	321	341	304	308	4	7	2	3	338	366	333	331	4	6	2	3	360	397	358	360	4	6	2	2
System 21 T_P = 4.13 sec μ_{ref} = 0.038	324	356	337	338	6	9	3	4	338	381	372	366	6	9	3	4	370	410	404	400	5	9	3	4
System 31 T_P = 4.86 sec μ_{ref} = 0.038	342	364	362	352	8	12	4	6	364	387	389	381	7	12	3	6	399	413	420	419	7	10	3	6
System 41 T_P = 5.57 sec μ_{ref} = 0.039	398	377	365	358	10	17	5	8	419	403	396	388	10	15	5	8	432	430	438	429	9	14	4	7
System 12 T_P = 3.40 sec μ_{ref} = 0.054	266	286	249	257	6	7	4	4	300	307	284	279	4	7	3	3	323	336	310	307	4	7	2	3
System 22 T_P = 4.13 sec μ_{ref} = 0.056	272	296	257	279	9	13	5	6	282	317	289	302	7	10	4	5	311	347	333	334	7	9	3	5
System 32 T_P = 4.86 sec μ_{ref} = 0.057	298	307	284	288	12	18	7	9	298	327	313	314	11	16	6	8	334	351	360	348	9	13	5	8
System 42 T_P = 5.57 sec μ_{ref} = 0.058	313	316	289	295	16	23	9	11	310	336	317	318	15	21	8	11	350	359	357	350	12	19	7	10
System 13 T_P = 3.40 sec μ_{ref} = 0.070	239	257	229	229	7	11	5	5	257	276	247	248	7	9	4	5	296	303	284	278	6	8	3	4
System 23 T_P = 4.13 sec μ_{ref} = 0.074	256	268	244	247	14	16	7	8	266	286	258	268	12	15	6	7	287	312	290	300	9	13	5	6
System 33 T_P = 4.86 sec μ_{ref} = 0.075	268	277	252	256	17	21	10	11	286	295	273	277	15	20	9	10	315	322	316	310	13	19	6	9
System 43 T_P = 5.57 sec μ_{ref} = 0.076	274	285	260	264	22	27	12	15	311	304	283	283	20	25	11	13	321	330	312	315	17	23	10	12
System 14 T_P = 3.40 sec μ_{ref} = 0.087	216	241	207	214	9	12	6	7	241	258	231	229	8	11	5	6	263	283	256	258	8	10	4	5
System 24 T_P = 4.13 sec μ_{ref} = 0.091	231	253	211	228	13	17	11	11	251	269	243	248	14	17	8	9	272	292	274	279	13	16	6	8
System 34 T_P = 4.86 sec μ_{ref} = 0.094	249	262	241	238	20	23	14	16	273	278	254	257	19	22	12	13	311	302	285	288	16	21	9	11
System 44 T_P = 5.57 sec μ_{ref} = 0.095	258	270	248	248	26	30	18	21	281	287	264	266	23	28	14	17	320	311	297	295	21	26	12	14

μ_{ref} is the starting value of the coefficient of friction prior to any heating effects

Table 6-10 Mean, 84th Percentile and 90th Percentile Resultant Maximum Displacements of Triple FP Systems for S_{M1}=0.7g

	k_T = 2/3 at 200°C								k_T = 1/2 at 200°C								k_T = 1/3 at 200°C							
	Short-duration				Long-duration				Short-duration				Long-duration				Short-duration				Long-duration			
	Mean	84th	90th	90th / Mean	Mean	84th	90th	90th / Mean	Mean	84th	90th	90th / Mean	Mean	84th	90th	90th / Mean	Mean	84th	90th	90th / Mean	Mean	84th	90th	90th / Mean
System 11 T_P = 3.40 sec μ_{ref} = 0.037	341	464	526	**1.54**	308	390	434	**1.41**	366	514	553	**1.51**	331	425	447	**1.35**	397	538	574	**1.45**	360	436	477	**1.33**
System 21 T_P = 4.13 sec μ_{ref} = 0.038	356	495	510	**1.43**	338	433	472	**1.40**	381	509	563	**1.48**	366	462	497	**1.36**	410	537	600	**1.46**	400	506	528	**1.32**
System 31 T_P = 4.86 sec μ_{ref} = 0.038	364	495	511	**1.40**	352	467	493	**1.40**	387	511	540	**1.40**	381	498	529	**1.39**	413	549	598	**1.45**	419	545	574	**1.37**
System 41 T_P = 5.57 sec μ_{ref} = 0.039	377	512	583	**1.55**	358	486	518	**1.45**	403	571	644	**1.60**	388	534	550	**1.42**	430	607	704	**1.64**	429	581	609	**1.42**
System 12 T_P = 3.40 sec μ_{ref} = 0.054	286	399	433	**1.51**	257	336	373	**1.45**	307	426	464	**1.51**	279	371	410	**1.47**	336	465	517	**1.54**	307	408	428	**1.39**
System 22 T_P = 4.13 sec μ_{ref} = 0.056	296	426	484	**1.64**	279	389	413	**1.48**	317	466	498	**1.57**	302	419	435	**1.44**	347	502	512	**1.48**	334	444	470	**1.41**
System 32 T_P = 4.86 sec μ_{ref} = 0.057	307	436	506	**1.65**	288	404	428	**1.49**	327	460	514	**1.57**	314	446	464	**1.48**	351	498	513	**1.46**	348	483	503	**1.45**
System 42 T_P = 5.57 sec μ_{ref} = 0.058	316	456	512	**1.62**	295	404	440	**1.49**	336	496	514	**1.53**	318	443	481	**1.51**	359	513	535	**1.49**	350	495	525	**1.50**
System 13 T_P = 3.40 sec μ_{ref} = 0.070	257	356	396	**1.54**	229	308	343	**1.50**	276	387	409	**1.48**	248	326	377	**1.52**	303	425	453	**1.50**	278	373	410	**1.47**
System 23 T_P = 4.13 sec μ_{ref} = 0.074	268	362	405	**1.51**	247	347	368	**1.49**	286	378	427	**1.49**	268	380	395	**1.47**	312	470	496	**1.59**	300	420	445	**1.48**
System 33 T_P = 4.86 sec μ_{ref} = 0.075	277	367	445	**1.61**	256	353	376	**1.47**	295	414	482	**1.63**	277	392	415	**1.50**	322	457	504	**1.57**	310	447	468	**1.51**
System 43 T_P = 5.57 sec μ_{ref} = 0.076	285	400	481	**1.69**	264	354	369	**1.40**	304	429	509	**1.67**	283	390	418	**1.48**	330	478	514	**1.56**	315	446	477	**1.51**
System 14 T_P = 3.40 sec μ_{ref} = 0.087	241	340	392	**1.63**	214	290	316	**1.48**	258	356	401	**1.55**	229	307	350	**1.53**	283	393	413	**1.46**	258	345	383	**1.48**
System 24 T_P = 4.13 sec μ_{ref} = 0.091	253	340	392	**1.55**	228	312	342	**1.50**	269	371	407	**1.51**	248	353	367	**1.48**	292	389	436	**1.49**	279	396	420	**1.51**
System 34 T_P = 4.86 sec μ_{ref} = 0.094	262	359	416	**1.59**	238	327	349	**1.47**	278	372	440	**1.58**	257	361	385	**1.50**	302	422	471	**1.56**	288	410	436	**1.51**
System 44 T_P = 5.57 sec μ_{ref} = 0.095	270	362	451	**1.67**	248	339	368	**1.48**	287	388	464	**1.62**	266	362	375	**1.41**	311	445	502	**1.61**	295	411	431	**1.46**
Average 90th / Mean				**1.57**				**1.46**				**1.54**				**1.46**				**1.52**				**1.45**

μ_{ref} is the starting value of the coefficient of friction prior to any heating effects

Table 6-11 Mean and Median Resultant Maximum Displacements and Residual Displacements of Triple FP Systems for S_{M1}=0.9g

	k_T = 2/3 at 200°C								k_T = 1/2 at 200°C								k_T = 1/3 at 200°C							
	Maximum Resultant Displacement (mm)				Residual Resultant Displacement (mm)				Maximum Resultant Displacement (mm)				Residual Resultant Displacement (mm)				Maximum Resultant Displacement (mm)				Residual Resultant Displacement (mm)			
	Short-duration		Long-duration		Short-duration		Long-duration		Short-duration		Long-duration		Short-duration		Long-duration		Short-duration		Long-duration		Short-duration		Long-duration	
	Median	Mean	Median	Mean	Median	Mean	Median	Mean	Median	Mean	Median	Mean	Median	Mean	Median	Mean	Median	Mean	Median	Mean	Median	Mean	Median	Mean
System 11 T_P = 3.40 sec μ_{ref} = 0.037	470	510	461	462	5	8	2	3	490	543	499	498	5	7	2	3	517	580	549	546	5	7	2	3
System 21 T_P = 4.13 sec μ_{ref} = 0.038	505	532	512	515	7	11	4	5	544	567	538	556	6	11	3	4	560	604	601	605	5	9	2	4
System 31 T_P = 4.86 sec μ_{ref} = 0.038	539	543	542	541	9	14	4	7	561	579	581	586	9	15	4	6	592	615	622	637	8	14	3	5
System 41 T_P = 5.57 sec μ_{ref} = 0.039	559	570	555	559	12	17	5	8	578	612	599	608	12	19	5	8	625	650	674	667	11	20	4	7
System 12 T_P = 3.40 sec μ_{ref} = 0.054	402	428	387	390	6	10	3	4	433	467	421	428	6	8	3	4	466	517	479	477	5	8	3	4
System 22 T_P = 4.13 sec μ_{ref} = 0.056	407	444	419	422	10	14	4	6	440	482	472	467	8	12	4	6	484	530	528	521	8	13	4	5
System 32 T_P = 4.86 sec μ_{ref} = 0.057	428	453	449	438	13	17	6	9	469	488	496	484	12	17	5	8	513	530	539	545	10	15	4	8
System 42 T_P = 5.57 sec μ_{ref} = 0.058	463	466	441	444	17	24	8	12	531	501	503	492	15	23	6	11	556	551	568	555	15	20	5	10
System 13 T_P = 3.40 sec μ_{ref} = 0.070	368	379	346	347	8	10	4	5	398	414	382	381	7	11	3	4	434	468	421	432	6	10	3	4
System 23 T_P = 4.13 sec μ_{ref} = 0.074	359	391	348	374	12	15	6	8	385	427	402	410	10	15	5	7	439	477	480	468	9	14	4	6
System 33 T_P = 4.86 sec μ_{ref} = 0.075	386	404	386	386	17	23	9	12	385	434	431	425	15	19	8	10	456	480	499	482	14	19	6	9
System 43 T_P = 5.57 sec μ_{ref} = 0.076	425	414	395	393	24	30	13	16	445	443	433	429	17	26	10	14	498	488	494	487	16	23	7	12
System 14 T_P = 3.40 sec μ_{ref} = 0.087	330	353	318	320	9	13	6	6	376	383	347	350	8	11	4	5	406	431	401	399	7	10	3	4
System 24 T_P = 4.13 sec μ_{ref} = 0.091	343	365	333	345	15	20	8	10	363	394	354	376	13	16	6	8	400	443	437	429	9	13	5	7
System 34 T_P = 4.86 sec μ_{ref} = 0.094	366	377	351	355	20	26	12	14	391	405	380	387	17	25	9	12	429	446	460	444	13	18	7	11
System 44 T_P = 5.57 sec μ_{ref} = 0.095	388	386	368	364	28	34	16	19	425	416	400	392	22	31	13	16	445	454	458	448	18	27	9	15

μ_{ref} is the starting value of the coefficient of friction prior to any heating effects

Table 6-12 Mean, 84th Percentile and 90th Percentile Resultant Maximum Displacements of Triple FP Systems for S_{M1}=0.9g

	k_T = 2/3 at 200°C								k_T = 1/2 at 200°C								k_T = 1/3 at 200°C							
	Short-duration				Long-duration				Short-duration				Long-duration				Short-duration				Long-duration			
	Mean	84th	90th	90th / Mean	Mean	84th	90th	90th / Mean	Mean	84th	90th	90th / Mean	Mean	84th	90th	90th / Mean	Mean	84th	90th	90th / Mean	Mean	84th	90th	90th / Mean
System 11 T_P = 3.40 sec μ_{ref} = 0.037	510	693	752	**1.47**	462	560	604	**1.31**	543	741	791	**1.46**	498	605	644	**1.29**	580	742	808	**1.39**	546	659	692	**1.27**
System 21 T_P = 4.13 sec μ_{ref} = 0.038	532	685	762	**1.43**	515	641	685	**1.33**	567	712	769	**1.36**	556	684	721	**1.30**	604	737	819	**1.36**	605	737	765	**1.26**
System 31 T_P = 4.86 sec μ_{ref} = 0.038	543	719	781	**1.44**	541	698	722	**1.33**	579	771	859	**1.48**	586	735	800	**1.37**	615	833	924	**1.50**	637	800	849	**1.33**
System 41 T_P = 5.57 sec μ_{ref} = 0.039	570	814	897	**1.57**	559	729	767	**1.37**	612	906	1009	**1.65**	608	786	826	**1.36**	650	940	1085	**1.67**	667	848	903	**1.35**
System 12 T_P = 3.40 sec μ_{ref} = 0.054	428	564	642	**1.50**	390	494	551	**1.41**	467	646	686	**1.47**	428	544	574	**1.34**	517	696	737	**1.43**	477	593	627	**1.31**
System 22 T_P = 4.13 sec μ_{ref} = 0.056	444	619	649	**1.46**	422	555	594	**1.41**	482	647	719	**1.49**	467	594	635	**1.36**	530	682	765	**1.44**	521	654	690	**1.32**
System 32 T_P = 4.86 sec μ_{ref} = 0.057	453	620	651	**1.44**	438	606	623	**1.42**	488	652	704	**1.44**	484	641	676	**1.40**	530	715	778	**1.47**	545	709	737	**1.35**
System 42 T_P = 5.57 sec μ_{ref} = 0.058	466	643	702	**1.51**	444	602	660	**1.49**	501	698	776	**1.55**	492	687	706	**1.43**	551	808	875	**1.59**	555	748	785	**1.41**
System 13 T_P = 3.40 sec μ_{ref} = 0.070	379	511	571	**1.51**	347	453	495	**1.43**	414	562	623	**1.50**	381	496	543	**1.43**	468	634	685	**1.46**	432	545	571	**1.32**
System 23 T_P = 4.13 sec μ_{ref} = 0.074	391	564	627	**1.60**	374	520	545	**1.46**	427	625	649	**1.52**	410	552	587	**1.43**	477	654	706	**1.48**	468	600	640	**1.37**
System 33 T_P = 4.86 sec μ_{ref} = 0.075	404	563	649	**1.61**	386	548	563	**1.46**	434	597	655	**1.51**	425	587	616	**1.45**	480	650	709	**1.48**	482	652	677	**1.40**
System 43 T_P = 5.57 sec μ_{ref} = 0.076	414	582	662	**1.60**	393	540	576	**1.47**	443	626	648	**1.46**	429	589	649	**1.51**	488	698	728	**1.49**	487	700	704	**1.45**
System 14 T_P = 3.40 sec μ_{ref} = 0.087	353	489	522	**1.48**	320	425	461	**1.44**	383	520	563	**1.47**	350	454	504	**1.44**	431	591	624	**1.45**	399	515	547	**1.37**
System 24 T_P = 4.13 sec μ_{ref} = 0.091	365	485	541	**1.48**	345	481	507	**1.47**	394	572	611	**1.55**	376	517	547	**1.45**	443	620	674	**1.52**	429	571	597	**1.39**
System 34 T_P = 4.86 sec μ_{ref} = 0.094	377	517	609	**1.62**	355	494	519	**1.46**	405	563	648	**1.60**	387	537	572	**1.48**	446	633	674	**1.51**	444	607	640	**1.44**
System 44 T_P = 5.57 sec μ_{ref} = 0.095	386	549	631	**1.63**	364	496	531	**1.46**	416	577	662	**1.59**	392	537	584	**1.49**	454	646	677	**1.49**	448	636	671	**1.50**
Average 90th / Mean				**1.52**				**1.42**				**1.51**				**1.41**				**1.48**				**1.37**

μ_{ref} is the starting value of the coefficient of friction prior to any heating effects

Table 6-13 Mean and Median Resultant Maximum Displacements and Residual Displacements of Triple FP Systems for S_{M1}=1.1g

	k_T = 2/3 at 200°C								k_T = 1/2 at 200°C								k_T = 1/3 at 200°C							
	Maximum Resultant Displacement (mm)				Residual Resultant Displacement (mm)				Maximum Resultant Displacement (mm)				Residual Resultant Displacement (mm)				Maximum Resultant Displacement (mm)				Residual Resultant Displacement (mm)			
	Short-duration		Long-duration		Short-duration		Long-duration		Short-duration		Long-duration		Short-duration		Long-duration		Short-duration		Long-duration		Short-duration		Long-duration	
	Median	Mean	Median	Mean	Median	Mean	Median	Mean	Median	Mean	Median	Mean	Median	Mean	Median	Mean	Median	Mean	Median	Mean	Median	Mean	Median	Mean
System 11 T_P = 3.40 sec μ_{ref} = 0.037	586	685	621	631	6	10	3	3	618	725	668	678	5	8	2	3	653	768	706	739	5	8	2	3
System 21 T_P = 4.13 sec μ_{ref} = 0.038	660	718	701	708	7	12	3	5	694	757	740	759	7	13	3	5	714	798	811	818	7	11	2	4
System 31 T_P = 4.86 sec μ_{ref} = 0.038	699	737	743	750	11	19	4	6	756	780	786	804	10	17	4	6	768	824	853	872	10	15	3	6
System 41 T_P = 5.57 sec μ_{ref} = 0.039	741	782	769	784	15	21	5	9	766	836	871	847	13	25	5	8	802	884	925	921	11	24	4	6
System 12 T_P = 3.40 sec μ_{ref} = 0.054	512	590	547	540	7	10	4	5	553	640	588	592	7	9	3	4	595	693	627	659	6	9	3	4
System 22 T_P = 4.13 sec μ_{ref} = 0.056	547	611	600	592	10	15	5	7	613	659	639	650	8	14	4	6	667	715	723	724	7	13	4	6
System 32 T_P = 4.86 sec μ_{ref} = 0.057	591	621	623	616	12	20	6	9	652	666	677	681	11	17	5	9	690	721	734	758	12	19	5	6
System 42 T_P = 5.57 sec μ_{ref} = 0.058	663	645	634	626	19	26	8	12	686	697	699	701	17	23	6	11	710	758	813	789	15	23	6	10
System 13 T_P = 3.40 sec μ_{ref} = 0.070	491	525	477	483	8	13	4	5	523	578	530	534	7	11	4	5	562	643	600	604	7	11	3	4
System 23 T_P = 4.13 sec μ_{ref} = 0.074	493	542	523	520	13	18	6	7	542	593	586	580	11	16	5	7	601	655	651	656	10	15	4	6
System 33 T_P = 4.86 sec μ_{ref} = 0.075	519	551	555	537	17	22	8	12	583	597	609	599	15	21	7	10	633	653	666	684	12	19	5	9
System 43 T_P = 5.57 sec μ_{ref} = 0.076	563	567	539	544	22	31	11	16	630	612	621	607	21	29	8	12	680	676	704	699	17	25	7	12
System 14 T_P = 3.40 sec μ_{ref} = 0.087	476	480	444	444	9	13	4	6	485	528	481	490	10	13	4	5	529	603	572	564	8	11	4	4
System 24 T_P = 4.13 sec μ_{ref} = 0.091	448	495	458	476	14	17	7	9	490	541	525	526	12	17	6	7	573	612	623	608	12	17	4	6
System 34 T_P = 4.86 sec μ_{ref} = 0.094	475	508	498	490	23	28	10	14	516	549	566	542	18	22	8	12	607	609	622	629	16	20	7	11
System 44 T_P = 5.57 sec μ_{ref} = 0.095	509	519	488	498	27	35	13	18	552	557	546	547	21	31	11	17	647	622	651	637	22	27	9	13

μ_{ref} is the starting value of the coefficient of friction prior to any heating effects

Table 6-14 Mean, 84th Percentile and 90th Percentile Resultant Maximum Displacements of Triple FP Systems for S_{M1}=1.1g

	k_T = 2/3 at 200°C								k_T = 1/2 at 200°C								k_T = 1/3 at 200°C							
	Short-duration				Long-duration				Short-duration				Long-duration				Short-duration				Long-duration			
	Mean	84th	90th	90th / Mean	Mean	84th	90th	90th / Mean	Mean	84th	90th	90th / Mean	Mean	84th	90th	90th / Mean	Mean	84th	90th	90th / Mean	Mean	84th	90th	90th / Mean
System 11 T_P = 3.40 sec μ_{ref} = 0.037	685	759	800	**1.17**	631	752	790	**1.25**	725	794	820	**1.13**	678	792	839	**1.24**	768	831	851	**1.11**	739	841	864	**1.17**
System 21 T_P = 4.13 sec μ_{ref} = 0.038	718	852	934	**1.30**	708	869	908	**1.28**	757	898	960	**1.27**	759	912	950	**1.25**	798	939	995	**1.25**	818	982	1005	**1.23**
System 31 T_P = 4.86 sec μ_{ref} = 0.038	737	983	1045	**1.42**	750	914	1004	**1.34**	780	1054	1125	**1.44**	804	974	1050	**1.31**	824	1082	1222	**1.48**	872	1055	1132	**1.30**
System 41 T_P = 5.57 sec μ_{ref} = 0.039	782	1135	1287	**1.65**	784	985	1058	**1.35**	836	1227	1421	**1.70**	847	1085	1120	**1.32**	884	1267	1483	**1.68**	921	1134	1208	**1.31**
System 12 T_P = 3.40 sec μ_{ref} = 0.054	590	719	798	**1.35**	540	666	710	**1.31**	640	783	834	**1.30**	592	726	773	**1.31**	693	765	792	**1.14**	659	770	829	**1.26**
System 22 T_P = 4.13 sec μ_{ref} = 0.056	611	786	860	**1.41**	592	747	792	**1.34**	659	829	877	**1.33**	650	804	858	**1.32**	715	855	936	**1.31**	724	898	914	**1.26**
System 32 T_P = 4.86 sec μ_{ref} = 0.057	621	829	876	**1.41**	616	803	834	**1.35**	666	900	960	**1.44**	681	872	924	**1.36**	721	944	1051	**1.46**	758	952	1014	**1.34**
System 42 T_P = 5.57 sec μ_{ref} = 0.058	645	894	1003	**1.56**	626	844	873	**1.39**	697	984	1108	**1.59**	701	914	964	**1.38**	758	1083	1194	**1.58**	789	1010	1067	**1.35**
System 13 T_P = 3.40 sec μ_{ref} = 0.070	525	687	757	**1.44**	483	608	669	**1.39**	578	721	810	**1.40**	534	670	702	**1.31**	643	806	830	**1.29**	604	735	786	**1.30**
System 23 T_P = 4.13 sec μ_{ref} = 0.074	542	757	795	**1.47**	520	684	724	**1.39**	593	785	875	**1.48**	580	740	784	**1.35**	655	822	891	**1.36**	656	825	862	**1.31**
System 33 T_P = 4.86 sec μ_{ref} = 0.075	551	763	791	**1.44**	537	730	763	**1.42**	597	795	874	**1.46**	599	785	824	**1.38**	653	866	944	**1.45**	684	881	928	**1.36**
System 43 T_P = 5.57 sec μ_{ref} = 0.076	567	777	847	**1.49**	544	746	813	**1.49**	612	852	928	**1.52**	607	841	859	**1.42**	676	984	1060	**1.57**	699	923	970	**1.39**
System 14 T_P = 3.40 sec μ_{ref} = 0.087	480	631	697	**1.45**	444	577	632	**1.42**	528	696	760	**1.44**	490	624	669	**1.37**	603	767	827	**1.37**	564	699	742	**1.32**
System 24 T_P = 4.13 sec μ_{ref} = 0.091	495	708	782	**1.58**	476	655	679	**1.43**	541	767	792	**1.46**	526	687	731	**1.39**	612	810	911	**1.49**	608	768	820	**1.35**
System 34 T_P = 4.86 sec μ_{ref} = 0.094	508	698	788	**1.55**	490	684	706	**1.44**	549	754	799	**1.46**	542	730	773	**1.43**	609	801	909	**1.49**	629	827	869	**1.38**
System 44 T_P = 5.57 sec μ_{ref} = 0.095	519	733	795	**1.53**	498	688	737	**1.48**	557	769	816	**1.46**	547	753	803	**1.47**	622	894	935	**1.50**	637	881	915	**1.44**
Average 90th / Mean				**1.45**				**1.38**				**1.43**				**1.35**				**1.41**				**1.32**

μ_{ref} is the starting value of the coefficient of friction prior to any heating effects

Table 6-15 Mean and Median Resultant Maximum Displacements and Residual Displacements of Additional Triple FP System LL

	S_{M1} = 0.7g							
	Maximum Resultant Displacement (mm)				Residual Resultant Displacement (mm)			
	Short-duration		Long-duration		Short-duration		Long-duration	
	Median	Mean	Median	Mean	Median	Mean	Median	Mean
k_T = 2/3 at 200°C	270	301	276	272	27	28	14	16
k_T = 1/2 at 200°C	297	319	283	288	23	26	12	15
k_T = 1/3 at 200°C	335	346	311	317	19	24	11	14
T_P = 5.49 sec, μ_{ref} = 0.074, μ_{1ref} = 0.08 μ_{ref} is the starting value of the ratio of zero-displacement force intercept and weight prior to any heating effects								

	S_{M1} = 0.9g							
	Maximum Resultant Displacement (mm)				Residual Resultant Displacement (mm)			
	Short-duration		Long-duration		Short-duration		Long-duration	
	Median	Mean	Median	Mean	Median	Mean	Median	Mean
k_T = 2/3 at 200°C	425	439	384	402	23	29	13	16
k_T = 1/2 at 200°C	457	470	429	437	18	26	11	15
k_T = 1/3 at 200°C	549	528	508	497	17	23	9	13
T_P = 5.49 sec, μ_{ref} = 0.074, μ_{1ref} = 0.08 μ_{ref} is the starting value of the ratio of zero-displacement force intercept and weight prior to any heating effects								

	S_{M1} = 1.1g							
	Maximum Resultant Displacement (mm)				Residual Resultant Displacement (mm)			
	Short-duration		Long-duration		Short-duration		Long-duration	
	Median	Mean	Median	Mean	Median	Mean	Median	Mean
k_T = 2/3 at 200°C	604	598	560	564	24	29	13	17
k_T = 1/2 at 200°C	700	666	632	632	21	27	9	14
k_T = 1/3 at 200°C	721	749	758	741	20	26	8	12
T_P = 5.49 sec, μ_{ref} = 0.074, μ_{1ref} = 0.08 μ_{ref} is the starting value of the ratio of zero-displacement force intercept and weight prior to any heating effects								

Table 6-16 Mean, 84th Percentile and 90th Percentile Resultant Maximum Displacements of Additional Triple FP System LL

	S_{M1} = 0.7g							
	Short-duration				Long-duration			
	Mean	84th	90th	90th / Mean	Mean	84th	90th	90th / Mean
k_T = 2/3 at 200°C	301	411	485	**1.61**	272	362	383	**1.41**
k_T = 1/2 at 200°C	319	442	511	**1.60**	288	394	408	**1.42**
k_T = 1/3 at 200°C	346	491	528	**1.53**	317	425	464	**1.46**

T_P = 5.49 sec, μ_{ref} = 0.074, μ_{1ref} = 0.08
μ_{ref} is the starting value of the ratio of zero-displacement force intercept and weight prior to any heating effects

	S_{M1} = 0.9g							
	Short-duration				Long-duration			
	Mean	84th	90th	90th / Mean	Mean	84th	90th	90th / Mean
k_T = 2/3 at 200°C	439	622	669	**1.52**	402	535	581	**1.45**
k_T = 1/2 at 200°C	470	660	707	**1.50**	437	597	640	**1.46**
k_T = 1/3 at 200°C	528	771	858	**1.63**	497	705	728	**1.46**

T_P = 5.49 sec, μ_{ref} = 0.074, μ_{1ref} = 0.08
μ_{ref} is the starting value of the ratio of zero-displacement force intercept and weight prior to any heating effects

	S_{M1} = 1.1g							
	Short-duration				Long-duration			
	Mean	84th	90th	90th / Mean	Mean	84th	90th	90th / Mean
k_T = 2/3 at 200°C	598	820	894	**1.49**	564	780	821	**1.46**
k_T = 1/2 at 200°C	666	954	1077	**1.62**	632	875	905	**1.43**
k_T = 1/3 at 200°C	749	1085	1191	**1.59**	741	998	1022	**1.38**

T_P = 5.49 sec, μ_{ref} = 0.074, μ_{1ref} = 0.08
μ_{ref} is the starting value of the ratio of zero-displacement force intercept and weight prior to any heating effects

Figures 6-7 and 6-8 present a sample of results on the distribution of the maximum resultant displacement and of the residual resultant displacement for the triple FP system 33 (μ_{1ref} =0.08, μ_{ref} =0.075, T_P =4.86s) when S_{M1} =0.9g. The results are for the case in which the friction coefficient-temperature relationship is given by equation (2-7), in which friction drops from the starting value at 20°C to a value equal to half that at temperature of about 200°C. Appendix E contains detailed results for all studied triple FP systems.

Median and dispersion values in each of Figures 6-7 and 6-8 may be used to construct the lognormal distributions which were fitted to the empirical data. The various percentile values listed in each figure are also fitted values. As also observed for single FP systems, triple FP systems have smaller residual displacements in long-duration ground motions than in short-duration ground motions.

Figures 6-9 and Figure 6-10 present sample results on the computed histories of cumulative energy and of temperature at the sliding interface for triple FP system 33 (μ_{1ref} =0.08, μ_{ref} =0.075, T_P =4.86s) when S_{M1} =0.9g and the friction coefficient-temperature relationship is given by equation (2-7), in which friction drops from the starting value at 20°C to a value equal to half that at temperature of about 200°C. Also, Tables 6-17 and 6-18 present results of the goodness-of-fit tests for the lognormal distributions of cumulative energy and temperature histories for the triple FP system 33 (μ_{1ref}=0.08, μ_{ref}=0.075, T_P =4.86s) when S_{M1} =0.9g (friction case when k_T =0.5 at 200°C), which were presented in Figures 6-9 and 6-10. Appendix E contains detailed results for all studied triple FP systems. The graphs include 16th, 50th (median), 84th and 90th percentile counted values (empirical data) and fitted values (based on lognormal distributions).

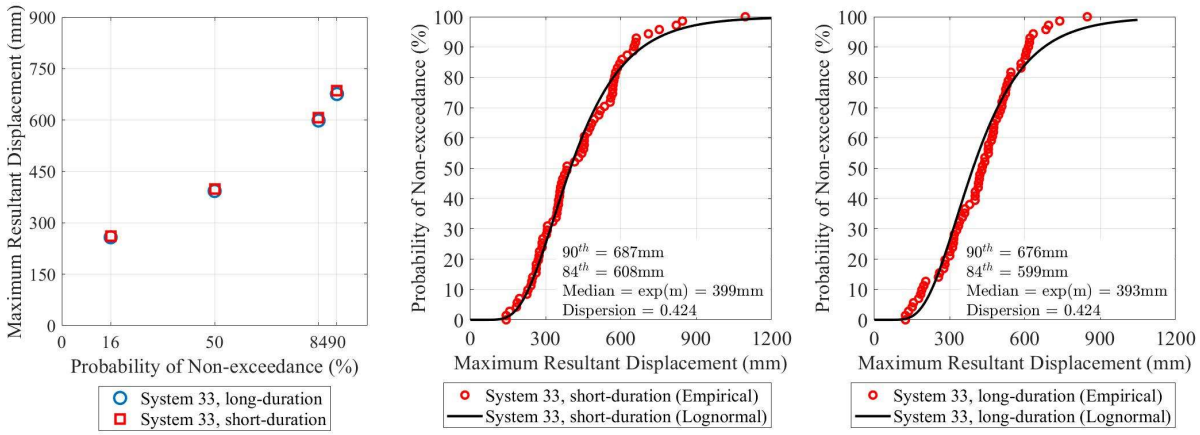

Figure 6-7 Distributions of Maximum Resultant Displacement for Triple FP System 33 (μ_{1ref} = 0.08, μ_{ref} = 0.075, T_P = 4.86s) when S_{M1} = 0.9g (friction case when k_T=0.5 at 200°C)

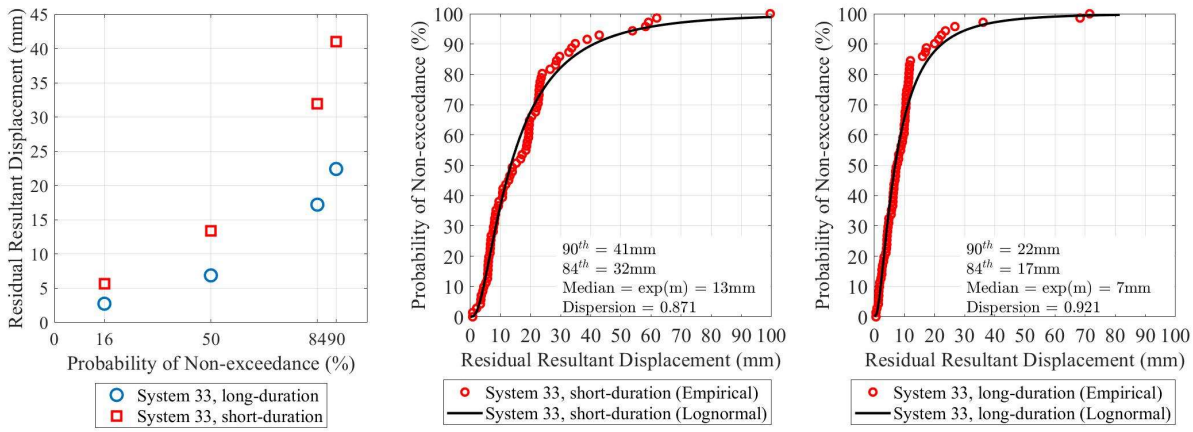

Figure 6-8 Distributions of Residual Resultant Displacement for Triple FP System 33 (μ_{1ref} = 0.08, μ_{ref} = 0.075, T_P = 4.86s) when S_{M1} = 0.9g (friction case when k_T=0.5 at 200°C)

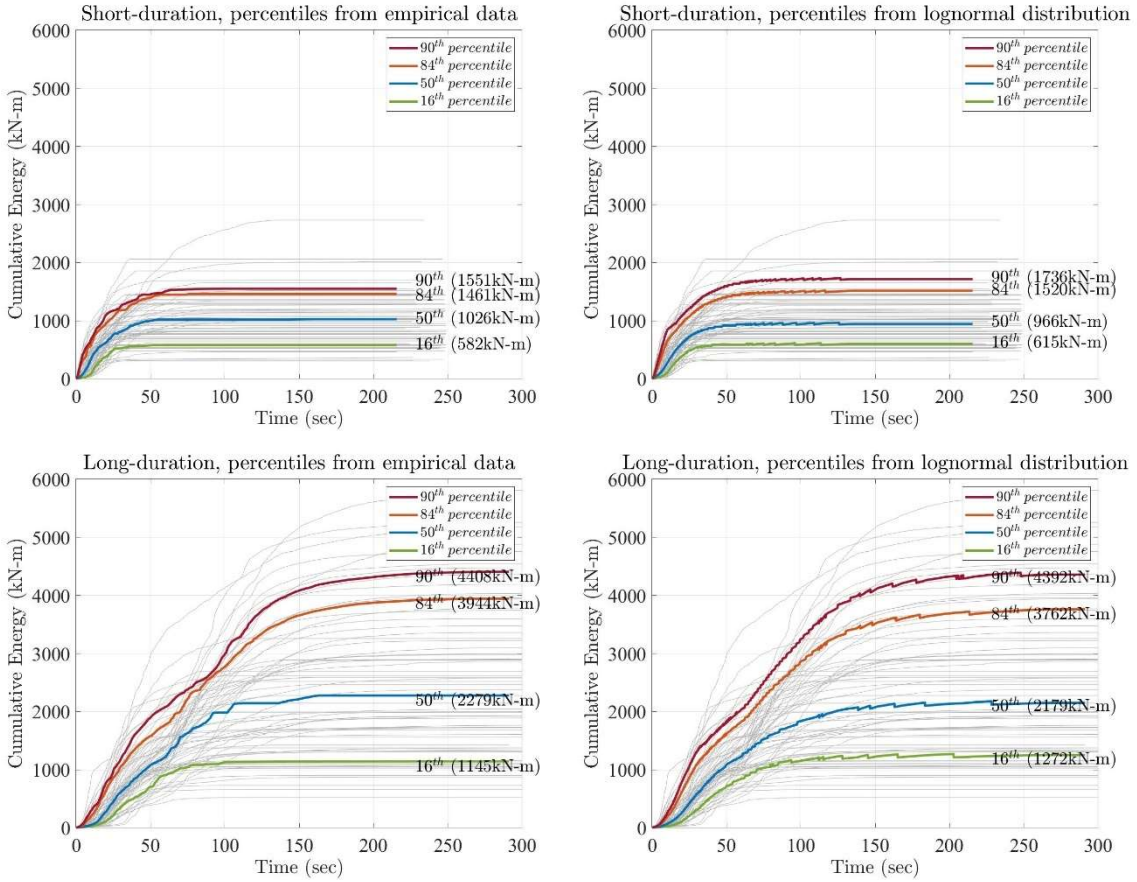

Figure 6-9 Histories of Cumulative Energy for Triple FP System 33 (μ_{1ref} = 0.08, μ_{ref} = 0.075, T_P = 4.86s) when S_{M1} = 0.9g (friction case when k_T=0.5 at 200°C)

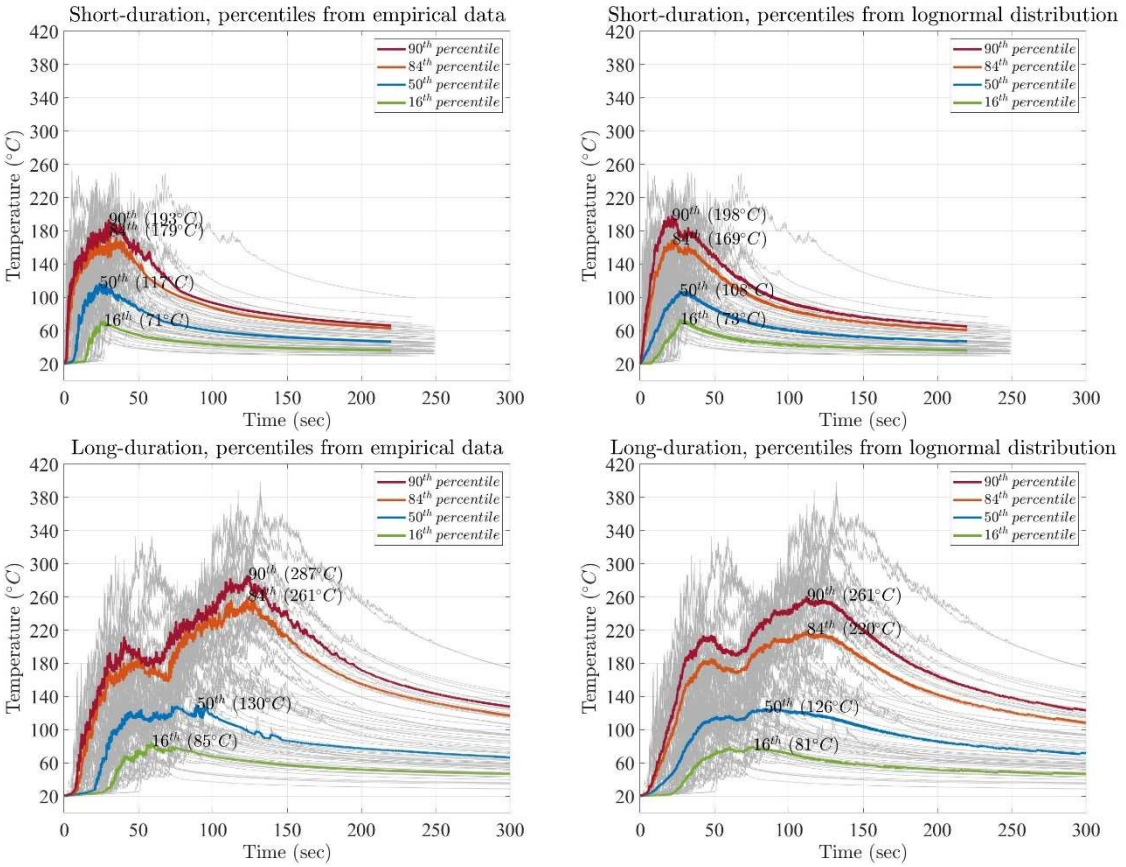

Figure 6-10 Histories of Temperature at the Sliding Interface for Triple FP System 33 (μ_{1ref} = 0.08, μ_{ref} = 0.075, T_P = 4.86s) when S_{M1} = 0.9g (friction case when k_T=0.5 at 200°C)

Table 6-17 Goodness-of-Fit Results for Lognormal Distributions of Cumulative Energy Histories for Triple FP System 33 (μ_{1ref} = 0.08, μ_{ref} = 0.075, T_P = 4.86s) when S_{M1} = 0.9g (friction case when k_T=0.5 at 200°C)

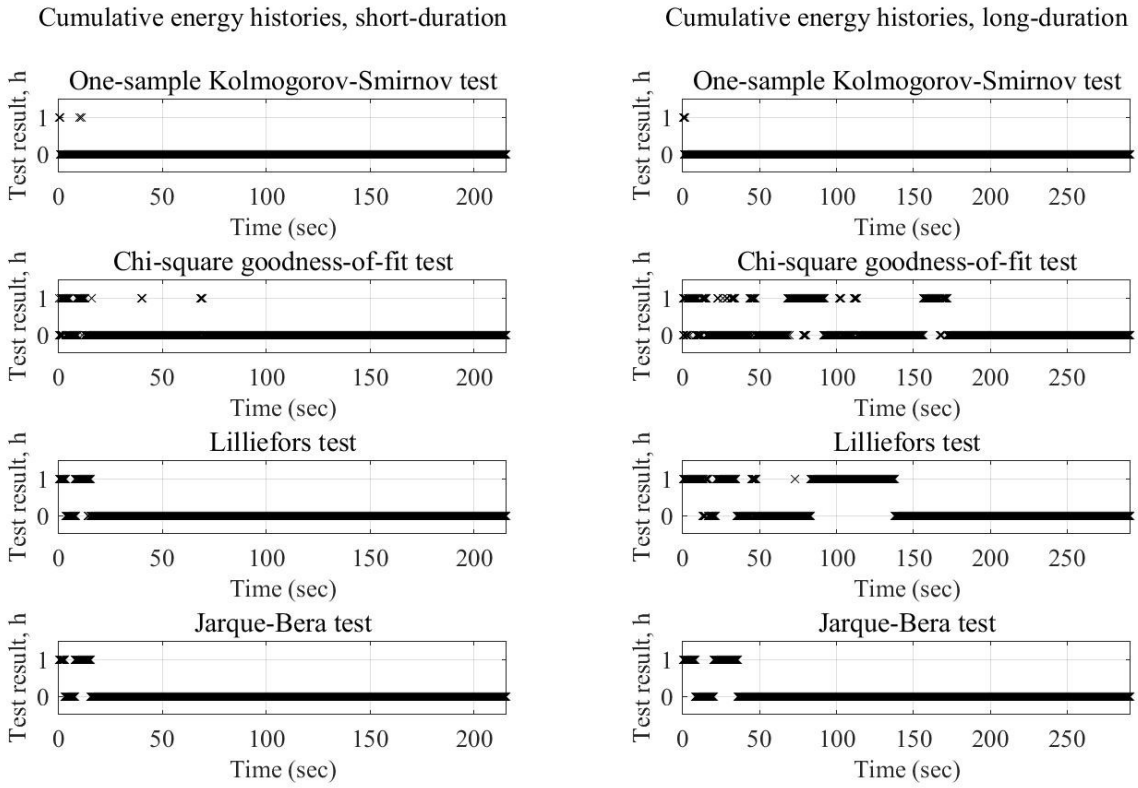

Goodness-of-fit test	Test Passing Rate (%)	
	Short-duration	Long-duration
One-sample Kolmogorov-Smirnov	99.6	99.5
Chi-square	96.3	81.7
Lilliefors	95.3	70.8
Jarque-Bera	95.2	91.9

Table 6-18 Goodness-of-Fit Results for Lognormal Distributions of Temperature Histories for Triple FP System 33 (μ_{1ref} = 0.08, μ_{ref} = 0.075, T_P = 4.86s) when S_{M1} = 0.9g (friction case when k_T=0.5 at 200°C)

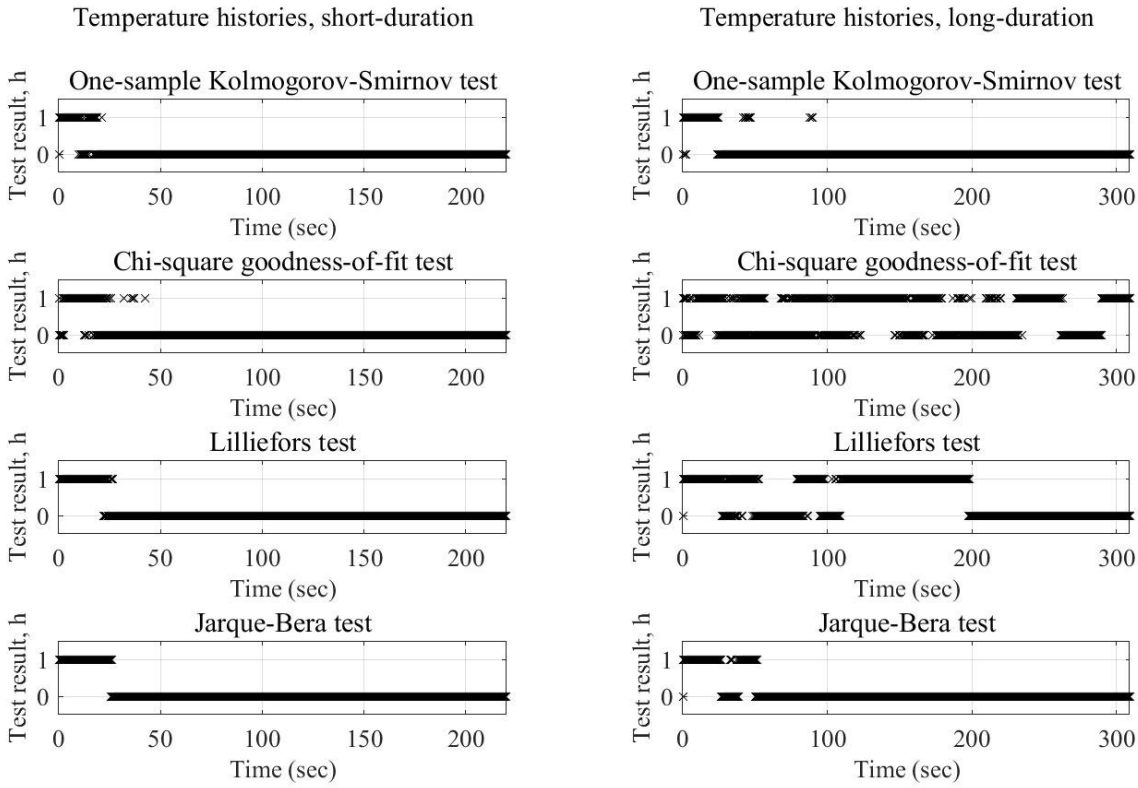

Goodness-of-fit test	Test Passing Rate (%)	
	Short-duration	Long-duration
One-sample Kolmogorov-Smirnov	93.2	91.9
Chi-square	91.7	51.2
Lilliefors	89.2	52.3
Jarque-Bera	88.2	87.3

6.4 Results for Lead-rubber Isolation Systems

Tables 6-19 to 6-26 present results on the resultant maximum displacements and residual displacements for the lead-rubber systems. The results include values of mean, median, 84th and 90th percentile counted values from the empirical data. Also, the tables present values of the 90th percentile isolator maximum resultant displacement to the mean value, which can be utilized in the design of isolators. The results in Tables 6-19 to 6-26 show that a value of for the 90th/mean scale factor for the isolator displacement of lead-rubber systems is 1.5 to 1.6, which is like the scale factor for single FP systems and is a little larger than the scale factor for triple FP systems. The difference likely has to do with heating effects which are larger in the single FP (for which the heat flux is larger due to the larger sliding velocity on its single interface) and the lead-rubber systems (for which heating is continuous) than in the triple FP systems (in which the heat flux is smaller due to the smaller sliding velocity on its two main sliding interfaces). Further evidence that heating is the reason for the difference is the case of the special triple FP system LL for which the heat flux is continuous unlike any of the other triple FP systems-for the LL triple FP system the scaling factor is larger than the other triple FP systems.

As in the case of the single FP systems, the values of the scale factor for long-duration ground motions are a little smaller than those for the short-duration motions.

Table 6-19 Mean and Median Resultant Maximum Displacements and Residual Displacements of Lead-rubber Systems for S_{M1}=0.7g

		Maximum Resultant Displacement (mm)				Residual Resultant Displacement (mm)			
		Short-duration		Long-duration		Short-duration		Long-duration	
		Median (mm)	Mean (mm)	Median (mm)	Mean (mm)	Median (mm)	Mean (mm)	Median (mm)	Mean (mm)
$a/h_L = 0.3$	**System 111** (T_d = 2 sec, $(Q_d/W)_{ref}$ = 0.08)	170	180	165	170	1	1	0	0
	System 211 (T_d = 3 sec, $(Q_d/W)_{ref}$ = 0.08)	204	223	228	221	2	3	0	1
	System 311 (T_d = 4 sec, $(Q_d/W)_{ref}$ = 0.08)	241	251	261	271	5	7	1	2
	System 121 (T_d = 2 sec, $(Q_d/W)_{ref}$ = 0.16)	108	121	107	108	1	1	0	0
	System 221 (T_d = 3 sec, $(Q_d/W)_{ref}$ = 0.16)	119	137	114	130	4	4	1	1
	System 321 (T_d = 4 sec, $(Q_d/W)_{ref}$ = 0.16)	136	151	135	149	9	9	1	2
	System 131 (T_d = 2 sec, $(Q_d/W)_{ref}$ = 0.24)	76	91	73	79	1	2	0	0
	System 231 (T_d = 3 sec, $(Q_d/W)_{ref}$ = 0.24)	88	105	87	96	5	6	1	1
	System 331 (T_d = 4 sec, $(Q_d/W)_{ref}$ = 0.24)	87	109	90	105	10	13	2	3
$a/h_L = 0.6$	**System 112** (T_d = 2 sec, $(Q_d/W)_{ref}$ = 0.08)	184	200	196	199	1	1	0	0
	System 212 (T_d = 3 sec, $(Q_d/W)_{ref}$ = 0.08)	250	258	270	258	2	3	0	1
	System 312 (T_d = 4 sec, $(Q_d/W)_{ref}$ = 0.08)	273	293	329	325	4	6	1	2
	System 122 (T_d = 2 sec, $(Q_d/W)_{ref}$ = 0.16)	111	128	115	120	1	1	0	0
	System 222 (T_d = 3 sec, $(Q_d/W)_{ref}$ = 0.16)	135	150	133	146	4	4	0	1
	System 322 (T_d = 4 sec, $(Q_d/W)_{ref}$ = 0.16)	145	162	152	170	7	8	1	2
	System 132 (T_d = 2 sec, $(Q_d/W)_{ref}$ = 0.24)	76	94	83	87	1	2	0	0
	System 232 (T_d = 3 sec, $(Q_d/W)_{ref}$ = 0.24)	91	108	94	105	4	5	1	1
	System 332 (T_d = 4 sec, $(Q_d/W)_{ref}$ = 0.24)	97	114	97	116	10	13	2	3

$(Q_d/W)_{ref}$ is the starting value of the characteristic strength divided by weight prior to any heating effects

Table 6-20 Mean, 84th Percentile and 90th Percentile Resultant Maximum Displacements of Lead-rubber Systems for S_{M1}=0.7g

		Short-duration				Long-duration			
		Mean	84th	90th	90th / Mean	Mean	84th	90th	90th / Mean
$\alpha/h_L = 0.3$	**System 111** (T_d = 2 sec, $(Q_d/W)_{ref}$ = 0.08)	180	243	259	**1.44**	170	216	229	**1.35**
	System 211 (T_d = 3 sec, $(Q_d/W)_{ref}$ = 0.08)	223	323	348	**1.56**	221	290	318	**1.44**
	System 311 (T_d = 4 sec, $(Q_d/W)_{ref}$ = 0.08)	251	352	387	**1.54**	271	375	381	**1.41**
	System 121 (T_d = 2 sec, $(Q_d/W)_{ref}$ = 0.16)	121	167	189	**1.56**	108	152	158	**1.46**
	System 221 (T_d = 3 sec, $(Q_d/W)_{ref}$ = 0.16)	137	196	230	**1.68**	130	174	225	**1.73**
	System 321 (T_d = 4 sec, $(Q_d/W)_{ref}$ = 0.16)	151	229	242	**1.60**	149	212	248	**1.66**
	System 131 (T_d = 2 sec, $(Q_d/W)_{ref}$ = 0.24)	91	139	151	**1.66**	79	102	119	**1.51**
	System 231 (T_d = 3 sec, $(Q_d/W)_{ref}$ = 0.24)	105	160	172	**1.64**	96	134	157	**1.64**
	System 331 (T_d = 4 sec, $(Q_d/W)_{ref}$ = 0.24)	109	156	178	**1.63**	105	146	176	**1.68**
				Average 90th / Mean	**1.59**				**1.54**
$\alpha/h_L = 0.6$	**System 112** (T_d = 2 sec, $(Q_d/W)_{ref}$ = 0.08)	200	277	302	**1.51**	199	249	255	**1.28**
	System 212 (T_d = 3 sec, $(Q_d/W)_{ref}$ = 0.08)	258	346	384	**1.49**	258	329	341	**1.32**
	System 312 (T_d = 4 sec, $(Q_d/W)_{ref}$ = 0.08)	293	395	459	**1.57**	325	440	461	**1.42**
	System 122 (T_d = 2 sec, $(Q_d/W)_{ref}$ = 0.16)	128	174	203	**1.59**	120	167	187	**1.56**
	System 222 (T_d = 3 sec, $(Q_d/W)_{ref}$ = 0.16)	150	230	248	**1.65**	146	222	255	**1.75**
	System 322 (T_d = 4 sec, $(Q_d/W)_{ref}$ = 0.16)	162	249	266	**1.64**	170	257	298	**1.75**
	System 132 (T_d = 2 sec, $(Q_d/W)_{ref}$ = 0.24)	94	141	155	**1.65**	87	120	134	**1.54**
	System 232 (T_d = 3 sec, $(Q_d/W)_{ref}$ = 0.24)	108	162	172	**1.59**	105	154	173	**1.65**
	System 332 (T_d = 4 sec, $(Q_d/W)_{ref}$ = 0.24)	114	163	182	**1.60**	116	166	196	**1.69**
				Average 90th / Mean	**1.59**				**1.55**

$(Q_d/W)_{ref}$ is the starting value of the characteristic strength divided by weight prior to any heating effects

Table 6-21 Mean and Median Resultant Maximum Displacements and Residual Displacements of Lead-rubber Systems for S_{M1}=0.9g

		Maximum Resultant Displacement (mm)				Residual Resultant Displacement (mm)			
		Short-duration		Long-duration		Short-duration		Long-duration	
		Median (mm)	Mean (mm)	Median (mm)	Mean (mm)	Median (mm)	Mean (mm)	Median (mm)	Mean (mm)
$a/h_L = 0.3$	**System 111** (T_d = 2 sec, $(Q_d/W)_{ref}$ = 0.08)	248	272	264	268	1	1	0	0
	System 211 (T_d = 3 sec, $(Q_d/W)_{ref}$ = 0.08)	350	357	365	347	3	4	1	1
	System 311 (T_d = 4 sec, $(Q_d/W)_{ref}$ = 0.08)	358	404	443	435	4	8	1	2
	System 121 (T_d = 2 sec, $(Q_d/W)_{ref}$ = 0.16)	155	175	160	163	1	2	0	0
	System 221 (T_d = 3 sec, $(Q_d/W)_{ref}$ = 0.16)	187	208	189	202	4	5	1	1
	System 321 (T_d = 4 sec, $(Q_d/W)_{ref}$ = 0.16)	201	227	220	241	8	10	1	3
	System 131 (T_d = 2 sec, $(Q_d/W)_{ref}$ = 0.24)	109	135	117	121	2	2	0	0
	System 231 (T_d = 3 sec, $(Q_d/W)_{ref}$ = 0.24)	132	157	125	145	5	6	1	1
	System 331 (T_d = 4 sec, $(Q_d/W)_{ref}$ = 0.24)	141	168	143	161	11	14	2	3
$a/h_L = 0.6$	**System 112** (T_d = 2 sec, $(Q_d/W)_{ref}$ = 0.08)	299	313	331	325	1	1	0	0
	System 212 (T_d = 3 sec, $(Q_d/W)_{ref}$ = 0.08)	428	435	420	419	3	4	1	1
	System 312 (T_d = 4 sec, $(Q_d/W)_{ref}$ = 0.08)	447	490	546	529	4	6	1	2
	System 122 (T_d = 2 sec, $(Q_d/W)_{ref}$ = 0.16)	174	195	187	192	1	2	0	1
	System 222 (T_d = 3 sec, $(Q_d/W)_{ref}$ = 0.16)	208	236	235	247	4	6	1	1
	System 322 (T_d = 4 sec, $(Q_d/W)_{ref}$ = 0.16)	245	267	312	307	7	11	1	3
	System 132 (T_d = 2 sec, $(Q_d/W)_{ref}$ = 0.24)	120	143	133	140	1	2	0	0
	System 232 (T_d = 3 sec, $(Q_d/W)_{ref}$ = 0.24)	140	169	158	171	5	6	1	1
	System 332 (T_d = 4 sec, $(Q_d/W)_{ref}$ = 0.24)	151	185	174	194	11	12	2	3

$(Q_d/W)_{ref}$ is the starting value of the characteristic strength divided by weight prior to any heating effects

Table 6-22 Mean, 84th Percentile and 90th Percentile Resultant Maximum Displacements of Lead-rubber Systems for S_{M1}=0.9g

		Short-duration				Long-duration			
		Mean	84th	90th	90th / Mean	Mean	84th	90th	90th / Mean
$\alpha/h_L = 0.3$	**System 111** (T_d = 2 sec, $(Q_d/W)_{ref}$ = 0.08)	272	367	387	**1.42**	268	326	331	**1.24**
	System 211 (T_d = 3 sec, $(Q_d/W)_{ref}$ = 0.08)	357	479	510	**1.43**	347	433	451	**1.30**
	System 311 (T_d = 4 sec, $(Q_d/W)_{ref}$ = 0.08)	404	571	628	**1.55**	435	587	611	**1.40**
	System 121 (T_d = 2 sec, $(Q_d/W)_{ref}$ = 0.16)	175	243	273	**1.56**	163	230	246	**1.51**
	System 221 (T_d = 3 sec, $(Q_d/W)_{ref}$ = 0.16)	208	314	344	**1.65**	202	307	346	**1.71**
	System 321 (T_d = 4 sec, $(Q_d/W)_{ref}$ = 0.16)	227	354	379	**1.67**	241	346	401	**1.66**
	System 131 (T_d = 2 sec, $(Q_d/W)_{ref}$ = 0.24)	135	199	224	**1.66**	121	171	186	**1.54**
	System 231 (T_d = 3 sec, $(Q_d/W)_{ref}$ = 0.24)	157	222	255	**1.62**	145	200	252	**1.74**
	System 331 (T_d = 4 sec, $(Q_d/W)_{ref}$ = 0.24)	168	240	294	**1.75**	161	219	265	**1.65**
				Average 90th / Mean	**1.59**				**1.53**
$\alpha/h_L = 0.6$	**System 112** (T_d = 2 sec, $(Q_d/W)_{ref}$ = 0.08)	313	402	480	**1.53**	325	371	396	**1.22**
	System 212 (T_d = 3 sec, $(Q_d/W)_{ref}$ = 0.08)	435	567	626	**1.44**	419	504	519	**1.24**
	System 312 (T_d = 4 sec, $(Q_d/W)_{ref}$ = 0.08)	490	668	763	**1.56**	529	676	699	**1.32**
	System 122 (T_d = 2 sec, $(Q_d/W)_{ref}$ = 0.16)	195	274	311	**1.59**	192	262	294	**1.53**
	System 222 (T_d = 3 sec, $(Q_d/W)_{ref}$ = 0.16)	236	368	394	**1.67**	247	366	399	**1.62**
	System 322 (T_d = 4 sec, $(Q_d/W)_{ref}$ = 0.16)	267	413	438	**1.64**	307	440	459	**1.50**
	System 132 (T_d = 2 sec, $(Q_d/W)_{ref}$ = 0.24)	143	215	229	**1.60**	140	197	228	**1.63**
	System 232 (T_d = 3 sec, $(Q_d/W)_{ref}$ = 0.24)	169	247	274	**1.62**	171	260	303	**1.77**
	System 332 (T_d = 4 sec, $(Q_d/W)_{ref}$ = 0.24)	185	269	323	**1.75**	194	302	337	**1.74**
				Average 90th / Mean	**1.60**				**1.51**

$(Q_d/W)_{ref}$ is the starting value of the characteristic strength divided by weight prior to any heating effects

Table 6-23 Mean and Median Resultant Maximum Displacements and Residual Displacements of Lead-rubber Systems for S_{M1}=1.1g

		Maximum Resultant Displacement (mm)				Residual Resultant Displacement (mm)			
		Short-duration		Long-duration		Short-duration		Long-duration	
		Median (mm)	Mean (mm)	Median (mm)	Mean (mm)	Median (mm)	Mean (mm)	Median (mm)	Mean (mm)
a/h_L = 0.3	**System 111** (T_d = 2 sec, $(Q_d/W)_{ref}$ = 0.08)	360	381	396	388	1	1	0	1
	System 211 (T_d = 3 sec, $(Q_d/W)_{ref}$ = 0.08)	515	527	511	501	3	5	1	2
	System 311 (T_d = 4 sec, $(Q_d/W)_{ref}$ = 0.08)	540	595	649	632	5	8	1	3
	System 121 (T_d = 2 sec, $(Q_d/W)_{ref}$ = 0.16)	218	244	229	235	1	2	0	1
	System 221 (T_d = 3 sec, $(Q_d/W)_{ref}$ = 0.16)	272	295	292	303	4	7	1	2
	System 321 (T_d = 4 sec, $(Q_d/W)_{ref}$ = 0.16)	317	332	374	372	9	13	1	3
	System 131 (T_d = 2 sec, $(Q_d/W)_{ref}$ = 0.24)	159	186	166	173	2	2	0	1
	System 231 (T_d = 3 sec, $(Q_d/W)_{ref}$ = 0.24)	191	219	201	213	6	7	1	1
	System 331 (T_d = 4 sec, $(Q_d/W)_{ref}$ = 0.24)	212	236	214	241	13	14	2	3
a/h_L = 0.6	**System 112** (T_d = 2 sec, $(Q_d/W)_{ref}$ = 0.08)	396	427	451	461	1	1	0	0
	System 212 (T_d = 3 sec, $(Q_d/W)_{ref}$ = 0.08)	593	632	598	614	5	5	1	2
	System 312 (T_d = 4 sec, $(Q_d/W)_{ref}$ = 0.08)	632	707	799	785	6	9	1	3
	System 122 (T_d = 2 sec, $(Q_d/W)_{ref}$ = 0.16)	251	277	282	288	1	2	0	1
	System 222 (T_d = 3 sec, $(Q_d/W)_{ref}$ = 0.16)	332	354	385	374	4	7	1	2
	System 322 (T_d = 4 sec, $(Q_d/W)_{ref}$ = 0.16)	401	405	484	477	8	13	2	3
	System 132 (T_d = 2 sec, $(Q_d/W)_{ref}$ = 0.24)	171	201	193	202	2	3	0	1
	System 232 (T_d = 3 sec, $(Q_d/W)_{ref}$ = 0.24)	216	244	237	259	6	6	1	2
	System 332 (T_d = 4 sec, $(Q_d/W)_{ref}$ = 0.24)	226	258	297	314	10	13	2	4

$(Q_d/W)_{ref}$ is the starting value of the characteristic strength divided by weight prior to any heating effects

Table 6-24 Mean, 84th Percentile and 90th Percentile Resultant Maximum Displacements of Lead-rubber Systems for S_{M1}=1.1g

		Short-duration				Long-duration			
		Mean	84th	90th	90th / Mean	Mean	84th	90th	90th / Mean
$\alpha/h_L = 0.3$	**System 111** (T_d = 2 sec, $(Q_d/W)_{ref}$ = 0.08)	381	486	580	**1.52**	388	443	470	**1.21**
	System 211 (T_d = 3 sec, $(Q_d/W)_{ref}$ = 0.08)	527	689	776	**1.47**	501	599	618	**1.23**
	System 311 (T_d = 4 sec, $(Q_d/W)_{ref}$ = 0.08)	595	813	925	**1.55**	632	806	843	**1.33**
	System 121 (T_d = 2 sec, $(Q_d/W)_{ref}$ = 0.16)	244	335	370	**1.52**	235	315	350	**1.49**
	System 221 (T_d = 3 sec, $(Q_d/W)_{ref}$ = 0.16)	295	450	490	**1.66**	303	444	488	**1.61**
	System 321 (T_d = 4 sec, $(Q_d/W)_{ref}$ = 0.16)	332	478	519	**1.56**	372	527	553	**1.49**
	System 131 (T_d = 2 sec, $(Q_d/W)_{ref}$ = 0.24)	186	263	289	**1.55**	173	241	267	**1.54**
	System 231 (T_d = 3 sec, $(Q_d/W)_{ref}$ = 0.24)	219	334	381	**1.74**	213	319	386	**1.81**
	System 331 (T_d = 4 sec, $(Q_d/W)_{ref}$ = 0.24)	236	363	392	**1.66**	241	367	416	**1.73**
				Average 90th / Mean	**1.58**				**1.49**
$\alpha/h_L = 0.6$	**System 112** (T_d = 2 sec, $(Q_d/W)_{ref}$ = 0.08)	427	522	643	**1.51**	461	536	575	**1.25**
	System 212 (T_d = 3 sec, $(Q_d/W)_{ref}$ = 0.08)	632	823	954	**1.51**	614	723	772	**1.26**
	System 312 (T_d = 4 sec, $(Q_d/W)_{ref}$ = 0.08)	707	1028	1158	**1.64**	785	949	996	**1.27**
	System 122 (T_d = 2 sec, $(Q_d/W)_{ref}$ = 0.16)	277	385	452	**1.63**	288	368	406	**1.41**
	System 222 (T_d = 3 sec, $(Q_d/W)_{ref}$ = 0.16)	354	524	549	**1.55**	374	515	539	**1.44**
	System 322 (T_d = 4 sec, $(Q_d/W)_{ref}$ = 0.16)	405	560	636	**1.57**	477	699	747	**1.57**
	System 132 (T_d = 2 sec, $(Q_d/W)_{ref}$ = 0.24)	201	283	330	**1.64**	202	284	343	**1.70**
	System 232 (T_d = 3 sec, $(Q_d/W)_{ref}$ = 0.24)	244	362	407	**1.67**	259	422	455	**1.76**
	System 332 (T_d = 4 sec, $(Q_d/W)_{ref}$ = 0.24)	258	392	433	**1.68**	314	458	541	**1.72**
				Average 90th / Mean	**1.60**				**1.49**

$(Q_d/W)_{ref}$ is the starting value of the characteristic strength divided by weight prior to any heating effects

Table 6-25 Mean and Median Resultant Maximum Displacements and Residual Displacements of Additional Lead-rubber Systems

	S_{M1} = 0.7g							
	Maximum Resultant Displacement (mm)				Residual Resultant Displacement (mm)			
	Short-duration		Long-duration		Short-duration		Long-duration	
	Median (mm)	Mean (mm)	Median (mm)	Mean (mm)	Median (mm)	Mean (mm)	Median (mm)	Mean (mm)
System 4 (T_d = 4 sec, $(Q_d/W)_{ref}$ = 0.121)	169	190	192	201	4	7	1	2
System 5 (T_d = 3 sec, $(Q_d/W)_{ref}$ = 0.121)	154	172	156	169	2	3	1	1
System 6 (T_d = 2 sec, $(Q_d/W)_{ref}$ = 0.241)	72	90	71	79	2	2	0	0

	S_{M1} = 0.9g							
	Maximum Resultant Displacement (mm)				Residual Resultant Displacement (mm)			
	Short-duration		Long-duration		Short-duration		Long-duration	
	Median (mm)	Mean (mm)	Median (mm)	Mean (mm)	Median (mm)	Mean (mm)	Median (mm)	Mean (mm)
System 4 (T_d = 4 sec, $(Q_d/W)_{ref}$ = 0.121)	282	300	338	341	7	9	1	3
System 5 (T_d = 3 sec, $(Q_d/W)_{ref}$ = 0.121)	237	267	270	272	3	5	1	1
System 6 (T_d = 2 sec, $(Q_d/W)_{ref}$ = 0.241)	102	132	107	119	2	2	0	1

	S_{M1} = 1.1g							
	Maximum Resultant Displacement (mm)				Residual Resultant Displacement (mm)			
	Short-duration		Long-duration		Short-duration		Long-duration	
	Median (mm)	Mean (mm)	Median (mm)	Mean (mm)	Median (mm)	Mean (mm)	Median (mm)	Mean (mm)
System 4 (T_d = 4 sec, $(Q_d/W)_{ref}$ = 0.121)	421	445	522	506	7	11	1	3
System 5 (T_d = 3 sec, $(Q_d/W)_{ref}$ = 0.121)	372	391	414	399	3	6	1	2
System 6 (T_d = 2 sec, $(Q_d/W)_{ref}$ = 0.241)	157	184	159	166	2	2	0	1

Table 6-26 Mean, 84th Percentile and 90th Percentile Resultant Maximum Displacements of Additional Lead-rubber Systems

	S_{M1} = 0.7g							
	Short-duration				Long-duration			
	Mean	84th	90th	90th / Mean	Mean	84th	90th	90th / Mean
System 4 (T_d = 4 sec, $(Q_d/W)_{ref}$ = 0.121)	190	297	318	**1.67**	201	287	317	**1.58**
System 5 (T_d = 3 sec, $(Q_d/W)_{ref}$ = 0.121)	172	258	283	**1.65**	169	249	274	**1.62**
System 6 (T_d = 2 sec, $(Q_d/W)_{ref}$ = 0.241)	90	138	153	**1.70**	79	106	123	**1.56**
Average 90th / Mean				**1.67**				**1.59**

	S_{M1} = 0.9g							
	Short-duration				Long-duration			
	Mean	84th	90th	90th / Mean	Mean	84th	90th	90th / Mean
System 4 (T_d = 4 sec, $(Q_d/W)_{ref}$ = 0.121)	300	444	470	**1.57**	341	492	501	**1.47**
System 5 (T_d = 3 sec, $(Q_d/W)_{ref}$ = 0.121)	267	399	430	**1.61**	272	377	421	**1.55**
System 6 (T_d = 2 sec, $(Q_d/W)_{ref}$ = 0.241)	132	191	223	**1.69**	119	172	185	**1.55**
Average 90th / Mean				**1.62**				**1.52**

	S_{M1} = 1.1g							
	Short-duration				Long-duration			
	Mean	84th	90th	90th / Mean	Mean	84th	90th	90th / Mean
System 4 (T_d = 4 sec, $(Q_d/W)_{ref}$ = 0.121)	445	641	697	**1.57**	506	711	747	**1.48**
System 5 (T_d = 3 sec, $(Q_d/W)_{ref}$ = 0.121)	391	549	614	**1.57**	399	521	539	**1.35**
System 6 (T_d = 2 sec, $(Q_d/W)_{ref}$ = 0.241)	184	261	296	**1.61**	166	232	256	**1.54**
Average 90th / Mean				**1.58**				**1.46**

Figures 6-11 and 6-12 present a sample of results on the distribution of the maximum resultant displacement and of the residual resultant displacement for the lead-rubber system 221 (T_d =3s, $(Q_d/W)_{ref}$ =0.16, α/h_L =0.3) when S_{M1} =0.9g. Appendix F contains detailed results for all studied lead-rubber systems.

Median and dispersion values in each of Figures 6-11 and 6-12 may be used to construct the lognormal distributions which were fitted to the empirical data. The various percentile values listed in each figure are also fitted values. As also observed for the single and triple FP systems, the residual displacements are smaller for long-duration ground motions than for short-duration ground motions.

Figures 6-13 and Figure 6-14 present sample results on the computed histories of cumulative energy and of temperature at the sliding interface for lead-rubber system 221 (T_d =3s, $(Q_d/W)_{ref}$ =0.16, α/h_L =0.3) when S_{M1} =0.9g. Goodness-of-fit tests were performed for the lognormally fitted cumulative energy and temperature histories in Figures 6-13 and 14 and the test results are presented in Tables 6-27 and 28. Appendix F contains detailed results for all studied lead-rubber systems. The graphs include 16th, 50th (median), 84th and 90th percentile counted values (empirical data) and fitted values (based on lognormal distributions).

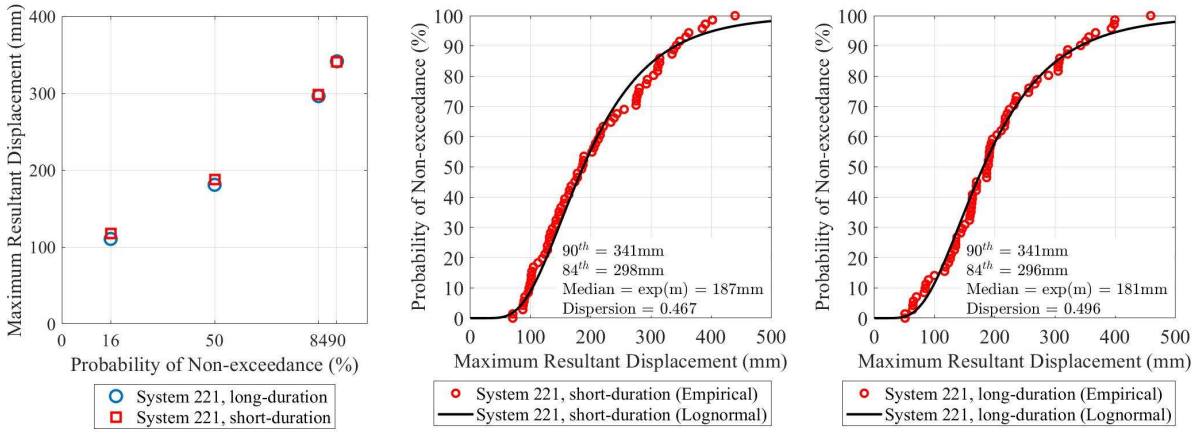

Figure 6-11 Distributions of Maximum Resultant Displacement for Lead-rubber System 221 (T_d = 3s, $(Q_d/W)_{ref}$ = 0.16, a/h_L =0.3) when S_{M1} = 0.9g

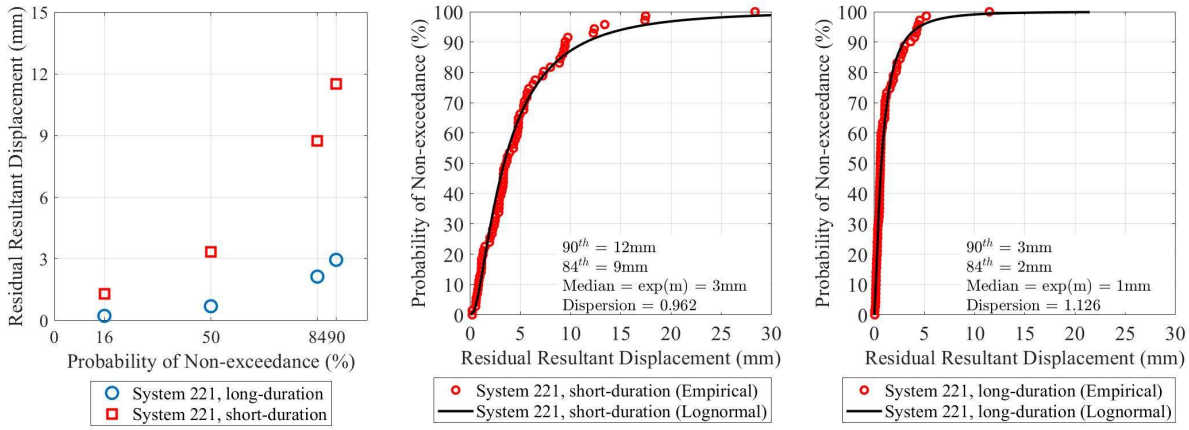

Figure 6-12 Distributions of Residual Resultant Displacement for Lead-rubber System 221 (T_d = 3s, $(Q_d/W)_{ref}$= 0.16, a/h_L =0.3) when S_{M1} = 0.9g

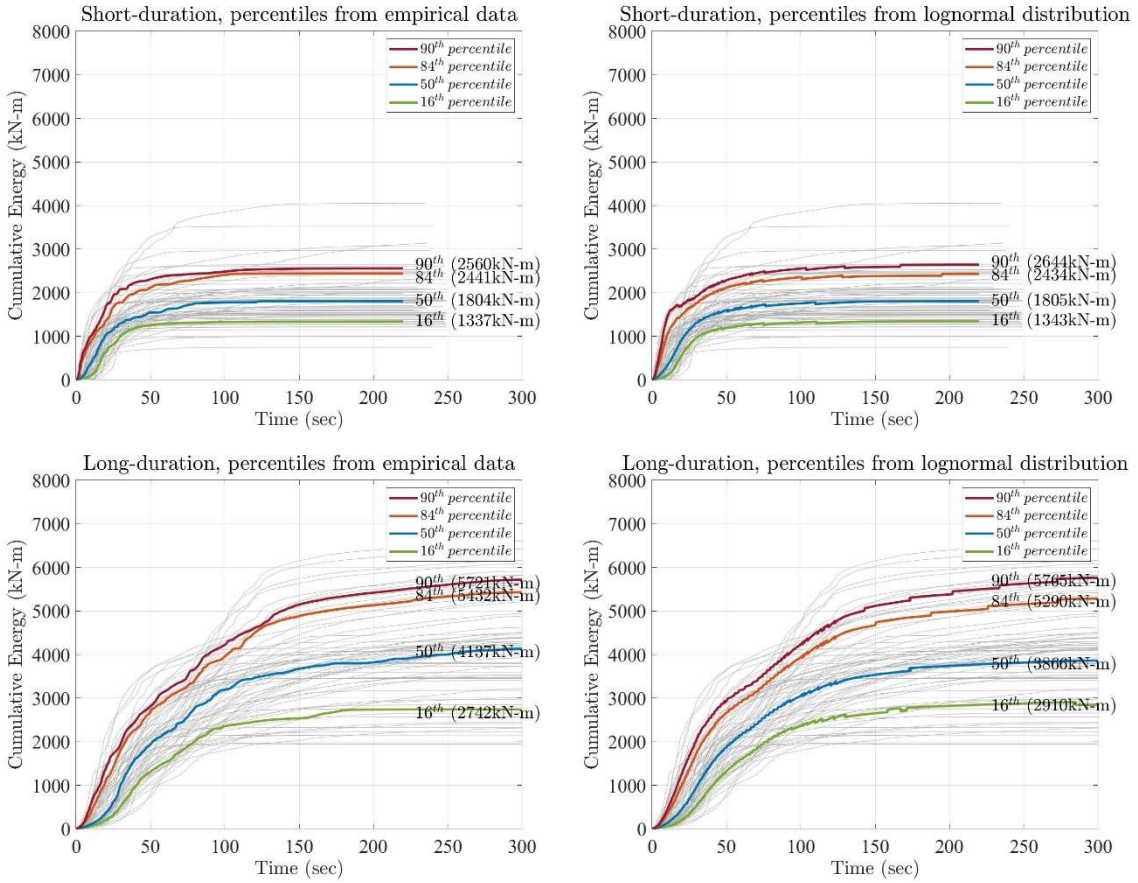

Figure 6-13 Histories of Cumulative Energy for Lead-rubber System 221 (T_d = 3s, $(Q_d/W)_{ref}$= 0.16, a/h_L =0.3) when S_{M1} = 0.9g

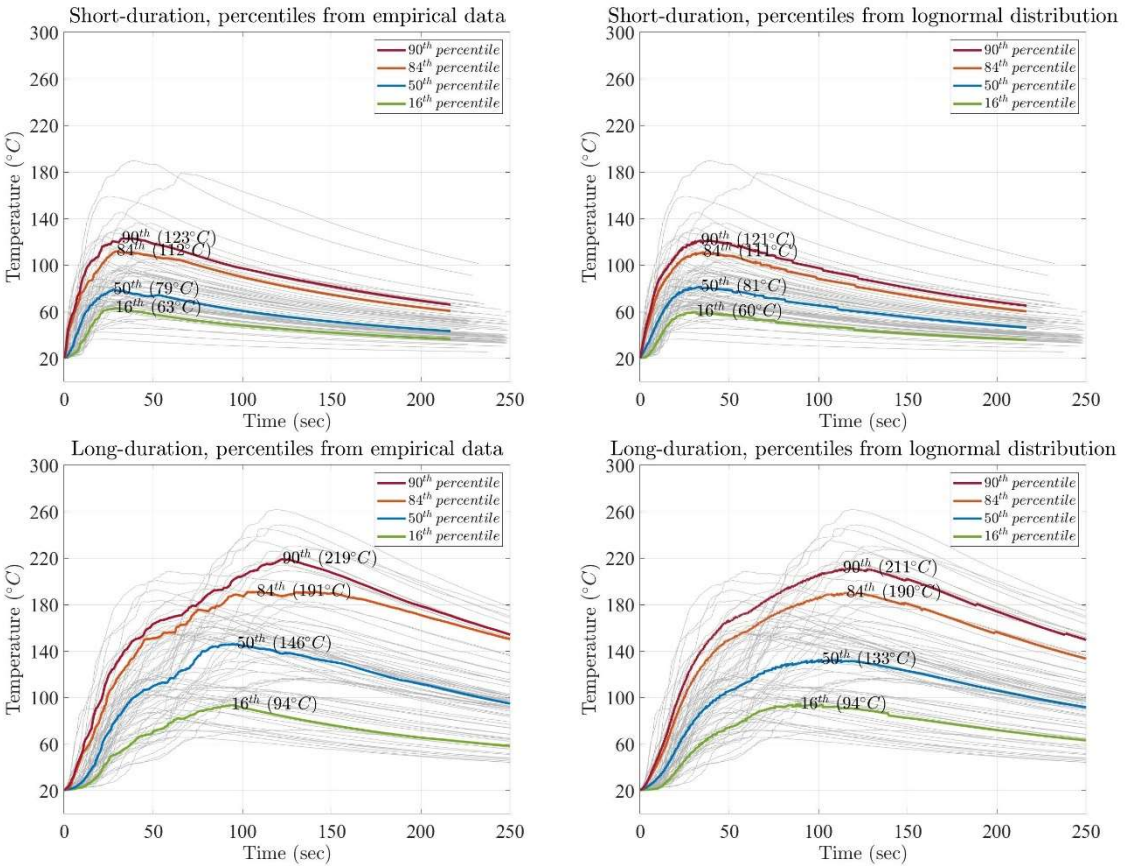

Figure 6-14 Histories of Temperature in Lead Core for Lead-rubber System 221 (T_d = 3s, $(Q_d/W)_{ref}$ = 0.16, a/h_L =0.3) when S_{M1} = 0.9g

Table 6-27 Goodness-of-Fit Results for Lognormal Distributions of Cumulative Energy Histories for Lead-rubber System 221 (T_d = 3s, $(Q_d/W)_{ref}$ = 0.16, a/h_L =0.3) when S_{M1} = 0.9g

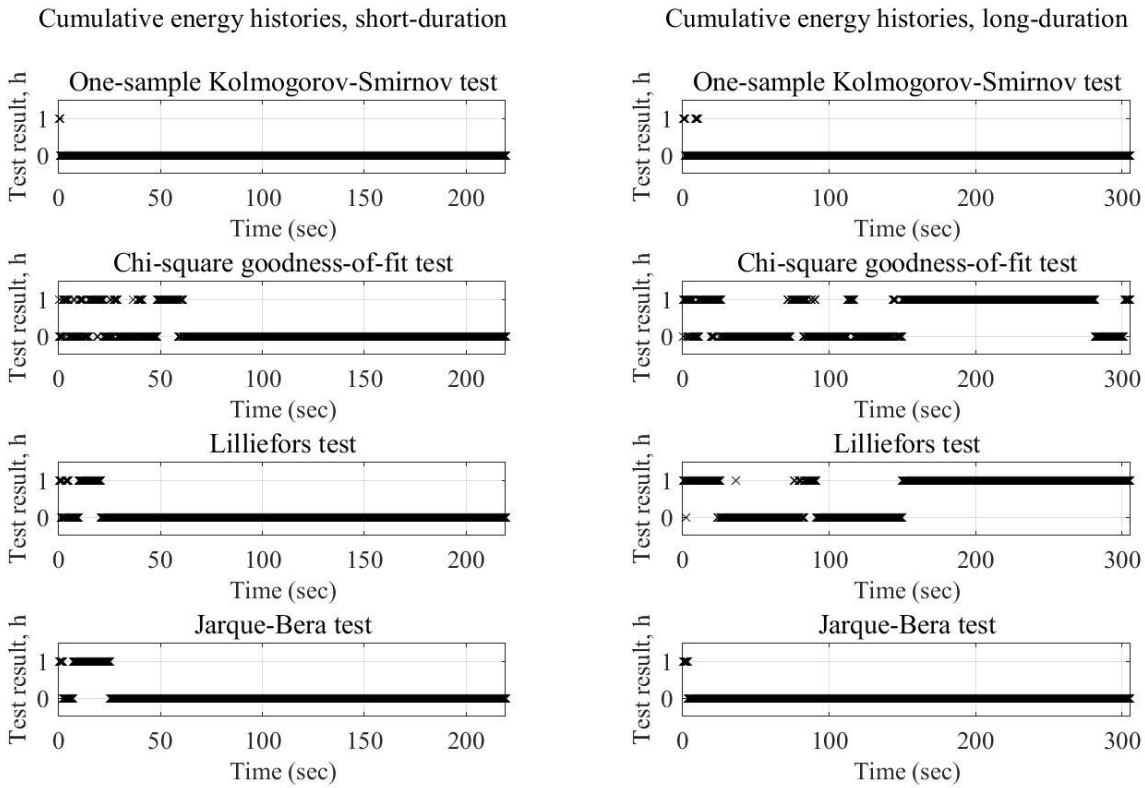

Goodness-of-fit test	Test Passing Rate (%)	
	Short-duration	Long-duration
One-sample Kolmogorov-Smirnov	99.6	99.2
Chi-square	87.8	42.8
Lilliefors	93.7	37.4
Jarque-Bera	90.9	98.9

Table 6-28 Goodness-of-Fit Results for Lognormal Distributions of Temperature Histories for Lead-rubber System 221 (T_d = 3s, $(Q_d/W)_{ref}$ = 0.16, a/h_L =0.3) when S_{M1} = 0.9g

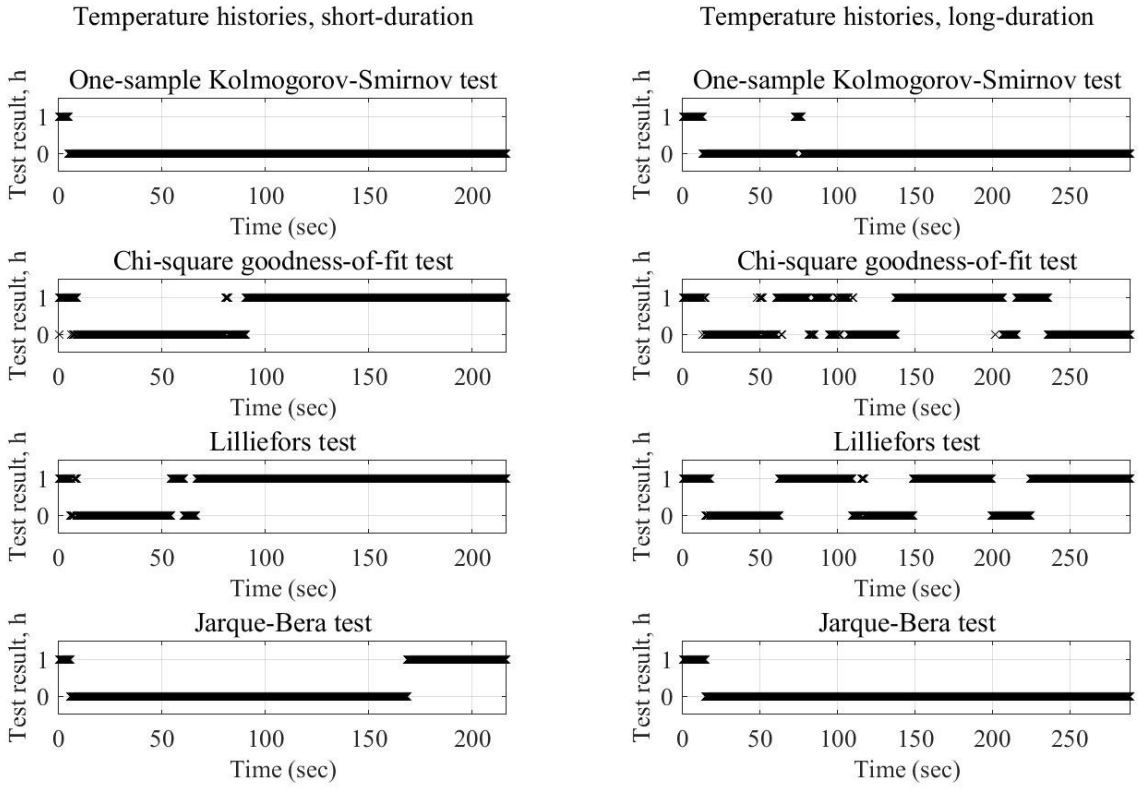

Goodness-of-fit test	Test Passing Rate (%)	
	Short-duration	Long-duration
One-sample Kolmogorov-Smirnov	97.8	94.1
Chi-square	37.6	51.1
Lilliefors	24.5	37.7
Jarque-Bera	75.3	94.9

6.5 Validity of Results on Computed Temperature of FP Bearings

The results obtained in response history analysis are dependent on the computation of temperature at the sliding interfaces of FP bearings. The computation of the temperature is based on a theory of which an assumption is that the concave plate on which the slider moves has indefinite depth as shown in Figure 6-15a (Constantinou et al, 2007; Carslaw and Jaeger, 1959) and subject to heat flux at its surface. In reality, the concave plate has finite depth where it may be assumed to be insulated when bearing against concrete, as shown in Figure 6-15b when subject to heat flux at the sliding surface. The implication of the finite depth is that the temperature at the sliding surface is larger than when computed based on the assumption of indefinite depth. This is expected to be intensified in long-duration motions.

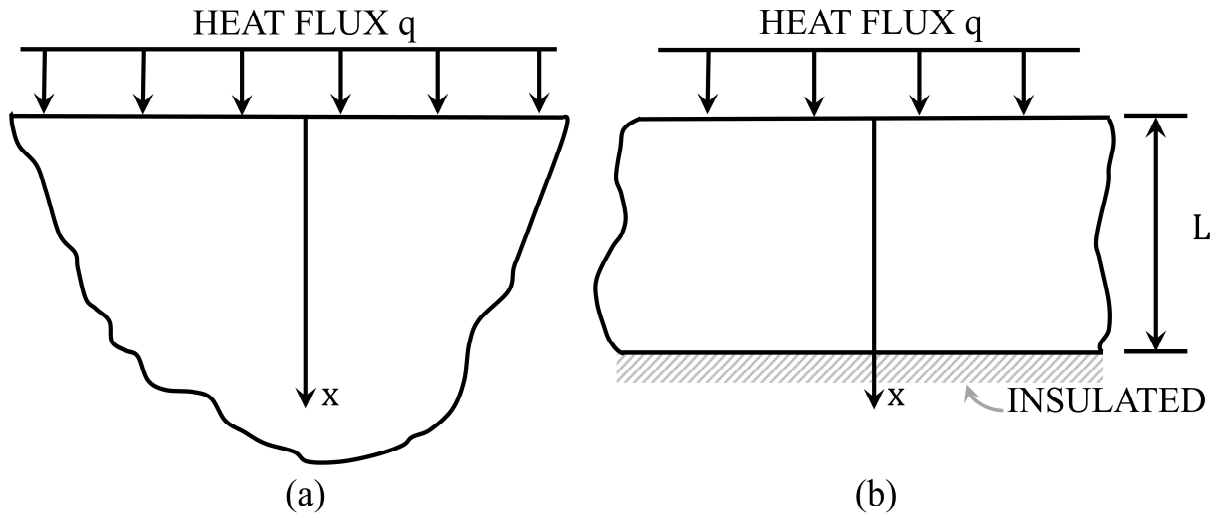

Figure 6-15 Indefinite Depth (a) and Finite Depth (b) Models of Heated Sliding Plate

Generally, the solution based on the infinite depth assumption is checked by computing the temperature over the depth of the concave plate and accepting the solution when the temperature increase at a depth equal to the thickness of the plate is small by comparison to that at the surface (Constantinou et al., 2007). As an example, Figure 6-16 presents histories of the temperature at the sliding surface and at various depths for the case of the Triple FP system LL (T_P =5.49 sec, μ_{1ref}=0.08, μ_{ref}=0.074) in the friction case when k_T =0.5 at 200ºC. The results are for a short-duration ground motion (1999 Chi-Chi CHY006, Taiwan, scale factor of 1.95) and for a long-duration ground motion (2011 Tohoku Iwanuma, Japan, scale factor of 1.52). Both motions were part of the scaled bins of motions representing the S_{M1} =0.9g spectra. The maximum depth used in the results of Figure 6-16 is 50mm, which is the minimum depth of the actual isolator used for the Lima Linda University Medical Center excluding any additional base plates. It is evident that at

depth of 50mm there is insignificant increase in temperature for the short-duration motion, but there is about a 30°C increase in temperature at that depth for the long-duration ground motion. However, this does not mean that the computed temperature at the sliding surface would have been significantly affected. For that an analysis with a model of finite depth is needed.

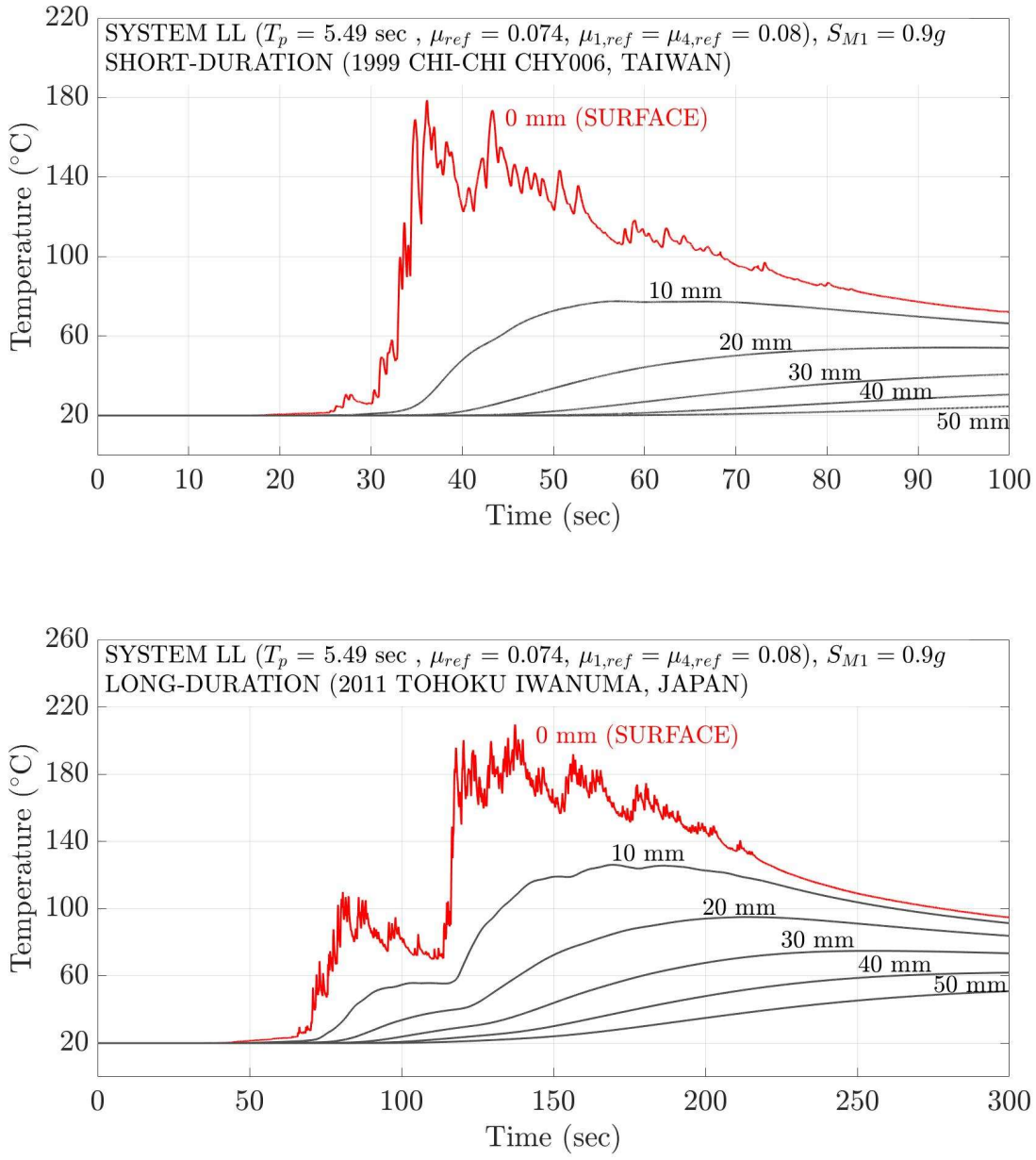

Figure 6-16 Temperature Histories at the Sliding Surfaces and at Various Depths of Triple FP System LL (T_P = 5.49 sec, μ_{ref} = 0.074) (friction case when k_T=0.5 at 200°C) in a Short-duration and in a Long-duration Ground Motion

The histories of temperature in Figure 6-16 were computed using the theory in Constantinou et al. (2007), which was based on analytic solutions obtained from Carslaw and Jaeger (1959). The temperature increase at any depth *x* (per Figure 6-16) of a plate of indefinite depth is given by:

$$\Delta T(x,t) = \frac{\sqrt{D}}{k\sqrt{\pi}} \int_0^t q(t-\tau) \exp\left(-\frac{x^2}{4D\tau}\right) \frac{d\tau}{\sqrt{\tau}} \qquad (6-2)$$

In this equation, q is the heat flux as given by equation (2-3). Equation (6-1) reduces to equation (2-2) when *x*=0, which is the sliding surface.

The solution for the temperature increase at the sliding interface (where the heat flux applies) and at depth L for the two cases of indefinite depth (Figure 6-15a) and finite insulated depth (Figure 6-15b) are known (Constantinou et al, 2007 and Carslaw and Jaeger, 1954) when the constant heat flux is constant over time. The solutions are given by the following equations:

Solution for Indefinite Depth, Constant Heat Flux q (special cases of equation 6-2)

$$\Delta T_{Surface} = \frac{2q}{K}\sqrt{\frac{Dt}{\pi}} \qquad (6-3)$$

$$\Delta T_{Depth\,L} = \frac{q\sqrt{D}}{k\sqrt{\pi}} \int_0^t \exp\left(-\frac{L^2}{4D\tau}\right) \frac{d\tau}{\sqrt{\tau}} \qquad (6-4)$$

Solution for Finite Insulated Depth L, Constant Heat Flux q

$$\Delta T_{Surface} = \frac{2q}{K}\sqrt{Dt} \sum_{n=0}^{\infty} \left\{ ierfc\left[\frac{nL}{\sqrt{Dt}}\right] + ierfc\left[\frac{(n+1)L}{\sqrt{Dt}}\right] \right\} \qquad (6-5)$$

$$\Delta T_{Depth\,L} = \frac{4q}{K}\sqrt{Dt} \sum_{n=0}^{\infty} ierfc\left[\frac{(2n+1)L}{2\sqrt{Dt}}\right] \qquad (6-6)$$

In equations (6-5) and (6-6),

$$ierfc(z) = \int_z^{\infty} erfc(\zeta)d\zeta = \frac{e^{-z^2}}{\sqrt{\pi}} - zerfc(z) \qquad (6-7)$$

In equation (6-7), *erfc* is the complimentary error function (Abramowitz and Stegun, 1965).

A comparison of results for the case of constant heat flux q=0.1MW/m^2 (all other thermal properties are as in Table 2-1) is presented in Figure 6-17, where histories of the temperature increase at the surface and at depth of 50mm are shown for sustained heat input of 200 second. Evidently, there is insignificant difference in the computed surface temperature but there is difference in the computed temperature at the insulated depth of 50mm. Important in the analysis is only the surface temperature so that we conclude that the results presented for FP isolators are valid. However, it is noted that the surface temperature calculated by the indefinite depth assumption is a lower bound estimate affected by the insulated depth and by the duration of the heating process.

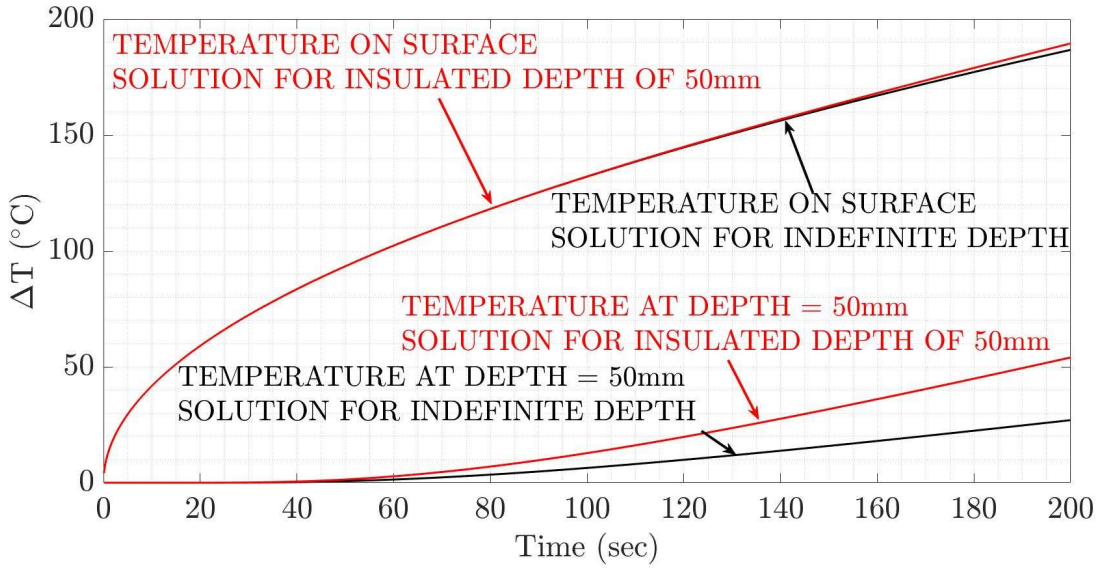

Figure 6-17 Histories of Temperature Increase on Surface and at Depth of 50mm as Computed by Theories Assuming Indefinite Depth or Finite Insulated Depth

6.6 Validity of Results on Computed Temperature of Lead-rubber Bearings

Like the case of the FP isolators investigated in Section 6.5, there is interest in investigating the validity of the solutions obtained for the temperature of the lead core in lead rubber bearings. Particularly, there are two issues to investigate: (a) the validity of the solutions which are based on analytic solutions valid for half space and full space of infinite dimensions, and (b) the validity of approximations to these analytic solutions using asymptotic expansions. The work of Kalpakidis and Constantinou (2008, 2009a, 2009b) on modeling the heating effects in lead-rubber bearings concentrated on analytic solutions only for temperature of the lead core and on some results of thermal finite element analysis of entire bearings to justify some assumptions made. It did not present solutions for the distribution of temperature in the steel end and shim plates that can be used to investigate the validity of the solutions. A later work by Lee and Constantinou (2016) presented such solutions, which are utilized in this section.

The model used in the theory of Kalpakidis and Constantinou (2008, 2009a, 2009b) utilizes analytic solutions, obtained from Carslaw and Jaeger (1959) and Beck (1979), for the following problems:

1) A half space heated at its surface by uniform heat flux q_P over an area of radius a (the radius of the lead core), which represents the heat conduction through the steel end plates (assumed to have indefinite depth), and

2) An infinite hollow cylinder of radius a (the radius of the lead core) heated over the cylindrical surface by uniform heat flux q_S, which represents heat conduction through the steel shim plates.

Figure 6-18 illustrates the problems considered for the heating in lead-rubber bearings. The increase of temperature in the end plates is $T_P(t, z)$, which is only dependent on depth z and time t, and the increase in temperature in the shim plates is $T_S(t, r)$, which is only dependent on the radial distance r and time t.

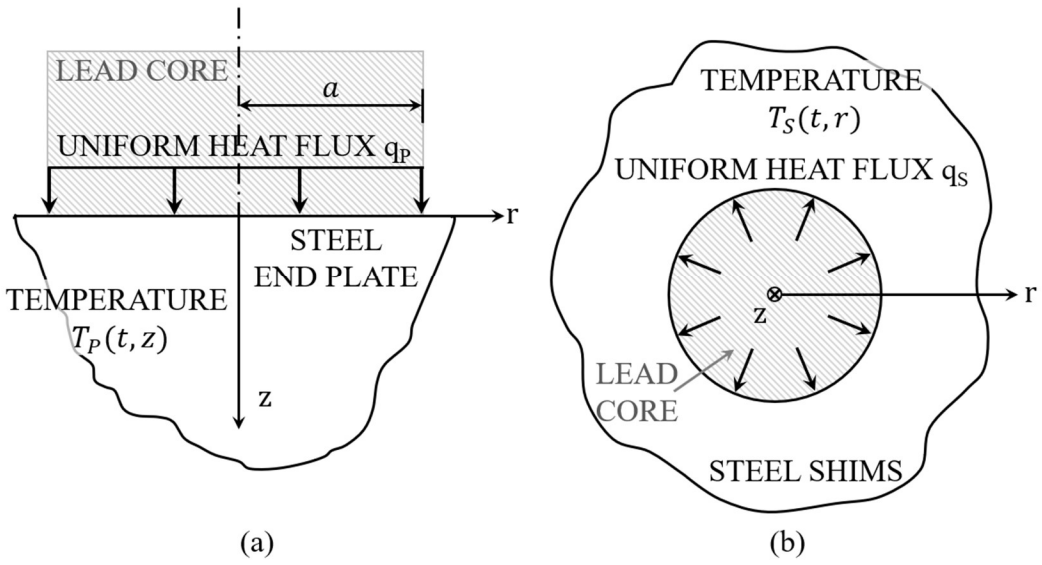

Figure 6-18 Problems Considered in Modeling Heating of Lead-Rubber Bearings (a) Half-Space Heated over a Circular Area 0 < r < a and z = 0, (b) Infinite Heated Hollow Cylinder

Analytic solutions for the temperature increase T_P and T_S are (Lee and Constantinou, 2016; Carlaw and Jaeger, 1959; Beck, 1979) are:

$$T_P^+(\tau, z^+) = \frac{k_s T_P(t,z)}{q_P a} = 2\sqrt{\tau}\left[ierfc\left(\frac{z^+}{2\sqrt{\tau}}\right) - ierfc\left(\frac{C}{\sqrt{\tau}}\right)\right] - \frac{1}{4C}erfc\left(\frac{C}{\sqrt{\tau}}\right) - I_a \qquad (6-8)$$

In equation (6-8), k_s is the thermal conductivity of steel, parameters τ and z^+ are dimensionless time and depth, defined by equations (6-9) and (6-10), α_S is the thermal diffusivity of steel, parameter C is defined by equation (6-11) and parameter I_a is defined by equation (6-12).

$$\tau = \frac{\alpha_s \cdot t}{a^2} \qquad (6-9)$$

$$z^+ = \frac{z}{a} \qquad (6-10)$$

$$C = \sqrt{\frac{1}{2} + \left(\frac{z^+}{2}\right)^2} \qquad (6-11)$$

$$I_a = \sqrt{\frac{C^2}{\pi}} \sum_{n=1}^{\infty} \frac{1}{(4C^2)^{2n}(n!)^2} \left[\Gamma\left(2n - \frac{1}{2}, \frac{C^2}{\tau}\right) + \frac{1}{(n+1)4C^2} \Gamma\left(2n + \frac{1}{2}, \frac{C^2}{\tau}\right) \right] \qquad (6-12)$$

In equation (6-12), function Γ(α, *x*) is the incomplete gamma function (Abramowitz and Stegun, 1965), defined by:

$$\Gamma(\alpha, x) = \int_x^{\infty} e^{-t} t^{\alpha-1} dt \qquad (6-13)$$

The complexity of equation (6-8) led Kalpakidis and Constantinou (2008, 2009a, 2009b), to instead use asymptotic expansions of the equation for z=0 given by equation (6-14), which is identical to function F given by equation (2-14).

$$T_P^+(z=0) = \begin{cases} 2\left(\frac{\tau}{\pi}\right)^{\frac{1}{2}} - \left(\frac{\tau}{\pi}\right) \cdot \left[2 - \left(\frac{\tau}{4}\right) - \left(\frac{\tau}{4}\right)^2 - \frac{15}{4} \cdot \left(\frac{\tau}{4}\right)^3\right], & \tau < 0.6 \\ \frac{8}{3\pi} - \frac{1}{2(\pi \cdot \tau)^{\frac{1}{2}}} \cdot \left[1 - \left(\frac{1}{3 \cdot (4\tau)}\right) - \frac{1}{6 \cdot (4\tau)^2} - \frac{1}{12 \cdot (4\tau)^3}\right], & \tau \geq 0.6 \end{cases} \qquad (6-14)$$

For temperature increase $T_S(t, r)$, the solution is:

$$T_S^+(t,r) = \frac{k_s T_S(t,r)}{q_s a} = -\frac{2}{\pi a} \int_0^{\infty} \left(1 - e^{-\alpha_s \theta^2 t}\right) \frac{J_0(\theta r) Y_1(\theta a) - Y_0(\theta r) J_1(\theta a)}{\theta^2 [J_1^2(\theta a) + Y_1^2(\theta a)]} d\theta \qquad (6-15)$$

In equation (6-15), J(*x*) and Y(*x*) are the Bessel functions of the first and second kind, respectively (Abramowitz and Stegun, 1965).

Again, the complexity of equation (6-15) led Kalpakidis and Constantinou (2008, 2009a, 2009b) and Lee and Constantinou (2016), to instead use asymptotic expansions or other approximations of the equation for r = a given by the following equations, of which equation (6-18) is used in the Kalpakidis model of equation (2-13):

$$T_S^+(\tau, r=a) = 2(\tau)^{0.5} \left[\frac{1}{\sqrt{\pi}} - \frac{\tau^{0.5}}{4}\right], \qquad \tau \leq 0.25 \qquad (6-16)$$

$$T_S^+(\tau, r=a) = 0.5 \ln(2.246\tau), \qquad \tau \geq 20 \qquad (6-17)$$

$$T_S^+(\tau, r = a) = 0.785\tau^{\frac{1}{3}} \qquad (6-18)$$

Equation (6-18) is not valid for all values of time. Figure 6-19 presents a comparison of the dimensionless temperature $T_S^+(\tau, r = a)$ as computed by equations (6-15) to (6-18), where it may be seen that equation (6-18) is valid to values of dimensionless time τ less than about 10. To better understand the significance of this limit, we use data for the lead-rubber bearing of system 5 (see Table 4-11), for which the radius of the lead core is a=0.153m, and a value for the thermal diffusivity of steel, $\alpha_S=1.41\times10^{-5}m^2/s$ to obtain for τ=10, a time t=16600sec. That is, the approximation in the Kalpakidis and Constantinou theory by use of equation (6-18) is valid to very large times.

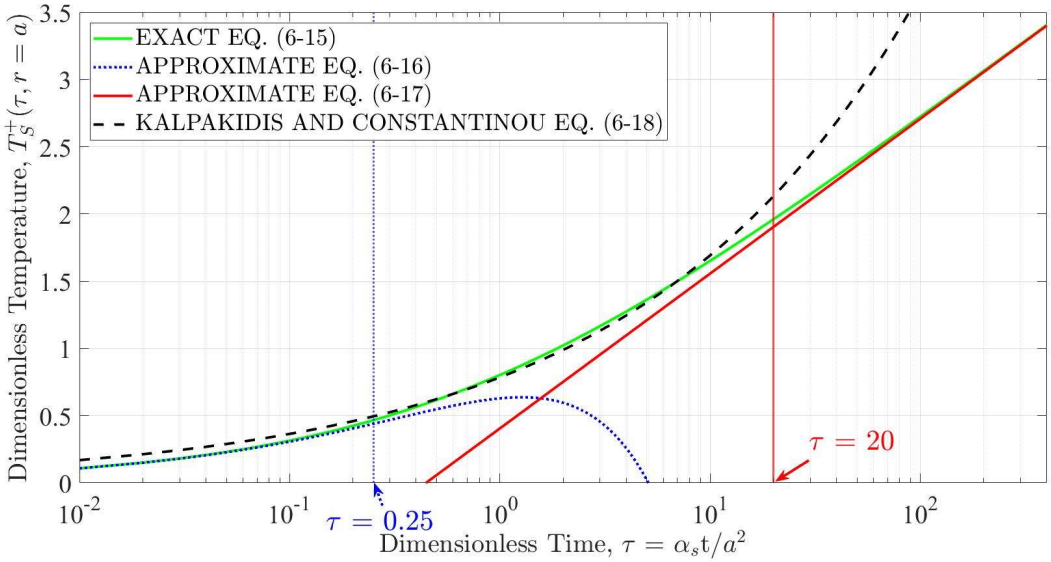

Figure 6-19 Comparison of Histories of Dimensionless Temperature Increase in Steel Shim Plates T^+_S at Interface with Lead Core

To compare exact results (however based on the infinite space solutions) on the temperature increase in the lead core and in the end and shim plates, the basic theory of Kalpakidis and Constantinou for the lead core, described by equations (2-13) and (2-14), was modified as follows. For the exact lead core temperature increase T_L,

$$\frac{dT_L}{dt} = \frac{\sigma_{YL}(T_L)\cdot|\dot{U}|}{\rho_L\cdot c_L\cdot h_L} - \frac{2p\cdot k_s\cdot T_L}{a\cdot\rho_L\cdot c_L\cdot h_L}\left[\frac{1}{T_P^+(z=0)} + \frac{t_s}{a}\frac{1}{T_S^+(r=a)}\right] \qquad (6-19)$$

In this equation, $T_P^+(z=0)$ and $T_S^+(\tau, r=a)$ are computed using equations (6-8) and (6-15), respectively. In the Kalpakidis and Constantinou theory equations (2-13) and (2-14) are used (the same results are obtained using equation (6-19), (6-14) and (6-18)).

An example is presented for the bearing of system 5 (Table 4-11). Detailed geometric parameters and properties of the bearing are presented in Figure 6-20 and Table 6-29 (this bearing is one of the isolators used in the Erzurum Hospital in Turkey, Constantinou et al, 2007). Note the t_s is the total thickness of the steel shims. The analysis is for a sustained motion of 200second duration with constant velocity of 0.2m/sec (in a test with sawtooth displacement history). Results are presented in Figure 6-21 for the lead core temperature increase, in Figure 6-22 for the temperature increase in the end plates (which have depth of 83mm) and in Figure 6-23 for the temperature increase in the shim plates (which have a diameter of 1118mm). It is evident in these results that the theory of Kalpakidis and Constantinou is valid and accurate in its prediction of the lead core temperature. Also, the temperature increase at the end of the steel shim plates where they meet the rubber cover is effectively zero, and the temperature increase at the bottom of the steel end plates where they are in contact with concrete is small enough to conclude that the theory based on infinite space solutions are valid.

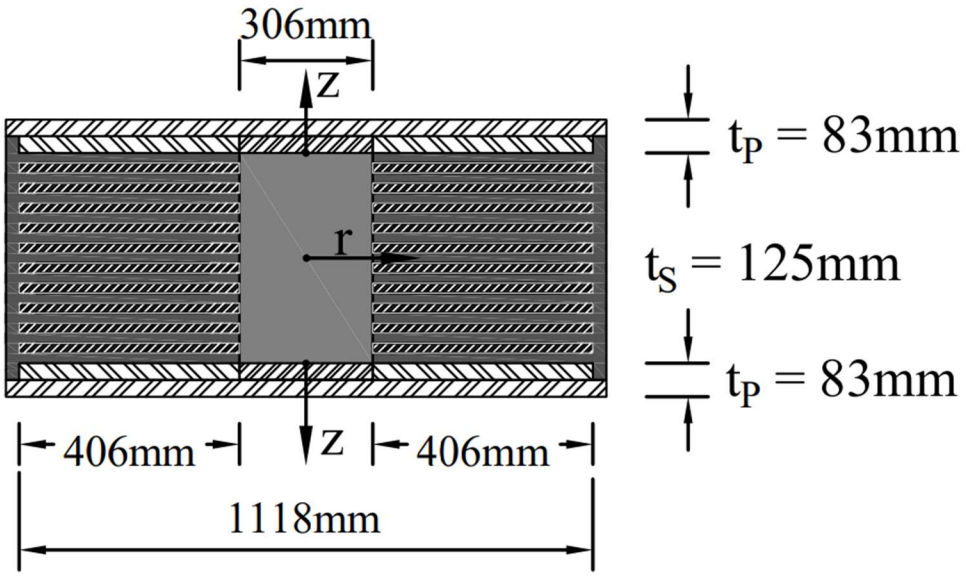

Figure 6-20 Cross Section of Lead-Rubber Bearing of System 5 (T_d = 3 sec, $(Q_d/W)_{ref}$ = 0.121)

Table 6-29 Geometric and Thermal Properties of Lead-rubber System 5

Parameters	System 5
Initial effective yield stress of lead, σ_{YL0} (MPa)	16.9
Lead core radius, a (m)	0.153
Lead core height, h_L (m)	0.333
End plate thickness, t_P (m)	0.083
Shim plate diameter (m)	1.118
Steel shim total thickness, t_s (m)	0.125
Density of lead, ρ_L (kg/m^3)	11300
Specific heat of lead, c_L (Joule/(kg·°C)	130
Thermal conductivity of steel, k_S (Watt/(m·°C)	50
Thermal diffusivity of steel, α_S (m^2/s)	1.41×10^{-5}
Parameter E_2 (1/°C)	0.0069

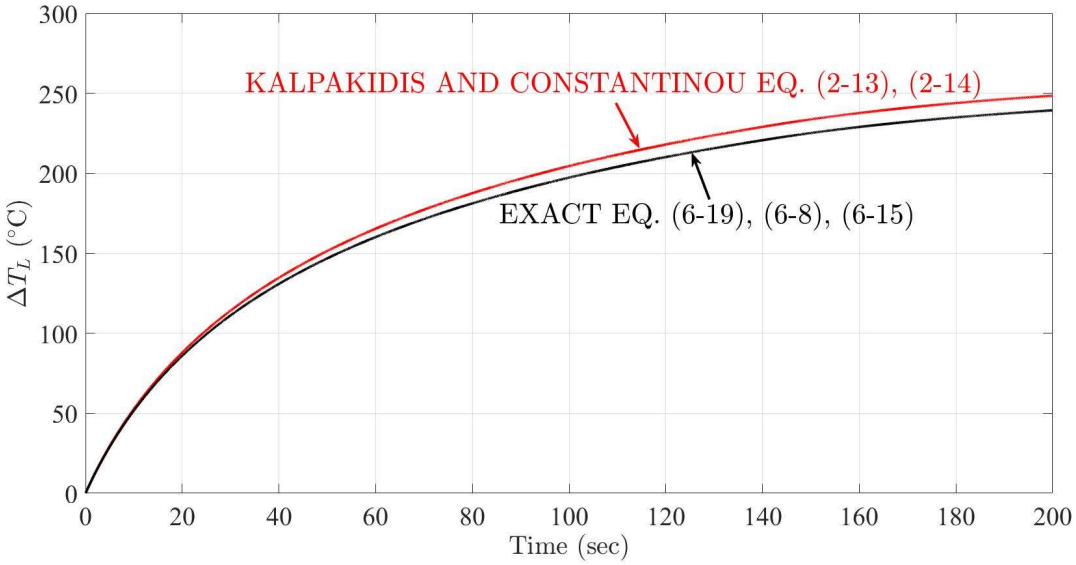

Figure 6-21 Comparison of Histories of Temperature Increase in Lead Core

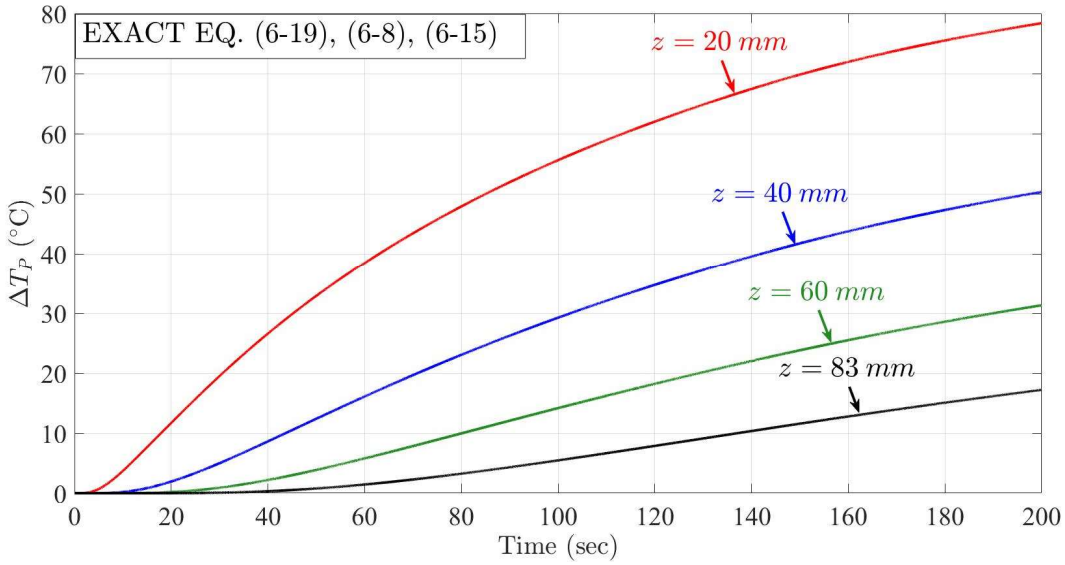

Figure 6-22 Exact Histories of Temperature Increase in Steel End Plates at Various Depths (83 mm is the interface of steel end plates with concrete)

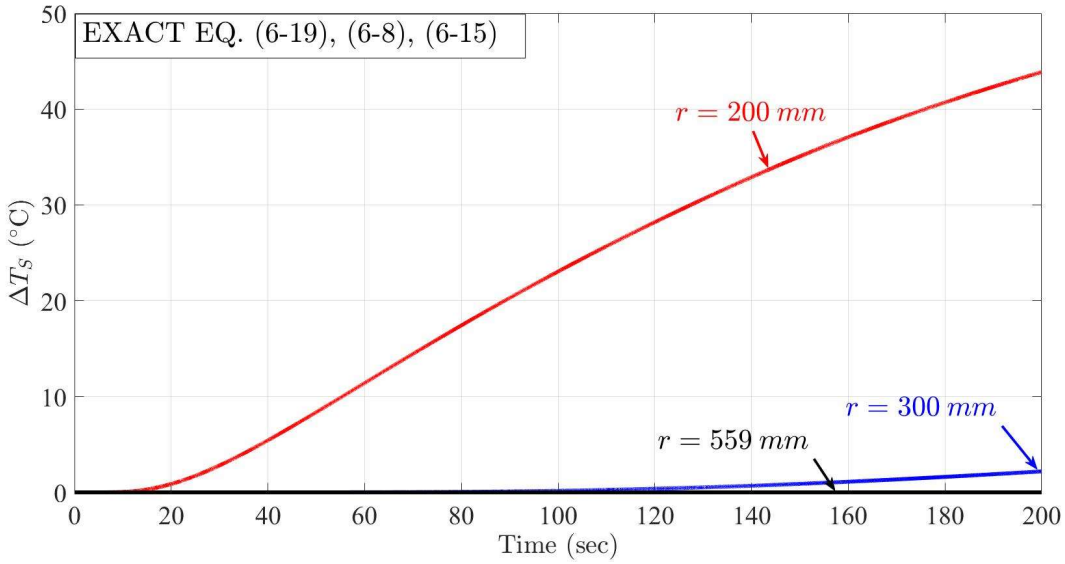

Figure 6-23 Exact Histories of Temperature Increase in Steel Shim Plates at Various Distances in the Radial Direction (r=559mm is the shim plate to rubber cover interface)

In further discussing the results of Figures 6-21 and 6-22, we note that the results are based on solutions that assume the steel end plates to be indefinite in depth. There is no available analytic solution for the problem of a heated plate as shown in Figure 6-18a but with finite insulated depth to be able to further investigate as done for the sliding bearings in Section 6.5. However, the results for the sliding bearing in

Figure 6-17 show that the temperature at the sliding interface is practically unaffected by the assumptions of indefinite depth plate, even for large times. This is true even when there some noticeable increase in temperature at the insulated depth, which as seen in Figure 6-17 is higher when a plate of insulated small finite depth is considered. In similarity, Figure 6-22 shows a small but noticeable increase in temperature at the depth where the steel plate terminates in insulated contact with concrete, but this should have no impact on the temperature at the steel to lead interface, and particularly on the temperature of the bulk of the lead core, which is used to determine instantaneous values of the characteristic strength of lead-rubber bearings.

“This Page Intentionally Left Blank”

SECTION 7
RESULTS FOR TEST TO REPRESENT EFFECTS OF THE MAXIMUM EARTHQUAKE

7.1 Procedure for Test Design

The procedure for designing a test to represent the effects of the maximum earthquake starts with the assumption that the isolator in the test is subject to the average gravity load in the actual application and cyclic lateral motion of specified amplitude of displacement and period of motion. Analysis then using the same isolator models used in the response history analysis reported in Section 6 determines the number of cycles needed to (a) approximately reach the maximum value of the cumulative energy computed in the response history analysis, or (b) approximately reproduce the cumulative energy history energy as in the response history analysis, or (c) approximately reproduce the history of temperature at the sliding interface or in the lead core as in the response history analysis. Results on the conditions of testing are presented for these three cases using the empirical data for the 50^{th} (median) and 90^{th} percentile response history analysis results of Section 6 for each of the systems analyzed (96 isolation systems, 3 seismic intensities, long and short-duration motions for a total of 576 cases).

All tests were designed for the following amplitude of displacement and period of motions: (a) Amplitude of D_M and period of T_M when the test approximately reaches the maximum value of the cumulative energy computed in the response history analysis, and (b) amplitude $0.4D_M$ or $0.5D_M$ and period T_M when the tests approximately reproduce the histories of cumulative energy and temperature at sliding interfaces or the lead core computed in the response history analysis. Values of displacement D_M and period T_M have been reported in Section 5, Tables 5-1 to 5-11.

Detailed results for each of the analyzed single FP, triple FP and lead-rubber systems are presented in Appendices G, H and I, respectively. Sample results are presented in the following sections.

7.2 Results for Test Based on Cumulative Energy

Tables 7-1 to 7-3 present results in terms of the required number of cycles for the studied single FP systems. Also, Tables 7-4 to 7-7 present results for the triple FP systems and Tables 7-8 to 7-11 present results for the lead-rubber systems.

Table 7-1 Required Number of Cycles for Maximum Earthquake Effect Test Based on Cumulative Energy for Single FP Systems when S_{M1}=0.7g

	Test Amplitude (D)	Test Period (T)	k_T = 2/3 at 200°C				k_T = 1/2 at 200°C				k_T = 1/3 at 200°C			
			Short-duration		Long-duration		Short-duration		Long-duration		Short-duration		Long-duration	
			50th	90th	50th	90th	50th	90th	50th	90th	50th	90th	50th	90th
System 11 (T_P = 3.50 sec, μ_{ref} = 0.040)	D_M	T_M	4	8	12	25	5	8	11	23	5	9	11	22
	$0.4D_M$	T_M	11	22	33	71	13	23	34	70	14	27	35	70
System 31 (T_P = 4.93 sec, μ_{ref} = 0.040)	D_M	T_M	4	7	10	24	4	7	10	21	4	8	9	20
	$0.4D_M$	T_M	10	21	29	69	11	21	28	64	11	24	29	62
System 12 (T_P = 3.50 sec, μ_{ref} = 0.060)	D_M	T_M	4	8	13	30	4	8	12	28	4	9	11	26
	$0.4D_M$	T_M	10	22	35	86	11	23	36	83	13	28	37	83
System 32 (T_P = 4.93 sec, μ_{ref} = 0.060)	D_M	T_M	3	8	11	27	4	7	11	25	4	7	9	22
	$0.4D_M$	T_M	9	21	32	77	10	21	32	75	12	24	30	73
System 13 (T_P = 3.50 sec, μ_{ref} = 0.080)	D_M	T_M	3	9	13	33	4	8	13	30	4	9	12	27
	$0.4D_M$	T_M	9	23	35	92	11	24	37	87	12	28	39	87
System 33 (T_P = 4.93 sec, μ_{ref} = 0.080)	D_M	T_M	3	8	12	30	3	8	12	28	4	7	10	25
	$0.4D_M$	T_M	8	21	34	84	10	21	33	81	11	23	34	81
System 14 (T_P = 3.50 sec, μ_{ref} = 0.100)	D_M	T_M	3	9	13	36	3	9	13	32	4	9	12	28
	$0.4D_M$	T_M	8	24	35	96	10	24	37	90	12	28	38	86
System 34 (T_P = 4.93 sec, μ_{ref} = 0.100)	D_M	T_M	3	8	13	33	3	8	12	31	4	8	11	27
	$0.4D_M$	T_M	8	20	33	89	9	22	35	85	11	24	35	83

Table 7-2 Required Number of Cycles for Maximum Earthquake Effect Test Based on Cumulative Energy for Single FP Systems when S_{M1}=0.9g

	Test Amplitude (D)	Test Period (T)	k_T = 2/3 at 200°C				k_T = 1/2 at 200°C				k_T = 1/3 at 200°C			
			Short-duration		Long-duration		Short-duration		Long-duration		Short-duration		Long-duration	
			50th	90th	50th	90th	50th	90th	50th	90th	50th	90th	50th	90th
System 11 (T_P = 3.50 sec, μ_{ref} = 0.040)	D_M	T_M	4	8	11	22	5	9	11	21	5	10	11	20
	$0.4D_M$	T_M	12	23	31	63	13	26	32	62	15	31	34	64
System 31 (T_P = 4.93 sec, μ_{ref} = 0.040)	D_M	T_M	4	8	10	20	4	8	9	19	4	8	9	17
	$0.4D_M$	T_M	10	21	27	58	11	23	27	56	12	26	28	55
System 12 (T_P = 3.50 sec, μ_{ref} = 0.060)	D_M	T_M	4	8	11	25	4	9	11	25	4	10	11	24
	$0.4D_M$	T_M	11	23	34	75	12	27	35	77	13	33	37	78
System 32 (T_P = 4.93 sec, μ_{ref} = 0.060)	D_M	T_M	4	7	10	23	4	7	9	21	4	8	9	19
	$0.4D_M$	T_M	10	20	28	69	11	22	28	63	12	26	29	61
System 13 (T_P = 3.50 sec, μ_{ref} = 0.080)	D_M	T_M	4	8	12	27	4	8	11	26	4	10	11	25
	$0.4D_M$	T_M	11	25	36	84	12	25	34	79	13	32	37	83
System 33 (T_P = 4.93 sec, μ_{ref} = 0.080)	D_M	T_M	3	7	11	26	4	7	10	23	4	7	9	20
	$0.4D_M$	T_M	10	22	32	80	11	22	31	71	12	24	30	67
System 14 (T_P = 3.50 sec, μ_{ref} = 0.100)	D_M	T_M	4	9	12	28	4	9	11	27	4	9	11	26
	$0.4D_M$	T_M	11	26	37	91	12	26	33	81	13	32	37	85
System 34 (T_P = 4.93 sec, μ_{ref} = 0.100)	D_M	T_M	3	8	11	28	3	8	11	25	4	8	10	22
	$0.4D_M$	T_M	10	24	35	87	11	23	33	76	12	26	32	72

Table 7-3 Required Number of Cycles for Maximum Earthquake Effect Test Based on Cumulative Energy for Single FP Systems when S_{M1}=1.1g

	Test Amplitude (D)	Test Period (T)	k_T = 2/3 at 200°C				k_T = 1/2 at 200°C				k_T = 1/3 at 200°C			
			Short-duration		Long-duration		Short-duration		Long-duration		Short-duration		Long-duration	
			50th	90th	50th	90th	50th	90th	50th	90th	50th	90th	50th	90th
System 11 (T_P = 3.50 sec, μ_{ref} = 0.040)	D_M	T_M	5	9	11	20	5	10	11	20	5	11	11	20
	$0.4D_M$	T_M	13	25	31	60	15	29	33	61	17	35	35	65
System 31 (T_P = 4.93 sec, μ_{ref} = 0.040)	D_M	T_M	4	8	9	19	4	8	9	18	4	9	8	17
	$0.4D_M$	T_M	10	22	26	54	11	24	26	54	11	27	25	55
System 12 (T_P = 3.50 sec, μ_{ref} = 0.060)	D_M	T_M	4	9	11	26	4	10	11	24	4	11	10	23
	$0.4D_M$	T_M	12	26	32	78	13	30	34	75	14	37	34	77
System 32 (T_P = 4.93 sec, μ_{ref} = 0.060)	D_M	T_M	4	8	9	20	4	8	9	19	4	9	9	17
	$0.4D_M$	T_M	10	22	27	61	11	24	27	58	12	28	28	56
System 13 (T_P = 3.50 sec, μ_{ref} = 0.080)	D_M	T_M	4	9	12	26	4	9	11	26	4	11	10	23
	$0.4D_M$	T_M	12	26	35	82	12	29	33	79	14	36	35	76
System 33 (T_P = 4.93 sec, μ_{ref} = 0.080)	D_M	T_M	4	7	10	22	4	7	9	21	4	8	9	18
	$0.4D_M$	T_M	10	21	30	69	11	22	29	64	12	27	29	60
System 14 (T_P = 3.50 sec, μ_{ref} = 0.100)	D_M	T_M	4	9	11	27	4	9	11	27	4	11	11	24
	$0.4D_M$	T_M	12	27	35	86	12	28	34	81	13	37	36	79
System 34 (T_P = 4.93 sec, μ_{ref} = 0.100)	D_M	T_M	3	8	10	24	4	7	10	23	4	8	9	20
	$0.4D_M$	T_M	10	23	31	75	11	23	31	69	12	27	29	65

Table 7-4 Required Number of Cycles for Maximum Earthquake Effect Test Based on Cumulative Energy for Triple FP Systems when S_{M1}=0.7g

	Test Amplitude (D)	Test Period (T)	k_T = 2/3 at 200°C				k_T = 1/2 at 200°C				k_T = 1/3 at 200°C			
			Short-duration		Long-duration		Short-duration		Long-duration		Short-duration		Long-duration	
			50th	90th	50th	90th	50th	90th	50th	90th	50th	90th	50th	90th
System 11 (T_P = 3.40 sec, μ_{ref} = 0.037)	D_M	T_M	5	8	12	26	5	9	13	25	5	10	12	24
	$0.4D_M$	T_M	12	20	30	63	12	21	30	60	12	25	29	59
System 21 (T_P = 4.13 sec, μ_{ref} = 0.038)	D_M	T_M	4	7	11	26	4	8	11	24	5	9	11	22
	$0.4D_M$	T_M	11	19	28	63	11	20	26	60	12	22	27	57
System 31 (T_P = 4.86 sec, μ_{ref} = 0.038)	D_M	T_M	4	8	11	25	4	8	11	23	4	8	11	21
	$0.4D_M$	T_M	11	19	28	62	11	19	27	58	11	19	27	55
System 41 (T_P = 5.57 sec, μ_{ref} = 0.039)	D_M	T_M	4	8	12	26	4	9	11	25	4	8	10	23
	$0.4D_M$	T_M	10	21	29	65	9	22	28	63	10	22	27	60
System 12 (T_P = 3.40 sec, μ_{ref} = 0.054)	D_M	T_M	5	9	15	33	5	9	14	31	5	9	14	30
	$0.4D_M$	T_M	13	21	34	74	13	21	32	70	12	20	32	67
System 22 (T_P = 4.13 sec, μ_{ref} = 0.056)	D_M	T_M	5	9	14	32	5	8	14	31	5	8	13	28
	$0.4D_M$	T_M	12	21	33	73	12	20	31	70	11	19	30	66
System 32 (T_P = 4.86 sec, μ_{ref} = 0.057)	D_M	T_M	5	8	13	33	5	8	13	30	5	8	12	27
	$0.4D_M$	T_M	11	20	31	76	12	19	30	70	12	19	29	64
System 42 (T_P = 5.57 sec, μ_{ref} = 0.058)	D_M	T_M	5	8	14	32	4	9	14	29	4	8	14	27
	$0.4D_M$	T_M	12	21	32	73	10	21	32	68	10	21	32	65
System 13 (T_P = 3.40 sec, μ_{ref} = 0.070)	D_M	T_M	6	10	17	38	6	10	17	37	6	10	17	35
	$0.4D_M$	T_M	13	22	38	82	13	21	37	78	13	21	35	75
System 23 (T_P = 4.13 sec, μ_{ref} = 0.074)	D_M	T_M	5	10	17	38	6	9	17	36	6	9	16	34
	$0.4D_M$	T_M	13	22	38	82	13	20	37	78	13	20	35	75
System 33 (T_P = 4.86 sec, μ_{ref} = 0.075)	D_M	T_M	5	9	16	38	5	9	15	36	5	9	15	32
	$0.4D_M$	T_M	13	22	37	83	12	21	34	79	12	20	33	72
System 43 (T_P = 5.57 sec, μ_{ref} = 0.076)	D_M	T_M	5	9	15	39	5	9	16	36	5	9	15	32
	$0.4D_M$	T_M	12	22	34	83	12	21	35	79	11	20	34	72
System 14 (T_P = 3.40 sec, μ_{ref} = 0.087)	D_M	T_M	6	10	19	42	6	10	19	40	6	10	19	40
	$0.4D_M$	T_M	14	23	41	90	14	23	41	86	13	21	39	82
System 24 (T_P = 4.13 sec, μ_{ref} = 0.091)	D_M	T_M	6	10	19	43	6	10	18	40	6	10	18	38
	$0.4D_M$	T_M	14	23	42	91	13	22	39	85	13	21	38	80
System 34 (T_P = 4.86 sec, μ_{ref} = 0.094)	D_M	T_M	6	10	19	43	6	10	19	40	6	9	18	37
	$0.4D_M$	T_M	14	23	41	90	14	22	41	86	13	21	37	79
System 44 (T_P = 5.57 sec, μ_{ref} = 0.095)	D_M	T_M	6	10	18	42	6	10	17	39	6	9	17	37
	$0.4D_M$	T_M	13	23	40	89	13	22	38	85	13	21	35	80

Table 7-5 Required Number of Cycles for Maximum Earthquake Effect Test Based on Cumulative Energy for Triple FP Systems when S_{M1}=0.9g

	Test Amplitude (D)	Test Period (T)	k_T = 2/3 at 200°C				k_T = 1/2 at 200°C				k_T = 1/3 at 200°C			
			Short-duration		Long-duration		Short-duration		Long-duration		Short-duration		Long-duration	
			50th	90th	50th	90th	50th	90th	50th	90th	50th	90th	50th	90th
System 11 (T_P = 3.40 sec, μ_{ref} = 0.037)	D_M	T_M	5	9	12	22	5	10	11	22	5	11	12	21
	$0.4D_M$	T_M	13	24	30	59	14	27	30	59	15	31	33	61
System 21 (T_P = 4.13 sec, μ_{ref} = 0.038)	D_M	T_M	5	8	10	21	5	8	10	20	4	9	10	18
	$0.4D_M$	T_M	12	22	27	58	12	23	28	56	12	27	29	55
System 31 (T_P = 4.86 sec, μ_{ref} = 0.038)	D_M	T_M	4	8	10	21	5	8	10	20	4	8	9	18
	$0.4D_M$	T_M	11	20	28	56	12	23	28	56	11	24	27	55
System 41 (T_P = 5.57 sec, μ_{ref} = 0.039)	D_M	T_M	4	8	10	23	4	8	9	21	3	8	8	19
	$0.4D_M$	T_M	10	23	26	63	10	24	26	61	10	25	25	60
System 12 (T_P = 3.40 sec, μ_{ref} = 0.054)	D_M	T_M	5	8	13	27	5	9	12	25	5	10	11	23
	$0.4D_M$	T_M	13	21	31	66	13	23	32	64	14	28	31	62
System 22 (T_P = 4.13 sec, μ_{ref} = 0.056)	D_M	T_M	5	8	12	26	4	8	11	24	4	8	11	21
	$0.4D_M$	T_M	12	19	30	67	12	21	29	63	13	24	30	60
System 32 (T_P = 4.86 sec, μ_{ref} = 0.057)	D_M	T_M	4	8	12	26	4	8	11	23	4	8	11	20
	$0.4D_M$	T_M	12	20	31	67	12	20	30	62	12	22	31	59
System 42 (T_P = 5.57 sec, μ_{ref} = 0.058)	D_M	T_M	4	8	12	26	4	9	11	25	4	9	10	22
	$0.4D_M$	T_M	10	22	31	68	10	23	30	68	11	25	29	66
System 13 (T_P = 3.40 sec, μ_{ref} = 0.070)	D_M	T_M	5	9	15	32	5	8	14	29	5	9	13	26
	$0.4D_M$	T_M	13	22	35	74	13	21	34	70	14	25	34	67
System 23 (T_P = 4.13 sec, μ_{ref} = 0.074)	D_M	T_M	5	8	14	31	5	8	13	28	5	8	12	24
	$0.4D_M$	T_M	13	21	34	74	12	21	32	71	13	23	32	66
System 33 (T_P = 4.86 sec, μ_{ref} = 0.075)	D_M	T_M	5	8	13	31	5	8	12	27	5	8	11	23
	$0.4D_M$	T_M	12	20	32	75	12	20	32	70	13	21	32	65
System 43 (T_P = 5.57 sec, μ_{ref} = 0.076)	D_M	T_M	5	8	14	29	4	8	13	27	4	8	12	24
	$0.4D_M$	T_M	12	21	35	73	11	22	34	69	11	24	33	68
System 14 (T_P = 3.40 sec, μ_{ref} = 0.087)	D_M	T_M	6	9	17	36	5	9	16	32	5	9	14	29
	$0.4D_M$	T_M	14	22	38	82	14	23	37	77	14	22	35	73
System 24 (T_P = 4.13 sec, μ_{ref} = 0.091)	D_M	T_M	6	9	17	35	5	8	15	31	5	8	13	28
	$0.4D_M$	T_M	13	22	39	81	13	21	37	76	13	21	34	73
System 34 (T_P = 4.86 sec, μ_{ref} = 0.094)	D_M	T_M	5	9	15	35	5	8	14	31	5	8	12	26
	$0.4D_M$	T_M	13	22	36	82	13	21	35	76	13	21	33	70
System 44 (T_P = 5.57 sec, μ_{ref} = 0.095)	D_M	T_M	5	9	16	34	5	8	14	31	4	9	14	26
	$0.4D_M$	T_M	13	22	38	82	13	21	35	76	12	23	37	71

Table 7-6 Required Number of Cycles for Maximum Earthquake Effect Test Based on Cumulative Energy for Triple FP Systems when S_{M1}=1.1g

	Test Amplitude (D)	Test Period (T)	k_T = 2/3 at 200°C				k_T = 1/2 at 200°C				k_T = 1/3 at 200°C			
			Short-duration		Long-duration		Short-duration		Long-duration		Short-duration		Long-duration	
			50th	90th	50th	90th	50th	90th	50th	90th	50th	90th	50th	90th
System 11 (T_P = 3.40 sec, μ_{ref} = 0.037)	D_M	T_M	5	11	11	21	6	11	12	20	5	13	11	19
	$0.4D_M$	T_M	15	30	31	60	16	33	34	60	16	39	34	60
System 21 (T_P = 4.13 sec, μ_{ref} = 0.038)	D_M	T_M	4	9	10	19	4	9	10	18	4	10	10	17
	$0.4D_M$	T_M	12	25	28	55	12	25	28	53	13	30	29	52
System 31 (T_P = 4.86 sec, μ_{ref} = 0.038)	D_M	T_M	4	8	9	19	4	8	9	17	4	8	8	16
	$0.4D_M$	T_M	11	21	26	53	11	23	26	51	12	26	25	49
System 41 (T_P = 5.57 sec, μ_{ref} = 0.039)	D_M	T_M	4	8	9	20	3	8	8	19	3	9	8	18
	$0.4D_M$	T_M	10	23	24	58	10	24	24	56	10	26	24	55
System 12 (T_P = 3.40 sec, μ_{ref} = 0.054)	D_M	T_M	5	8	12	23	5	9	11	21	5	11	11	20
	$0.4D_M$	T_M	14	23	32	64	14	27	32	62	16	35	35	65
System 22 (T_P = 4.13 sec, μ_{ref} = 0.056)	D_M	T_M	5	8	10	22	4	9	11	20	4	9	10	18
	$0.4D_M$	T_M	13	22	29	63	13	25	31	60	14	29	31	57
System 32 (T_P = 4.86 sec, μ_{ref} = 0.057)	D_M	T_M	4	8	11	21	4	8	10	19	4	8	9	17
	$0.4D_M$	T_M	12	21	30	62	12	23	30	58	12	25	29	55
System 42 (T_P = 5.57 sec, μ_{ref} = 0.058)	D_M	T_M	4	9	10	23	4	8	9	22	3	8	8	19
	$0.4D_M$	T_M	10	24	29	68	11	25	28	65	11	27	27	61
System 13 (T_P = 3.40 sec, μ_{ref} = 0.070)	D_M	T_M	5	8	13	26	5	10	12	24	5	9	11	21
	$0.4D_M$	T_M	13	22	34	70	15	28	33	66	15	30	34	66
System 23 (T_P = 4.13 sec, μ_{ref} = 0.074)	D_M	T_M	5	8	12	25	4	8	11	23	4	9	11	19
	$0.4D_M$	T_M	13	21	33	70	13	23	32	65	14	28	34	62
System 33 (T_P = 4.86 sec, μ_{ref} = 0.075)	D_M	T_M	5	8	12	25	4	8	11	22	4	8	10	19
	$0.4D_M$	T_M	12	21	33	70	13	22	32	65	14	25	33	61
System 43 (T_P = 5.57 sec, μ_{ref} = 0.076)	D_M	T_M	4	8	12	25	4	9	11	24	4	8	9	21
	$0.4D_M$	T_M	11	23	34	71	12	25	32	71	12	27	30	67
System 14 (T_P = 3.40 sec, μ_{ref} = 0.087)	D_M	T_M	5	9	14	29	5	8	13	26	5	8	12	23
	$0.4D_M$	T_M	14	23	36	76	14	23	35	71	15	26	36	68
System 24 (T_P = 4.13 sec, μ_{ref} = 0.091)	D_M	T_M	5	8	14	29	5	8	12	26	4	8	11	21
	$0.4D_M$	T_M	14	22	36	77	13	22	33	71	14	27	34	66
System 34 (T_P = 4.86 sec, μ_{ref} = 0.094)	D_M	T_M	5	8	13	28	5	8	12	25	5	8	10	21
	$0.4D_M$	T_M	13	21	36	76	14	21	33	71	15	25	34	66
System 44 (T_P = 5.57 sec, μ_{ref} = 0.095)	D_M	T_M	5	8	14	27	4	8	13	25	4	8	10	22
	$0.4D_M$	T_M	12	23	37	75	12	24	36	71	13	27	34	72

Table 7-7 Required Number of Cycles for Maximum Earthquake Effect Test Based on Cumulative Energy for Additional Triple FP System LL

	Test Amplitude (D)	Test Period (T)	S_{M1} = 0.7g											
			k_T = 2/3 at 200°C				k_T = 1/2 at 200°C				k_T = 1/3 at 200°C			
			Short-duration		Long-duration		Short-duration		Long-duration		Short-duration		Long-duration	
			50th	90th	50th	90th	50th	90th	50th	90th	50th	90th	50th	90th
System LL (T_P = 5.49 sec, μ_{ref} = 0.074)	D_M	T_M	5	9	15	39	5	10	16	38	5	9	16	36
	0.4D_M	T_M	12	22	34	85	12	22	36	81	11	20	33	72

	Test Amplitude (D)	Test Period (T)	S_{M1} = 0.9g											
			k_T = 2/3 at 200°C				k_T = 1/2 at 200°C				k_T = 1/3 at 200°C			
			Short-duration		Long-duration		Short-duration		Long-duration		Short-duration		Long-duration	
			50th	90th	50th	90th	50th	90th	50th	90th	50th	90th	50th	90th
System LL (T_P = 5.49 sec, μ_{ref} = 0.074)	D_M	T_M	5	9	15	34	5	9	15	32	5	10	15	31
	0.4D_M	T_M	12	21	34	72	10	20	31	68	10	20	30	62

	Test Amplitude (D)	Test Period (T)	S_{M1} = 1.1g											
			k_T = 2/3 at 200°C				k_T = 1/2 at 200°C				k_T = 1/3 at 200°C			
			Short-duration		Long-duration		Short-duration		Short-duration		Long-duration		Short-duration	
			50th	90th	50th	50th	90th	50th	50th	90th	50th	50th	90th	50th
System LL (T_P = 5.49 sec, μ_{ref} = 0.074)	D_M	T_M	5	9	14	32	5	10	13	29	4	10	13	26
	0.4D_M	T_M	11	21	30	66	10	20	29	61	10	21	27	57

Table 7-8 Required Number of Cycles for Maximum Earthquake Effect Test Based on Cumulative Energy for Lead-rubber Systems when S_{M1}=0.7g

		Test Amplitude (D)	Test Period (T)	Short-duration		Long-duration	
				50th	90th	50th	90th
α/h_L =0.3	System 111 (T_d = 2 sec, $(Q_d/W)_{ref}$ = 0.08)	D_M	T_M	9	15	28	52
		$0.5D_M$	T_M	16	27	50	87
	System 211 (T_d = 3 sec, $(Q_d/W)_{ref}$ = 0.08)	D_M	T_M	7	12	23	43
		$0.5D_M$	T_M	14	23	41	72
	System 311 (T_d = 4 sec, $(Q_d/W)_{ref}$ = 0.08)	D_M	T_M	7	12	20	39
		$0.5D_M$	T_M	13	22	35	64
	System 121 (T_d = 2 sec, $(Q_d/W)_{ref}$ = 0.16)	D_M	T_M	11	16	42	72
		$0.5D_M$	T_M	21	31	76	126
	System 221 (T_d = 3 sec, $(Q_d/W)_{ref}$ = 0.16)	D_M	T_M	10	15	36	62
		$0.5D_M$	T_M	19	28	67	109
	System 321 (T_d = 4 sec, $(Q_d/W)_{ref}$ = 0.16)	D_M	T_M	9	14	34	56
		$0.5D_M$	T_M	18	27	62	98
	System 131 (T_d = 2 sec, $(Q_d/W)_{ref}$ = 0.24)	D_M	T_M	14	21	57	90
		$0.5D_M$	T_M	26	40	103	156
	System 231 (T_d = 3 sec, $(Q_d/W)_{ref}$ = 0.24)	D_M	T_M	13	20	48	81
		$0.5D_M$	T_M	25	38	87	142
	System 331 (T_d = 4 sec, $(Q_d/W)_{ref}$ = 0.24)	D_M	T_M	12	19	43	75
		$0.5D_M$	T_M	23	36	79	133
α/h_L =0.6	System 112 (T_d = 2 sec, $(Q_d/W)_{ref}$ = 0.08)	D_M	T_M	9	17	30	54
		$0.5D_M$	T_M	16	30	48	78
	System 212 (T_d = 3 sec, $(Q_d/W)_{ref}$ = 0.08)	D_M	T_M	7	14	25	44
		$0.5D_M$	T_M	13	25	40	64
	System 312 (T_d = 4 sec, $(Q_d/W)_{ref}$ = 0.08)	D_M	T_M	7	12	20	37
		$0.5D_M$	T_M	12	21	32	53
	System 122 (T_d = 2 sec, $(Q_d/W)_{ref}$ = 0.16)	D_M	T_M	10	16	41	73
		$0.5D_M$	T_M	20	29	70	115
	System 222 (T_d = 3 sec, $(Q_d/W)_{ref}$ = 0.16)	D_M	T_M	9	15	36	62
		$0.5D_M$	T_M	17	27	62	97
	System 322 (T_d = 4 sec, $(Q_d/W)_{ref}$ = 0.16)	D_M	T_M	9	14	32	55
		$0.5D_M$	T_M	18	26	55	86
	System 132 (T_d = 2 sec, $(Q_d/W)_{ref}$ = 0.24)	D_M	T_M	13	20	59	90
		$0.5D_M$	T_M	25	38	100	147
	System 232 (T_d = 3 sec, $(Q_d/W)_{ref}$ = 0.24)	D_M	T_M	13	19	50	84
		$0.5D_M$	T_M	25	36	86	135
	System 332 (T_d = 4 sec, $(Q_d/W)_{ref}$ = 0.24)	D_M	T_M	12	18	42	77
		$0.5D_M$	T_M	23	34	73	124

Table 7-9 Required Number of Cycles for Maximum Earthquake Effect Test Based on Cumulative Energy for Lead-rubber Systems when S_{M1}=0.9g

		Test Amplitude (D)	Test Period (T)	Short-duration		Long-duration	
				50th	90th	50th	90th
α/h_L =0.3	System 111 (T_d = 2 sec, $(Q_d/W)_{ref}$ = 0.08)	D_M	T_M	8	17	24	47
		$0.5D_M$	T_M	18	36	52	86
	System 211 (T_d = 3 sec, $(Q_d/W)_{ref}$ = 0.08)	D_M	T_M	6	13	20	40
		$0.5D_M$	T_M	15	28	42	72
	System 311 (T_d = 4 sec, $(Q_d/W)_{ref}$ = 0.08)	D_M	T_M	6	11	17	34
		$0.5D_M$	T_M	15	25	35	60
	System 121 (T_d = 2 sec, $(Q_d/W)_{ref}$ = 0.16)	D_M	T_M	9	14	33	62
		$0.5D_M$	T_M	22	32	74	127
	System 221 (T_d = 3 sec, $(Q_d/W)_{ref}$ = 0.16)	D_M	T_M	8	13	29	51
		$0.5D_M$	T_M	19	30	63	105
	System 321 (T_d = 4 sec, $(Q_d/W)_{ref}$ = 0.16)	D_M	T_M	7	12	25	47
		$0.5D_M$	T_M	18	28	55	95
	System 131 (T_d = 2 sec, $(Q_d/W)_{ref}$ = 0.24)	D_M	T_M	11	17	44	75
		$0.5D_M$	T_M	26	41	97	157
	System 231 (T_d = 3 sec, $(Q_d/W)_{ref}$ = 0.24)	D_M	T_M	10	15	38	70
		$0.5D_M$	T_M	24	36	83	147
	System 331 (T_d = 4 sec, $(Q_d/W)_{ref}$ = 0.24)	D_M	T_M	9	14	33	62
		$0.5D_M$	T_M	22	34	74	131
α/h_L =0.6	System 112 (T_d = 2 sec, $(Q_d/W)_{ref}$ = 0.08)	D_M	T_M	8	19	29	52
		$0.5D_M$	T_M	18	36	48	77
	System 212 (T_d = 3 sec, $(Q_d/W)_{ref}$ = 0.08)	D_M	T_M	6	17	24	41
		$0.5D_M$	T_M	14	30	40	62
	System 312 (T_d = 4 sec, $(Q_d/W)_{ref}$ = 0.08)	D_M	T_M	6	12	18	32
		$0.5D_M$	T_M	13	23	31	49
	System 122 (T_d = 2 sec, $(Q_d/W)_{ref}$ = 0.16)	D_M	T_M	9	14	33	64
		$0.5D_M$	T_M	20	31	65	108
	System 222 (T_d = 3 sec, $(Q_d/W)_{ref}$ = 0.16)	D_M	T_M	7	13	27	52
		$0.5D_M$	T_M	17	28	54	87
	System 322 (T_d = 4 sec, $(Q_d/W)_{ref}$ = 0.16)	D_M	T_M	7	12	24	44
		$0.5D_M$	T_M	16	27	47	74
	System 132 (T_d = 2 sec, $(Q_d/W)_{ref}$ = 0.24)	D_M	T_M	11	17	42	80
		$0.5D_M$	T_M	25	39	86	143
	System 232 (T_d = 3 sec, $(Q_d/W)_{ref}$ = 0.24)	D_M	T_M	10	15	37	69
		$0.5D_M$	T_M	22	34	76	122
	System 332 (T_d = 4 sec, $(Q_d/W)_{ref}$ = 0.24)	D_M	T_M	9	14	31	60
		$0.5D_M$	T_M	20	31	65	107

Table 7-10 Required Number of Cycles for Maximum Earthquake Effect Test Based on Cumulative Energy for Lead-rubber Systems when S_{M1}=1.1g

		Test Amplitude (D)	Test Period (T)	Short-duration		Long-duration	
				50th	90th	50th	90th
α/h_L =0.3	System 111 (T_d = 2 sec, $(Q_d/W)_{ref}$ = 0.08)	D_M	T_M	8	19	24	48
		$0.5D_M$	T_M	14	33	40	68
	System 211 (T_d = 3 sec, $(Q_d/W)_{ref}$ = 0.08)	D_M	T_M	6	15	20	39
		$0.5D_M$	T_M	11	26	32	56
	System 311 (T_d = 4 sec, $(Q_d/W)_{ref}$ = 0.08)	D_M	T_M	6	12	16	31
		$0.5D_M$	T_M	11	21	27	44
	System 121 (T_d = 2 sec, $(Q_d/W)_{ref}$ = 0.16)	D_M	T_M	8	13	28	56
		$0.5D_M$	T_M	16	25	52	92
	System 221 (T_d = 3 sec, $(Q_d/W)_{ref}$ = 0.16)	D_M	T_M	7	12	23	47
		$0.5D_M$	T_M	13	22	42	77
	System 321 (T_d = 4 sec, $(Q_d/W)_{ref}$ = 0.16)	D_M	T_M	6	11	20	41
		$0.5D_M$	T_M	12	21	36	66
	System 131 (T_d = 2 sec, $(Q_d/W)_{ref}$ = 0.24)	D_M	T_M	9	15	34	67
		$0.5D_M$	T_M	18	28	63	118
	System 231 (T_d = 3 sec, $(Q_d/W)_{ref}$ = 0.24)	D_M	T_M	8	13	32	57
		$0.5D_M$	T_M	16	26	59	100
	System 331 (T_d = 4 sec, $(Q_d/W)_{ref}$ = 0.24)	D_M	T_M	7	13	28	50
		$0.5D_M$	T_M	15	24	51	88
α/h_L =0.6	System 112 (T_d = 2 sec, $(Q_d/W)_{ref}$ = 0.08)	D_M	T_M	8	21	30	51
		$0.5D_M$	T_M	15	31	41	65
	System 212 (T_d = 3 sec, $(Q_d/W)_{ref}$ = 0.08)	D_M	T_M	7	19	24	39
		$0.5D_M$	T_M	12	27	32	50
	System 312 (T_d = 4 sec, $(Q_d/W)_{ref}$ = 0.08)	D_M	T_M	6	13	18	31
		$0.5D_M$	T_M	11	19	25	40
	System 122 (T_d = 2 sec, $(Q_d/W)_{ref}$ = 0.16)	D_M	T_M	8	14	30	58
		$0.5D_M$	T_M	15	26	46	80
	System 222 (T_d = 3 sec, $(Q_d/W)_{ref}$ = 0.16)	D_M	T_M	7	14	24	46
		$0.5D_M$	T_M	13	25	37	63
	System 322 (T_d = 4 sec, $(Q_d/W)_{ref}$ = 0.16)	D_M	T_M	6	12	20	38
		$0.5D_M$	T_M	12	21	31	53
	System 132 (T_d = 2 sec, $(Q_d/W)_{ref}$ = 0.24)	D_M	T_M	9	14	33	73
		$0.5D_M$	T_M	17	27	57	105
	System 232 (T_d = 3 sec, $(Q_d/W)_{ref}$ = 0.24)	D_M	T_M	8	13	30	60
		$0.5D_M$	T_M	15	24	51	86
	System 332 (T_d = 4 sec, $(Q_d/W)_{ref}$ = 0.24)	D_M	T_M	7	12	26	50
		$0.5D_M$	T_M	14	23	43	72

Table 7-11 Required Number of Cycles for Maximum Earthquake Effect Test Based on Cumulative Energy for Additional Lead-rubber Systems

	Test Amplitude (D)	Test Period (T)	S_{M1} = 0.7g			
			Short-duration		Long-duration	
			50th	90th	50th	90th
System 4 (T_d = 4 sec, a/h_L = 0.46, $(Q_d/W)_{ref}$ = 0.121)	D_M	T_M	8	12	25	48
	$0.5D_M$	T_M	15	23	46	80
System 5 (T_d = 3 sec, a/h_L = 0.46, $(Q_d/W)_{ref}$ = 0.121)	D_M	T_M	9	14	28	51
	$0.5D_M$	T_M	17	26	52	88
System 6 (T_d = 2 sec, a/h_L = 0.35, $(Q_d/W)_{ref}$ = 0.241)	D_M	T_M	13	21	53	88
	$0.5D_M$	T_M	26	41	98	158

	Test Amplitude (D)	Test Period (T)	S_{M1} = 0.9g			
			Short-duration		Long-duration	
			50th	90th	50th	90th
System 4 (T_d = 4 sec, a/h_L = 0.46, $(Q_d/W)_{ref}$ = 0.121)	D_M	T_M	7	11	19	42
	$0.5D_M$	T_M	13	21	34	65
System 5 (T_d = 3 sec, a/h_L = 0.46, $(Q_d/W)_{ref}$ = 0.121)	D_M	T_M	7	12	23	48
	$0.5D_M$	T_M	13	23	42	75
System 6 (T_d = 2 sec, a/h_L = 0.35, $(Q_d/W)_{ref}$ = 0.241)	D_M	T_M	11	17	42	75
	$0.5D_M$	T_M	21	34	79	135

	Test Amplitude (D)	Test Period (T)	S_{M1} = 1.1g			
			Short-duration		Long-duration	
			50th	90th	50th	90th
System 4 (T_d = 4 sec, a/h_L = 0.46, $(Q_d/W)_{ref}$ = 0.121)	D_M	T_M	6	11	17	38
	$0.5D_M$	T_M	12	21	30	54
System 5 (T_d = 3 sec, a/h_L = 0.46, $(Q_d/W)_{ref}$ = 0.121)	D_M	T_M	6	13	20	45
	$0.5D_M$	T_M	12	25	36	66
System 6 (T_d = 2 sec, a/h_L = 0.35, $(Q_d/W)_{ref}$ = 0.241)	D_M	T_M	9	14	35	67
	$0.5D_M$	T_M	18	28	65	121

Figures 7-1 to 7-3 present a sample of graphs comparing results on the 50th (median) and 90th cumulative energy computed using response history analysis and the corresponding test in short- and long-duration motions for representative single FP, triple FP, and lead-rubber systems. The choice of using an amplitude of $0.4D_M$ or $0.5D_M$ in the test to reproduce the history of the cumulative energy is such that in many, but not all, cases the test and the response history analysis provide similar histories of cumulative energy. Important consideration in the selection of the amplitude was to be the same for all 576 cases studied.

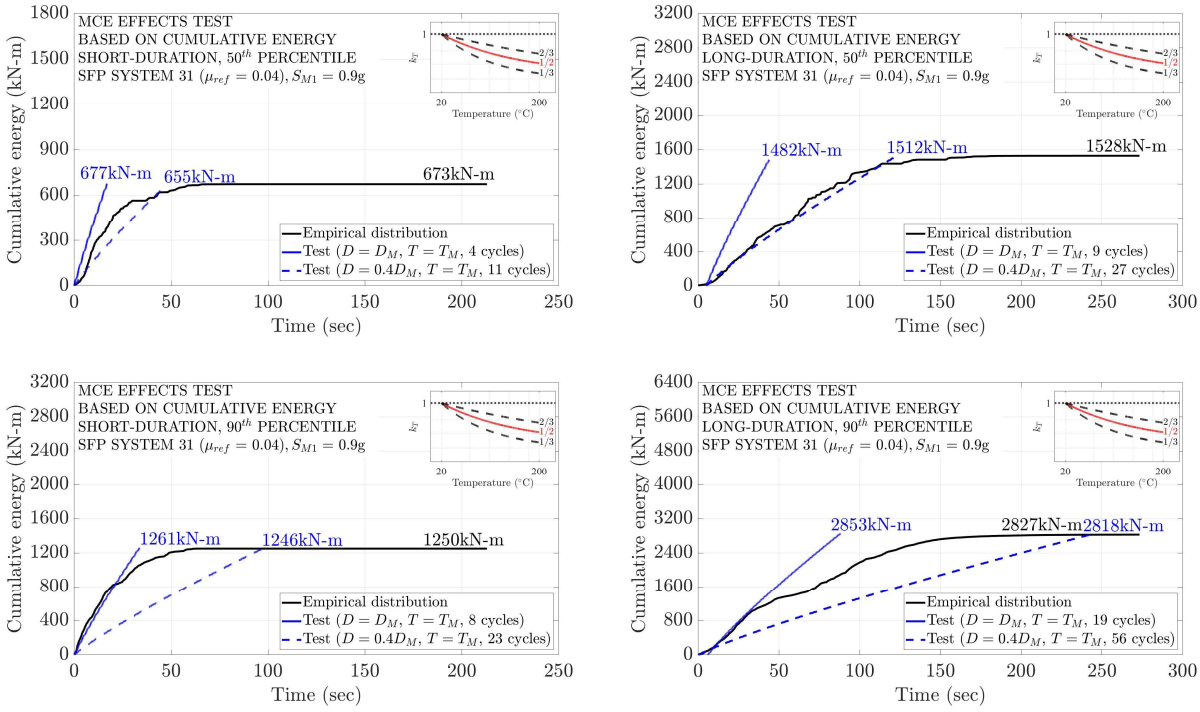

Figure 7-1 Comparison of 50th and 90th Percentile Histories of Cumulative Energy to Results of Test for Single FP System 31 (T_P = 4.93sec, μ_{ref} = 0.040) when S_{M1}=0.9g (friction case when k_T=0.5 at 200°C)

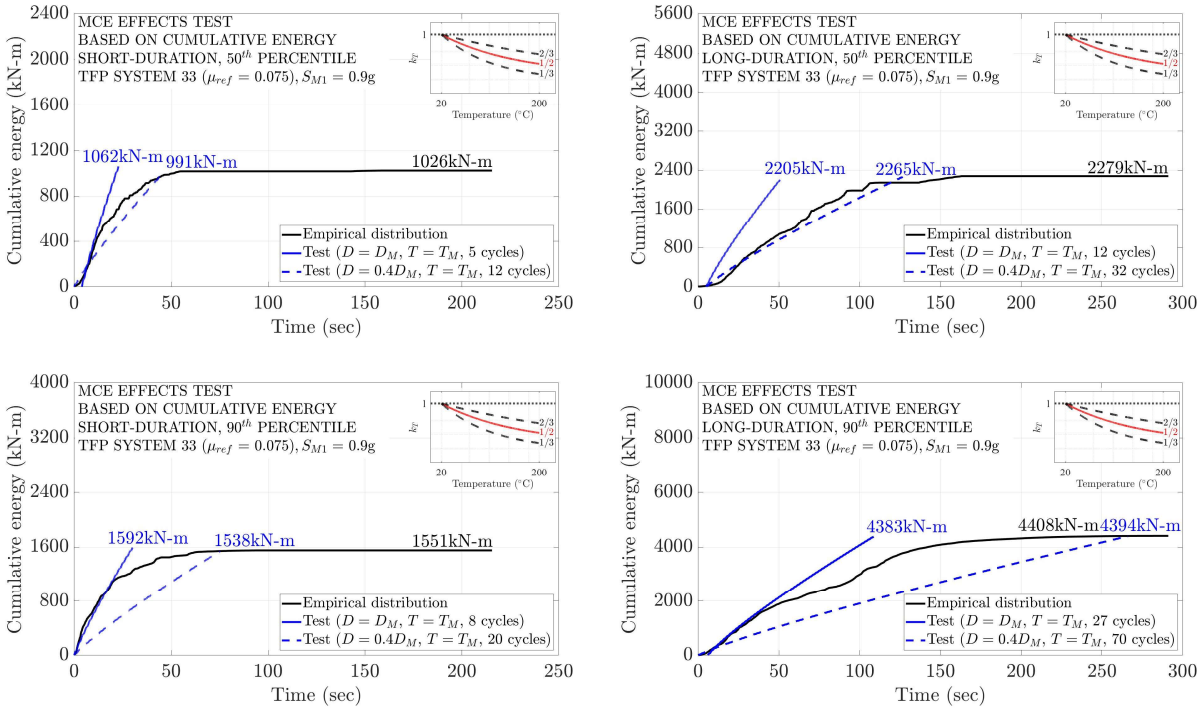

Figure 7-2 Comparison of 50th and 90th Percentile Histories of Cumulative Energy to Results of Test for Triple FP System 33 (μ_{1ref} = 0.08, μ_{ref} = 0.075, T_P = 4.86s) when S_{M1}=0.9g (friction case when k_T=0.5 at 200°C)

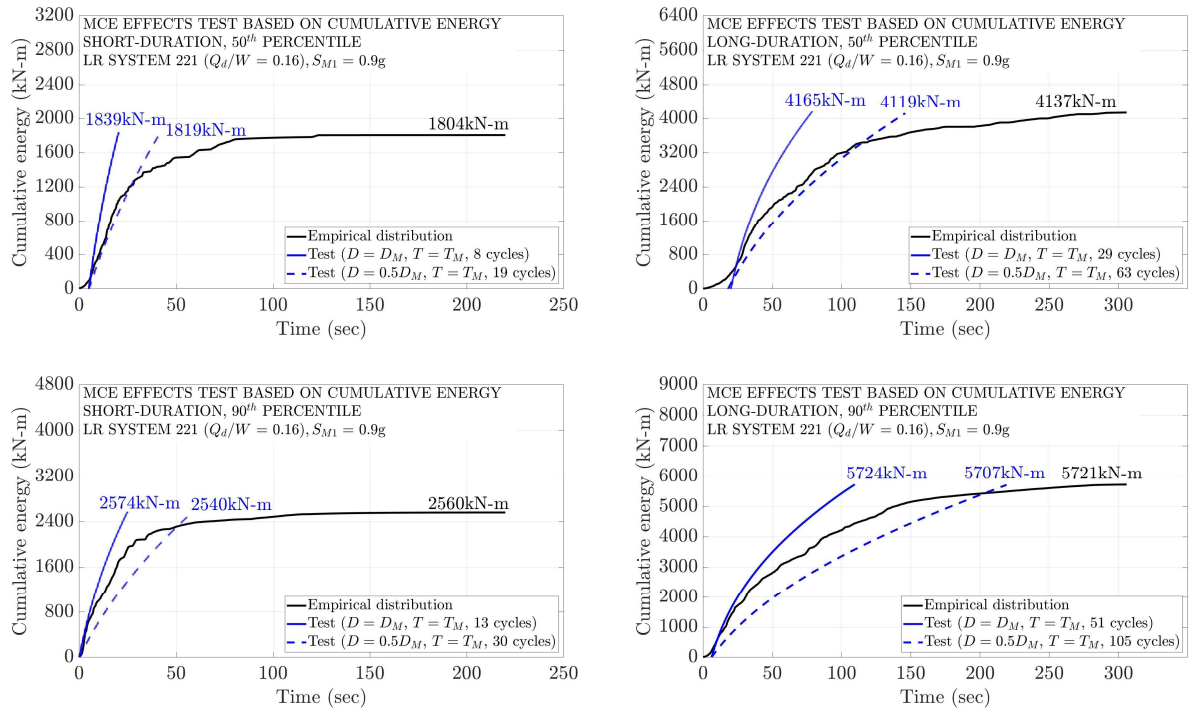

Figure 7-3 Comparison of 50th and 90th Percentile Histories of Cumulative Energy to Results of Test for Lead-rubber System 221 (T_d = 3s, $(Q_d/W)_{ref}$ = 0.16, a/h_L =0.3) when S_{M1} = 0.9g

Of interest is to note in Figure 7-3 that the cumulative energy in the tests of lead-rubber systems has nonlinear relationship with time. This is also true for the sliding systems but is less obvious in the graphs of Figures 7-1 and 7-2. This nonlinearity results from heating effects that reduce the strength of the isolators and thus more cycles (i.e., time) is required to achieve the target cumulative energy. The difference between sliding and lead-rubber systems is due to the relationship between the characteristic strength and temperature: for sliding systems the friction coefficient reaches a stable value at high temperatures, whereas for lead-rubber systems the characteristic strength continually declines to an essentially zero value as the temperature of lead approaches the melting point. This important difference leads to the requirement for more cycles of testing for lead-rubber than for sliding systems. The importance of heating effects is best seen in the results for the test to just reproduce the maximum value of the cumulative energy, performed at amplitude D_M and period T_M. This test should be compared to the ASCE/SEI-7 prototype test Item 4 in section 17.8.2.2, in which the isolator is subjected to at least 10 cycles of motion at amplitude of $0.75D_M$ and period of T_M (it is allowed to be performed in sets consisting of five continuous cycles followed by pause-thus effectively this test is one of five cycles that is repeated). Also, it should be compared to similar

results obtained with models of constant friction or characteristic strength (without heating effects) as those of Warn and Whittaker (2004).

Figures 7-4 to 7-15 presents results of the required number of cycles in the test match the maximum cumulative energy for the case of the median (50^{th} percentile) results (test at amplitude D_M and period T_M). The results demonstrate that for short-duration ground motions, sliding systems require 3 to 6 cycles, and lead-rubber systems require 6 to 14 cycles. The larger number of cycles is required when the friction or the characteristic strength (values at start of motion or reference values) are larger-thus when heating effects are pronounced. By comparison, the study of Warn and Whittaker (2004) resulted in for the same type of test (at amplitude D_M and period T_M, short-duration motions and matching the median of the maximum cumulative energy), a number of required cycles between 2 to 8 (but based on a wider range of invariable characteristic strength to weight values-0.03 to 0.12). These results are consistent with those obtained in this study for sliding systems but for an interesting difference. The Warn and Whittaker study (2004) predicts an increasing number of cycles as the ratio of the invariant characteristic strength to weight reduces, whereas this study predicts an increasing number of cycles as the ratio of the temperature-dependent initial value of friction or characteristic strength/weight increases. The difference is due to heating effects which are more intense in high strength systems and are more important in lead-rubber systems.

The number of cycles required for the test to match the 90^{th} percentile maximum value of the cumulative energy (test at amplitude D_M and period T_M) for short-duration ground motions is in the range of 8 to 13 for the sliding systems and in the range of 12 to 21 for the lead-rubber systems (see Tables 7-1 to 7-11). If we accept the maximum value of cumulative energy as the criterion for designing a test for the effects of the maximum earthquake and considering the 90^{th} percentile as the appropriate value to use, the ASCE/SEI-7 prototype test Item 4 in section 17.8.2.2 needs modification to increase the number of cycles without interruptions as currently allowed, to clarify the conditions of ground motion (short- and long-duration) and to distinguish between sliding and lead-rubber systems. Nevertheless, the number of cycles is too large-for long-duration ground motions for a test to match the 90^{th} percentile maximum value of the cumulative energy (test at amplitude D_M and period T_M) is in the range of 17 to 43 for the sliding systems and in the range of 31 to 90 for the lead-rubber systems (see Tables 7-1 to 7-11). The number of required number of cycles is so large that one may conclude that the cumulative energy is a problematic measure for use in designing isolator tests. As originally identified by Kitayama and Constantinou (2020), the reason is that the cumulative energy increases monotonically and does not account for fluctuations in the intensity of the ground motion. Rather, we recommend tests based on the history of temperature at the sliding interfaces or the lead core, on which we concentrate in the next section.

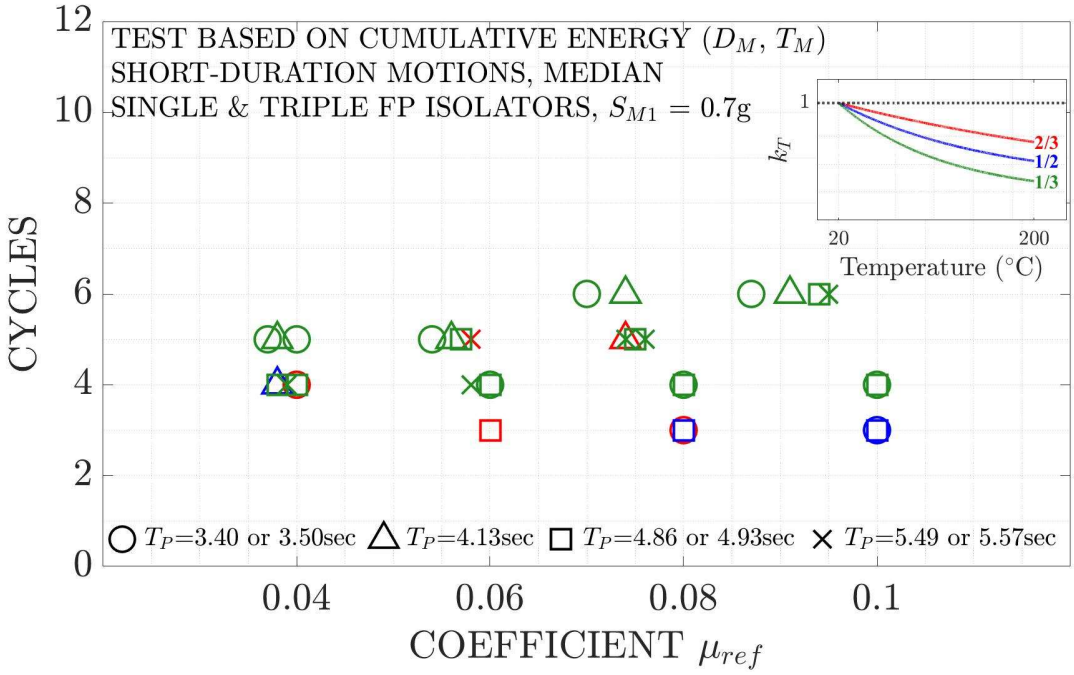

Figure 7-4 Required Number of Cycles for Test to Match Median Maximum Value of Cumulative Energy of Single and Triple FP Isolators in Short-duration Ground Motions when S_{M1} = 0.7g

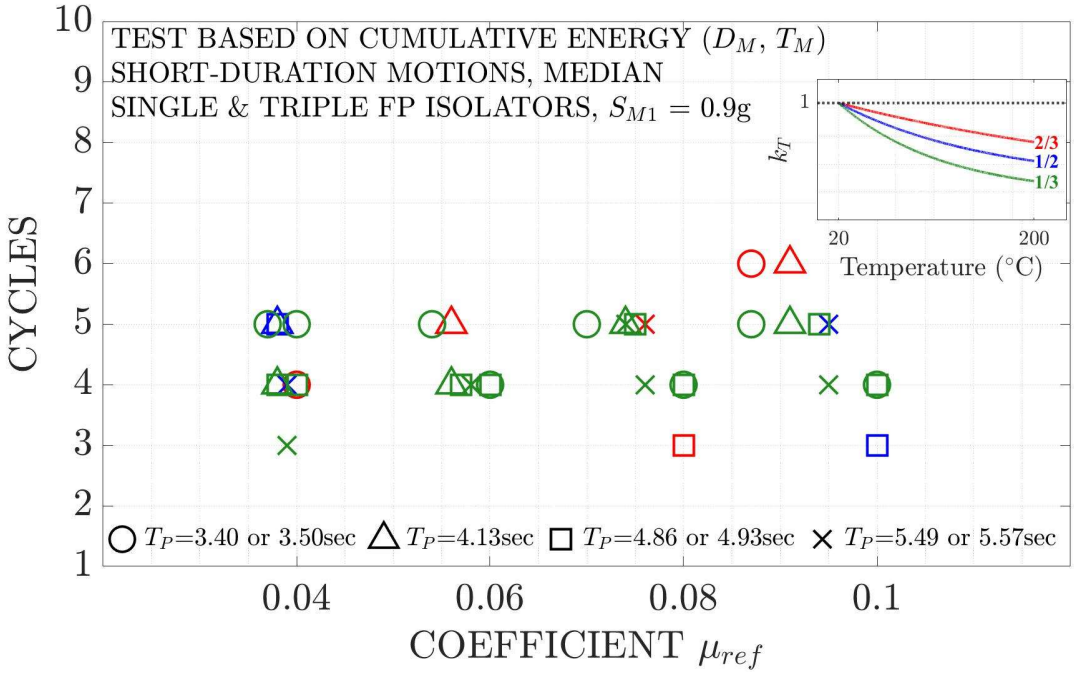

Figure 7-5 Required Number of Cycles for Test to Match Median Maximum Value of Cumulative Energy of Single and Triple FP Isolators in Short-duration Ground Motions when S_{M1} = 0.9g

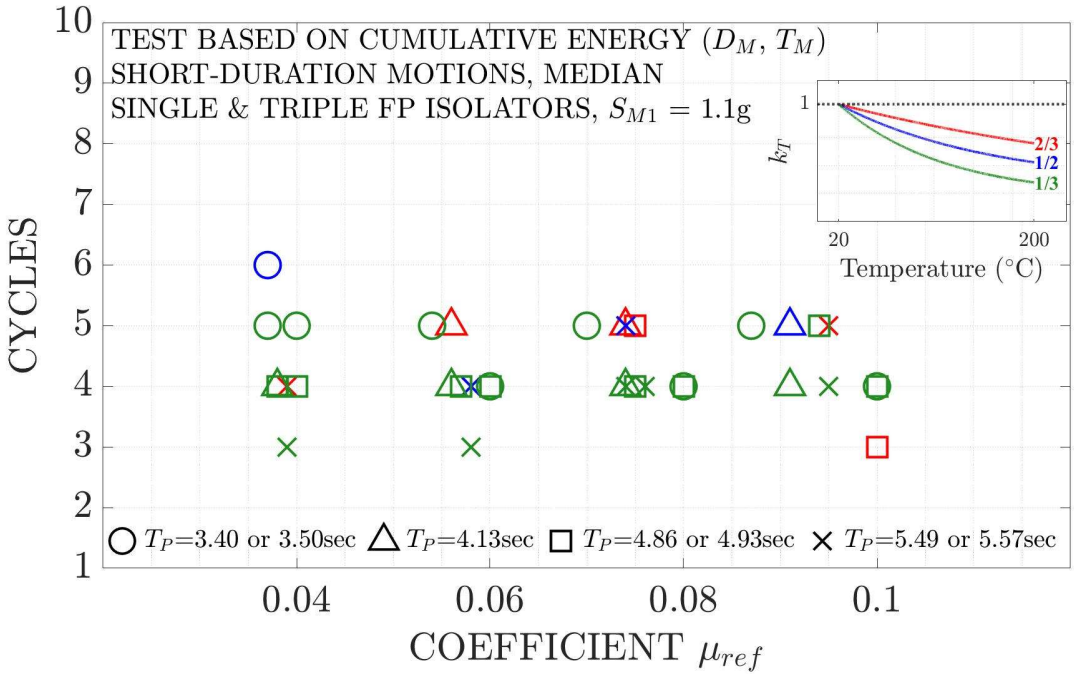

Figure 7-6 Required Number of Cycles for Test to Match Median Maximum Value of Cumulative Energy of Single and Triple FP Isolators in Short-duration Ground Motions when S_{M1} = 1.1g

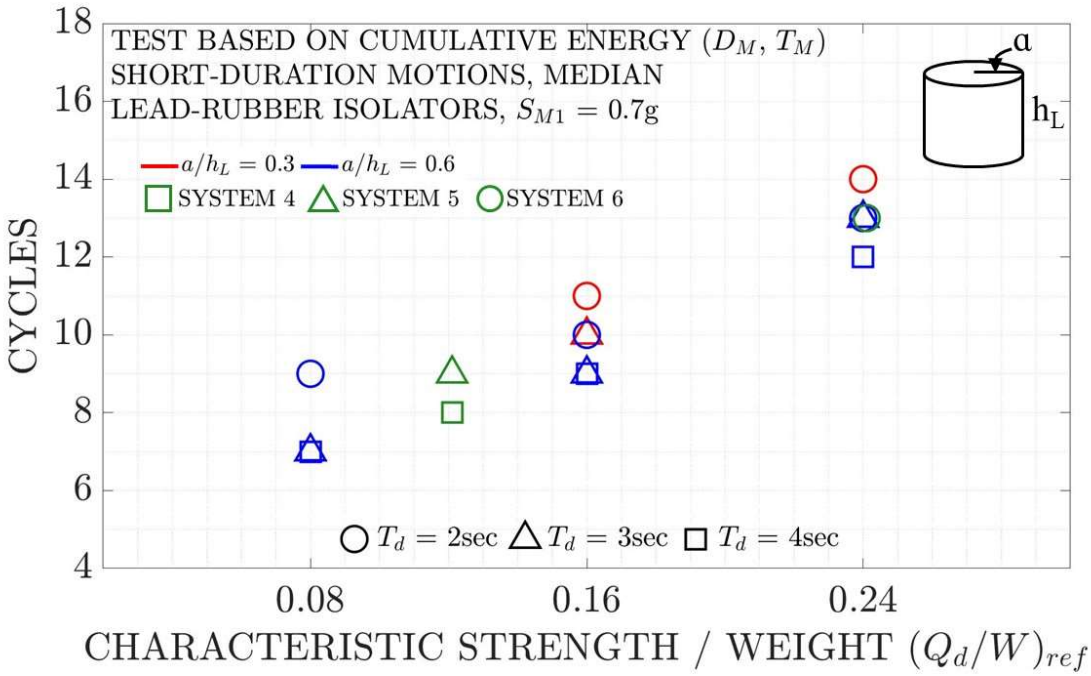

Figure 7-7 Required Number of Cycles for Test to Match Median Maximum Value of Cumulative Energy of Lead-rubber Isolators in Short-duration Ground Motions when S_{M1} = 0.7g

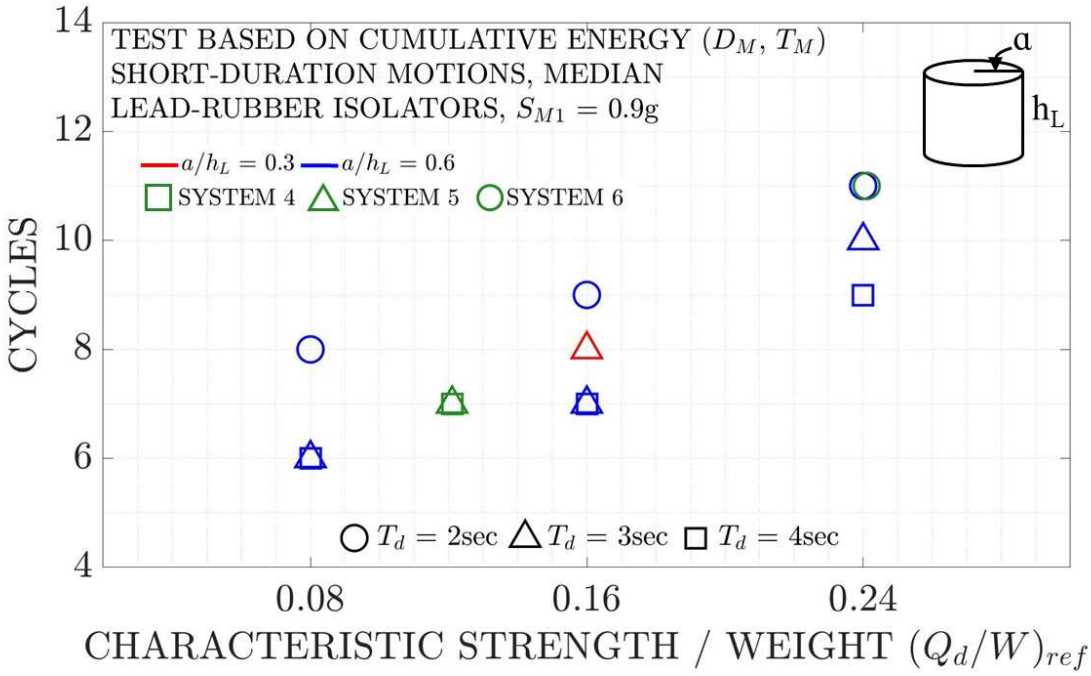

Figure 7-8 Required Number of Cycles for Test to Match Median Maximum Value of Cumulative Energy of Lead-rubber Isolators in Short-duration Ground Motions when S_{M1} = 0.9g

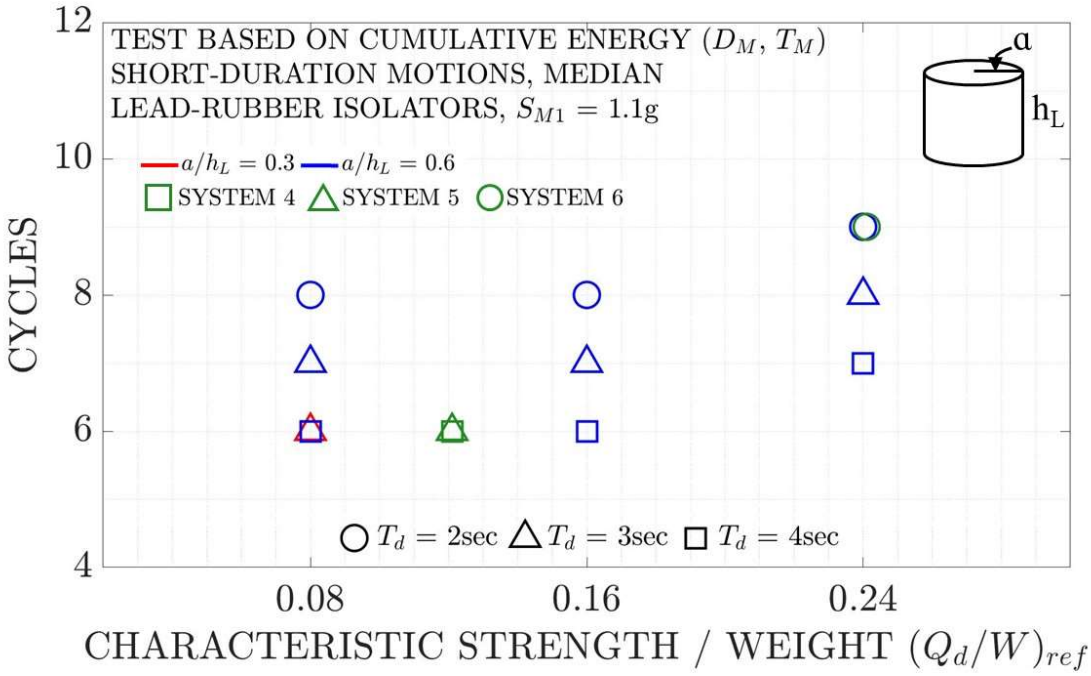

Figure 7-9 Required Number of Cycles for Test to Match Median Maximum Value of Cumulative Energy of Lead-rubber Isolators in Short-duration Ground Motions when S_{M1} = 1.1g

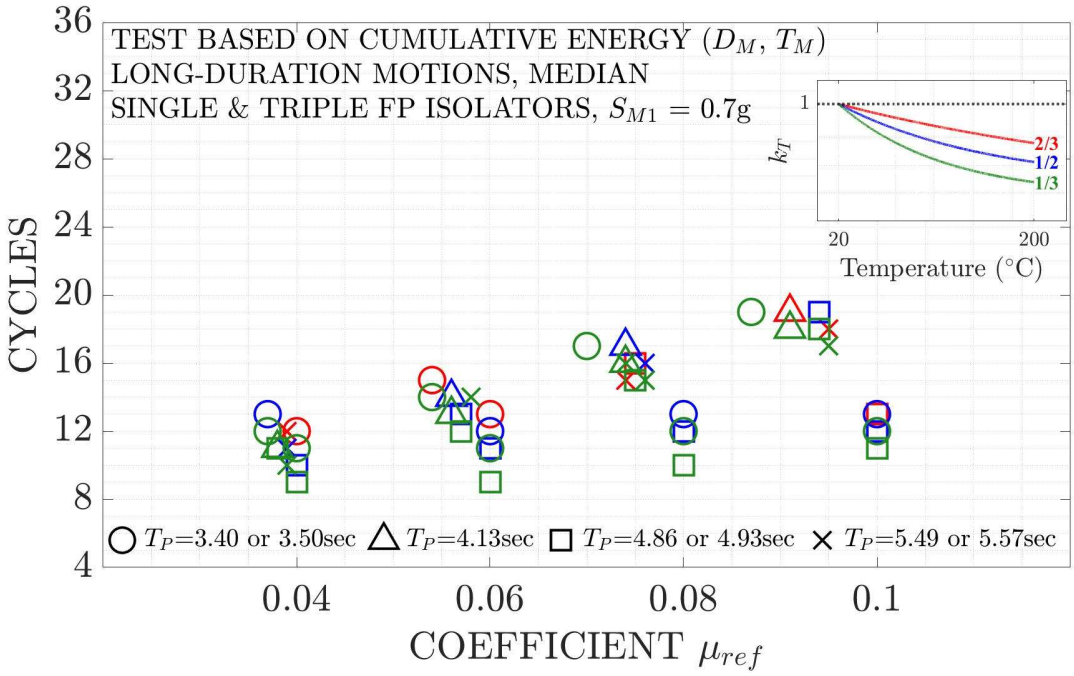

Figure 7-10 Required Number of Cycles for Test to Match Median Maximum Value of Cumulative Energy of Single and Triple FP Isolators in Long-duration Ground Motions when S_{M1} = 0.7g

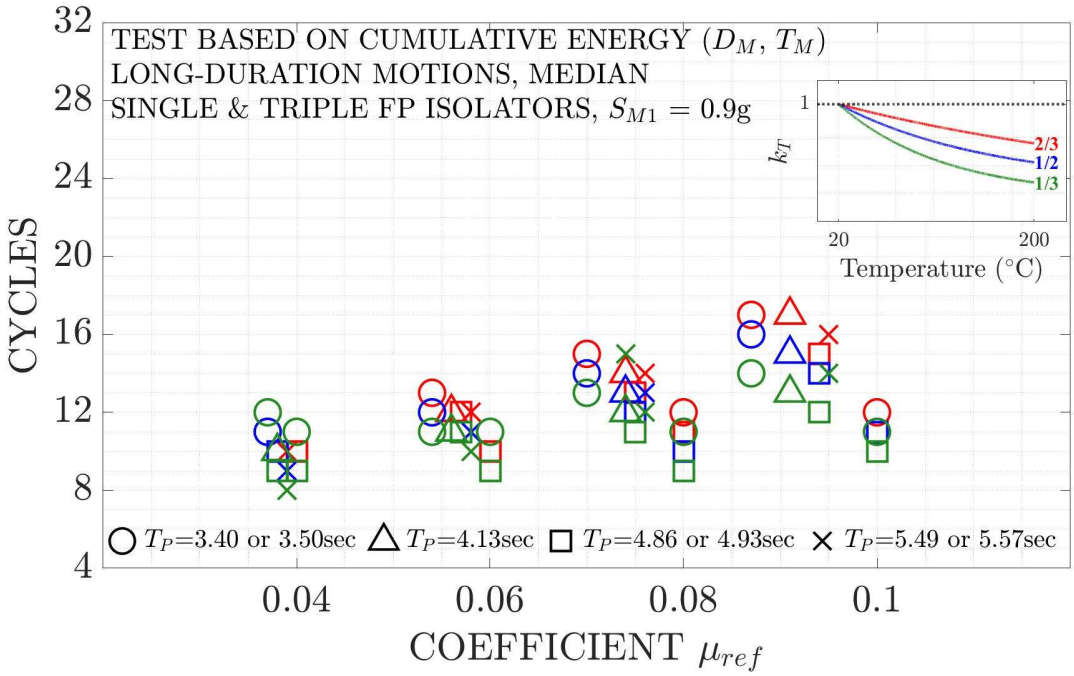

Figure 7-11 Required Number of Cycles for Test to Match Median Maximum Value of Cumulative Energy of Single and Triple FP Isolators in Long-duration Ground Motions when S_{M1} = 0.9g

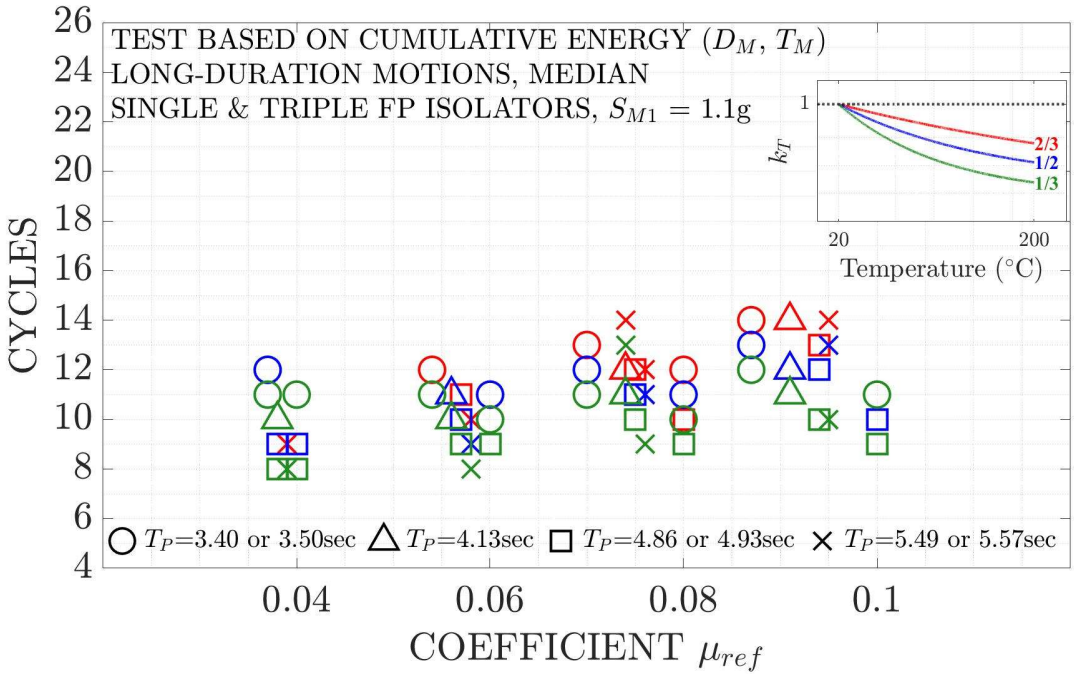

Figure 7-12 Required Number of Cycles for Test to Match Median Maximum Value of Cumulative Energy of Single and Triple FP Isolators in Long-duration Ground Motions when S_{M1} = 1.1g

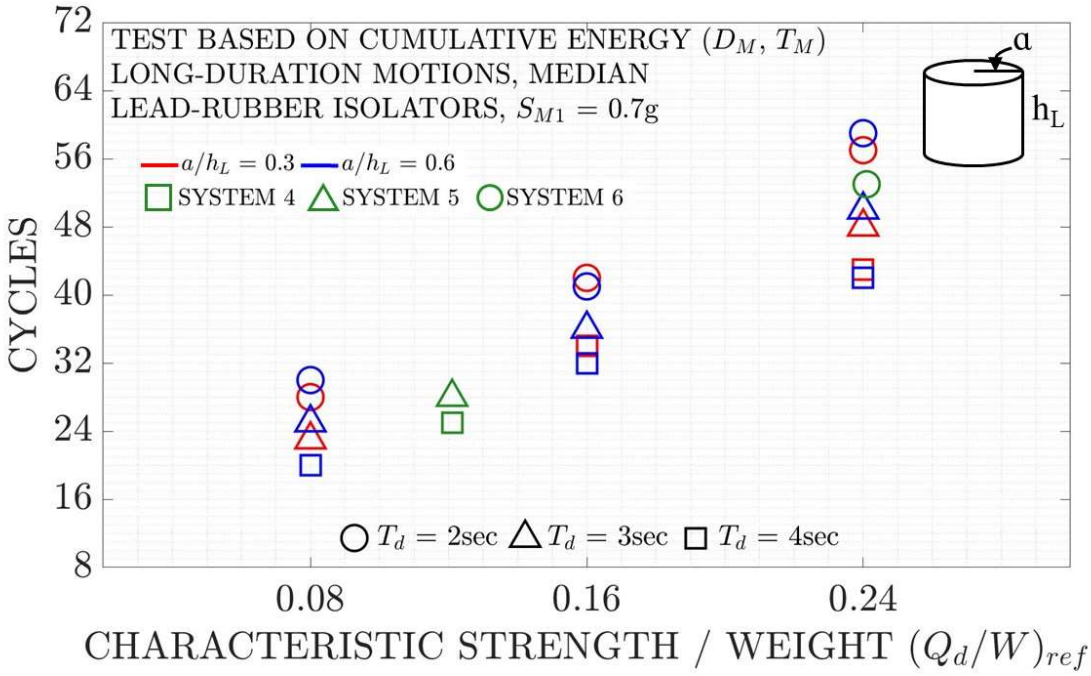

Figure 7-13 Required Number of Cycles for Test to Match Median Maximum Value of Cumulative Energy of Lead-rubber Isolators in Long-duration Ground Motions when S_{M1} = 0.7g

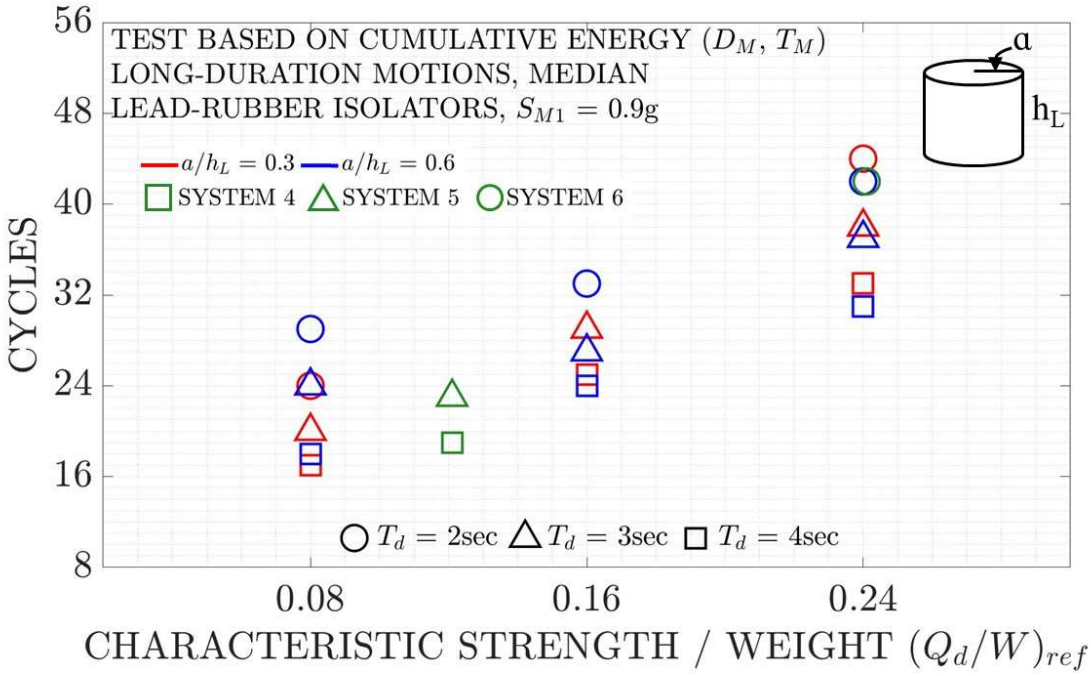

Figure 7-14 Required Number of Cycles for Test to Match Median Maximum Value of Cumulative Energy of Lead-rubber Isolators in Long-duration Ground Motions S_{M1} = 0.9g

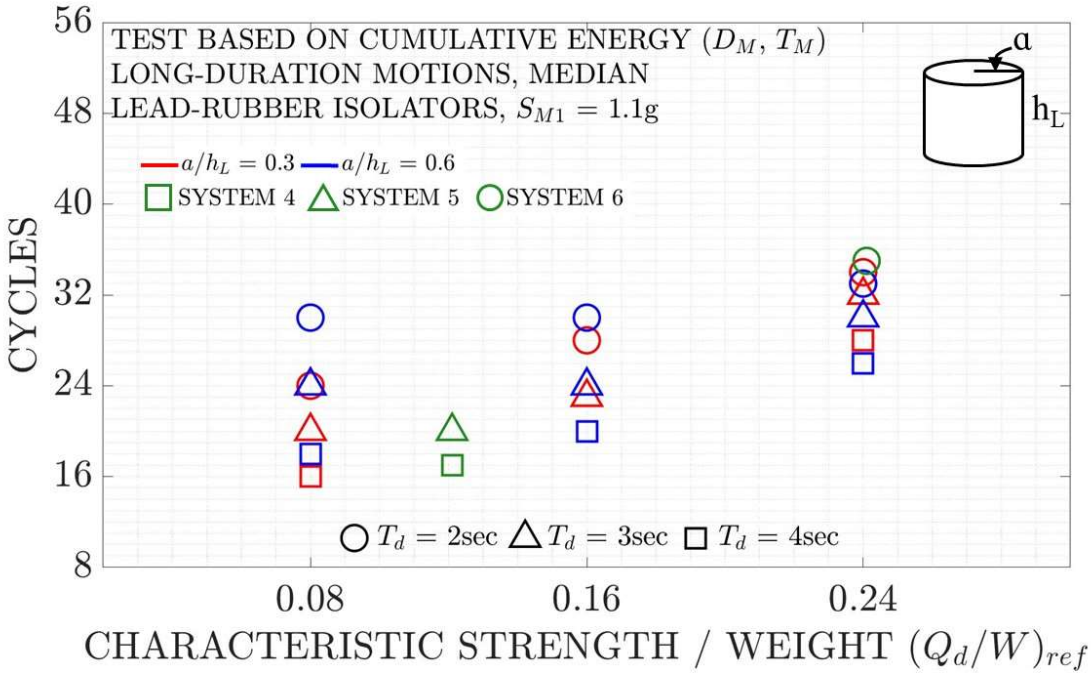

Figure 7-15 Required Number of Cycles for Test to Match Median Maximum Value of Cumulative Energy of Lead-rubber Isolators in Long-duration Ground Motions when S_{M1} = 1.1g

7.3 Results for Test Based on History of Temperature at Sliding Interfaces and in Lead Core

Table 7-12 presents results in terms of the required number of cycles for the studied single FP systems. Also, Tables 7-13 and 7-14 present results for the triple FP systems and Tables 7-15 and 7-16 present results for the lead-rubber systems. The tests were designed to approximately reproduce the 50^{th} (median) and 90^{th} percentile histories of temperature at the main sliding interfaces of single and triple FP isolators or at the lead core of lead-rubber systems. The tests were selected to have amplitude of $0.4D_M$ for sliding systems and $0.5D_M$ for lead-rubber systems, and period T_M. These values of amplitude resulted in the best approximation of the computed histories of temperature in the response history for all cases. This is demonstrated in selected cases of single, triple and lead-rubber systems in Figures 7-16 to 7-18, where the computed 50^{th} and 90^{th} percentile histories of temperature in the response history analysis are compared to those of the tests. Note that tests could have been designed with amplitude of $0.75D_M$ as in test Item 4 of section 17.8.2.2 of ASCE/SEI-7 but then the duration of the test would have been shorter, thus not subjecting the tested isolators to the proper duration of the high temperatures as computed in the response history analysis.

The duration of exposure to high temperatures is known to affect wear in sliding bearings (Constantinou et al., 2007), and thus is important in the testing isolators for the effects of the maximum earthquake. While there is no known comparable mechanism that affects the properties of lead or causes damage to the lead for lead-rubber isolators, one can think of possible damage to rubber at the rubber to lead core interface due to the combination of large temperature and long exposure to that temperature. This is of much interest in long-duration ground motions when the temperature of lead may approach the melting point of 327^oC, and then damage to rubber is possible and it could be affected by the duration of exposure to the high temperature.

Table 7-12 Required Number of Cycles for Maximum Earthquake Effect Test Based on History of Temperature for Single FP Systems

	Test Amplitude (D)	Test Period (T)	S_{M1} = 0.7g, 0.9g and 1.1g											
			k_T = 2/3 at 200°C				k_T = 1/2 at 200°C				k_T = 1/3 at 200°C			
			Short-duration		Long-duration		Short-duration		Long-duration		Short-duration		Long-duration	
			50th	90th	50th	90th	50th	90th	50th	90th	50th	90th	50th	90th
System 11 (T_P = 3.50 sec, μ_{ref} = 0.040)	$0.4D_M$	T_M	6	12	18	36	6	12	18	36	6	12	18	36
System 31 (T_P = 4.93 sec, μ_{ref} = 0.040)	$0.4D_M$	T_M	6	12	18	36	6	12	18	36	6	12	18	36
System 12 (T_P = 3.50 sec, μ_{ref} = 0.060)	$0.4D_M$	T_M	6	12	18	36	6	12	18	36	6	12	18	36
System 32 (T_P = 4.93 sec, μ_{ref} = 0.060)	$0.4D_M$	T_M	6	12	18	36	6	12	18	36	6	12	18	36
System 13 (T_P = 3.50 sec, μ_{ref} = 0.080)	$0.4D_M$	T_M	6	12	18	36	6	12	18	36	6	12	18	36
System 33 (T_P = 4.93 sec, μ_{ref} = 0.080)	$0.4D_M$	T_M	6	12	18	36	6	12	18	36	6	12	18	36
System 14 (T_P = 3.50 sec, μ_{ref} = 0.100)	$0.4D_M$	T_M	6	12	18	36	6	12	18	36	6	12	18	36
System 34 (T_P = 4.93 sec, μ_{ref} = 0.100)	$0.4D_M$	T_M	6	12	18	36	6	12	18	36	6	12	18	36

Table 7-13 Required Number of Cycles for Maximum Earthquake Effect Test Based on History of Temperature for Triple FP Systems

	Test Amplitude (D)	Test Period (T)	S_{M1} = 0.7g, 0.9g and 1.1g											
			k_T = 2/3 at 200°C				k_T = 1/2 at 200°C				k_T = 1/3 at 200°C			
			Short-duration		Long-duration		Short-duration		Long-duration		Short-duration		Long-duration	
			50th	90th	50th	90th	50th	90th	50th	90th	50th	90th	50th	90th
System 11 (T_P = 3.40 sec, μ_{ref} = 0.037)	$0.4D_M$	T_M	8	16	18	36	8	16	18	36	8	16	18	36
System 21 (T_P = 4.13 sec, μ_{ref} = 0.038)	$0.4D_M$	T_M	8	16	18	36	8	16	18	36	8	16	18	36
System 31 (T_P = 4.86 sec, μ_{ref} = 0.038)	$0.4D_M$	T_M	8	16	18	36	8	16	18	36	8	16	18	36
System 41 (T_P = 5.57 sec, μ_{ref} = 0.039)	$0.4D_M$	T_M	8	16	18	36	8	16	18	36	8	16	18	36
System 12 (T_P = 3.40 sec, μ_{ref} = 0.054)	$0.4D_M$	T_M	8	16	18	36	8	16	18	36	8	16	18	36
System 22 (T_P = 4.13 sec, μ_{ref} = 0.056)	$0.4D_M$	T_M	8	16	18	36	8	16	18	36	8	16	18	36
System 32 (T_P = 4.86 sec, μ_{ref} = 0.057)	$0.4D_M$	T_M	8	16	18	36	8	16	18	36	8	16	18	36
System 42 (T_P = 5.57 sec, μ_{ref} = 0.058)	$0.4D_M$	T_M	8	16	18	36	8	16	18	36	8	16	18	36
System 13 (T_P = 3.40 sec, μ_{ref} = 0.070)	$0.4D_M$	T_M	8	16	18	36	8	16	18	36	8	16	18	36
System 23 (T_P = 4.13 sec, μ_{ref} = 0.074)	$0.4D_M$	T_M	8	16	18	36	8	16	18	36	8	16	18	36
System 33 (T_P = 4.86 sec, μ_{ref} = 0.075)	$0.4D_M$	T_M	8	16	18	36	8	16	18	36	8	16	18	36
System 43 (T_P = 5.57 sec, μ_{ref} = 0.076)	$0.4D_M$	T_M	8	16	18	36	8	16	18	36	8	16	18	36
System 14 (T_P = 3.40 sec, μ_{ref} = 0.087)	$0.4D_M$	T_M	8	16	18	36	8	16	18	36	8	16	18	36
System 24 (T_P = 4.13 sec, μ_{ref} = 0.091)	$0.4D_M$	T_M	8	16	18	36	8	16	18	36	8	16	18	36
System 34 (T_P = 4.86 sec, μ_{ref} = 0.094)	$0.4D_M$	T_M	8	16	18	36	8	16	18	36	8	16	18	36
System 44 (T_P = 5.57 sec, μ_{ref} = 0.095)	$0.4D_M$	T_M	8	16	18	36	8	16	18	36	8	16	18	36

Table 7-14 Required Number of Cycles for Maximum Earthquake Effect Test Based on History of Temperature for Triple FP System LL

	Test Amplitude (D)	Test Period (T)	S_{M1} = 0.7g, 0.9g and 1.1g											
			k_T = 2/3 at 200°C				k_T = 2/3 at 200°C				k_T = 2/3 at 200°C			
			Short-duration		Long-duration		Short-duration		Long-duration		Short-duration		Long-duration	
			50th	90th	50th	90th	50th	90th	50th	90th	50th	90th	50th	90th
System LL (T_P = 3.40 sec, μ_{ref} = 0.037)	$0.4D_M$	T_M	8	16	18	36	8	16	18	36	8	16	18	36

Table 7-15 Required Number of Cycles for Maximum Earthquake Effect Test Based on History of Temperature for Lead-rubber Systems

		S_{M1} = 0.7g, 0.9g and 1.1g					
		Test Amplitude (D)	Test Period (T)	Short-duration		Long-duration	
				50th	90th	50th	90th
α/h_L =0.3	System 111 (T_d = 2 sec, $(Q_d/W)_{ref}$ = 0.08)	$0.5D_M$	T_M	12	24	30	60
	System 211 (T_d = 3 sec, $(Q_d/W)_{ref}$ = 0.08)	$0.5D_M$	T_M	12	24	30	60
	System 311 (T_d = 4 sec, $(Q_d/W)_{ref}$ = 0.08)	$0.5D_M$	T_M	12	24	30	60
	System 121 (T_d = 2 sec, $(Q_d/W)_{ref}$ = 0.16)	$0.5D_M$	T_M	12	24	30	60
	System 221 (T_d = 3 sec, $(Q_d/W)_{ref}$ = 0.16)	$0.5D_M$	T_M	12	24	30	60
	System 321 (T_d = 4 sec, $(Q_d/W)_{ref}$ = 0.16)	$0.5D_M$	T_M	12	24	30	60
	System 131 (T_d = 2 sec, $(Q_d/W)_{ref}$ = 0.24)	$0.5D_M$	T_M	12	24	30	60
	System 231 (T_d = 3 sec, $(Q_d/W)_{ref}$ = 0.24)	$0.5D_M$	T_M	12	24	30	60
	System 331 (T_d = 4 sec, $(Q_d/W)_{ref}$ = 0.24)	$0.5D_M$	T_M	12	24	30	60
α/h_L =0.6	System 112 (T_d = 2 sec, $(Q_d/W)_{ref}$ = 0.08)	$0.5D_M$	T_M	12	24	30	60
	System 212 (T_d = 3 sec, $(Q_d/W)_{ref}$ = 0.08)	$0.5D_M$	T_M	12	24	30	60
	System 312 (T_d = 4 sec, $(Q_d/W)_{ref}$ = 0.08)	$0.5D_M$	T_M	12	24	30	60
	System 122 (T_d = 2 sec, $(Q_d/W)_{ref}$ = 0.16)	$0.5D_M$	T_M	12	24	30	60
	System 222 (T_d = 3 sec, $(Q_d/W)_{ref}$ = 0.16)	$0.5D_M$	T_M	12	24	30	60
	System 322 (T_d = 4 sec, $(Q_d/W)_{ref}$ = 0.16)	$0.5D_M$	T_M	12	24	30	60
	System 132 (T_d = 2 sec, $(Q_d/W)_{ref}$ = 0.24)	$0.5D_M$	T_M	12	24	30	60
	System 232 (T_d = 3 sec, $(Q_d/W)_{ref}$ = 0.24)	$0.5D_M$	T_M	12	24	30	60
	System 332 (T_d = 4 sec, $(Q_d/W)_{ref}$ = 0.24)	$0.5D_M$	T_M	12	24	30	60

Table 7-16 Required Number of Cycles for Maximum Earthquake Effect Test Based on History of Temperature for Additional Lead-rubber Systems

	S_{M1} = 0.7g, 0.9g and 1.1g					
	Test Amplitude (D)	Test Period (T)	Short-duration		Long-duration	
			50th	90th	50th	90th
System 4 (T_d = 4 sec, α/h_L = 0.46, $(Q_d/W)_{ref}$ = 0.121)	$0.5D_M$	T_M	12	24	30	60
System 5 (T_d = 3 sec, α/h_L = 0.46, $(Q_d/W)_{ref}$ = 0.121)	$0.5D_M$	T_M	12	24	30	60
System 6 (T_d = 2 sec, α/h_L = 0.35, $(Q_d/W)_{ref}$ = 0.241)	$0.5D_M$	T_M	12	24	30	60

The results presented in Tables 7-12 to 7-14 show a much simpler picture than when the cumulative energy is used as the criterion for designing the test. Specifically, the intensity of the seismic excitation and the properties of the isolation system (period and friction coefficient or characteristic strength) do not affect the number of cycles. A summary of the required number of cycles is presented in Table 7-17. The number of required cycles (amplitude $0.4D_M$ for sliding systems and $0.5D_M$ for lead-rubber systems, period T_M) for short-duration motions are: 6 to 12 for the 50^{th} percentile results and is 12 to 24 for the 90^{th} percentile results. For long-duration motions are: 18 to 36 for the 50^{th} percentile results and is 30 to 60 for the 90^{th} percentile results. Also, the number of cycles required for the 90^{th} percentile results is twice that for the 50^{th} percentile results for all systems and for short- or long-duration ground motions.

Table 7-17 Summary of Required Number of Cycles for Maximum Earthquake Effect Test (Amplitude $0.4D_M$ for Sliding Systems, $0.5D_M$ for Lead-rubber Systems, Period T_M) Based on History of Temperature

System	Short-duration Motions		Long-duration Motions	
	50^{th} Percentile	90^{th} Percentile	50^{th} Percentile	90^{th} Percentile
Single FP	6	12	18	36
Triple FP	8	16	18	36
Lead-rubber	12	24	30	60

The required number of cycles is systematically larger for lead-rubber systems, due to the more profound heating effects in the lead core than at the sliding interfaces. This was discussed in Section 7.2, where it was stated that the difference between sliding and lead-rubber systems is due to the relationship of the characteristic strength to temperature: for sliding systems the friction coefficient reaches a stable value at high temperatures, whereas for lead-rubber systems the characteristic strength continually declines to an essentially zero value as the temperature of lead approaches the melting point.

Interesting also is that the required number of cycles is a little smaller for single FP systems than for triple FP systems in short-duration ground motions. This difference may be explained as follows. Firstly, in many cases the number of cycles listed in Tables 7-12 to 7-16 may result in overestimation of the peak temperature as seen in many graphs of Appendices G, H, and I, and in the results of Figures 7-16 to 7-18, so that the reported number of cycles is more or less than needed by one or two. The interest in the study was to produce results that systematically provide good information on the required number of cycles with the minimum complexity. Secondly, there are differences in heating effects between single and triple FP

systems. Generally, it is commonly stated that single FP isolators experience higher temperatures than triple (also the similar double) FP systems due to higher heat flux caused by the higher velocity of sliding (which is partitioned mainly between the two main sliding interfaces of the triple FP, Kim and Constantinou, 2022, 2023). While indeed the heat flux is larger in the single FP, its duration may be different due to larger sliding displacements by comparison to the diameter of the contact area. For example, single FP system 31 (case of Figure 7-16) has D_M=529mm and contact area diameter equal to 279.4mm. Triple FP system 31 (has essentially the same period and reference friction coefficient, and same contact area) has for the same motions and conditions as single FP system 31, D_M=579mm. The test is conducted at amplitude $0.4D_M$, thus at 212mm for the single FP system 31-the entire 212mm amplitude is traversed on the single sliding interface, of which 140mm (half the diameter of the contact area) in contact and the remaining 72mm not in contact. That is the heat flux is intermittent. For the triple FP system 31, the amplitude of the test is 232mm, but less than half of this is traversed on a single main sliding interface (the displacement is partitioned between several sliding interfaces), say approximately 110mm, which is less than half of the diameter of the contact area. Thus, for the triple FP system, the heat flux, while less, is essentially continuous and may lead to more heating. This is demonstrated in Figure 7-19 that shows histories of heat flux for the single FP system 31 (left) and the triple FP system 31 (right) in the analysis for the tests to represent the 50th percentile effects in short-duration ground motions.

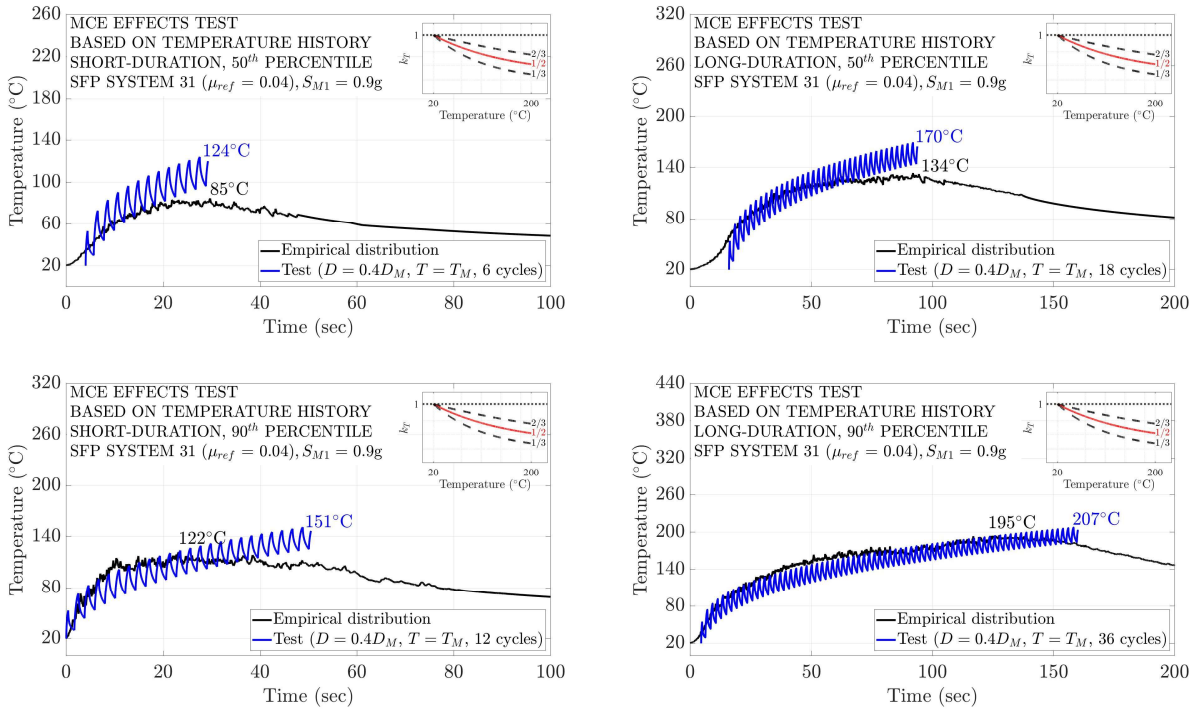

Figure 7-16 Comparison of 50th and 90th Percentile Histories of Temperature to Results of Test for Single FP System 31 (T_P = 4.93sec, μ_{ref} = 0.040) when S_{M1}=0.9g (friction case when k_T=0.5 at 200ºC)

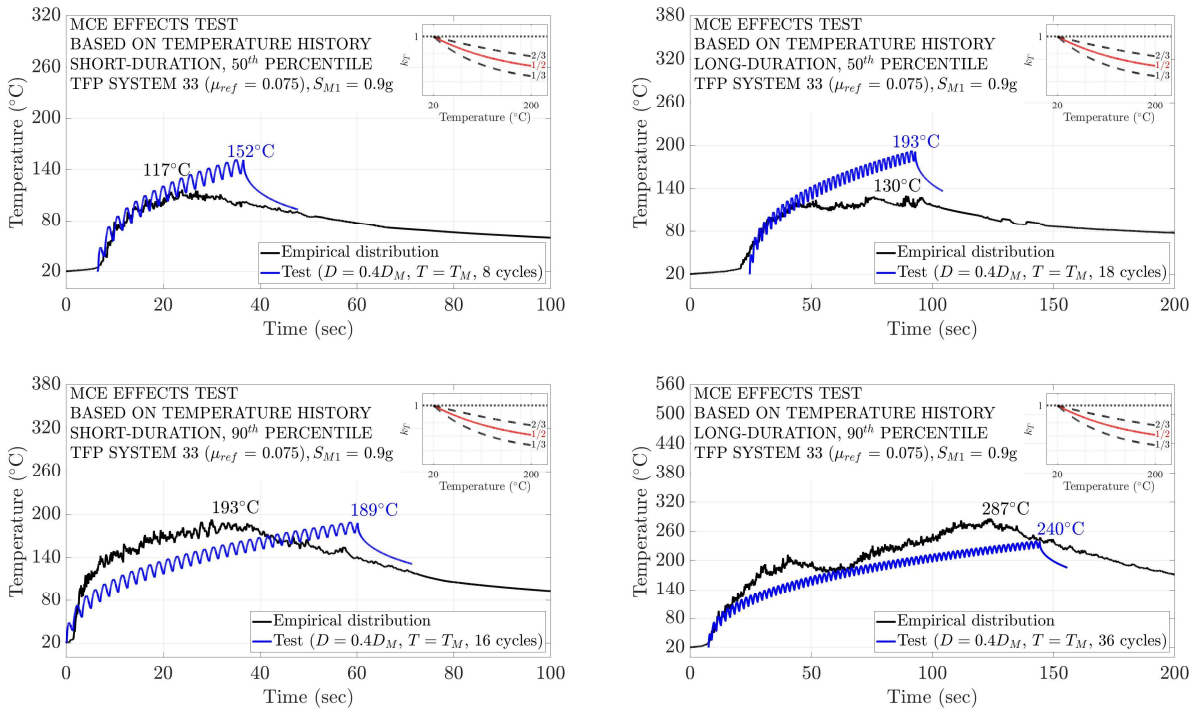

Figure 7-17 Comparison of 50th and 90th Percentile Histories of Temperature to Results of Test for Triple FP System 33 (μ_{1ref} = 0.08, μ_{ref} = 0.075, T_P = 4.86s) when S_{M1}=0.9g (friction case when k_T=0.5 at 200°C)

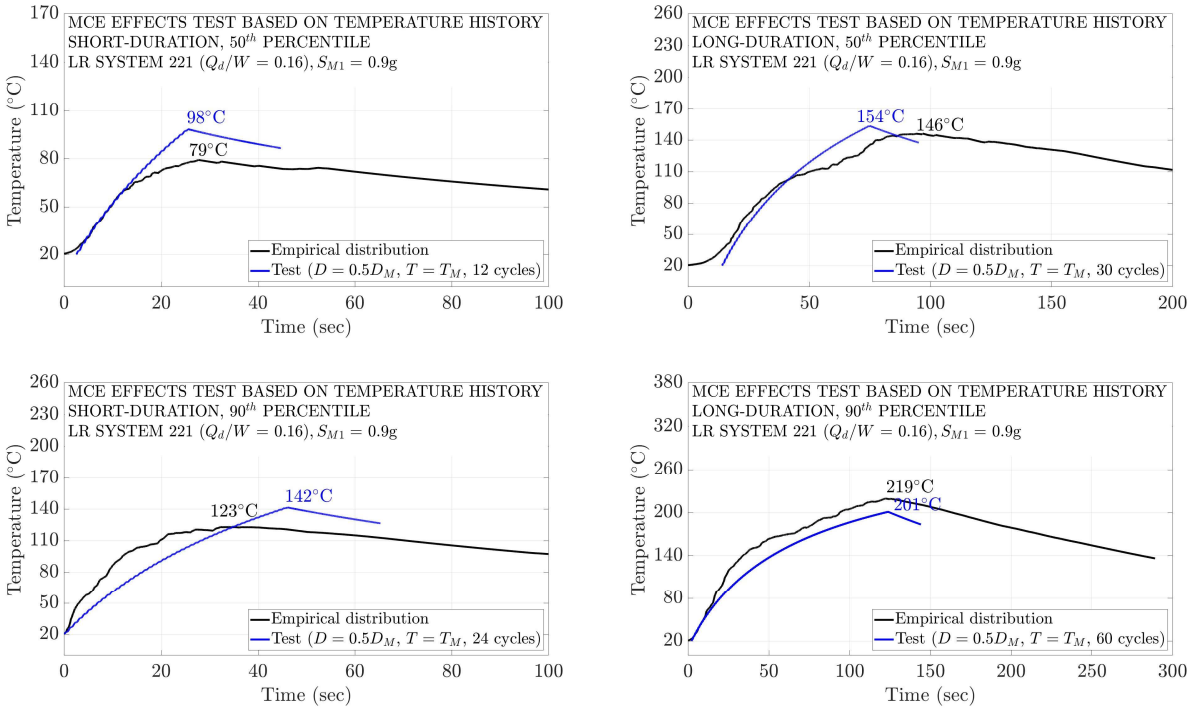

Figure 7-18 Comparison of 50th and 90th Percentile Histories of Temperature to Results of Test for Lead-rubber System 221 (T_d = 3s, $(Q_d/W)_{ref}$ = 0.16, α/h_L =0.3) when S_{M1} = 0.9g

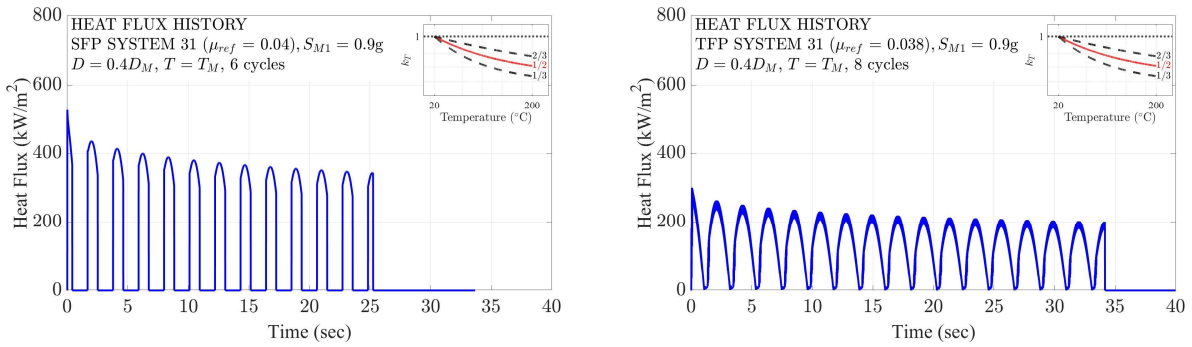

Figure 7-19 Histories of Heat Flux for Single FP System 31 (μ_{ref} = 0.040, T_P = 4.93sec) (left) and Triple FP System 31 (μ_{1ref} = 0.040, μ_{ref} = 0.038, T_P = 4.86s) (right) when S_{M1}=0.9g (friction case when k_T=0.5 at 200°C)

7.4 Recommendations for Test to Represent the Effects of the Maximum Earthquake

Based on the results presented in this section, we recommend:

1) The cumulative energy is not used as measure for designing a test to represent the effects of the maximum earthquake because it monotonically increases without accounting for fluctuations in the seismic ground motion intensity-a fact that results in unrealistically onerous tests.

2) The history of temperature at the sliding interfaces of sliding isolators and in the lead core of lead-rubber isolators is an appropriate measure for designing tests to represents the effects of the maximum earthquake.

3) Based on the history of temperature, the recommended test to represent the maximum earthquake effects is performed at a vertical load equal to the gravity load (or average gravity of a group of isolators) and harmonic lateral displacement of amplitude $0.4D_M$ for sliding isolators or $0.5D_M$ for lead-rubber isolators, and a period equal to T_M, for specified number of cycles as follows.

4) For short-duration ground motions, the number of cycles to represent the 50th percentile effects is 8 for sliding isolators and 12 for lead-rubber isolators. The number of cycles to represent the 90th percentile effects is 16 for sliding isolators and 24 for lead-rubber isolators, that is, twice those for the 50th percentile effects.

5) For long-duration ground motions, the number of cycles to represent the 50^{th} percentile effects is 18 for sliding isolators and 30 for lead-rubber isolators. The number of cycles to represent the 90^{th} percentile effects is 36 for sliding isolators and 60 for lead-rubber isolators, that is, twice those for the 50^{th} percentile effects.

SECTION 8
SUMMARY AND CONCLUSIONS

This report presented a study for the design of two important tests in the prototype testing of seismic isolators:

1) A test for determining the bounding properties of isolators for use in analysis and design. The test conditions are determined by first performing analyses with models that account for the time-variant properties of the isolators and computing the resultant isolator displacements. Then the analyses are repeated using models with time-invariant isolator properties that result in the same isolator resultant displacement. With the time-invariant isolator properties known and defined as those of the lower bound analysis, a test is designed to result in lower bound properties at the last cycle of the test, whereas the first cycle results in the upper bound properties. In this way, tests are designed that correctly result in the properties for use in bounding analysis (specifically to determine factors $\lambda_{(test,\ max)}$ and $\lambda_{(test,\ min)}$ in ASCE/SEI-7). The lower bound properties are used to compute the isolation system resultant peak displacement (quantity D_M as defined in ASCE/SEI-7). The test is meant to be a replacement for the tests Items 2(a) and 3 described in ASCE/SEI-7.
2) A test for determining the adequacy of the isolators in the maximum considered earthquake, with consideration for the probability of exceedance of these effects (e.g., median effects, 90% percentile effects). The test is meant to be a replacement for the test Item 4 described in ASCE/SEI-7. The approach followed in determining the conditions of testing was based on using the histories of temperature computed at the sliding interfaces of sliding bearings or in the lead core of lead-rubber bearings. Moreover, conditions of testing were determined when using the cumulative dissipated energy histories instead of the temperature histories.

In performing the work, a large number of isolation systems (96 systems, comprising single friction pendulum, triple friction pendulum and lead-rubber), three different seismic hazards as measured by the spectral acceleration at the period of one second, and a large collection of bi-directional ground motions with short- and long-duration characteristics (71 pairs of each duration, 96 systems, three seismic hazards, for a total of 40896 ground motion pairs) were considered. The short-duration motions had a geomean duration $Ds_{5\text{-}75}$ (Chandramohan et al., 2016; Kitayama and Constantinou, 2021) of less than 20 secs, whereas long-duration motions had a geomean duration $Ds_{5\text{-}75}$ between 15 and 80 sec. The ground motions were selected such that for each long-duration pair of ground motions, there was a corresponding pair of short-duration motions that had response spectra in the two orthogonal directions that were essentially the same

as the spectra of the corresponding long-duration pair; such motions are called "spectrally equivalent". All ground motions were appropriate for far field conditions.

In performing the analysis, isolator models with time-variant properties were needed. These models were based on validated theories for sliding isolators (Constantinou et al., 2007; Kumar et al., 2015; Kim and Constantinou, 2022, 2023) and lead-rubber isolators (Kalpakidis et al., 2010; Kumar et al., 2014). However, enhancements in these models were made that were needed to better represent the behavior of sliding and lead-rubber bearings.

One the basis of this work, the following have been concluded:

1) For all seismic isolation systems and for short-duration motions, a test of three cycles at amplitude D_M and period T_M suffices to determine the lower bound properties for analysis. That is, test Items 2(a) and 3 of Section 17.8.2.2 of ASCE/SEI-7 are sufficient to determine factors $\lambda_{(test,\ max)}$ and $\lambda_{(test,\ min)}$ for short-duration motions.

2) An alternative test per ASCE/SEI-7 Item 2(b) in section 17.8.2.2 (one cycle at D_M, followed by single cycles at $0.67D_M$, $0.5D_M$ and $0.25D_M$, all at period T_M) will result in values of properties in the fourth cycle that are essentially the same or conservative by comparison to those obtained in the third cycle of a test per ASCE/SEI-7 Items 2(a) and 3 in section 17.8.2.2 (three cycles at D_M and period T_M) for single and triple FP systems provided that the amplitude D_M is large by comparison to the diameter of the contact area so that the heat flux conditions are intermittent. That is, the alternative test of ASCE/SEI-7 Item 2(b) in section 17.8.2.2 is acceptable for single FP and triple FP sliding isolators in location with short duration ground motions. This alternative test was found to be not generally valid for lead-rubber systems, in which the 4-cycle test may overestimate the lower bound properties by comparison to the 3-cycle test, although the overestimation is not significant.

3) For long-duration motions, a test of five cycles at amplitude D_M and period T_M is needed to determine the lower bound properties for analysis.

4) The cumulative energy is not a useful measure for designing a test to represent the effects of the maximum earthquake because it monotonically increases without accounting for fluctuations in the seismic ground motion intensity, a fact that results in unrealistically onerous tests.

5) The history of temperature at the sliding interfaces of sliding isolators and in the lead core of lead-rubber isolators is an appropriate measure for designing tests to represent the effects of the maximum earthquake.

6) Based on the history of temperature, the recommended test to represent the maximum earthquake effects is performed at a vertical load equal to the gravity load (or average gravity of a group of isolators) and harmonic lateral displacement of amplitude $0.4D_M$ for sliding isolators or $0.5D_M$ for lead-rubber isolators, and a period equal to T_M, for specified number of cycles as follows.

    a. For short-duration ground motions, the number of cycles to represent the 50^{th} percentile effects is 8 for sliding isolators and 12 for lead-rubber isolators. The number of cycles to represent the 90^{th} percentile effects is 16 for sliding isolators and 24 for lead-rubber isolators; that is, twice those for the 50^{th} percentile effects.

    b. For long-duration ground motions, the number of cycles to represent the 50^{th} percentile effects is 18 for sliding isolators and 30 for lead-rubber isolators. The number of cycles to represent the 90^{th} percentile effects is 36 for sliding isolators and 60 for lead-rubber isolators; that is, twice those for the 50^{th} percentile effects.

The difference between sliding and lead-rubber systems in the required number of cycles in the adequacy tests is related to the dependency of the strength of the isolators (friction force or characteristic strength) on temperature. For sliding isolators, the strength does not diminish but reaches a stable value as temperature increases, whereas in lead-rubber isolators the strength may vanish as the temperature approaches the melting point of lead. While the number of cycles is less in the sliding isolators than in the lead-rubber isolators, the effects of the test may be more important due to wear of the materials of the sliding interface, whereas for the lead-rubber isolators, lead recovers its strength after many cycles of motion.

Moreover, the following results of the response-history for all studied systems have been documented in the report:

1) Tabulated values of mean, median, 84th percentile and 90th percentile values of the peak resultant isolator displacement and of the resultant residual displacement. The values are counted values based on the empirical data.

2) Graphs of probability distributions of the empirical data and lognormal representations for the probability of non-exceedance vs the maximum displacement and vs the residual displacement. Also, plotted counted values (empirical data) of the resultant isolator displacement and of the resultant residual displacement for 16%, 50% (median), 84% and 90% probabilities of being exceeded.

3) 16th, 50th (median), 84th and 90th percentile histories of cumulative energy as obtained from the empirical data (counted) and again from the lognormal distributions (fitted). Comparisons of histories of the cumulative energy obtained using the empirical data and the lognormal distributions are also presented to demonstrate differences.

4) 16th, 50th (median), 84th and 90th percentile histories of temperature at the main sliding interface or the bulk of the lead core as obtained from the empirical data (counted) and again from the lognormal distributions (fitted). Comparisons of histories of the temperature obtained using the empirical data and the lognormal distributions are also presented to demonstrate differences.

Results from these data have been processed to determine an appropriate factor for the ratio of the 90th percentile isolator peak resultant displacement to the mean isolator peak resultant displacement. This ratio provides a simple scale factor for computing a value that has an acceptable probability of exceedance. Kammerer et al. (2019) recommended the use of a scale factor of 1.6 for obtaining the 90th percentile isolator displacement from the mean value. The results of this study found that the 90th/mean scale factor for the isolator peak resultant displacement to be in the range of 1.4 to 1.6 for single FP isolation systems, 1.3 to 1.5, triple FP isolation systems and 1.5 to 1.6 for lead-rubber systems.

An appropriate scale factor for the ratio of the 90th/mean isolator peak resultant displacement, applicable to all systems and for short or long-duration far field ground motions, is 1.6.

Goodness-of-fit statistical tests were performed to check whether the data could be represented with lognormal distributions for all studied systems. These goodness-of-fit tests were also performed for the lognormally fitted cumulative energy and temperature histories at each time step. The lognormally fitted

analysis data have not been used in this work to design the isolator tests (for which only empirical data have been used) but are presented for the interested reader for other possible uses.

“This Page Intentionally Left Blank”

SECTION 9

REFERENCES

Abramowitz, M., and Stegun, I. A. (1965). *Handbook of mathematical functions*, Dover Publications, NY, 361.

Al-Hussaini, T.M., Zayas, V.A. and Constantinou, M.C. (1994). "Seismic isolation of multi-story frame structures using spherical sliding isolation system." Report No. NCEER-94-0007, National Center for Earthquake Engineering Research, Buffalo, New York.

ASCE/SEI–7. (2017). "Minimum design loads and associated criteria for buildings and other structures", American Society of Civil Engineers, Reston, VA. doi.org/10.1061/9780784414248

Beck, J. (1979). "Closed-form exact solution for the average transient temperature of a circular region within a semi-infinite body heated by a disk heat source", In *17th Aerospace Sciences Meeting* (p. 175). doi.org/10.2514/6.1979-175.

Boore, D. M., and Bommer, J. J. (2005). "Processing of strong-motion accelerograms: needs, options and consequences", Soil Dynamics and Earthquake Engineering, 25(2), 93-115. doi.org/10.1016/j.soildyn.2004.10.007.

Boore, D. M. (2005). "On pads and filters: Processing strong-motion data", Bulletin of the Seismological Society of America, 95(2), 745-750. doi.org/10.1785/0120040160.

Carslaw, H.S. and Jaeger, J.C. (1959). *Conduction of Heat in Solids*, 2nd Edition, Oxford University Press, London, UK.

CEN. EN 1998–1. (2004) "Eurocode 8: Design of structures for earthquake resistance. General rules, seismic actions and rules for buildings", European Committee for Standardization.

CEN. EN15129. (2009). "European Standard: anti-seismic devices", European Committee for Standardization.

Chandramohan, R., Baker, J. W., and Deierlein, G. G. (2016). "Quantifying the influence of ground motion duration on structural collapse capacity using spectrally equivalent records", Earthquake Spectra, 32(2), 927-950. doi.org/10.1193/122813eqs298mr2.

Cilsalar, H. and Constantinou, M. C. (2017). "Effect of vertical ground motion on the response of structures isolated with friction pendulum isolators", International Journal of Earthquake and Impact Engineering, 2(2), 135-157. 10.1504/IJEIE.2017.10010024.

Computers and Structures, Inc. (2011). "SAP 2000—Integrated Software for Structural Analysis and Design".

Constantinou, M. C., Whittaker, A. S., Kalpakidis, Y., Fenz, D. M. and Warn, G. P. (2007). "Performance of seismic isolation hardware under service and seismic loading", Report No. MCEER-07-0012, Multidisciplinary Center for Earthquake Engineering Research, Buffalo, NY.

Constantinou, M. C., Kalpakidis, I., Filiatrault, A., and Ecker Lay, R. A. (2011). "LRFD-based analysis and design procedures for bridge bearings and seismic isolators", Report No. MCEER-11-0004, Multidisciplinary Center for Earthquake Engineering Research, Buffalo, NY.

Dao, N. D., Ryan, K. L., Sato, E. and Sasaki, T. (2013). "Predicting the displacement of triple pendulum bearings in a full-scale shaking experiment using a three-dimensional element", Earthquake engineering and structural dynamics, 42(11), 1677-1695. doi.org/10.1002/eqe.2293.

Fenz, D. M. and Constantinou, M. C. (2008a), "Spherical sliding isolation bearings with adaptive behavior: Theory", Earthquake Engineering and Structural Dynamics, Vol. 37, No. 2, 163-183. doi.org/10.1002/eqe.751 .

Fenz, D. M. and Constantinou, M. C. (2008b), "Spherical sliding isolation bearings with adaptive behavior: Experimental verification", Earthquake Engineering and Structural Dynamics, Vol. 37, No. 2, 185-205. doi.org/10.1002/eqe.750.

Fenz, D. M. and Constantinou, M. C. (2008c). "Mechanical behavior of multi-spherical sliding bearings", Report No. MCEER 08-0007, Multidisciplinary Center for Earthquake Engineering Research, Buffalo, NY.

Fenz, D. M. and Constantinou, M. C. (2008d), "Development, implementation and verification of dynamic analysis models for multi-spherical sliding bearings", Report No. MCEER-08-0018, Multidisciplinary Center for Earthquake Engineering Research, Buffalo, NY.

Fenz, D. M. and Constantinou, M. C. (2009), "Modelling triple friction pendulum bearings for response-history analysis", Earthquake Spectra, Vol. 24, No. 4, 1011-1028.

Fenz, D. M., Reed, R., Slatnick, S., Stewart, H. R. and Constantinou, M. C. (2011). "Development of performance-based testing specifications for the Arkutun-Dagi friction pendulum bearings", In OTC Arctic Technology Conference, OnePetro, Houston, Texas, 7–9 February, 2011. doi.org/10.4043/22160-MS.

Huang, Y.-N., Whittaker, A. S., Kennedy, R. P., and Mayes, R. L. (2009). "Assessment of base-isolated nuclear structures for design and beyond-design basis earthquake shaking." Report No. MCEER-09-0008, Multidisciplinary Center for Earthquake Engineering Research, Buffalo, NY.

Hwang, J. S. and Hsu, T. Y. (2000). "Experimental study of isolated building under triaxial ground excitations", Journal of Structural Engineering, 126(8), 879-886. doi.org/10.1061/(ASCE)0733-9445(2000)126:8(879).

Jarque, C. M., and Bera, A. K. (1987). "A test for normality of observations and regression residuals". International Statistical Review/Revue Internationale de Statistique, 163-172. https://doi.org/10.2307/1403192.

Kalpakidis, I. V. and Constantinou, M. C. (2008). "Effects of heating and load history on the behavior of lead-rubber bearings", Report No. MCEER-08-0027, Multidisciplinary Center for Earthquake Engineering Research, Buffalo, NY.

Kalpakidis, I. V. and Constantinou, M. C. (2009a). “Effects of heating on the behavior of lead-rubber bearings. I: Theory”, Journal of Structural Engineering, 135(12), 1440-1449. doi.org/10.1061/(ASCE)ST.1943-541X.0000072.

Kalpakidis, I. V. and Constantinou, M. C. (2009b). “Effects of heating on the behavior of lead-rubber bearings. II: Verification of theory”, Journal of Structural Engineering, 135(12), 1450-1461. doi.org/10.1061/(ASCE)ST.1943-541X.0000071.

Kalpakidis, I. V., Constantinou, M. C. and Whittaker, A. S. (2010). “Modeling strength degradation in lead–rubber bearings under earthquake shaking”, Earthquake Engineering & Structural Dynamics, 39(13), 1533-1549. doi.org/10.1002/eqe.1039.

Kammerer, A. M., Whittaker, A. S., and Constantinou, M. C. (2019). "Technical considerations for seismic isolation of nuclear facilities." NUREG/CR-7253, United States Nuclear Regulatory Commission, Washington, DC.

Kim, H-M., and Constantinou, M. C. (2022). “Modeling triple friction pendulum bearings in program OpenSees including frictional heating effects”, Report No. MCEER-22-0001, Multidisciplinary Center for Earthquake Engineering Research, Buffalo, NY.

Kim, H-M., and Constantinou, M. C. (2023). “Modeling frictional heating effects in triple friction pendulum isolators”, Earthquake Engineering & Structural Dynamics, 52(4), 979–997. doi.org/10.1002/eqe.3797

Kircher, C. A., and Lashkari, B. (1989) “Statistical evaluation of nonlinear response of seismic isolation systems”, Volume I. Report JBA 109-070, Jack R. Benjamin & Associates, Inc. Consulting Engineers, June 30. 1989.

Kitayama, S., and Constantinou, M. C. (2018). “Collapse performance of seismically isolated buildings designed by the procedures of ASCE/SEI 7”, Engineering Structures, 164, 243-258. doi.org/10.1016/j.engstruct.2018.03.008.

Kitayama, S., and Constantinou, M. C. (2019b). “Effect of displacement restraint on the collapse performance of seismically isolated buildings”. Bulletin of Earthquake Engineering, 17(5), 2767-2786. doi.org/10.1007/s10518-019-00554-y.

Kitayama, S., and Constantinou, M. C. (2021). “Implications of strong earthquake ground motion duration on the response and testing of seismic isolation systems”, Earthquake Engineering & Structural Dynamics, 50(2), 290-308. doi.org/10.1002/eqe.3330.

Kumar, M., Whittaker, A. S., and Constantinou, M. C. (2014). “An advanced numerical model of elastomeric seismic isolation bearings”, Earthquake Engineering & Structural Dynamics, 43(13), 1955-1974. doi.org/10.1002/eqe.2431.

Kumar, M., Whittaker, A. S., and Constantinou, M. C. (2015). “Characterizing friction in sliding isolation bearings”, Earthquake Engineering & Structural Dynamics, 44(9), 1409-1425. doi.org/10.1002/eqe.2524.

Lee, D., and Constantinou, M. C. (2016). “Further results on the heating of single and multi-core lead-rubber bearings and dampers”, Bulletin of Earthquake Engineering, 14, 999-1016. doi.org/10.1007/s10518-015-9830-2.

Lilliefors, H. W. (1969). “On the Kolmogorov-Smirnov test for the exponential distribution with mean unknown”. Journal of the American Statistical Association, 64(325), 387-389. https://doi.org/10.2307/2283748.

Massey Jr, F. J. (1951). “The Kolmogorov-Smirnov test for goodness of fit”. Journal of the American statistical Association, 46(253), 68-78. https://doi.org/10.2307/2280095.

McKenna, F., Scott, M. H. and Fenves, G. L. (2010). “Nonlinear finite-element analysis software architecture using object composition”, Journal of Computing in Civil Engineering, 24(1), 95-107. doi.org/10.1061/(ASCE)CP.1943-5487.0000002.

McVitty, W. J., and Constantinou, M. C. (2015). “Property modification factors for seismic isolators: design guidance for buildings”, Report No. MCEER-15-0005, Multidisciplinary Center for Earthquake Engineering Research, Buffalo, NY.

Mokha, A., Constantinou, M. C. and Reinhorn, A. M. (1990). “Teflon bearings in base isolation I: Testing”, Journal of Structural Engineering, 116(2), 438-454. doi.org/10.1061/(ASCE)0733-9445(1990)116:2(438).

O'Reilly, G. J., Yasumoto, H., Suzuki, Y., Calvi, G. M., and Nakashima, M. (2022). “Risk-based seismic design of base-isolated structures with single surface friction sliders”, Earthquake Engineering & Structural Dynamics, 51(10), 2378-2398. doi.org/10.1002/eqe.3668.

Pearson, K. (1900). “X. On the criterion that a given system of deviations from the probable in the case of a correlated system of variables is such that it can be reasonably supposed to have arisen from random sampling.” The London, Edinburgh, and Dublin Philosophical Magazine and Journal of Science, 50(302), 157–175. https://doi.org/10.1080/14786440009463897.

Sarlis, A. A. and Constantinou, M. C. (2010), “Modeling triple friction pendulum isolators in Program SAP2000”, document distributed to the engineering community together with example files, University at Buffalo.

Sarlis, A. A. and Constantinou, M. C. (2013). “Model of triple friction pendulum bearing for general geometric and frictional parameters and for uplift conditions”, Report No. MCEER-13-0010, Multidisciplinary Center for Earthquake Engineering Research, State University of New York at Buffalo, Buffalo, NY.

Sarlis, A. A., Constantinou, M. C. and Reinhorn, A. M. (2013). “Shake table testing of triple friction pendulum isolators under extreme conditions”, Report No. MCEER-13-0011, Multidisciplinary Center for Earthquake Engineering Research, State University of New York at Buffalo, Buffalo, NY.

Sarlis, A. A. and Constantinou, M. C. (2016). “A model of triple friction pendulum bearing for general geometric and frictional parameters”, Earthquake Engineering & Structural Dynamics, 45(11), 1837-1853. doi.org/10.1002/eqe.2738.

Structural Engineers Association of Northern California (SEAONC). Base isolation subcommittee of the seismology committee. (1986). “Tentative seismic isolation design requirements”, SEAONC.

The Mathworks Inc. (Mathworks). (2020). MATLAB. version 9.8.0.1451342 (R2020a), Natick, MA.

Warn, G. P., and Whittaker, A. S. (2004). “Performance estimates in seismically isolated bridge structures”, Engineering Structures, 26(9), 1261-1278. doi.org/10.1016/j.engstruct.2004.04.006.

Zayas, V. A., Low, S. S. and Mahin, S. A. (1987). “The FPS earthquake resisting system: Experimental report”, Report No. UCB/EERC-87/01. University of California, Berkeley, CA, Berkeley.

“This Page Intentionally Left Blank”

MCEER Technical Reports

MCEER publishes technical reports on a variety of subjects written by authors funded through MCEER. These reports can be downloaded from the MCEER website at http://www.buffalo.edu/mceer. They can also be requested through NTIS, P.O. Box 1425, Springfield, Virginia 22151. NTIS accession numbers are shown in parenthesis, if available.

NCEER-87-0001 "First-Year Program in Research, Education and Technology Transfer," 3/5/87, (PB88-134275, A04, MF-A01).

NCEER-87-0002 "Experimental Evaluation of Instantaneous Optimal Algorithms for Structural Control," by R.C. Lin, T.T. Soong and A.M. Reinhorn, 4/20/87, (PB88-134341, A04, MF-A01).

NCEER-87-0003 "Experimentation Using the Earthquake Simulation Facilities at University at Buffalo," by A.M. Reinhorn and R.L. Ketter, not available.

NCEER-87-0004 "The System Characteristics and Performance of a Shaking Table," by J.S. Hwang, K.C. Chang and G.C. Lee, 6/1/87, (PB88-134259, A03, MF-A01). This report is available only through NTIS (see address given above).

NCEER-87-0005 "A Finite Element Formulation for Nonlinear Viscoplastic Material Using a Q Model," by O. Gyebi and G. Dasgupta, 11/2/87, (PB88-213764, A08, MF-A01).

NCEER-87-0006 "Symbolic Manipulation Program (SMP) - Algebraic Codes for Two and Three Dimensional Finite Element Formulations," by X. Lee and G. Dasgupta, 11/9/87, (PB88-218522, A05, MF-A01).

NCEER-87-0007 "Instantaneous Optimal Control Laws for Tall Buildings Under Seismic Excitations," by J.N. Yang, A. Akbarpour and P. Ghaemmaghami, 6/10/87, (PB88-134333, A06, MF-A01). This report is only available through NTIS (see address given above).

NCEER-87-0008 "IDARC: Inelastic Damage Analysis of Reinforced Concrete Frame - Shear-Wall Structures," by Y.J. Park, A.M. Reinhorn and S.K. Kunnath, 7/20/87, (PB88-134325, A09, MF-A01). This report is only available through NTIS (see address given above).

NCEER-87-0009 "Liquefaction Potential for New York State: A Preliminary Report on Sites in Manhattan and Buffalo," by M. Budhu, V. Vijayakumar, R.F. Giese and L. Baumgras, 8/31/87, (PB88-163704, A03, MF-A01). This report is available only through NTIS (see address given above).

NCEER-87-0010 "Vertical and Torsional Vibration of Foundations in Inhomogeneous Media," by A.S. Veletsos and K.W. Dotson, 6/1/87, (PB88-134291, A03, MF-A01). This report is only available through NTIS (see address given above).

NCEER-87-0011 "Seismic Probabilistic Risk Assessment and Seismic Margins Studies for Nuclear Power Plants," by Howard H.M. Hwang, 6/15/87, (PB88-134267, A03, MF-A01). This report is only available through NTIS (see address given above).

NCEER-87-0012 "Parametric Studies of Frequency Response of Secondary Systems Under Ground-Acceleration Excitations," by Y. Yong and Y.K. Lin, 6/10/87, (PB88-134309, A03, MF-A01). This report is only available through NTIS (see address given above).

NCEER-87-0013 "Frequency Response of Secondary Systems Under Seismic Excitation," by J.A. HoLung, J. Cai and Y.K. Lin, 7/31/87, (PB88-134317, A05, MF-A01). This report is only available through NTIS (see address given above).

NCEER-87-0014 "Modelling Earthquake Ground Motions in Seismically Active Regions Using Parametric Time Series Methods," by G.W. Ellis and A.S. Cakmak, 8/25/87, (PB88-134283, A08, MF-A01). This report is only available through NTIS (see address given above).

NCEER-87-0015 "Detection and Assessment of Seismic Structural Damage," by E. DiPasquale and A.S. Cakmak, 8/25/87, (PB88-163712, A05, MF-A01). This report is only available through NTIS (see address given above).

NCEER-87-0016 "Pipeline Experiment at Parkfield, California," by J. Isenberg and E. Richardson, 9/15/87, (PB88-163720, A03, MF-A01). This report is available only through NTIS (see address given above).

NCEER-87-0017 "Digital Simulation of Seismic Ground Motion," by M. Shinozuka, G. Deodatis and T. Harada, 8/31/87, (PB88-155197, A04, MF-A01). This report is available only through NTIS (see address given above).

NCEER-87-0018 "Practical Considerations for Structural Control: System Uncertainty, System Time Delay and Truncation of Small Control Forces," J.N. Yang and A. Akbarpour, 8/10/87, (PB88-163738, A08, MF-A01). This report is only available through NTIS (see address given above).

NCEER-87-0019 "Modal Analysis of Nonclassically Damped Structural Systems Using Canonical Transformation," by J.N. Yang, S. Sarkani and F.X. Long, 9/27/87, (PB88-187851, A04, MF-A01).

NCEER-87-0020 "A Nonstationary Solution in Random Vibration Theory," by J.R. Red-Horse and P.D. Spanos, 11/3/87, (PB88-163746, A03, MF-A01).

NCEER-87-0021 "Horizontal Impedances for Radially Inhomogeneous Viscoelastic Soil Layers," by A.S. Veletsos and K.W. Dotson, 10/15/87, (PB88-150859, A04, MF-A01).

NCEER-87-0022 "Seismic Damage Assessment of Reinforced Concrete Members," by Y.S. Chung, C. Meyer and M. Shinozuka, 10/9/87, (PB88-150867, A05, MF-A01). This report is available only through NTIS (see address given above).

NCEER-87-0023 "Active Structural Control in Civil Engineering," by T.T. Soong, 11/11/87, (PB88-187778, A03, MF-A01).

NCEER-87-0024 "Vertical and Torsional Impedances for Radially Inhomogeneous Viscoelastic Soil Layers," by K.W. Dotson and A.S. Veletsos, 12/87, (PB88-187786, A03, MF-A01).

NCEER-87-0025 "Proceedings from the Symposium on Seismic Hazards, Ground Motions, Soil-Liquefaction and Engineering Practice in Eastern North America," October 20-22, 1987, edited by K.H. Jacob, 12/87, (PB88-188115, A23, MF-A01). This report is available only through NTIS (see address given above).

NCEER-87-0026 "Report on the Whittier-Narrows, California, Earthquake of October 1, 1987," by J. Pantelic and A. Reinhorn, 11/87, (PB88-187752, A03, MF-A01). This report is available only through NTIS (see address given above).

NCEER-87-0027 "Design of a Modular Program for Transient Nonlinear Analysis of Large 3-D Building Structures," by S. Srivastav and J.F. Abel, 12/30/87, (PB88-187950, A05, MF-A01). This report is only available through NTIS (see address given above).

NCEER-87-0028 "Second-Year Program in Research, Education and Technology Transfer," 3/8/88, (PB88-219480, A04, MF-A01).

NCEER-88-0001 "Workshop on Seismic Computer Analysis and Design of Buildings With Interactive Graphics," by W. McGuire, J.F. Abel and C.H. Conley, 1/18/88, (PB88-187760, A03, MF-A01). This report is only available through NTIS (see address given above).

NCEER-88-0002 "Optimal Control of Nonlinear Flexible Structures," by J.N. Yang, F.X. Long and D. Wong, 1/22/88, (PB88-213772, A06, MF-A01).

NCEER-88-0003 "Substructuring Techniques in the Time Domain for Primary-Secondary Structural Systems," by G.D. Manolis and G. Juhn, 2/10/88, (PB88-213780, A04, MF-A01).

NCEER-88-0004 "Iterative Seismic Analysis of Primary-Secondary Systems," by A. Singhal, L.D. Lutes and P.D. Spanos, 2/23/88, (PB88-213798, A04, MF-A01).

NCEER-88-0005 "Stochastic Finite Element Expansion for Random Media," by P.D. Spanos and R. Ghanem, 3/14/88, (PB88-213806, A03, MF-A01).

NCEER-88-0006 "Combining Structural Optimization and Structural Control," by F.Y. Cheng and C.P. Pantelides, 1/10/88, (PB88-213814, A05, MF-A01).

NCEER-88-0007 "Seismic Performance Assessment of Code-Designed Structures," by H.H-M. Hwang, J-W. Jaw and H-J. Shau, 3/20/88, (PB88-219423, A04, MF-A01). This report is only available through NTIS (see address given above).

NCEER-88-0008 "Reliability Analysis of Code-Designed Structures Under Natural Hazards," by H.H-M. Hwang, H. Ushiba and M. Shinozuka, 2/29/88, (PB88-229471, A07, MF-A01). This report is only available through NTIS (see address given above).

NCEER-88-0009 "Seismic Fragility Analysis of Shear Wall Structures," by J-W Jaw and H.H-M. Hwang, 4/30/88, (PB89-102867, A04, MF-A01).

NCEER-88-0010 "Base Isolation of a Multi-Story Building Under a Harmonic Ground Motion - A Comparison of Performances of Various Systems," by F-G Fan, G. Ahmadi and I.G. Tadjbakhsh, 5/18/88, (PB89-122238, A06, MF-A01). This report is only available through NTIS (see address given above).

NCEER-88-0011 "Seismic Floor Response Spectra for a Combined System by Green's Functions," by F.M. Lavelle, L.A. Bergman and P.D. Spanos, 5/1/88, (PB89-102875, A03, MF-A01).

NCEER-88-0012 "A New Solution Technique for Randomly Excited Hysteretic Structures," by G.Q. Cai and Y.K. Lin, 5/16/88, (PB89-102883, A03, MF-A01).

NCEER-88-0013 "A Study of Radiation Damping and Soil-Structure Interaction Effects in the Centrifuge," by K. Weissman, supervised by J.H. Prevost, 5/24/88, (PB89-144703, A06, MF-A01).

NCEER-88-0014 "Parameter Identification and Implementation of a Kinematic Plasticity Model for Frictional Soils," by J.H. Prevost and D.V. Griffiths, not available.

NCEER-88-0015 "Two- and Three- Dimensional Dynamic Finite Element Analyses of the Long Valley Dam," by D.V. Griffiths and J.H. Prevost, 6/17/88, (PB89-144711, A04, MF-A01).

NCEER-88-0016 "Damage Assessment of Reinforced Concrete Structures in Eastern United States," by A.M. Reinhorn, M.J. Seidel, S.K. Kunnath and Y.J. Park, 6/15/88, (PB89-122220, A04, MF-A01). This report is only available through NTIS (see address given above).

NCEER-88-0017 "Dynamic Compliance of Vertically Loaded Strip Foundations in Multilayered Viscoelastic Soils," by S. Ahmad and A.S.M. Israil, 6/17/88, (PB89-102891, A04, MF-A01).

NCEER-88-0018 "An Experimental Study of Seismic Structural Response With Added Viscoelastic Dampers," by R.C. Lin, Z. Liang, T.T. Soong and R.H. Zhang, 6/30/88, (PB89-122212, A05, MF-A01). This report is available only through NTIS (see address given above).

NCEER-88-0019 "Experimental Investigation of Primary - Secondary System Interaction," by G.D. Manolis, G. Juhn and A.M. Reinhorn, 5/27/88, (PB89-122204, A04, MF-A01).

NCEER-88-0020 "A Response Spectrum Approach For Analysis of Nonclassically Damped Structures," by J.N. Yang, S. Sarkani and F.X. Long, 4/22/88, (PB89-102909, A04, MF-A01).

NCEER-88-0021 "Seismic Interaction of Structures and Soils: Stochastic Approach," by A.S. Veletsos and A.M. Prasad, 7/21/88, (PB89-122196, A04, MF-A01). This report is only available through NTIS (see address given above).

NCEER-88-0022 "Identification of the Serviceability Limit State and Detection of Seismic Structural Damage," by E. DiPasquale and A.S. Cakmak, 6/15/88, (PB89-122188, A05, MF-A01). This report is available only through NTIS (see address given above).

NCEER-88-0023 "Multi-Hazard Risk Analysis: Case of a Simple Offshore Structure," by B.K. Bhartia and E.H. Vanmarcke, 7/21/88, (PB89-145213, A05, MF-A01).

NCEER-88-0024 "Automated Seismic Design of Reinforced Concrete Buildings," by Y.S. Chung, C. Meyer and M. Shinozuka, 7/5/88, (PB89-122170, A06, MF-A01). This report is available only through NTIS (see address given above).

NCEER-88-0025 "Experimental Study of Active Control of MDOF Structures Under Seismic Excitations," by L.L. Chung, R.C. Lin, T.T. Soong and A.M. Reinhorn, 7/10/88, (PB89-122600, A04, MF-A01).

NCEER-88-0026 "Earthquake Simulation Tests of a Low-Rise Metal Structure," by J.S. Hwang, K.C. Chang, G.C. Lee and R.L. Ketter, 8/1/88, (PB89-102917, A04, MF-A01).

NCEER-88-0027 "Systems Study of Urban Response and Reconstruction Due to Catastrophic Earthquakes," by F. Kozin and H.K. Zhou, 9/22/88, (PB90-162348, A04, MF-A01).

NCEER-88-0028 "Seismic Fragility Analysis of Plane Frame Structures," by H.H-M. Hwang and Y.K. Low, 7/31/88, (PB89-131445, A06, MF-A01).

NCEER-88-0029 "Response Analysis of Stochastic Structures," by A. Kardara, C. Bucher and M. Shinozuka, 9/22/88, (PB89-174429, A04, MF-A01).

NCEER-88-0030 "Nonnormal Accelerations Due to Yielding in a Primary Structure," by D.C.K. Chen and L.D. Lutes, 9/19/88, (PB89-131437, A04, MF-A01).

NCEER-88-0031 "Design Approaches for Soil-Structure Interaction," by A.S. Veletsos, A.M. Prasad and Y. Tang, 12/30/88, (PB89-174437, A03, MF-A01). This report is available only through NTIS (see address given above).

NCEER-88-0032 "A Re-evaluation of Design Spectra for Seismic Damage Control," by C.J. Turkstra and A.G. Tallin, 11/7/88, (PB89-145221, A05, MF-A01).

NCEER-88-0033 "The Behavior and Design of Noncontact Lap Splices Subjected to Repeated Inelastic Tensile Loading," by V.E. Sagan, P. Gergely and R.N. White, 12/8/88, (PB89-163737, A08, MF-A01).

NCEER-88-0034 "Seismic Response of Pile Foundations," by S.M. Mamoon, P.K. Banerjee and S. Ahmad, 11/1/88, (PB89-145239, A04, MF-A01).

NCEER-88-0035 "Modeling of R/C Building Structures With Flexible Floor Diaphragms (IDARC2)," by A.M. Reinhorn, S.K. Kunnath and N. Panahshahi, 9/7/88, (PB89-207153, A07, MF-A01).

NCEER-88-0036 "Solution of the Dam-Reservoir Interaction Problem Using a Combination of FEM, BEM with Particular Integrals, Modal Analysis, and Substructuring," by C-S. Tsai, G.C. Lee and R.L. Ketter, 12/31/88, (PB89-207146, A04, MF-A01).

NCEER-88-0037 "Optimal Placement of Actuators for Structural Control," by F.Y. Cheng and C.P. Pantelides, 8/15/88, (PB89-162846, A05, MF-A01).

NCEER-88-0038 "Teflon Bearings in Aseismic Base Isolation: Experimental Studies and Mathematical Modeling," by A. Mokha, M.C. Constantinou and A.M. Reinhorn, 12/5/88, (PB89-218457, A10, MF-A01). This report is available only through NTIS (see address given above).

NCEER-88-0039 "Seismic Behavior of Flat Slab High-Rise Buildings in the New York City Area," by P. Weidlinger and M. Ettouney, 10/15/88, (PB90-145681, A04, MF-A01).

NCEER-88-0040 "Evaluation of the Earthquake Resistance of Existing Buildings in New York City," by P. Weidlinger and M. Ettouney, 10/15/88, not available.

NCEER-88-0041 "Small-Scale Modeling Techniques for Reinforced Concrete Structures Subjected to Seismic Loads," by W. Kim, A. El-Attar and R.N. White, 11/22/88, (PB89-189625, A05, MF-A01).

NCEER-88-0042 "Modeling Strong Ground Motion from Multiple Event Earthquakes," by G.W. Ellis and A.S. Cakmak, 10/15/88, (PB89-174445, A03, MF-A01).

NCEER-88-0043 "Nonstationary Models of Seismic Ground Acceleration," by M. Grigoriu, S.E. Ruiz and E. Rosenblueth, 7/15/88, (PB89-189617, A04, MF-A01).

NCEER-88-0044 "SARCF User's Guide: Seismic Analysis of Reinforced Concrete Frames," by Y.S. Chung, C. Meyer and M. Shinozuka, 11/9/88, (PB89-174452, A08, MF-A01).

NCEER-88-0045 "First Expert Panel Meeting on Disaster Research and Planning," edited by J. Pantelic and J. Stoyle, 9/15/88, (PB89-174460, A05, MF-A01).

NCEER-88-0046 "Preliminary Studies of the Effect of Degrading Infill Walls on the Nonlinear Seismic Response of Steel Frames," by C.Z. Chrysostomou, P. Gergely and J.F. Abel, 12/19/88, (PB89-208383, A05, MF-A01).

NCEER-88-0047 "Reinforced Concrete Frame Component Testing Facility - Design, Construction, Instrumentation and Operation," by S.P. Pessiki, C. Conley, T. Bond, P. Gergely and R.N. White, 12/16/88, (PB89-174478, A04, MF-A01).

NCEER-89-0001 "Effects of Protective Cushion and Soil Compliancy on the Response of Equipment Within a Seismically Excited Building," by J.A. HoLung, 2/16/89, (PB89-207179, A04, MF-A01).

NCEER-89-0002 "Statistical Evaluation of Response Modification Factors for Reinforced Concrete Structures," by H.H-M. Hwang and J-W. Jaw, 2/17/89, (PB89-207187, A05, MF-A01).

NCEER-89-0003 "Hysteretic Columns Under Random Excitation," by G-Q. Cai and Y.K. Lin, 1/9/89, (PB89-196513, A03, MF-A01).

NCEER-89-0004 "Experimental Study of `Elephant Foot Bulge' Instability of Thin-Walled Metal Tanks," by Z-H. Jia and R.L. Ketter, 2/22/89, (PB89-207195, A03, MF-A01).

NCEER-89-0005 "Experiment on Performance of Buried Pipelines Across San Andreas Fault," by J. Isenberg, E. Richardson and T.D. O'Rourke, 3/10/89, (PB89-218440, A04, MF-A01). This report is available only through NTIS (see address given above).

NCEER-89-0006 "A Knowledge-Based Approach to Structural Design of Earthquake-Resistant Buildings," by M. Subramani, P. Gergely, C.H. Conley, J.F. Abel and A.H. Zaghw, 1/15/89, (PB89-218465, A06, MF-A01).

NCEER-89-0007 "Liquefaction Hazards and Their Effects on Buried Pipelines," by T.D. O'Rourke and P.A. Lane, 2/1/89, (PB89-218481, A09, MF-A01).

NCEER-89-0008 "Fundamentals of System Identification in Structural Dynamics," by H. Imai, C-B. Yun, O. Maruyama and M. Shinozuka, 1/26/89, (PB89-207211, A04, MF-A01).

NCEER-89-0009 "Effects of the 1985 Michoacan Earthquake on Water Systems and Other Buried Lifelines in Mexico," by A.G. Ayala and M.J. O'Rourke, 3/8/89, (PB89-207229, A06, MF-A01).

NCEER-89-R010 "NCEER Bibliography of Earthquake Education Materials," by K.E.K. Ross, Second Revision, 9/1/89, (PB90-125352, A05, MF-A01). This report is replaced by NCEER-92-0018.

NCEER-89-0011 "Inelastic Three-Dimensional Response Analysis of Reinforced Concrete Building Structures (IDARC-3D), Part I - Modeling," by S.K. Kunnath and A.M. Reinhorn, 4/17/89, (PB90-114612, A07, MF-A01). This report is available only through NTIS (see address given above).

NCEER-89-0012 "Recommended Modifications to ATC-14," by C.D. Poland and J.O. Malley, 4/12/89, (PB90-108648, A15, MF-A01).

NCEER-89-0013 "Repair and Strengthening of Beam-to-Column Connections Subjected to Earthquake Loading," by M. Corazao and A.J. Durrani, 2/28/89, (PB90-109885, A06, MF-A01).

NCEER-89-0014 "Program EXKAL2 for Identification of Structural Dynamic Systems," by O. Maruyama, C-B. Yun, M. Hoshiya and M. Shinozuka, 5/19/89, (PB90-109877, A09, MF-A01).

NCEER-89-0015 "Response of Frames With Bolted Semi-Rigid Connections, Part I - Experimental Study and Analytical Predictions," by P.J. DiCorso, A.M. Reinhorn, J.R. Dickerson, J.B. Radziminski and W.L. Harper, 6/1/89, not available.

NCEER-89-0016 "ARMA Monte Carlo Simulation in Probabilistic Structural Analysis," by P.D. Spanos and M.P. Mignolet, 7/10/89, (PB90-109893, A03, MF-A01).

NCEER-89-P017 "Preliminary Proceedings from the Conference on Disaster Preparedness - The Place of Earthquake Education in Our Schools," Edited by K.E.K. Ross, 6/23/89, (PB90-108606, A03, MF-A01).

NCEER-89-0017 "Proceedings from the Conference on Disaster Preparedness - The Place of Earthquake Education in Our Schools," Edited by K.E.K. Ross, 12/31/89, (PB90-207895, A012, MF-A02). This report is available only through NTIS (see address given above).

NCEER-89-0018 "Multidimensional Models of Hysteretic Material Behavior for Vibration Analysis of Shape Memory Energy Absorbing Devices, by E.J. Graesser and F.A. Cozzarelli, 6/7/89, (PB90-164146, A04, MF-A01).

NCEER-89-0019 "Nonlinear Dynamic Analysis of Three-Dimensional Base Isolated Structures (3D-BASIS)," by S. Nagarajaiah, A.M. Reinhorn and M.C. Constantinou, 8/3/89, (PB90-161936, A06, MF-A01). This report has been replaced by NCEER-93-0011.

NCEER-89-0020 "Structural Control Considering Time-Rate of Control Forces and Control Rate Constraints," by F.Y. Cheng and C.P. Pantelides, 8/3/89, (PB90-120445, A04, MF-A01).

NCEER-89-0021 "Subsurface Conditions of Memphis and Shelby County," by K.W. Ng, T-S. Chang and H-H.M. Hwang, 7/26/89, (PB90-120437, A03, MF-A01).

NCEER-89-0022 "Seismic Wave Propagation Effects on Straight Jointed Buried Pipelines," by K. Elhmadi and M.J. O'Rourke, 8/24/89, (PB90-162322, A10, MF-A02).

NCEER-89-0023 "Workshop on Serviceability Analysis of Water Delivery Systems," edited by M. Grigoriu, 3/6/89, (PB90-127424, A03, MF-A01).

NCEER-89-0024 "Shaking Table Study of a 1/5 Scale Steel Frame Composed of Tapered Members," by K.C. Chang, J.S. Hwang and G.C. Lee, 9/18/89, (PB90-160169, A04, MF-A01).

NCEER-89-0025 "DYNA1D: A Computer Program for Nonlinear Seismic Site Response Analysis - Technical Documentation," by Jean H. Prevost, 9/14/89, (PB90-161944, A07, MF-A01). This report is available only through NTIS (see address given above).

NCEER-89-0026 "1:4 Scale Model Studies of Active Tendon Systems and Active Mass Dampers for Aseismic Protection," by A.M. Reinhorn, T.T. Soong, R.C. Lin, Y.P. Yang, Y. Fukao, H. Abe and M. Nakai, 9/15/89, (PB90-173246, A10, MF-A02). This report is available only through NTIS (see address given above).

NCEER-89-0027 "Scattering of Waves by Inclusions in a Nonhomogeneous Elastic Half Space Solved by Boundary Element Methods," by P.K. Hadley, A. Askar and A.S. Cakmak, 6/15/89, (PB90-145699, A07, MF-A01).

NCEER-89-0028 "Statistical Evaluation of Deflection Amplification Factors for Reinforced Concrete Structures," by H.H.M. Hwang, J-W. Jaw and A.L. Ch'ng, 8/31/89, (PB90-164633, A05, MF-A01).

NCEER-89-0029 "Bedrock Accelerations in Memphis Area Due to Large New Madrid Earthquakes," by H.H.M. Hwang, C.H.S. Chen and G. Yu, 11/7/89, (PB90-162330, A04, MF-A01).

NCEER-89-0030 "Seismic Behavior and Response Sensitivity of Secondary Structural Systems," by Y.Q. Chen and T.T. Soong, 10/23/89, (PB90-164658, A08, MF-A01).

NCEER-89-0031 "Random Vibration and Reliability Analysis of Primary-Secondary Structural Systems," by Y. Ibrahim, M. Grigoriu and T.T. Soong, 11/10/89, (PB90-161951, A04, MF-A01).

NCEER-89-0032 "Proceedings from the Second U.S. - Japan Workshop on Liquefaction, Large Ground Deformation and Their Effects on Lifelines, September 26-29, 1989," Edited by T.D. O'Rourke and M. Hamada, 12/1/89, (PB90-209388, A22, MF-A03).

NCEER-89-0033 "Deterministic Model for Seismic Damage Evaluation of Reinforced Concrete Structures," by J.M. Bracci, A.M. Reinhorn, J.B. Mander and S.K. Kunnath, 9/27/89, (PB91-108803, A06, MF-A01).

NCEER-89-0034 "On the Relation Between Local and Global Damage Indices," by E. DiPasquale and A.S. Cakmak, 8/15/89, (PB90-173865, A05, MF-A01).

NCEER-89-0035 "Cyclic Undrained Behavior of Nonplastic and Low Plasticity Silts," by A.J. Walker and H.E. Stewart, 7/26/89, (PB90-183518, A10, MF-A01).

NCEER-89-0036 "Liquefaction Potential of Surficial Deposits in the City of Buffalo, New York," by M. Budhu, R. Giese and L. Baumgrass, 1/17/89, (PB90-208455, A04, MF-A01).

NCEER-89-0037 "A Deterministic Assessment of Effects of Ground Motion Incoherence," by A.S. Veletsos and Y. Tang, 7/15/89, (PB90-164294, A03, MF-A01).

NCEER-89-0038 "Workshop on Ground Motion Parameters for Seismic Hazard Mapping," July 17-18, 1989, edited by R.V. Whitman, 12/1/89, (PB90-173923, A04, MF-A01).

NCEER-89-0039 "Seismic Effects on Elevated Transit Lines of the New York City Transit Authority," by C.J. Costantino, C.A. Miller and E. Heymsfield, 12/26/89, (PB90-207887, A06, MF-A01).

NCEER-89-0040 "Centrifugal Modeling of Dynamic Soil-Structure Interaction," by K. Weissman, Supervised by J.H. Prevost, 5/10/89, (PB90-207879, A07, MF-A01).

NCEER-89-0041 "Linearized Identification of Buildings With Cores for Seismic Vulnerability Assessment," by I-K. Ho and A.E. Aktan, 11/1/89, (PB90-251943, A07, MF-A01).

NCEER-90-0001 "Geotechnical and Lifeline Aspects of the October 17, 1989 Loma Prieta Earthquake in San Francisco," by T.D. O'Rourke, H.E. Stewart, F.T. Blackburn and T.S. Dickerman, 1/90, (PB90-208596, A05, MF-A01).

NCEER-90-0002 "Nonnormal Secondary Response Due to Yielding in a Primary Structure," by D.C.K. Chen and L.D. Lutes, 2/28/90, (PB90-251976, A07, MF-A01).

NCEER-90-0003 "Earthquake Education Materials for Grades K-12," by K.E.K. Ross, 4/16/90, (PB91-251984, A05, MF-A05). This report has been replaced by NCEER-92-0018.

NCEER-90-0004 "Catalog of Strong Motion Stations in Eastern North America," by R.W. Busby, 4/3/90, (PB90-251984, A05, MF-A01).

NCEER-90-0005 "NCEER Strong-Motion Data Base: A User Manual for the GeoBase Release (Version 1.0 for the Sun3)," by P. Friberg and K. Jacob, 3/31/90 (PB90-258062, A04, MF-A01).

NCEER-90-0006 "Seismic Hazard Along a Crude Oil Pipeline in the Event of an 1811-1812 Type New Madrid Earthquake," by H.H.M. Hwang and C-H.S. Chen, 4/16/90, (PB90-258054, A04, MF-A01).

NCEER-90-0007 "Site-Specific Response Spectra for Memphis Sheahan Pumping Station," by H.H.M. Hwang and C.S. Lee, 5/15/90, (PB91-108811, A05, MF-A01).

NCEER-90-0008 "Pilot Study on Seismic Vulnerability of Crude Oil Transmission Systems," by T. Ariman, R. Dobry, M. Grigoriu, F. Kozin, M. O'Rourke, T. O'Rourke and M. Shinozuka, 5/25/90, (PB91-108837, A06, MF-A01).

NCEER-90-0009 "A Program to Generate Site Dependent Time Histories: EQGEN," by G.W. Ellis, M. Srinivasan and A.S. Cakmak, 1/30/90, (PB91-108829, A04, MF-A01).

NCEER-90-0010 "Active Isolation for Seismic Protection of Operating Rooms," by M.E. Talbott, Supervised by M. Shinozuka, 6/8/9, (PB91-110205, A05, MF-A01).

NCEER-90-0011 "Program LINEARID for Identification of Linear Structural Dynamic Systems," by C-B. Yun and M. Shinozuka, 6/25/90, (PB91-110312, A08, MF-A01).

NCEER-90-0012 "Two-Dimensional Two-Phase Elasto-Plastic Seismic Response of Earth Dams," by A.N. Yiagos, Supervised by J.H. Prevost, 6/20/90, (PB91-110197, A13, MF-A02).

NCEER-90-0013 "Secondary Systems in Base-Isolated Structures: Experimental Investigation, Stochastic Response and Stochastic Sensitivity," by G.D. Manolis, G. Juhn, M.C. Constantinou and A.M. Reinhorn, 7/1/90, (PB91-110320, A08, MF-A01).

NCEER-90-0014 "Seismic Behavior of Lightly-Reinforced Concrete Column and Beam-Column Joint Details," by S.P. Pessiki, C.H. Conley, P. Gergely and R.N. White, 8/22/90, (PB91-108795, A11, MF-A02).

NCEER-90-0015 "Two Hybrid Control Systems for Building Structures Under Strong Earthquakes," by J.N. Yang and A. Danielians, 6/29/90, (PB91-125393, A04, MF-A01).

NCEER-90-0016 "Instantaneous Optimal Control with Acceleration and Velocity Feedback," by J.N. Yang and Z. Li, 6/29/90, (PB91-125401, A03, MF-A01).

NCEER-90-0017 "Reconnaissance Report on the Northern Iran Earthquake of June 21, 1990," by M. Mehrain, 10/4/90, (PB91-125377, A03, MF-A01).

NCEER-90-0018 "Evaluation of Liquefaction Potential in Memphis and Shelby County," by T.S. Chang, P.S. Tang, C.S. Lee and H. Hwang, 8/10/90, (PB91-125427, A09, MF-A01).

NCEER-90-0019 "Experimental and Analytical Study of a Combined Sliding Disc Bearing and Helical Steel Spring Isolation System," by M.C. Constantinou, A.S. Mokha and A.M. Reinhorn, 10/4/90, (PB91-125385, A06, MF-A01). This report is available only through NTIS (see address given above).

NCEER-90-0020 "Experimental Study and Analytical Prediction of Earthquake Response of a Sliding Isolation System with a Spherical Surface," by A.S. Mokha, M.C. Constantinou and A.M. Reinhorn, 10/11/90, (PB91-125419, A05, MF-A01).

NCEER-90-0021 "Dynamic Interaction Factors for Floating Pile Groups," by G. Gazetas, K. Fan, A. Kaynia and E. Kausel, 9/10/90, (PB91-170381, A05, MF-A01).

NCEER-90-0022 "Evaluation of Seismic Damage Indices for Reinforced Concrete Structures," by S. Rodriguez-Gomez and A.S. Cakmak, 9/30/90, PB91-171322, A06, MF-A01).

NCEER-90-0023 "Study of Site Response at a Selected Memphis Site," by H. Desai, S. Ahmad, E.S. Gazetas and M.R. Oh, 10/11/90, (PB91-196857, A03, MF-A01).

NCEER-90-0024 "A User's Guide to Strongmo: Version 1.0 of NCEER's Strong-Motion Data Access Tool for PCs and Terminals," by P.A. Friberg and C.A.T. Susch, 11/15/90, (PB91-171272, A03, MF-A01).

NCEER-90-0025 "A Three-Dimensional Analytical Study of Spatial Variability of Seismic Ground Motions," by L-L. Hong and A.H.-S. Ang, 10/30/90, (PB91-170399, A09, MF-A01).

NCEER-90-0026 "MUMOID User's Guide - A Program for the Identification of Modal Parameters," by S. Rodriguez-Gomez and E. DiPasquale, 9/30/90, (PB91-171298, A04, MF-A01).

NCEER-90-0027 "SARCF-II User's Guide - Seismic Analysis of Reinforced Concrete Frames," by S. Rodriguez-Gomez, Y.S. Chung and C. Meyer, 9/30/90, (PB91-171280, A05, MF-A01).

NCEER-90-0028 "Viscous Dampers: Testing, Modeling and Application in Vibration and Seismic Isolation," by N. Makris and M.C. Constantinou, 12/20/90 (PB91-190561, A06, MF-A01).

NCEER-90-0029 "Soil Effects on Earthquake Ground Motions in the Memphis Area," by H. Hwang, C.S. Lee, K.W. Ng and T.S. Chang, 8/2/90, (PB91-190751, A05, MF-A01).

NCEER-91-0001 "Proceedings from the Third Japan-U.S. Workshop on Earthquake Resistant Design of Lifeline Facilities and Countermeasures for Soil Liquefaction, December 17-19, 1990," edited by T.D. O'Rourke and M. Hamada, 2/1/91, (PB91-179259, A99, MF-A04).

NCEER-91-0002 "Physical Space Solutions of Non-Proportionally Damped Systems," by M. Tong, Z. Liang and G.C. Lee, 1/15/91, (PB91-179242, A04, MF-A01).

NCEER-91-0003 "Seismic Response of Single Piles and Pile Groups," by K. Fan and G. Gazetas, 1/10/91, (PB92-174994, A04, MF-A01).

NCEER-91-0004 "Damping of Structures: Part 1 - Theory of Complex Damping," by Z. Liang and G. Lee, 10/10/91, (PB92-197235, A12, MF-A03).

NCEER-91-0005 "3D-BASIS - Nonlinear Dynamic Analysis of Three Dimensional Base Isolated Structures: Part II," by S. Nagarajaiah, A.M. Reinhorn and M.C. Constantinou, 2/28/91, (PB91-190553, A07, MF-A01). This report has been replaced by NCEER-93-0011.

NCEER-91-0006 "A Multidimensional Hysteretic Model for Plasticity Deforming Metals in Energy Absorbing Devices," by E.J. Graesser and F.A. Cozzarelli, 4/9/91, (PB92-108364, A04, MF-A01).

NCEER-91-0007 "A Framework for Customizable Knowledge-Based Expert Systems with an Application to a KBES for Evaluating the Seismic Resistance of Existing Buildings," by E.G. Ibarra-Anaya and S.J. Fenves, 4/9/91, (PB91-210930, A08, MF-A01).

NCEER-91-0008 "Nonlinear Analysis of Steel Frames with Semi-Rigid Connections Using the Capacity Spectrum Method," by G.G. Deierlein, S-H. Hsieh, Y-J. Shen and J.F. Abel, 7/2/91, (PB92-113828, A05, MF-A01).

NCEER-91-0009 "Earthquake Education Materials for Grades K-12," by K.E.K. Ross, 4/30/91, (PB91-212142, A06, MF-A01). This report has been replaced by NCEER-92-0018.

NCEER-91-0010 "Phase Wave Velocities and Displacement Phase Differences in a Harmonically Oscillating Pile," by N. Makris and G. Gazetas, 7/8/91, (PB92-108356, A04, MF-A01).

NCEER-91-0011 "Dynamic Characteristics of a Full-Size Five-Story Steel Structure and a 2/5 Scale Model," by K.C. Chang, G.C. Yao, G.C. Lee, D.S. Hao and Y.C. Yeh," 7/2/91, (PB93-116648, A06, MF-A02).

NCEER-91-0012 "Seismic Response of a 2/5 Scale Steel Structure with Added Viscoelastic Dampers," by K.C. Chang, T.T. Soong, S-T. Oh and M.L. Lai, 5/17/91, (PB92-110816, A05, MF-A01).

NCEER-91-0013 "Earthquake Response of Retaining Walls; Full-Scale Testing and Computational Modeling," by S. Alampalli and A-W.M. Elgamal, 6/20/91, not available.

NCEER-91-0014 "3D-BASIS-M: Nonlinear Dynamic Analysis of Multiple Building Base Isolated Structures," by P.C. Tsopelas, S. Nagarajaiah, M.C. Constantinou and A.M. Reinhorn, 5/28/91, (PB92-113885, A09, MF-A02).

NCEER-91-0015 "Evaluation of SEAOC Design Requirements for Sliding Isolated Structures," by D. Theodossiou and M.C. Constantinou, 6/10/91, (PB92-114602, A11, MF-A03).

NCEER-91-0016 "Closed-Loop Modal Testing of a 27-Story Reinforced Concrete Flat Plate-Core Building," by H.R. Somaprasad, T. Toksoy, H. Yoshiyuki and A.E. Aktan, 7/15/91, (PB92-129980, A07, MF-A02).

NCEER-91-0017 "Shake Table Test of a 1/6 Scale Two-Story Lightly Reinforced Concrete Building," by A.G. El-Attar, R.N. White and P. Gergely, 2/28/91, (PB92-222447, A06, MF-A02).

NCEER-91-0018 "Shake Table Test of a 1/8 Scale Three-Story Lightly Reinforced Concrete Building," by A.G. El-Attar, R.N. White and P. Gergely, 2/28/91, (PB93-116630, A08, MF-A02).

NCEER-91-0019 "Transfer Functions for Rigid Rectangular Foundations," by A.S. Veletsos, A.M. Prasad and W.H. Wu, 7/31/91, not available.

NCEER-91-0020 "Hybrid Control of Seismic-Excited Nonlinear and Inelastic Structural Systems," by J.N. Yang, Z. Li and A. Danielians, 8/1/91, (PB92-143171, A06, MF-A02).

NCEER-91-0021 "The NCEER-91 Earthquake Catalog: Improved Intensity-Based Magnitudes and Recurrence Relations for U.S. Earthquakes East of New Madrid," by L. Seeber and J.G. Armbruster, 8/28/91, (PB92-176742, A06, MF-A02).

NCEER-91-0022 "Proceedings from the Implementation of Earthquake Planning and Education in Schools: The Need for Change - The Roles of the Changemakers," by K.E.K. Ross and F. Winslow, 7/23/91, (PB92-129998, A12, MF-A03).

NCEER-91-0023 "A Study of Reliability-Based Criteria for Seismic Design of Reinforced Concrete Frame Buildings," by H.H.M. Hwang and H-M. Hsu, 8/10/91, (PB92-140235, A09, MF-A02).

NCEER-91-0024 "Experimental Verification of a Number of Structural System Identification Algorithms," by R.G. Ghanem, H. Gavin and M. Shinozuka, 9/18/91, (PB92-176577, A18, MF-A04).

NCEER-91-0025 "Probabilistic Evaluation of Liquefaction Potential," by H.H.M. Hwang and C.S. Lee," 11/25/91, (PB92-143429, A05, MF-A01).

NCEER-91-0026 "Instantaneous Optimal Control for Linear, Nonlinear and Hysteretic Structures - Stable Controllers," by J.N. Yang and Z. Li, 11/15/91, (PB92-163807, A04, MF-A01).

NCEER-91-0027 "Experimental and Theoretical Study of a Sliding Isolation System for Bridges," by M.C. Constantinou, A. Kartoum, A.M. Reinhorn and P. Bradford, 11/15/91, (PB92-176973, A10, MF-A03).

NCEER-92-0001 "Case Studies of Liquefaction and Lifeline Performance During Past Earthquakes, Volume 1: Japanese Case Studies," Edited by M. Hamada and T. O'Rourke, 2/17/92, (PB92-197243, A18, MF-A04).

NCEER-92-0002 "Case Studies of Liquefaction and Lifeline Performance During Past Earthquakes, Volume 2: United States Case Studies," Edited by T. O'Rourke and M. Hamada, 2/17/92, (PB92-197250, A20, MF-A04).

NCEER-92-0003 "Issues in Earthquake Education," Edited by K. Ross, 2/3/92, (PB92-222389, A07, MF-A02).

NCEER-92-0004 "Proceedings from the First U.S. - Japan Workshop on Earthquake Protective Systems for Bridges," Edited by I.G. Buckle, 2/4/92, (PB94-142239, A99, MF-A06).

NCEER-92-0005 "Seismic Ground Motion from a Haskell-Type Source in a Multiple-Layered Half-Space," A.P. Theoharis, G. Deodatis and M. Shinozuka, 1/2/92, not available.

NCEER-92-0006 "Proceedings from the Site Effects Workshop," Edited by R. Whitman, 2/29/92, (PB92-197201, A04, MF-A01).

NCEER-92-0007 "Engineering Evaluation of Permanent Ground Deformations Due to Seismically-Induced Liquefaction," by M.H. Baziar, R. Dobry and A-W.M. Elgamal, 3/24/92, (PB92-222421, A13, MF-A03).

NCEER-92-0008 "A Procedure for the Seismic Evaluation of Buildings in the Central and Eastern United States," by C.D. Poland and J.O. Malley, 4/2/92, (PB92-222439, A20, MF-A04).

NCEER-92-0009 "Experimental and Analytical Study of a Hybrid Isolation System Using Friction Controllable Sliding Bearings," by M.Q. Feng, S. Fujii and M. Shinozuka, 5/15/92, (PB93-150282, A06, MF-A02).

NCEER-92-0010 "Seismic Resistance of Slab-Column Connections in Existing Non-Ductile Flat-Plate Buildings," by A.J. Durrani and Y. Du, 5/18/92, (PB93-116812, A06, MF-A02).

NCEER-92-0011 "The Hysteretic and Dynamic Behavior of Brick Masonry Walls Upgraded by Ferrocement Coatings Under Cyclic Loading and Strong Simulated Ground Motion," by H. Lee and S.P. Prawel, 5/11/92, not available.

NCEER-92-0012 "Study of Wire Rope Systems for Seismic Protection of Equipment in Buildings," by G.F. Demetriades, M.C. Constantinou and A.M. Reinhorn, 5/20/92, (PB93-116655, A08, MF-A02).

NCEER-92-0013 "Shape Memory Structural Dampers: Material Properties, Design and Seismic Testing," by P.R. Witting and F.A. Cozzarelli, 5/26/92, (PB93-116663, A05, MF-A01).

NCEER-92-0014 "Longitudinal Permanent Ground Deformation Effects on Buried Continuous Pipelines," by M.J. O'Rourke, and C. Nordberg, 6/15/92, (PB93-116671, A08, MF-A02).

NCEER-92-0015 "A Simulation Method for Stationary Gaussian Random Functions Based on the Sampling Theorem," by M. Grigoriu and S. Balopoulou, 6/11/92, (PB93-127496, A05, MF-A01).

NCEER-92-0016 "Gravity-Load-Designed Reinforced Concrete Buildings: Seismic Evaluation of Existing Construction and Detailing Strategies for Improved Seismic Resistance," by G.W. Hoffmann, S.K. Kunnath, A.M. Reinhorn and J.B. Mander, 7/15/92, (PB94-142007, A08, MF-A02).

NCEER-92-0017 "Observations on Water System and Pipeline Performance in the Limón Area of Costa Rica Due to the April 22, 1991 Earthquake," by M. O'Rourke and D. Ballantyne, 6/30/92, (PB93-126811, A06, MF-A02).

NCEER-92-0018 "Fourth Edition of Earthquake Education Materials for Grades K-12," Edited by K.E.K. Ross, 8/10/92, (PB93-114023, A07, MF-A02).

NCEER-92-0019 "Proceedings from the Fourth Japan-U.S. Workshop on Earthquake Resistant Design of Lifeline Facilities and Countermeasures for Soil Liquefaction," Edited by M. Hamada and T.D. O'Rourke, 8/12/92, (PB93-163939, A99, MF-E11).

NCEER-92-0020 "Active Bracing System: A Full Scale Implementation of Active Control," by A.M. Reinhorn, T.T. Soong, R.C. Lin, M.A. Riley, Y.P. Wang, S. Aizawa and M. Higashino, 8/14/92, (PB93-127512, A06, MF-A02).

NCEER-92-0021 "Empirical Analysis of Horizontal Ground Displacement Generated by Liquefaction-Induced Lateral Spreads," by S.F. Bartlett and T.L. Youd, 8/17/92, (PB93-188241, A06, MF-A02).

NCEER-92-0022 "IDARC Version 3.0: Inelastic Damage Analysis of Reinforced Concrete Structures," by S.K. Kunnath, A.M. Reinhorn and R.F. Lobo, 8/31/92, (PB93-227502, A07, MF-A02).

NCEER-92-0023 "A Semi-Empirical Analysis of Strong-Motion Peaks in Terms of Seismic Source, Propagation Path and Local Site Conditions, by M. Kamiyama, M.J. O'Rourke and R. Flores-Berrones, 9/9/92, (PB93-150266, A08, MF-A02).

NCEER-92-0024 "Seismic Behavior of Reinforced Concrete Frame Structures with Nonductile Details, Part I: Summary of Experimental Findings of Full Scale Beam-Column Joint Tests," by A. Beres, R.N. White and P. Gergely, 9/30/92, (PB93-227783, A05, MF-A01).

NCEER-92-0025 "Experimental Results of Repaired and Retrofitted Beam-Column Joint Tests in Lightly Reinforced Concrete Frame Buildings," by A. Beres, S. El-Borgi, R.N. White and P. Gergely, 10/29/92, (PB93-227791, A05, MF-A01).

NCEER-92-0026 "A Generalization of Optimal Control Theory: Linear and Nonlinear Structures," by J.N. Yang, Z. Li and S. Vongchavalitkul, 11/2/92, (PB93-188621, A05, MF-A01).

NCEER-92-0027 "Seismic Resistance of Reinforced Concrete Frame Structures Designed Only for Gravity Loads: Part I - Design and Properties of a One-Third Scale Model Structure," by J.M. Bracci, A.M. Reinhorn and J.B. Mander, 12/1/92, (PB94-104502, A08, MF-A02).

NCEER-92-0028 "Seismic Resistance of Reinforced Concrete Frame Structures Designed Only for Gravity Loads: Part II - Experimental Performance of Subassemblages," by L.E. Aycardi, J.B. Mander and A.M. Reinhorn, 12/1/92, (PB94-104510, A08, MF-A02).

NCEER-92-0029 "Seismic Resistance of Reinforced Concrete Frame Structures Designed Only for Gravity Loads: Part III - Experimental Performance and Analytical Study of a Structural Model," by J.M. Bracci, A.M. Reinhorn and J.B. Mander, 12/1/92, (PB93-227528, A09, MF-A01).

NCEER-92-0030 "Evaluation of Seismic Retrofit of Reinforced Concrete Frame Structures: Part I - Experimental Performance of Retrofitted Subassemblages," by D. Choudhuri, J.B. Mander and A.M. Reinhorn, 12/8/92, (PB93-198307, A07, MF-A02).

NCEER-92-0031 "Evaluation of Seismic Retrofit of Reinforced Concrete Frame Structures: Part II - Experimental Performance and Analytical Study of a Retrofitted Structural Model," by J.M. Bracci, A.M. Reinhorn and J.B. Mander, 12/8/92, (PB93-198315, A09, MF-A03).

NCEER-92-0032 "Experimental and Analytical Investigation of Seismic Response of Structures with Supplemental Fluid Viscous Dampers," by M.C. Constantinou and M.D. Symans, 12/21/92, (PB93-191435, A10, MF-A03). This report is available only through NTIS (see address given above).

NCEER-92-0033 "Reconnaissance Report on the Cairo, Egypt Earthquake of October 12, 1992," by M. Khater, 12/23/92, (PB93-188621, A03, MF-A01).

NCEER-92-0034 "Low-Level Dynamic Characteristics of Four Tall Flat-Plate Buildings in New York City," by H. Gavin, S. Yuan, J. Grossman, E. Pekelis and K. Jacob, 12/28/92, (PB93-188217, A07, MF-A02).

NCEER-93-0001 "An Experimental Study on the Seismic Performance of Brick-Infilled Steel Frames With and Without Retrofit," by J.B. Mander, B. Nair, K. Wojtkowski and J. Ma, 1/29/93, (PB93-227510, A07, MF-A02).

NCEER-93-0002 "Social Accounting for Disaster Preparedness and Recovery Planning," by S. Cole, E. Pantoja and V. Razak, 2/22/93, (PB94-142114, A12, MF-A03).

NCEER-93-0003 "Assessment of 1991 NEHRP Provisions for Nonstructural Components and Recommended Revisions," by T.T. Soong, G. Chen, Z. Wu, R-H. Zhang and M. Grigoriu, 3/1/93, (PB93-188639, A06, MF-A02).

NCEER-93-0004 "Evaluation of Static and Response Spectrum Analysis Procedures of SEAOC/UBC for Seismic Isolated Structures," by C.W. Winters and M.C. Constantinou, 3/23/93, (PB93-198299, A10, MF-A03).

NCEER-93-0005 "Earthquakes in the Northeast - Are We Ignoring the Hazard? A Workshop on Earthquake Science and Safety for Educators," edited by K.E.K. Ross, 4/2/93, (PB94-103066, A09, MF-A02).

NCEER-93-0006 "Inelastic Response of Reinforced Concrete Structures with Viscoelastic Braces," by R.F. Lobo, J.M. Bracci, K.L. Shen, A.M. Reinhorn and T.T. Soong, 4/5/93, (PB93-227486, A05, MF-A02).

NCEER-93-0007 "Seismic Testing of Installation Methods for Computers and Data Processing Equipment," by K. Kosar, T.T. Soong, K.L. Shen, J.A. HoLung and Y.K. Lin, 4/12/93, (PB93-198299, A07, MF-A02).

NCEER-93-0008 "Retrofit of Reinforced Concrete Frames Using Added Dampers," by A. Reinhorn, M. Constantinou and C. Li, not available.

NCEER-93-0009 "Seismic Behavior and Design Guidelines for Steel Frame Structures with Added Viscoelastic Dampers," by K.C. Chang, M.L. Lai, T.T. Soong, D.S. Hao and Y.C. Yeh, 5/1/93, (PB94-141959, A07, MF-A02).

NCEER-93-0010 "Seismic Performance of Shear-Critical Reinforced Concrete Bridge Piers," by J.B. Mander, S.M. Waheed, M.T.A. Chaudhary and S.S. Chen, 5/12/93, (PB93-227494, A08, MF-A02).

NCEER-93-0011 "3D-BASIS-TABS: Computer Program for Nonlinear Dynamic Analysis of Three Dimensional Base Isolated Structures," by S. Nagarajaiah, C. Li, A.M. Reinhorn and M.C. Constantinou, 8/2/93, (PB94-141819, A09, MF-A02).

NCEER-93-0012 "Effects of Hydrocarbon Spills from an Oil Pipeline Break on Ground Water," by O.J. Helweg and H.H.M. Hwang, 8/3/93, (PB94-141942, A06, MF-A02).

NCEER-93-0013 "Simplified Procedures for Seismic Design of Nonstructural Components and Assessment of Current Code Provisions," by M.P. Singh, L.E. Suarez, E.E. Matheu and G.O. Maldonado, 8/4/93, (PB94-141827, A09, MF-A02).

NCEER-93-0014 "An Energy Approach to Seismic Analysis and Design of Secondary Systems," by G. Chen and T.T. Soong, 8/6/93, (PB94-142767, A11, MF-A03).

NCEER-93-0015 "Proceedings from School Sites: Becoming Prepared for Earthquakes - Commemorating the Third Anniversary of the Loma Prieta Earthquake," Edited by F.E. Winslow and K.E.K. Ross, 8/16/93, (PB94-154275, A16, MF-A02).

NCEER-93-0016 "Reconnaissance Report of Damage to Historic Monuments in Cairo, Egypt Following the October 12, 1992 Dahshur Earthquake," by D. Sykora, D. Look, G. Croci, E. Karaesmen and E. Karaesmen, 8/19/93, (PB94-142221, A08, MF-A02).

NCEER-93-0017 "The Island of Guam Earthquake of August 8, 1993," by S.W. Swan and S.K. Harris, 9/30/93, (PB94-141843, A04, MF-A01).

NCEER-93-0018 "Engineering Aspects of the October 12, 1992 Egyptian Earthquake," by A.W. Elgamal, M. Amer, K. Adalier and A. Abul-Fadl, 10/7/93, (PB94-141983, A05, MF-A01).

NCEER-93-0019 "Development of an Earthquake Motion Simulator and its Application in Dynamic Centrifuge Testing," by I. Krstelj, Supervised by J.H. Prevost, 10/23/93, (PB94-181773, A-10, MF-A03).

NCEER-93-0020 "NCEER-Taisei Corporation Research Program on Sliding Seismic Isolation Systems for Bridges: Experimental and Analytical Study of a Friction Pendulum System (FPS)," by M.C. Constantinou, P. Tsopelas, Y-S. Kim and S. Okamoto, 11/1/93, (PB94-142775, A08, MF-A02).

NCEER-93-0021 "Finite Element Modeling of Elastomeric Seismic Isolation Bearings," by L.J. Billings, Supervised by R. Shepherd, 11/8/93, not available.

NCEER-93-0022 "Seismic Vulnerability of Equipment in Critical Facilities: Life-Safety and Operational Consequences," by K. Porter, G.S. Johnson, M.M. Zadeh, C. Scawthorn and S. Eder, 11/24/93, (PB94-181765, A16, MF-A03).

NCEER-93-0023 "Hokkaido Nansei-oki, Japan Earthquake of July 12, 1993, by P.I. Yanev and C.R. Scawthorn, 12/23/93, (PB94-181500, A07, MF-A01).

NCEER-94-0001 "An Evaluation of Seismic Serviceability of Water Supply Networks with Application to the San Francisco Auxiliary Water Supply System," by I. Markov, Supervised by M. Grigoriu and T. O'Rourke, 1/21/94, (PB94-204013, A07, MF-A02).

NCEER-94-0002 "NCEER-Taisei Corporation Research Program on Sliding Seismic Isolation Systems for Bridges: Experimental and Analytical Study of Systems Consisting of Sliding Bearings, Rubber Restoring Force Devices and Fluid Dampers," Volumes I and II, by P. Tsopelas, S. Okamoto, M.C. Constantinou, D. Ozaki and S. Fujii, 2/4/94, (PB94-181740, A09, MF-A02 and PB94-181757, A12, MF-A03).

NCEER-94-0003 "A Markov Model for Local and Global Damage Indices in Seismic Analysis," by S. Rahman and M. Grigoriu, 2/18/94, (PB94-206000, A12, MF-A03).

NCEER-94-0004 "Proceedings from the NCEER Workshop on Seismic Response of Masonry Infills," edited by D.P. Abrams, 3/1/94, (PB94-180783, A07, MF-A02).

NCEER-94-0005 "The Northridge, California Earthquake of January 17, 1994: General Reconnaissance Report," edited by J.D. Goltz, 3/11/94, (PB94-193943, A10, MF-A03).

NCEER-94-0006 "Seismic Energy Based Fatigue Damage Analysis of Bridge Columns: Part I - Evaluation of Seismic Capacity," by G.A. Chang and J.B. Mander, 3/14/94, (PB94-219185, A11, MF-A03).

NCEER-94-0007 "Seismic Isolation of Multi-Story Frame Structures Using Spherical Sliding Isolation Systems," by T.M. Al-Hussaini, V.A. Zayas and M.C. Constantinou, 3/17/94, (PB94-193745, A09, MF-A02).

NCEER-94-0008 "The Northridge, California Earthquake of January 17, 1994: Performance of Highway Bridges," edited by I.G. Buckle, 3/24/94, (PB94-193851, A06, MF-A02).

NCEER-94-0009 "Proceedings of the Third U.S.-Japan Workshop on Earthquake Protective Systems for Bridges," edited by I.G. Buckle and I. Friedland, 3/31/94, (PB94-195815, A99, MF-A06).

NCEER-94-0010 "3D-BASIS-ME: Computer Program for Nonlinear Dynamic Analysis of Seismically Isolated Single and Multiple Structures and Liquid Storage Tanks," by P.C. Tsopelas, M.C. Constantinou and A.M. Reinhorn, 4/12/94, (PB94-204922, A09, MF-A02).

NCEER-94-0011 "The Northridge, California Earthquake of January 17, 1994: Performance of Gas Transmission Pipelines," by T.D. O'Rourke and M.C. Palmer, 5/16/94, (PB94-204989, A05, MF-A01).

NCEER-94-0012 "Feasibility Study of Replacement Procedures and Earthquake Performance Related to Gas Transmission Pipelines," by T.D. O'Rourke and M.C. Palmer, 5/25/94, (PB94-206638, A09, MF-A02).

NCEER-94-0013 "Seismic Energy Based Fatigue Damage Analysis of Bridge Columns: Part II - Evaluation of Seismic Demand," by G.A. Chang and J.B. Mander, 6/1/94, (PB95-18106, A08, MF-A02).

NCEER-94-0014 "NCEER-Taisei Corporation Research Program on Sliding Seismic Isolation Systems for Bridges: Experimental and Analytical Study of a System Consisting of Sliding Bearings and Fluid Restoring Force/Damping Devices," by P. Tsopelas and M.C. Constantinou, 6/13/94, (PB94-219144, A10, MF-A03).

NCEER-94-0015 "Generation of Hazard-Consistent Fragility Curves for Seismic Loss Estimation Studies," by H. Hwang and J-R. Huo, 6/14/94, (PB95-181996, A09, MF-A02).

NCEER-94-0016 "Seismic Study of Building Frames with Added Energy-Absorbing Devices," by W.S. Pong, C.S. Tsai and G.C. Lee, 6/20/94, (PB94-219136, A10, A03).

NCEER-94-0017 "Sliding Mode Control for Seismic-Excited Linear and Nonlinear Civil Engineering Structures," by J. Yang, J. Wu, A. Agrawal and Z. Li, 6/21/94, (PB95-138483, A06, MF-A02).

NCEER-94-0018 "3D-BASIS-TABS Version 2.0: Computer Program for Nonlinear Dynamic Analysis of Three Dimensional Base Isolated Structures," by A.M. Reinhorn, S. Nagarajaiah, M.C. Constantinou, P. Tsopelas and R. Li, 6/22/94, (PB95-182176, A08, MF-A02).

NCEER-94-0019 "Proceedings of the International Workshop on Civil Infrastructure Systems: Application of Intelligent Systems and Advanced Materials on Bridge Systems," Edited by G.C. Lee and K.C. Chang, 7/18/94, (PB95-252474, A20, MF-A04).

NCEER-94-0020 "Study of Seismic Isolation Systems for Computer Floors," by V. Lambrou and M.C. Constantinou, 7/19/94, (PB95-138533, A10, MF-A03).

NCEER-94-0021 "Proceedings of the U.S.-Italian Workshop on Guidelines for Seismic Evaluation and Rehabilitation of Unreinforced Masonry Buildings," Edited by D.P. Abrams and G.M. Calvi, 7/20/94, (PB95-138749, A13, MF-A03).

NCEER-94-0022 "NCEER-Taisei Corporation Research Program on Sliding Seismic Isolation Systems for Bridges: Experimental and Analytical Study of a System Consisting of Lubricated PTFE Sliding Bearings and Mild Steel Dampers," by P. Tsopelas and M.C. Constantinou, 7/22/94, (PB95-182184, A08, MF-A02).

NCEER-94-0023 “Development of Reliability-Based Design Criteria for Buildings Under Seismic Load,” by Y.K. Wen, H. Hwang and M. Shinozuka, 8/1/94, (PB95-211934, A08, MF-A02).

NCEER-94-0024 “Experimental Verification of Acceleration Feedback Control Strategies for an Active Tendon System,” by S.J. Dyke, B.F. Spencer, Jr., P. Quast, M.K. Sain, D.C. Kaspari, Jr. and T.T. Soong, 8/29/94, (PB95-212320, A05, MF-A01).

NCEER-94-0025 “Seismic Retrofitting Manual for Highway Bridges,” Edited by I.G. Buckle and I.F. Friedland, published by the Federal Highway Administration (PB95-212676, A15, MF-A03).

NCEER-94-0026 “Proceedings from the Fifth U.S.-Japan Workshop on Earthquake Resistant Design of Lifeline Facilities and Countermeasures Against Soil Liquefaction,” Edited by T.D. O’Rourke and M. Hamada, 11/7/94, (PB95-220802, A99, MF-E08).

NCEER-95-0001 “Experimental and Analytical Investigation of Seismic Retrofit of Structures with Supplemental Damping: Part 1 - Fluid Viscous Damping Devices,” by A.M. Reinhorn, C. Li and M.C. Constantinou, 1/3/95, (PB95-266599, A09, MF-A02).

NCEER-95-0002 “Experimental and Analytical Study of Low-Cycle Fatigue Behavior of Semi-Rigid Top-And-Seat Angle Connections,” by G. Pekcan, J.B. Mander and S.S. Chen, 1/5/95, (PB95-220042, A07, MF-A02).

NCEER-95-0003 “NCEER-ATC Joint Study on Fragility of Buildings,” by T. Anagnos, C. Rojahn and A.S. Kiremidjian, 1/20/95, (PB95-220026, A06, MF-A02).

NCEER-95-0004 “Nonlinear Control Algorithms for Peak Response Reduction,” by Z. Wu, T.T. Soong, V. Gattulli and R.C. Lin, 2/16/95, (PB95-220349, A05, MF-A01).

NCEER-95-0005 “Pipeline Replacement Feasibility Study: A Methodology for Minimizing Seismic and Corrosion Risks to Underground Natural Gas Pipelines,” by R.T. Eguchi, H.A. Seligson and D.G. Honegger, 3/2/95, (PB95-252326, A06, MF-A02).

NCEER-95-0006 “Evaluation of Seismic Performance of an 11-Story Frame Building During the 1994 Northridge Earthquake,” by F. Naeim, R. DiSulio, K. Benuska, A. Reinhorn and C. Li, not available.

NCEER-95-0007 “Prioritization of Bridges for Seismic Retrofitting,” by N. Basöz and A.S. Kiremidjian, 4/24/95, (PB95-252300, A08, MF-A02).

NCEER-95-0008 "Method for Developing Motion Damage Relationships for Reinforced Concrete Frames," by A. Singhal and A.S. Kiremidjian, 5/11/95, (PB95-266607, A06, MF-A02).

NCEER-95-0009 "Experimental and Analytical Investigation of Seismic Retrofit of Structures with Supplemental Damping: Part II - Friction Devices," by C. Li and A.M. Reinhorn, 7/6/95, (PB96-128087, A11, MF-A03).

NCEER-95-0010 "Experimental Performance and Analytical Study of a Non-Ductile Reinforced Concrete Frame Structure Retrofitted with Elastomeric Spring Dampers," by G. Pekcan, J.B. Mander and S.S. Chen, 7/14/95, (PB96-137161, A08, MF-A02).

NCEER-95-0011 "Development and Experimental Study of Semi-Active Fluid Damping Devices for Seismic Protection of Structures," by M.D. Symans and M.C. Constantinou, 8/3/95, (PB96-136940, A23, MF-A04).

NCEER-95-0012 "Real-Time Structural Parameter Modification (RSPM): Development of Innervated Structures," by Z. Liang, M. Tong and G.C. Lee, 4/11/95, (PB96-137153, A06, MF-A01).

NCEER-95-0013 "Experimental and Analytical Investigation of Seismic Retrofit of Structures with Supplemental Damping: Part III - Viscous Damping Walls," by A.M. Reinhorn and C. Li, 10/1/95, (PB96-176409, A11, MF-A03).

NCEER-95-0014 "Seismic Fragility Analysis of Equipment and Structures in a Memphis Electric Substation," by J-R. Huo and H.H.M. Hwang, 8/10/95, (PB96-128087, A09, MF-A02).

NCEER-95-0015 "The Hanshin-Awaji Earthquake of January 17, 1995: Performance of Lifelines," Edited by M. Shinozuka, 11/3/95, (PB96-176383, A15, MF-A03).

NCEER-95-0016 "Highway Culvert Performance During Earthquakes," by T.L. Youd and C.J. Beckman, available as NCEER-96-0015.

NCEER-95-0017 "The Hanshin-Awaji Earthquake of January 17, 1995: Performance of Highway Bridges," Edited by I.G. Buckle, 12/1/95, not available.

NCEER-95-0018 "Modeling of Masonry Infill Panels for Structural Analysis," by A.M. Reinhorn, A. Madan, R.E. Valles, Y. Reichmann and J.B. Mander, 12/8/95, (PB97-110886, MF-A01, A06).

NCEER-95-0019 "Optimal Polynomial Control for Linear and Nonlinear Structures," by A.K. Agrawal and J.N. Yang, 12/11/95, (PB96-168737, A07, MF-A02).

NCEER-95-0020 "Retrofit of Non-Ductile Reinforced Concrete Frames Using Friction Dampers," by R.S. Rao, P. Gergely and R.N. White, 12/22/95, (PB97-133508, A10, MF-A02).

NCEER-95-0021 "Parametric Results for Seismic Response of Pile-Supported Bridge Bents," by G. Mylonakis, A. Nikolaou and G. Gazetas, 12/22/95, (PB97-100242, A12, MF-A03).

NCEER-95-0022 "Kinematic Bending Moments in Seismically Stressed Piles," by A. Nikolaou, G. Mylonakis and G. Gazetas, 12/23/95, (PB97-113914, MF-A03, A13).

NCEER-96-0001 "Dynamic Response of Unreinforced Masonry Buildings with Flexible Diaphragms," by A.C. Costley and D.P. Abrams," 10/10/96, (PB97-133573, MF-A03, A15).

NCEER-96-0002 "State of the Art Review: Foundations and Retaining Structures," by I. Po Lam, not available.

NCEER-96-0003 "Ductility of Rectangular Reinforced Concrete Bridge Columns with Moderate Confinement," by N. Wehbe, M. Saiidi, D. Sanders and B. Douglas, 11/7/96, (PB97-133557, A06, MF-A02).

NCEER-96-0004 "Proceedings of the Long-Span Bridge Seismic Research Workshop," edited by I.G. Buckle and I.M. Friedland, not available.

NCEER-96-0005 "Establish Representative Pier Types for Comprehensive Study: Eastern United States," by J. Kulicki and Z. Prucz, 5/28/96, (PB98-119217, A07, MF-A02).

NCEER-96-0006 "Establish Representative Pier Types for Comprehensive Study: Western United States," by R. Imbsen, R.A. Schamber and T.A. Osterkamp, 5/28/96, (PB98-118607, A07, MF-A02).

NCEER-96-0007 "Nonlinear Control Techniques for Dynamical Systems with Uncertain Parameters," by R.G. Ghanem and M.I. Bujakov, 5/27/96, (PB97-100259, A17, MF-A03).

NCEER-96-0008 "Seismic Evaluation of a 30-Year Old Non-Ductile Highway Bridge Pier and Its Retrofit," by J.B. Mander, B. Mahmoodzadegan, S. Bhadra and S.S. Chen, 5/31/96, (PB97-110902, MF-A03, A10).

NCEER-96-0009 "Seismic Performance of a Model Reinforced Concrete Bridge Pier Before and After Retrofit," by J.B. Mander, J.H. Kim and C.A. Ligozio, 5/31/96, (PB97-110910, MF-A02, A10).

NCEER-96-0010 "IDARC2D Version 4.0: A Computer Program for the Inelastic Damage Analysis of Buildings," by R.E. Valles, A.M. Reinhorn, S.K. Kunnath, C. Li and A. Madan, 6/3/96, (PB97-100234, A17, MF-A03).

NCEER-96-0011 "Estimation of the Economic Impact of Multiple Lifeline Disruption: Memphis Light, Gas and Water Division Case Study," by S.E. Chang, H.A. Seligson and R.T. Eguchi, 8/16/96, (PB97-133490, A11, MF-A03).

NCEER-96-0012 "Proceedings from the Sixth Japan-U.S. Workshop on Earthquake Resistant Design of Lifeline Facilities and Countermeasures Against Soil Liquefaction, Edited by M. Hamada and T. O'Rourke, 9/11/96, (PB97-133581, A99, MF-A06).

NCEER-96-0013 "Chemical Hazards, Mitigation and Preparedness in Areas of High Seismic Risk: A Methodology for Estimating the Risk of Post-Earthquake Hazardous Materials Release," by H.A. Seligson, R.T. Eguchi, K.J. Tierney and K. Richmond, 11/7/96, (PB97-133565, MF-A02, A08).

NCEER-96-0014 "Response of Steel Bridge Bearings to Reversed Cyclic Loading," by J.B. Mander, D-K. Kim, S.S. Chen and G.J. Premus, 11/13/96, (PB97-140735, A12, MF-A03).

NCEER-96-0015 "Highway Culvert Performance During Past Earthquakes," by T.L. Youd and C.J. Beckman, 11/25/96, (PB97-133532, A06, MF-A01).

NCEER-97-0001 "Evaluation, Prevention and Mitigation of Pounding Effects in Building Structures," by R.E. Valles and A.M. Reinhorn, 2/20/97, (PB97-159552, A14, MF-A03).

NCEER-97-0002 "Seismic Design Criteria for Bridges and Other Highway Structures," by C. Rojahn, R. Mayes, D.G. Anderson, J. Clark, J.H. Hom, R.V. Nutt and M.J. O'Rourke, 4/30/97, (PB97-194658, A06, MF-A03).

NCEER-97-0003 "Proceedings of the U.S.-Italian Workshop on Seismic Evaluation and Retrofit," Edited by D.P. Abrams and G.M. Calvi, 3/19/97, (PB97-194666, A13, MF-A03).

NCEER-97-0004 "Investigation of Seismic Response of Buildings with Linear and Nonlinear Fluid Viscous Dampers," by A.A. Seleemah and M.C. Constantinou, 5/21/97, (PB98-109002, A15, MF-A03).

NCEER-97-0005 "Proceedings of the Workshop on Earthquake Engineering Frontiers in Transportation Facilities," edited by G.C. Lee and I.M. Friedland, 8/29/97, (PB98-128911, A25, MR-A04).

NCEER-97-0006 "Cumulative Seismic Damage of Reinforced Concrete Bridge Piers," by S.K. Kunnath, A. El-Bahy, A. Taylor and W. Stone, 9/2/97, (PB98-108814, A11, MF-A03).

NCEER-97-0007 "Structural Details to Accommodate Seismic Movements of Highway Bridges and Retaining Walls," by R.A. Imbsen, R.A. Schamber, E. Thorkildsen, A. Kartoum, B.T. Martin, T.N. Rosser and J.M. Kulicki, 9/3/97, (PB98-108996, A09, MF-A02).

NCEER-97-0008 "A Method for Earthquake Motion-Damage Relationships with Application to Reinforced Concrete Frames," by A. Singhal and A.S. Kiremidjian, 9/10/97, (PB98-108988, A13, MF-A03).

NCEER-97-0009 "Seismic Analysis and Design of Bridge Abutments Considering Sliding and Rotation," by K. Fishman and R. Richards, Jr., 9/15/97, (PB98-108897, A06, MF-A02).

NCEER-97-0010 "Proceedings of the FHWA/NCEER Workshop on the National Representation of Seismic Ground Motion for New and Existing Highway Facilities," edited by I.M. Friedland, M.S. Power and R.L. Mayes, 9/22/97, (PB98-128903, A21, MF-A04).

NCEER-97-0011 "Seismic Analysis for Design or Retrofit of Gravity Bridge Abutments," by K.L. Fishman, R. Richards, Jr. and R.C. Divito, 10/2/97, (PB98-128937, A08, MF-A02).

NCEER-97-0012 "Evaluation of Simplified Methods of Analysis for Yielding Structures," by P. Tsopelas, M.C. Constantinou, C.A. Kircher and A.S. Whittaker, 10/31/97, (PB98-128929, A10, MF-A03).

NCEER-97-0013 "Seismic Design of Bridge Columns Based on Control and Repairability of Damage," by C-T. Cheng and J.B. Mander, 12/8/97, (PB98-144249, A11, MF-A03).

NCEER-97-0014 "Seismic Resistance of Bridge Piers Based on Damage Avoidance Design," by J.B. Mander and C-T. Cheng, 12/10/97, (PB98-144223, A09, MF-A02).

NCEER-97-0015 “Seismic Response of Nominally Symmetric Systems with Strength Uncertainty,” by S. Balopoulou and M. Grigoriu, 12/23/97, (PB98-153422, A11, MF-A03).

NCEER-97-0016 “Evaluation of Seismic Retrofit Methods for Reinforced Concrete Bridge Columns,” by T.J. Wipf, F.W. Klaiber and F.M. Russo, 12/28/97, (PB98-144215, A12, MF-A03).

NCEER-97-0017 “Seismic Fragility of Existing Conventional Reinforced Concrete Highway Bridges,” by C.L. Mullen and A.S. Cakmak, 12/30/97, (PB98-153406, A08, MF-A02).

NCEER-97-0018 “Loss Asssessment of Memphis Buildings,” edited by D.P. Abrams and M. Shinozuka, 12/31/97, (PB98-144231, A13, MF-A03).

NCEER-97-0019 “Seismic Evaluation of Frames with Infill Walls Using Quasi-static Experiments,” by K.M. Mosalam, R.N. White and P. Gergely, 12/31/97, (PB98-153455, A07, MF-A02).

NCEER-97-0020 “Seismic Evaluation of Frames with Infill Walls Using Pseudo-dynamic Experiments,” by K.M. Mosalam, R.N. White and P. Gergely, 12/31/97, (PB98-153430, A07, MF-A02).

NCEER-97-0021 “Computational Strategies for Frames with Infill Walls: Discrete and Smeared Crack Analyses and Seismic Fragility,” by K.M. Mosalam, R.N. White and P. Gergely, 12/31/97, (PB98-153414, A10, MF-A02).

NCEER-97-0022 “Proceedings of the NCEER Workshop on Evaluation of Liquefaction Resistance of Soils,” edited by T.L. Youd and I.M. Idriss, 12/31/97, (PB98-155617, A15, MF-A03).

MCEER-98-0001 “Extraction of Nonlinear Hysteretic Properties of Seismically Isolated Bridges from Quick-Release Field Tests,” by Q. Chen, B.M. Douglas, E.M. Maragakis and I.G. Buckle, 5/26/98, (PB99-118838, A06, MF-A01).

MCEER-98-0002 “Methodologies for Evaluating the Importance of Highway Bridges,” by A. Thomas, S. Eshenaur and J. Kulicki, 5/29/98, (PB99-118846, A10, MF-A02).

MCEER-98-0003 “Capacity Design of Bridge Piers and the Analysis of Overstrength,” by J.B. Mander, A. Dutta and P. Goel, 6/1/98, (PB99-118853, A09, MF-A02).

MCEER-98-0004 “Evaluation of Bridge Damage Data from the Loma Prieta and Northridge, California Earthquakes,” by N. Basoz and A. Kiremidjian, 6/2/98, (PB99-118861, A15, MF-A03).

MCEER-98-0005 “Screening Guide for Rapid Assessment of Liquefaction Hazard at Highway Bridge Sites,” by T. L. Youd, 6/16/98, (PB99-118879, A06, not available on microfiche).

MCEER-98-0006 “Structural Steel and Steel/Concrete Interface Details for Bridges,” by P. Ritchie, N. Kauhl and J. Kulicki, 7/13/98, (PB99-118945, A06, MF-A01).

MCEER-98-0007 “Capacity Design and Fatigue Analysis of Confined Concrete Columns,” by A. Dutta and J.B. Mander, 7/14/98, (PB99-118960, A14, MF-A03).

MCEER-98-0008 “Proceedings of the Workshop on Performance Criteria for Telecommunication Services Under Earthquake Conditions,” edited by A.J. Schiff, 7/15/98, (PB99-118952, A08, MF-A02).

MCEER-98-0009 “Fatigue Analysis of Unconfined Concrete Columns,” by J.B. Mander, A. Dutta and J.H. Kim, 9/12/98, (PB99-123655, A10, MF-A02).

MCEER-98-0010 “Centrifuge Modeling of Cyclic Lateral Response of Pile-Cap Systems and Seat-Type Abutments in Dry Sands,” by A.D. Gadre and R. Dobry, 10/2/98, (PB99-123606, A13, MF-A03).

MCEER-98-0011 “IDARC-BRIDGE: A Computational Platform for Seismic Damage Assessment of Bridge Structures,” by A.M. Reinhorn, V. Simeonov, G. Mylonakis and Y. Reichman, 10/2/98, (PB99-162919, A15, MF-A03).

MCEER-98-0012 “Experimental Investigation of the Dynamic Response of Two Bridges Before and After Retrofitting with Elastomeric Bearings,” by D.A. Wendichansky, S.S. Chen and J.B. Mander, 10/2/98, (PB99-162927, A15, MF-A03).

MCEER-98-0013 “Design Procedures for Hinge Restrainers and Hinge Sear Width for Multiple-Frame Bridges,” by R. Des Roches and G.L. Fenves, 11/3/98, (PB99-140477, A13, MF-A03).

MCEER-98-0014 “Response Modification Factors for Seismically Isolated Bridges,” by M.C. Constantinou and J.K. Quarshie, 11/3/98, (PB99-140485, A14, MF-A03).

MCEER-98-0015 “Proceedings of the U.S.-Italy Workshop on Seismic Protective Systems for Bridges,” edited by I.M. Friedland and M.C. Constantinou, 11/3/98, (PB2000-101711, A22, MF-A04).

MCEER-98-0016 “Appropriate Seismic Reliability for Critical Equipment Systems: Recommendations Based on Regional Analysis of Financial and Life Loss,” by K. Porter, C. Scawthorn, C. Taylor and N. Blais, 11/10/98, (PB99-157265, A08, MF-A02).

MCEER-98-0017 “Proceedings of the U.S. Japan Joint Seminar on Civil Infrastructure Systems Research,” edited by M. Shinozuka and A. Rose, 11/12/98, (PB99-156713, A16, MF-A03).

MCEER-98-0018 “Modeling of Pile Footings and Drilled Shafts for Seismic Design,” by I. PoLam, M. Kapuskar and D. Chaudhuri, 12/21/98, (PB99-157257, A09, MF-A02).

MCEER-99-0001 "Seismic Evaluation of a Masonry Infilled Reinforced Concrete Frame by Pseudodynamic Testing," by S.G. Buonopane and R.N. White, 2/16/99, (PB99-162851, A09, MF-A02).

MCEER-99-0002 "Response History Analysis of Structures with Seismic Isolation and Energy Dissipation Systems: Verification Examples for Program SAP2000," by J. Scheller and M.C. Constantinou, 2/22/99, (PB99-162869, A08, MF-A02).

MCEER-99-0003 "Experimental Study on the Seismic Design and Retrofit of Bridge Columns Including Axial Load Effects," by A. Dutta, T. Kokorina and J.B. Mander, 2/22/99, (PB99-162877, A09, MF-A02).

MCEER-99-0004 "Experimental Study of Bridge Elastomeric and Other Isolation and Energy Dissipation Systems with Emphasis on Uplift Prevention and High Velocity Near-source Seismic Excitation," by A. Kasalanati and M. C. Constantinou, 2/26/99, (PB99-162885, A12, MF-A03).

MCEER-99-0005 "Truss Modeling of Reinforced Concrete Shear-flexure Behavior," by J.H. Kim and J.B. Mander, 3/8/99, (PB99-163693, A12, MF-A03).

MCEER-99-0006 "Experimental Investigation and Computational Modeling of Seismic Response of a 1:4 Scale Model Steel Structure with a Load Balancing Supplemental Damping System," by G. Pekcan, J.B. Mander and S.S. Chen, 4/2/99, (PB99-162893, A11, MF-A03).

MCEER-99-0007 "Effect of Vertical Ground Motions on the Structural Response of Highway Bridges," by M.R. Button, C.J. Cronin and R.L. Mayes, 4/10/99, (PB2000-101411, A10, MF-A03).

MCEER-99-0008 "Seismic Reliability Assessment of Critical Facilities: A Handbook, Supporting Documentation, and Model Code Provisions," by G.S. Johnson, R.E. Sheppard, M.D. Quilici, S.J. Eder and C.R. Scawthorn, 4/12/99, (PB2000-101701, A18, MF-A04).

MCEER-99-0009 "Impact Assessment of Selected MCEER Highway Project Research on the Seismic Design of Highway Structures," by C. Rojahn, R. Mayes, D.G. Anderson, J.H. Clark, D'Appolonia Engineering, S. Gloyd and R.V. Nutt, 4/14/99, (PB99-162901, A10, MF-A02).

MCEER-99-0010 "Site Factors and Site Categories in Seismic Codes," by R. Dobry, R. Ramos and M.S. Power, 7/19/99, (PB2000-101705, A08, MF-A02).

MCEER-99-0011 "Restrainer Design Procedures for Multi-Span Simply-Supported Bridges," by M.J. Randall, M. Saiidi, E. Maragakis and T. Isakovic, 7/20/99, (PB2000-101702, A10, MF-A02).

MCEER-99-0012 "Property Modification Factors for Seismic Isolation Bearings," by M.C. Constantinou, P. Tsopelas, A. Kasalanati and E. Wolff, 7/20/99, (PB2000-103387, A11, MF-A03).

MCEER-99-0013 "Critical Seismic Issues for Existing Steel Bridges," by P. Ritchie, N. Kauhl and J. Kulicki, 7/20/99, (PB2000-101697, A09, MF-A02).

MCEER-99-0014 "Nonstructural Damage Database," by A. Kao, T.T. Soong and A. Vender, 7/24/99, (PB2000-101407, A06, MF-A01).

MCEER-99-0015 "Guide to Remedial Measures for Liquefaction Mitigation at Existing Highway Bridge Sites," by H.G. Cooke and J. K. Mitchell, 7/26/99, (PB2000-101703, A11, MF-A03).

MCEER-99-0016 "Proceedings of the MCEER Workshop on Ground Motion Methodologies for the Eastern United States," edited by N. Abrahamson and A. Becker, 8/11/99, (PB2000-103385, A07, MF-A02).

MCEER-99-0017 "Quindío, Colombia Earthquake of January 25, 1999: Reconnaissance Report," by A.P. Asfura and P.J. Flores, 10/4/99, (PB2000-106893, A06, MF-A01).

MCEER-99-0018 "Hysteretic Models for Cyclic Behavior of Deteriorating Inelastic Structures," by M.V. Sivaselvan and A.M. Reinhorn, 11/5/99, (PB2000-103386, A08, MF-A02).

MCEER-99-0019 "Proceedings of the 7th U.S.- Japan Workshop on Earthquake Resistant Design of Lifeline Facilities and Countermeasures Against Soil Liquefaction," edited by T.D. O'Rourke, J.P. Bardet and M. Hamada, 11/19/99, (PB2000-103354, A99, MF-A06).

MCEER-99-0020 "Development of Measurement Capability for Micro-Vibration Evaluations with Application to Chip Fabrication Facilities," by G.C. Lee, Z. Liang, J.W. Song, J.D. Shen and W.C. Liu, 12/1/99, (PB2000-105993, A08, MF-A02).

MCEER-99-0021 "Design and Retrofit Methodology for Building Structures with Supplemental Energy Dissipating Systems," by G. Pekcan, J.B. Mander and S.S. Chen, 12/31/99, (PB2000-105994, A11, MF-A03).

MCEER-00-0001 "The Marmara, Turkey Earthquake of August 17, 1999: Reconnaissance Report," edited by C. Scawthorn; with major contributions by M. Bruneau, R. Eguchi, T. Holzer, G. Johnson, J. Mander, J. Mitchell, W. Mitchell, A. Papageorgiou, C. Scaethorn, and G. Webb, 3/23/00, (PB2000-106200, A11, MF-A03).

MCEER-00-0002 "Proceedings of the MCEER Workshop for Seismic Hazard Mitigation of Health Care Facilities," edited by G.C. Lee, M. Ettouney, M. Grigoriu, J. Hauer and J. Nigg, 3/29/00, (PB2000-106892, A08, MF-A02).

MCEER-00-0003 "The Chi-Chi, Taiwan Earthquake of September 21, 1999: Reconnaissance Report," edited by G.C. Lee and C.H. Loh, with major contributions by G.C. Lee, M. Bruneau, I.G. Buckle, S.E. Chang, P.J. Flores, T.D. O'Rourke, M. Shinozuka, T.T. Soong, C-H. Loh, K-C. Chang, Z-J. Chen, J-S. Hwang, M-L. Lin, G-Y. Liu, K-C. Tsai, G.C. Yao and C-L. Yen, 4/30/00, (PB2001-100980, A10, MF-A02).

MCEER-00-0004 "Seismic Retrofit of End-Sway Frames of Steel Deck-Truss Bridges with a Supplemental Tendon System: Experimental and Analytical Investigation," by G. Pekcan, J.B. Mander and S.S. Chen, 7/1/00, (PB2001-100982, A10, MF-A02).

MCEER-00-0005 "Sliding Fragility of Unrestrained Equipment in Critical Facilities," by W.H. Chong and T.T. Soong, 7/5/00, (PB2001-100983, A08, MF-A02).

MCEER-00-0006 "Seismic Response of Reinforced Concrete Bridge Pier Walls in the Weak Direction," by N. Abo-Shadi, M. Saiidi and D. Sanders, 7/17/00, (PB2001-100981, A17, MF-A03).

MCEER-00-0007 "Low-Cycle Fatigue Behavior of Longitudinal Reinforcement in Reinforced Concrete Bridge Columns," by J. Brown and S.K. Kunnath, 7/23/00, (PB2001-104392, A08, MF-A02).

MCEER-00-0008 "Soil Structure Interaction of Bridges for Seismic Analysis," I. PoLam and H. Law, 9/25/00, (PB2001-105397, A08, MF-A02).

MCEER-00-0009 "Proceedings of the First MCEER Workshop on Mitigation of Earthquake Disaster by Advanced Technologies (MEDAT-1), edited by M. Shinozuka, D.J. Inman and T.D. O'Rourke, 11/10/00, (PB2001-105399, A14, MF-A03).

MCEER-00-0010 "Development and Evaluation of Simplified Procedures for Analysis and Design of Buildings with Passive Energy Dissipation Systems, Revision 01," by O.M. Ramirez, M.C. Constantinou, C.A. Kircher, A.S. Whittaker, M.W. Johnson, J.D. Gomez and C. Chrysostomou, 11/16/01, (PB2001-105523, A23, MF-A04).

MCEER-00-0011 "Dynamic Soil-Foundation-Structure Interaction Analyses of Large Caissons," by C-Y. Chang, C-M. Mok, Z-L. Wang, R. Settgast, F. Waggoner, M.A. Ketchum, H.M. Gonnermann and C-C. Chin, 12/30/00, (PB2001-104373, A07, MF-A02).

MCEER-00-0012 "Experimental Evaluation of Seismic Performance of Bridge Restrainers," by A.G. Vlassis, E.M. Maragakis and M. Saiid Saiidi, 12/30/00, (PB2001-104354, A09, MF-A02).

MCEER-00-0013 "Effect of Spatial Variation of Ground Motion on Highway Structures," by M. Shinozuka, V. Saxena and G. Deodatis, 12/31/00, (PB2001-108755, A13, MF-A03).

MCEER-00-0014 "A Risk-Based Methodology for Assessing the Seismic Performance of Highway Systems," by S.D. Werner, C.E. Taylor, J.E. Moore, II, J.S. Walton and S. Cho, 12/31/00, (PB2001-108756, A14, MF-A03).

MCEER-01-0001 “Experimental Investigation of P-Delta Effects to Collapse During Earthquakes,” by D. Vian and M. Bruneau, 6/25/01, (PB2002-100534, A17, MF-A03).

MCEER-01-0002 “Proceedings of the Second MCEER Workshop on Mitigation of Earthquake Disaster by Advanced Technologies (MEDAT-2),” edited by M. Bruneau and D.J. Inman, 7/23/01, (PB2002-100434, A16, MF-A03).

MCEER-01-0003 “Sensitivity Analysis of Dynamic Systems Subjected to Seismic Loads,” by C. Roth and M. Grigoriu, 9/18/01, (PB2003-100884, A12, MF-A03).

MCEER-01-0004 “Overcoming Obstacles to Implementing Earthquake Hazard Mitigation Policies: Stage 1 Report,” by D.J. Alesch and W.J. Petak, 12/17/01, (PB2002-107949, A07, MF-A02).

MCEER-01-0005 “Updating Real-Time Earthquake Loss Estimates: Methods, Problems and Insights,” by C.E. Taylor, S.E. Chang and R.T. Eguchi, 12/17/01, (PB2002-107948, A05, MF-A01).

MCEER-01-0006 “Experimental Investigation and Retrofit of Steel Pile Foundations and Pile Bents Under Cyclic Lateral Loadings,” by A. Shama, J. Mander, B. Blabac and S. Chen, 12/31/01, (PB2002-107950, A13, MF-A03).

MCEER-02-0001 “Assessment of Performance of Bolu Viaduct in the 1999 Duzce Earthquake in Turkey” by P.C. Roussis, M.C. Constantinou, M. Erdik, E. Durukal and M. Dicleli, 5/8/02, (PB2003-100883, A08, MF-A02).

MCEER-02-0002 “Seismic Behavior of Rail Counterweight Systems of Elevators in Buildings,” by M.P. Singh, Rildova and L.E. Suarez, 5/27/02. (PB2003-100882, A11, MF-A03).

MCEER-02-0003 “Development of Analysis and Design Procedures for Spread Footings,” by G. Mylonakis, G. Gazetas, S. Nikolaou and A. Chauncey, 10/02/02, (PB2004-101636, A13, MF-A03, CD-A13).

MCEER-02-0004 “Bare-Earth Algorithms for Use with SAR and LIDAR Digital Elevation Models,” by C.K. Huyck, R.T. Eguchi and B. Houshmand, 10/16/02, (PB2004-101637, A07, CD-A07).

MCEER-02-0005 "Review of Energy Dissipation of Compression Members in Concentrically Braced Frames," by K.Lee and M. Bruneau, 10/18/02, (PB2004-101638, A10, CD-A10).

MCEER-03-0001 "Experimental Investigation of Light-Gauge Steel Plate Shear Walls for the Seismic Retrofit of Buildings" by J. Berman and M. Bruneau, 5/2/03, (PB2004-101622, A10, MF-A03, CD-A10).

MCEER-03-0002 "Statistical Analysis of Fragility Curves," by M. Shinozuka, M.Q. Feng, H. Kim, T. Uzawa and T. Ueda, 6/16/03, (PB2004-101849, A09, CD-A09).

MCEER-03-0003 "Proceedings of the Eighth U.S.-Japan Workshop on Earthquake Resistant Design f Lifeline Facilities and Countermeasures Against Liquefaction," edited by M. Hamada, J.P. Bardet and T.D. O'Rourke, 6/30/03, (PB2004-104386, A99, CD-A99).

MCEER-03-0004 "Proceedings of the PRC-US Workshop on Seismic Analysis and Design of Special Bridges," edited by L.C. Fan and G.C. Lee, 7/15/03, (PB2004-104387, A14, CD-A14).

MCEER-03-0005 "Urban Disaster Recovery: A Framework and Simulation Model," by S.B. Miles and S.E. Chang, 7/25/03, (PB2004-104388, A07, CD-A07).

MCEER-03-0006 "Behavior of Underground Piping Joints Due to Static and Dynamic Loading," by R.D. Meis, M. Maragakis and R. Siddharthan, 11/17/03, (PB2005-102194, A13, MF-A03, CD-A00).

MCEER-04-0001 "Experimental Study of Seismic Isolation Systems with Emphasis on Secondary System Response and Verification of Accuracy of Dynamic Response History Analysis Methods," by E. Wolff and M. Constantinou, 1/16/04 (PB2005-102195, A99, MF-E08, CD-A00).

MCEER-04-0002 "Tension, Compression and Cyclic Testing of Engineered Cementitious Composite Materials," by K. Kesner and S.L. Billington, 3/1/04, (PB2005-102196, A08, CD-A08).

MCEER-04-0003 "Cyclic Testing of Braces Laterally Restrained by Steel Studs to Enhance Performance During Earthquakes," by O.C. Celik, J.W. Berman and M. Bruneau, 3/16/04, (PB2005-102197, A13, MF-A03, CD-A00).

MCEER-04-0004 "Methodologies for Post Earthquake Building Damage Detection Using SAR and Optical Remote Sensing: Application to the August 17, 1999 Marmara, Turkey Earthquake," by C.K. Huyck, B.J. Adams, S. Cho, R.T. Eguchi, B. Mansouri and B. Houshmand, 6/15/04, (PB2005-104888, A10, CD-A00).

MCEER-04-0005 "Nonlinear Structural Analysis Towards Collapse Simulation: A Dynamical Systems Approach," by M.V. Sivaselvan and A.M. Reinhorn, 6/16/04, (PB2005-104889, A11, MF-A03, CD-A00).

MCEER-04-0006 "Proceedings of the Second PRC-US Workshop on Seismic Analysis and Design of Special Bridges," edited by G.C. Lee and L.C. Fan, 6/25/04, (PB2005-104890, A16, CD-A00).

MCEER-04-0007 "Seismic Vulnerability Evaluation of Axially Loaded Steel Built-up Laced Members," by K. Lee and M. Bruneau, 6/30/04, (PB2005-104891, A16, CD-A00).

MCEER-04-0008 "Evaluation of Accuracy of Simplified Methods of Analysis and Design of Buildings with Damping Systems for Near-Fault and for Soft-Soil Seismic Motions," by E.A. Pavlou and M.C. Constantinou, 8/16/04, (PB2005-104892, A08, MF-A02, CD-A00).

MCEER-04-0009 "Assessment of Geotechnical Issues in Acute Care Facilities in California," by M. Lew, T.D. O'Rourke, R. Dobry and M. Koch, 9/15/04, (PB2005-104893, A08, CD-A00).

MCEER-04-0010 "Scissor-Jack-Damper Energy Dissipation System," by A.N. Sigaher-Boyle and M.C. Constantinou, 12/1/04 (PB2005-108221).

MCEER-04-0011 "Seismic Retrofit of Bridge Steel Truss Piers Using a Controlled Rocking Approach," by M. Pollino and M. Bruneau, 12/20/04 (PB2006-105795).

MCEER-05-0001 "Experimental and Analytical Studies of Structures Seismically Isolated with an Uplift-Restraint Isolation System," by P.C. Roussis and M.C. Constantinou, 1/10/05 (PB2005-108222).

MCEER-05-0002 "A Versatile Experimentation Model for Study of Structures Near Collapse Applied to Seismic Evaluation of Irregular Structures," by D. Kusumastuti, A.M. Reinhorn and A. Rutenberg, 3/31/05 (PB2006-101523).

MCEER-05-0003 "Proceedings of the Third PRC-US Workshop on Seismic Analysis and Design of Special Bridges," edited by L.C. Fan and G.C. Lee, 4/20/05, (PB2006-105796).

MCEER-05-0004 "Approaches for the Seismic Retrofit of Braced Steel Bridge Piers and Proof-of-Concept Testing of an Eccentrically Braced Frame with Tubular Link," by J.W. Berman and M. Bruneau, 4/21/05 (PB2006-101524).

MCEER-05-0005 "Simulation of Strong Ground Motions for Seismic Fragility Evaluation of Nonstructural Components in Hospitals," by A. Wanitkorkul and A. Filiatrault, 5/26/05 (PB2006-500027).

MCEER-05-0006 "Seismic Safety in California Hospitals: Assessing an Attempt to Accelerate the Replacement or Seismic Retrofit of Older Hospital Facilities," by D.J. Alesch, L.A. Arendt and W.J. Petak, 6/6/05 (PB2006-105794).

MCEER-05-0007 "Development of Seismic Strengthening and Retrofit Strategies for Critical Facilities Using Engineered Cementitious Composite Materials," by K. Kesner and S.L. Billington, 8/29/05 (PB2006-111701).

MCEER-05-0008 "Experimental and Analytical Studies of Base Isolation Systems for Seismic Protection of Power Transformers," by N. Murota, M.Q. Feng and G-Y. Liu, 9/30/05 (PB2006-111702).

MCEER-05-0009 "3D-BASIS-ME-MB: Computer Program for Nonlinear Dynamic Analysis of Seismically Isolated Structures," by P.C. Tsopelas, P.C. Roussis, M.C. Constantinou, R. Buchanan and A.M. Reinhorn, 10/3/05 (PB2006-111703).

MCEER-05-0010 "Steel Plate Shear Walls for Seismic Design and Retrofit of Building Structures," by D. Vian and M. Bruneau, 12/15/05 (PB2006-111704).

MCEER-05-0011 "The Performance-Based Design Paradigm," by M.J. Astrella and A. Whittaker, 12/15/05 (PB2006-111705).

MCEER-06-0001 "Seismic Fragility of Suspended Ceiling Systems," H. Badillo-Almaraz, A.S. Whittaker, A.M. Reinhorn and G.P. Cimellaro, 2/4/06 (PB2006-111706).

MCEER-06-0002 "Multi-Dimensional Fragility of Structures," by G.P. Cimellaro, A.M. Reinhorn and M. Bruneau, 3/1/06 (PB2007-106974, A09, MF-A02, CD A00).

MCEER-06-0003 "Built-Up Shear Links as Energy Dissipators for Seismic Protection of Bridges," by P. Dusicka, A.M. Itani and I.G. Buckle, 3/15/06 (PB2006-111708).

MCEER-06-0004 "Analytical Investigation of the Structural Fuse Concept," by R.E. Vargas and M. Bruneau, 3/16/06 (PB2006-111709).

MCEER-06-0005 "Experimental Investigation of the Structural Fuse Concept," by R.E. Vargas and M. Bruneau, 3/17/06 (PB2006-111710).

MCEER-06-0006 "Further Development of Tubular Eccentrically Braced Frame Links for the Seismic Retrofit of Braced Steel Truss Bridge Piers," by J.W. Berman and M. Bruneau, 3/27/06 (PB2007-105147).

MCEER-06-0007 "REDARS Validation Report," by S. Cho, C.K. Huyck, S. Ghosh and R.T. Eguchi, 8/8/06 (PB2007-106983).

MCEER-06-0008 "Review of Current NDE Technologies for Post-Earthquake Assessment of Retrofitted Bridge Columns," by J.W. Song, Z. Liang and G.C. Lee, 8/21/06 (PB2007-106984).

MCEER-06-0009 "Liquefaction Remediation in Silty Soils Using Dynamic Compaction and Stone Columns," by S. Thevanayagam, G.R. Martin, R. Nashed, T. Shenthan, T. Kanagalingam and N. Ecemis, 8/28/06 (PB2007-106985).

MCEER-06-0010 "Conceptual Design and Experimental Investigation of Polymer Matrix Composite Infill Panels for Seismic Retrofitting," by W. Jung, M. Chiewanichakorn and A.J. Aref, 9/21/06 (PB2007-106986).

MCEER-06-0011 "A Study of the Coupled Horizontal-Vertical Behavior of Elastomeric and Lead-Rubber Seismic Isolation Bearings," by G.P. Warn and A.S. Whittaker, 9/22/06 (PB2007-108679).

MCEER-06-0012 "Proceedings of the Fourth PRC-US Workshop on Seismic Analysis and Design of Special Bridges: Advancing Bridge Technologies in Research, Design, Construction and Preservation," Edited by L.C. Fan, G.C. Lee and L. Ziang, 10/12/06 (PB2007-109042).

MCEER-06-0013 "Cyclic Response and Low Cycle Fatigue Characteristics of Plate Steels," by P. Dusicka, A.M. Itani and I.G. Buckle, 11/1/06 06 (PB2007-106987).

MCEER-06-0014 "Proceedings of the Second US-Taiwan Bridge Engineering Workshop," edited by W.P. Yen, J. Shen, J-Y. Chen and M. Wang, 11/15/06 (PB2008-500041).

MCEER-06-0015 "User Manual and Technical Documentation for the REDARS^{TM} Import Wizard," by S. Cho, S. Ghosh, C.K. Huyck and S.D. Werner, 11/30/06 (PB2007-114766).

MCEER-06-0016 "Hazard Mitigation Strategy and Monitoring Technologies for Urban and Infrastructure Public Buildings: Proceedings of the China-US Workshops," edited by X.Y. Zhou, A.L. Zhang, G.C. Lee and M. Tong, 12/12/06 (PB2008-500018).

MCEER-07-0001 "Static and Kinetic Coefficients of Friction for Rigid Blocks," by C. Kafali, S. Fathali, M. Grigoriu and A.S. Whittaker, 3/20/07 (PB2007-114767).

MCEER-07-0002 "Hazard Mitigation Investment Decision Making: Organizational Response to Legislative Mandate," by L.A. Arendt, D.J. Alesch and W.J. Petak, 4/9/07 (PB2007-114768).

MCEER-07-0003 "Seismic Behavior of Bidirectional-Resistant Ductile End Diaphragms with Unbonded Braces in Straight or Skewed Steel Bridges," by O. Celik and M. Bruneau, 4/11/07 (PB2008-105141).

MCEER-07-0004 "Modeling Pile Behavior in Large Pile Groups Under Lateral Loading," by A.M. Dodds and G.R. Martin, 4/16/07(PB2008-105142).

MCEER-07-0005 "Experimental Investigation of Blast Performance of Seismically Resistant Concrete-Filled Steel Tube Bridge Piers," by S. Fujikura, M. Bruneau and D. Lopez-Garcia, 4/20/07 (PB2008-105143).

MCEER-07-0006 "Seismic Analysis of Conventional and Isolated Liquefied Natural Gas Tanks Using Mechanical Analogs," by I.P. Christovasilis and A.S. Whittaker, 5/1/07, not available.

MCEER-07-0007 "Experimental Seismic Performance Evaluation of Isolation/Restraint Systems for Mechanical Equipment – Part 1: Heavy Equipment Study," by S. Fathali and A. Filiatrault, 6/6/07 (PB2008-105144).

MCEER-07-0008 "Seismic Vulnerability of Timber Bridges and Timber Substructures," by A.A. Sharma, J.B. Mander, I.M. Friedland and D.R. Allicock, 6/7/07 (PB2008-105145).

MCEER-07-0009 "Experimental and Analytical Study of the XY-Friction Pendulum (XY-FP) Bearing for Bridge Applications," by C.C. Marin-Artieda, A.S. Whittaker and M.C. Constantinou, 6/7/07 (PB2008-105191).

MCEER-07-0010 "Proceedings of the PRC-US Earthquake Engineering Forum for Young Researchers," Edited by G.C. Lee and X.Z. Qi, 6/8/07 (PB2008-500058).

MCEER-07-0011 "Design Recommendations for Perforated Steel Plate Shear Walls," by R. Purba and M. Bruneau, 6/18/07, (PB2008-105192).

MCEER-07-0012 "Performance of Seismic Isolation Hardware Under Service and Seismic Loading," by M.C. Constantinou, A.S. Whittaker, Y. Kalpakidis, D.M. Fenz and G.P. Warn, 8/27/07, (PB2008-105193).

MCEER-07-0013 "Experimental Evaluation of the Seismic Performance of Hospital Piping Subassemblies," by E.R. Goodwin, E. Maragakis and A.M. Itani, 9/4/07, (PB2008-105194).

MCEER-07-0014 "A Simulation Model of Urban Disaster Recovery and Resilience: Implementation for the 1994 Northridge Earthquake," by S. Miles and S.E. Chang, 9/7/07, (PB2008-106426).

MCEER-07-0015 "Statistical and Mechanistic Fragility Analysis of Concrete Bridges," by M. Shinozuka, S. Banerjee and S-H. Kim, 9/10/07, (PB2008-106427).

MCEER-07-0016 "Three-Dimensional Modeling of Inelastic Buckling in Frame Structures," by M. Schachter and AM. Reinhorn, 9/13/07, (PB2008-108125).

MCEER-07-0017 "Modeling of Seismic Wave Scattering on Pile Groups and Caissons," by I. Po Lam, H. Law and C.T. Yang, 9/17/07 (PB2008-108150).

MCEER-07-0018 "Bridge Foundations: Modeling Large Pile Groups and Caissons for Seismic Design," by I. Po Lam, H. Law and G.R. Martin (Coordinating Author), 12/1/07 (PB2008-111190).

MCEER-07-0019 "Principles and Performance of Roller Seismic Isolation Bearings for Highway Bridges," by G.C. Lee, Y.C. Ou, Z. Liang, T.C. Niu and J. Song, 12/10/07 (PB2009-110466).

MCEER-07-0020 "Centrifuge Modeling of Permeability and Pinning Reinforcement Effects on Pile Response to Lateral Spreading," by L.L Gonzalez-Lagos, T. Abdoun and R. Dobry, 12/10/07 (PB2008-111191).

MCEER-07-0021 "Damage to the Highway System from the Pisco, Perú Earthquake of August 15, 2007," by J.S. O'Connor, L. Mesa and M. Nykamp, 12/10/07, (PB2008-108126).

MCEER-07-0022 "Experimental Seismic Performance Evaluation of Isolation/Restraint Systems for Mechanical Equipment – Part 2: Light Equipment Study," by S. Fathali and A. Filiatrault, 12/13/07 (PB2008-111192).

MCEER-07-0023 "Fragility Considerations in Highway Bridge Design," by M. Shinozuka, S. Banerjee and S.H. Kim, 12/14/07 (PB2008-111193).

MCEER-07-0024 "Performance Estimates for Seismically Isolated Bridges," by G.P. Warn and A.S. Whittaker, 12/30/07 (PB2008-112230).

MCEER-08-0001 "Seismic Performance of Steel Girder Bridge Superstructures with Conventional Cross Frames," by L.P. Carden, A.M. Itani and I.G. Buckle, 1/7/08, (PB2008-112231).

MCEER-08-0002 "Seismic Performance of Steel Girder Bridge Superstructures with Ductile End Cross Frames with Seismic Isolators," by L.P. Carden, A.M. Itani and I.G. Buckle, 1/7/08 (PB2008-112232).

MCEER-08-0003 "Analytical and Experimental Investigation of a Controlled Rocking Approach for Seismic Protection of Bridge Steel Truss Piers," by M. Pollino and M. Bruneau, 1/21/08 (PB2008-112233).

MCEER-08-0004 "Linking Lifeline Infrastructure Performance and Community Disaster Resilience: Models and Multi-Stakeholder Processes," by S.E. Chang, C. Pasion, K. Tatebe and R. Ahmad, 3/3/08 (PB2008-112234).

MCEER-08-0005 "Modal Analysis of Generally Damped Linear Structures Subjected to Seismic Excitations," by J. Song, Y-L. Chu, Z. Liang and G.C. Lee, 3/4/08 (PB2009-102311).

MCEER-08-0006 "System Performance Under Multi-Hazard Environments," by C. Kafali and M. Grigoriu, 3/4/08 (PB2008-112235).

MCEER-08-0007 "Mechanical Behavior of Multi-Spherical Sliding Bearings," by D.M. Fenz and M.C. Constantinou, 3/6/08 (PB2008-112236).

MCEER-08-0008 "Post-Earthquake Restoration of the Los Angeles Water Supply System," by T.H.P. Tabucchi and R.A. Davidson, 3/7/08 (PB2008-112237).

MCEER-08-0009 "Fragility Analysis of Water Supply Systems," by A. Jacobson and M. Grigoriu, 3/10/08 (PB2009-105545).

MCEER-08-0010 "Experimental Investigation of Full-Scale Two-Story Steel Plate Shear Walls with Reduced Beam Section Connections," by B. Qu, M. Bruneau, C-H. Lin and K-C. Tsai, 3/17/08 (PB2009-106368).

MCEER-08-0011 "Seismic Evaluation and Rehabilitation of Critical Components of Electrical Power Systems," S. Ersoy, B. Feizi, A. Ashrafi and M. Ala Saadeghvaziri, 3/17/08 (PB2009-105546).

MCEER-08-0012 "Seismic Behavior and Design of Boundary Frame Members of Steel Plate Shear Walls," by B. Qu and M. Bruneau, 4/26/08 . (PB2009-106744).

MCEER-08-0013 "Development and Appraisal of a Numerical Cyclic Loading Protocol for Quantifying Building System Performance," by A. Filiatrault, A. Wanitkorkul and M. Constantinou, 4/27/08 (PB2009-107906).

MCEER-08-0014 "Structural and Nonstructural Earthquake Design: The Challenge of Integrating Specialty Areas in Designing Complex, Critical Facilities," by W.J. Petak and D.J. Alesch, 4/30/08 (PB2009-107907).

MCEER-08-0015 "Seismic Performance Evaluation of Water Systems," by Y. Wang and T.D. O'Rourke, 5/5/08 (PB2009-107908).

MCEER-08-0016 "Seismic Response Modeling of Water Supply Systems," by P. Shi and T.D. O'Rourke, 5/5/08 (PB2009-107910).

MCEER-08-0017 "Numerical and Experimental Studies of Self-Centering Post-Tensioned Steel Frames," by D. Wang and A. Filiatrault, 5/12/08 (PB2009-110479).

MCEER-08-0018 "Development, Implementation and Verification of Dynamic Analysis Models for Multi-Spherical Sliding Bearings," by D.M. Fenz and M.C. Constantinou, 8/15/08 (PB2009-107911).

MCEER-08-0019 "Performance Assessment of Conventional and Base Isolated Nuclear Power Plants for Earthquake Blast Loadings," by Y.N. Huang, A.S. Whittaker and N. Luco, 10/28/08 (PB2009-107912).

MCEER-08-0020 "Remote Sensing for Resilient Multi-Hazard Disaster Response – Volume I: Introduction to Damage Assessment Methodologies," by B.J. Adams and R.T. Eguchi, 11/17/08 (PB2010-102695).

MCEER-08-0021 "Remote Sensing for Resilient Multi-Hazard Disaster Response – Volume II: Counting the Number of Collapsed Buildings Using an Object-Oriented Analysis: Case Study of the 2003 Bam Earthquake," by L. Gusella, C.K. Huyck and B.J. Adams, 11/17/08 (PB2010-100925).

MCEER-08-0022 "Remote Sensing for Resilient Multi-Hazard Disaster Response – Volume III: Multi-Sensor Image Fusion Techniques for Robust Neighborhood-Scale Urban Damage Assessment," by B.J. Adams and A. McMillan, 11/17/08 (PB2010-100926).

MCEER-08-0023 "Remote Sensing for Resilient Multi-Hazard Disaster Response – Volume IV: A Study of Multi-Temporal and Multi-Resolution SAR Imagery for Post-Katrina Flood Monitoring in New Orleans," by A. McMillan, J.G. Morley, B.J. Adams and S. Chesworth, 11/17/08 (PB2010-100927).

MCEER-08-0024 "Remote Sensing for Resilient Multi-Hazard Disaster Response – Volume V: Integration of Remote Sensing Imagery and VIEWS^{TM} Field Data for Post-Hurricane Charley Building Damage Assessment," by J.A. Womble, K. Mehta and B.J. Adams, 11/17/08 (PB2009-115532).

MCEER-08-0025 "Building Inventory Compilation for Disaster Management: Application of Remote Sensing and Statistical Modeling," by P. Sarabandi, A.S. Kiremidjian, R.T. Eguchi and B. J. Adams, 11/20/08 (PB2009-110484).

MCEER-08-0026 "New Experimental Capabilities and Loading Protocols for Seismic Qualification and Fragility Assessment of Nonstructural Systems," by R. Retamales, G. Mosqueda, A. Filiatrault and A. Reinhorn, 11/24/08 (PB2009-110485).

MCEER-08-0027 "Effects of Heating and Load History on the Behavior of Lead-Rubber Bearings," by I.V. Kalpakidis and M.C. Constantinou, 12/1/08 (PB2009-115533).

MCEER-08-0028 "Experimental and Analytical Investigation of Blast Performance of Seismically Resistant Bridge Piers," by S.Fujikura and M. Bruneau, 12/8/08 (PB2009-115534).

MCEER-08-0029 "Evolutionary Methodology for Aseismic Decision Support," by Y. Hu and G. Dargush, 12/15/08.

MCEER-08-0030 "Development of a Steel Plate Shear Wall Bridge Pier System Conceived from a Multi-Hazard Perspective," by D. Keller and M. Bruneau, 12/19/08 (PB2010-102696).

MCEER-09-0001 "Modal Analysis of Arbitrarily Damped Three-Dimensional Linear Structures Subjected to Seismic Excitations," by Y.L. Chu, J. Song and G.C. Lee, 1/31/09 (PB2010-100922).

MCEER-09-0002 "Air-Blast Effects on Structural Shapes," by G. Ballantyne, A.S. Whittaker, A.J. Aref and G.F. Dargush, 2/2/09 (PB2010-102697).

MCEER-09-0003 "Water Supply Performance During Earthquakes and Extreme Events," by A.L. Bonneau and T.D. O'Rourke, 2/16/09 (PB2010-100923).

MCEER-09-0004 "Generalized Linear (Mixed) Models of Post-Earthquake Ignitions," by R.A. Davidson, 7/20/09 (PB2010-102698).

MCEER-09-0005 "Seismic Testing of a Full-Scale Two-Story Light-Frame Wood Building: NEESWood Benchmark Test," by I.P. Christovasilis, A. Filiatrault and A. Wanitkorkul, 7/22/09 (PB2012-102401).

MCEER-09-0006 "IDARC2D Version 7.0: A Program for the Inelastic Damage Analysis of Structures," by A.M. Reinhorn, H. Roh, M. Sivaselvan, S.K. Kunnath, R.E. Valles, A. Madan, C. Li, R. Lobo and Y.J. Park, 7/28/09 (PB2010-103199).

MCEER-09-0007 "Enhancements to Hospital Resiliency: Improving Emergency Planning for and Response to Hurricanes," by D.B. Hess and L.A. Arendt, 7/30/09 (PB2010-100924).

MCEER-09-0008 "Assessment of Base-Isolated Nuclear Structures for Design and Beyond-Design Basis Earthquake Shaking," by Y.N. Huang, A.S. Whittaker, R.P. Kennedy and R.L. Mayes, 8/20/09 (PB2010-102699).

MCEER-09-0009 "Quantification of Disaster Resilience of Health Care Facilities," by G.P. Cimellaro, C. Fumo, A.M Reinhorn and M. Bruneau, 9/14/09 (PB2010-105384).

MCEER-09-0010 "Performance-Based Assessment and Design of Squat Reinforced Concrete Shear Walls," by C.K. Gulec and A.S. Whittaker, 9/15/09 (PB2010-102700).

MCEER-09-0011 "Proceedings of the Fourth US-Taiwan Bridge Engineering Workshop," edited by W.P. Yen, J.J. Shen, T.M. Lee and R.B. Zheng, 10/27/09 (PB2010-500009).

MCEER-09-0012 "Proceedings of the Special International Workshop on Seismic Connection Details for Segmental Bridge Construction," edited by W. Phillip Yen and George C. Lee, 12/21/09 (PB2012-102402).

MCEER-10-0001 "Direct Displacement Procedure for Performance-Based Seismic Design of Multistory Woodframe Structures," by W. Pang and D. Rosowsky, 4/26/10 (PB2012-102403).

MCEER-10-0002 "Simplified Direct Displacement Design of Six-Story NEESWood Capstone Building and Pre-Test Seismic Performance Assessment," by W. Pang, D. Rosowsky, J. van de Lindt and S. Pei, 5/28/10 (PB2012-102404).

MCEER-10-0003 "Integration of Seismic Protection Systems in Performance-Based Seismic Design of Woodframed Structures," by J.K. Shinde and M.D. Symans, 6/18/10 (PB2012-102405).

MCEER-10-0004 "Modeling and Seismic Evaluation of Nonstructural Components: Testing Frame for Experimental Evaluation of Suspended Ceiling Systems," by A.M. Reinhorn, K.P. Ryu and G. Maddaloni, 6/30/10 (PB2012-102406).

MCEER-10-0005 "Analytical Development and Experimental Validation of a Structural-Fuse Bridge Pier Concept," by S. El-Bahey and M. Bruneau, 10/1/10 (PB2012-102407).

MCEER-10-0006 "A Framework for Defining and Measuring Resilience at the Community Scale: The PEOPLES Resilience Framework," by C.S. Renschler, A.E. Frazier, L.A. Arendt, G.P. Cimellaro, A.M. Reinhorn and M. Bruneau, 10/8/10 (PB2012-102408).

MCEER-10-0007 "Impact of Horizontal Boundary Elements Design on Seismic Behavior of Steel Plate Shear Walls," by R. Purba and M. Bruneau, 11/14/10 (PB2012-102409).

MCEER-10-0008 "Seismic Testing of a Full-Scale Mid-Rise Building: The NEESWood Capstone Test," by S. Pei, J.W. van de Lindt, S.E. Pryor, H. Shimizu, H. Isoda and D.R. Rammer, 12/1/10 (PB2012-102410).

MCEER-10-0009 "Modeling the Effects of Detonations of High Explosives to Inform Blast-Resistant Design," by P. Sherkar, A.S. Whittaker and A.J. Aref, 12/1/10 (PB2012-102411).

MCEER-10-0010 "L'Aquila Earthquake of April 6, 2009 in Italy: Rebuilding a Resilient City to Withstand Multiple Hazards," by G.P. Cimellaro, I.P. Christovasilis, A.M. Reinhorn, A. De Stefano and T. Kirova, 12/29/10.

MCEER-11-0001 "Numerical and Experimental Investigation of the Seismic Response of Light-Frame Wood Structures," by I.P. Christovasilis and A. Filiatrault, 8/8/11 (PB2012-102412).

MCEER-11-0002 "Seismic Design and Analysis of a Precast Segmental Concrete Bridge Model," by M. Anagnostopoulou, A. Filiatrault and A. Aref, 9/15/11.

MCEER-11-0003 'Proceedings of the Workshop on Improving Earthquake Response of Substation Equipment," Edited by A.M. Reinhorn, 9/19/11 (PB2012-102413).

MCEER-11-0004 "LRFD-Based Analysis and Design Procedures for Bridge Bearings and Seismic Isolators," by M.C. Constantinou, I. Kalpakidis, A. Filiatrault and R.A. Ecker Lay, 9/26/11.

MCEER-11-0005 "Experimental Seismic Evaluation, Model Parameterization, and Effects of Cold-Formed Steel-Framed Gypsum Partition Walls on the Seismic Performance of an Essential Facility," by R. Davies, R. Retamales, G. Mosqueda and A. Filiatrault, 10/12/11.

MCEER-11-0006 "Modeling and Seismic Performance Evaluation of High Voltage Transformers and Bushings," by A.M. Reinhorn, K. Oikonomou, H. Roh, A. Schiff and L. Kempner, Jr., 10/3/11.

MCEER-11-0007 "Extreme Load Combinations: A Survey of State Bridge Engineers," by G.C. Lee, Z. Liang, J.J. Shen and J.S. O'Connor, 10/14/11.

MCEER-12-0001 "Simplified Analysis Procedures in Support of Performance Based Seismic Design," by Y.N. Huang and A.S. Whittaker.

MCEER-12-0002 "Seismic Protection of Electrical Transformer Bushing Systems by Stiffening Techniques," by M. Koliou, A. Filiatrault, A.M. Reinhorn and N. Oliveto, 6/1/12.

MCEER-12-0003 "Post-Earthquake Bridge Inspection Guidelines," by J.S. O'Connor and S. Alampalli, 6/8/12.

MCEER-12-0004 "Integrated Design Methodology for Isolated Floor Systems in Single-Degree-of-Freedom Structural Fuse Systems," by S. Cui, M. Bruneau and M.C. Constantinou, 6/13/12.

MCEER-12-0005 "Characterizing the Rotational Components of Earthquake Ground Motion," by D. Basu, A.S. Whittaker and M.C. Constantinou, 6/15/12.

MCEER-12-0006 "Bayesian Fragility for Nonstructural Systems," by C.H. Lee and M.D. Grigoriu, 9/12/12.

MCEER-12-0007 "A Numerical Model for Capturing the In-Plane Seismic Response of Interior Metal Stud Partition Walls," by R.L. Wood and T.C. Hutchinson, 9/12/12.

MCEER-12-0008 "Assessment of Floor Accelerations in Yielding Buildings," by J.D. Wieser, G. Pekcan, A.E. Zaghi, A.M. Itani and E. Maragakis, 10/5/12.

MCEER-13-0001 "Experimental Seismic Study of Pressurized Fire Sprinkler Piping Systems," by Y. Tian, A. Filiatrault and G. Mosqueda, 4/8/13.

MCEER-13-0002 "Enhancing Resource Coordination for Multi-Modal Evacuation Planning," by D.B. Hess, B.W. Conley and C.M. Farrell, 2/8/13.

MCEER-13-0003 "Seismic Response of Base Isolated Buildings Considering Pounding to Moat Walls," by A. Masroor and G. Mosqueda, 2/26/13.

MCEER-13-0004 "Seismic Response Control of Structures Using a Novel Adaptive Passive Negative Stiffness Device," by D.T.R. Pasala, A.A. Sarlis, S. Nagarajaiah, A.M. Reinhorn, M.C. Constantinou and D.P. Taylor, 6/10/13.

MCEER-13-0005 "Negative Stiffness Device for Seismic Protection of Structures," by A.A. Sarlis, D.T.R. Pasala, M.C. Constantinou, A.M. Reinhorn, S. Nagarajaiah and D.P. Taylor, 6/12/13.

MCEER-13-0006 "Emilia Earthquake of May 20, 2012 in Northern Italy: Rebuilding a Resilient Community to Withstand Multiple Hazards," by G.P. Cimellaro, M. Chiriatti, A.M. Reinhorn and L. Tirca, June 30, 2013.

MCEER-13-0007 "Precast Concrete Segmental Components and Systems for Accelerated Bridge Construction in Seismic Regions," by A.J. Aref, G.C. Lee, Y.C. Ou and P. Sideris, with contributions from K.C. Chang, S. Chen, A. Filiatrault and Y. Zhou, June 13, 2013.

MCEER-13-0008 "A Study of U.S. Bridge Failures (1980-2012)," by G.C. Lee, S.B. Mohan, C. Huang and B.N. Fard, June 15, 2013.

MCEER-13-0009 "Development of a Database Framework for Modeling Damaged Bridges," by G.C. Lee, J.C. Qi and C. Huang, June 16, 2013.

MCEER-13-0010 "Model of Triple Friction Pendulum Bearing for General Geometric and Frictional Parameters and for Uplift Conditions," by A.A. Sarlis and M.C. Constantinou, July 1, 2013.

MCEER-13-0011 "Shake Table Testing of Triple Friction Pendulum Isolators under Extreme Conditions," by A.A. Sarlis, M.C. Constantinou and A.M. Reinhorn, July 2, 2013.

MCEER-13-0012 "Theoretical Framework for the Development of MH-LRFD," by G.C. Lee (coordinating author), H.A Capers, Jr., C. Huang, J.M. Kulicki, Z. Liang, T. Murphy, J.J.D. Shen, M. Shinozuka and P.W.H. Yen, July 31, 2013.

MCEER-13-0013 "Seismic Protection of Highway Bridges with Negative Stiffness Devices," by N.K.A. Attary, M.D. Symans, S. Nagarajaiah, A.M. Reinhorn, M.C. Constantinou, A.A. Sarlis, D.T.R. Pasala, and D.P. Taylor, September 3, 2014.

MCEER-14-0001 "Simplified Seismic Collapse Capacity-Based Evaluation and Design of Frame Buildings with and without Supplemental Damping Systems," by M. Hamidia, A. Filiatrault, and A. Aref, May 19, 2014.

MCEER-14-0002 "Comprehensive Analytical Seismic Fragility of Fire Sprinkler Piping Systems," by Siavash Soroushian, Emmanuel "Manos" Maragakis, Arash E. Zaghi, Alicia Echevarria, Yuan Tian and Andre Filiatrault, August 26, 2014.

MCEER-14-0003 "Hybrid Simulation of the Seismic Response of a Steel Moment Frame Building Structure through Collapse," by M. Del Carpio Ramos, G. Mosqueda and D.G. Lignos, October 30, 2014.

MCEER-14-0004 "Blast and Seismic Resistant Concrete-Filled Double Skin Tubes and Modified Steel Jacketed Bridge Columns," by P.P. Fouche and M. Bruneau, June 30, 2015.

MCEER-14-0005 "Seismic Performance of Steel Plate Shear Walls Considering Various Design Approaches," by R. Purba and M. Bruneau, October 31, 2014.

MCEER-14-0006 "Air-Blast Effects on Civil Structures," by Jinwon Shin, Andrew S. Whittaker, Amjad J. Aref and David Cormie, October 30, 2014.

MCEER-14-0007 "Seismic Performance Evaluation of Precast Girders with Field-Cast Ultra High Performance Concrete (UHPC) Connections," by G.C. Lee, C. Huang, J. Song, and J. S. O'Connor, July 31, 2014.

MCEER-14-0008 "Post-Earthquake Fire Resistance of Ductile Concrete-Filled Double-Skin Tube Columns," by Reza Imani, Gilberto Mosqueda and Michel Bruneau, December 1, 2014.

MCEER-14-0009 "Cyclic Inelastic Behavior of Concrete Filled Sandwich Panel Walls Subjected to In-Plane Flexure," by Y. Alzeni and M. Bruneau, December 19, 2014.

MCEER-14-0010 "Analytical and Experimental Investigation of Self-Centering Steel Plate Shear Walls," by D.M. Dowden and M. Bruneau, December 19, 2014.

MCEER-15-0001 "Seismic Analysis of Multi-story Unreinforced Masonry Buildings with Flexible Diaphragms," by J. Aleman, G. Mosqueda and A.S. Whittaker, June 12, 2015.

MCEER-15-0002 "Site Response, Soil-Structure Interaction and Structure-Soil-Structure Interaction for Performance Assessment of Buildings and Nuclear Structures," by C. Bolisetti and A.S. Whittaker, June 15, 2015.

MCEER-15-0003 "Stress Wave Attenuation in Solids for Mitigating Impulsive Loadings," by R. Rafiee-Dehkharghani, A.J. Aref and G. Dargush, August 15, 2015.

MCEER-15-0004 "Computational, Analytical, and Experimental Modeling of Masonry Structures," by K.M. Dolatshahi and A.J. Aref, November 16, 2015.

MCEER-15-0005 "Property Modification Factors for Seismic Isolators: Design Guidance for Buildings," by W.J. McVitty and M.C. Constantinou, June 30, 2015.

MCEER-15-0006 "Seismic Isolation of Nuclear Power Plants using Sliding Bearings," by Manish Kumar, Andrew S. Whittaker and Michael C. Constantinou, December 27, 2015.

MCEER-15-0007 "Quintuple Friction Pendulum Isolator Behavior, Modeling and Validation," by Donghun Lee and Michael C. Constantinou, December 28, 2015.

MCEER-15-0008 "Seismic Isolation of Nuclear Power Plants using Elastomeric Bearings," by Manish Kumar, Andrew S. Whittaker and Michael C. Constantinou, December 29, 2015.

MCEER-16-0001 "Experimental, Numerical and Analytical Studies on the Seismic Response of Steel-Plate Concrete (SC) Composite Shear Walls," by Siamak Epackachi and Andrew S. Whittaker, June 15, 2016.

MCEER-16-0002 "Seismic Demand in Columns of Steel Frames," by Lisa Shrestha and Michel Bruneau, June 17, 2016.

MCEER-16-0003 "Development and Evaluation of Procedures for Analysis and Design of Buildings with Fluidic Self-Centering Systems" by Shoma Kitayama and Michael C. Constantinou, July 21, 2016.

MCEER-16-0004 "Real Time Control of Shake Tables for Nonlinear Hysteretic Systems," by Ki Pung Ryu and Andrei M. Reinhorn, October 22, 2016.

MCEER-16-0006 "Seismic Isolation of High Voltage Electrical Power Transformers," by Kostis Oikonomou, Michael C. Constantinou, Andrei M. Reinhorn and Leon Kemper, Jr., November 2, 2016.

MCEER-16-0007 "Open Space Damping System Theory and Experimental Validation," by Erkan Polat and Michael C. Constantinou, December 13, 2016.

MCEER-16-0008 "Seismic Response of Low Aspect Ratio Reinforced Concrete Walls for Buildings and Safety-Related Nuclear Applications," by Bismarck N. Luna and Andrew S. Whittaker.

MCEER-16-0009 "Buckling Restrained Braces Applications for Superstructure and Substructure Protection in Bridges," by Xiaone Wei and Michel Bruneau, December 28, 2016.

MCEER-16-0010 "Procedures and Results of Assessment of Seismic Performance of Seismically Isolated Electrical Transformers with Due Consideration for Vertical Isolation and Vertical Ground Motion Effects," by Shoma Kitayama, Michael C. Constantinou and Donghun Lee, December 31, 2016.

MCEER-17-0001 "Diagonal Tension Field Inclination Angle in Steel Plate Shear Walls," by Yushan Fu, Fangbo Wang and Michel Bruneau, February 10, 2017.

MCEER-17-0002 "Behavior of Steel Plate Shear Walls Subjected to Long Duration Earthquakes," by Ramla Qureshi and Michel Bruneau, September 1, 2017.

MCEER-17-0003 "Response of Steel-plate Concrete (SC) Wall Piers to Combined In-plane and Out-of-plane Seismic Loadings," by Brian Terranova, Andrew S. Whittaker, Siamak Epackachi and Nebojsa Orbovic, July 17, 2017.

MCEER-17-0004 "Design of Reinforced Concrete Panels for Wind-borne Missile Impact," by Brian Terranova, Andrew S. Whittaker and Len Schwer, July 18, 2017.

MCEER-17-0005 "A Simple Strategy for Dynamic Substructuring and its Application to Soil-Foundation-Structure Interaction," by Aikaterini Stefanaki and Metttupalayam V. Sivaselvan, December 15, 2017.

MCEER-17-0006 "Dynamics of Cable Structures: Modeling and Applications," by Nicholas D. Oliveto and Mettupalayam V. Sivaselvan, December 1, 2017.

MCEER-17-0007 "Development and Validation of a Combined Horizontal-Vertical Seismic Isolation System for High-Voltage-Power Transformers," by Donghun Lee and Michael C. Constantinou, November 3, 2017.

MCEER-18-0001 "Reduction of Seismic Acceleration Parameters for Temporary Bridge Design," by Conor Stucki and Michel Bruneau, March 22, 2018.

MCEER-18-0002 "Seismic Response of Low Aspect Ratio Reinforced Concrete Walls," by Bismarck N. Luna, Jonathan P. Rivera, Siamak Epackachi and Andrew S. Whittaker, April 21, 2018.

MCEER-18-0003 "Seismic Damage Assessment of Low Aspect Ratio Reinforced Concrete Shear Walls," by Jonathan P. Rivera, Bismarck N. Luna and Andrew S. Whittaker, April 16, 2018.

MCEER-18-0004 "Seismic Performance Assessment of Seismically Isolated Buildings Designed by the Procedures of ASCE/ SEI 7," by Shoma Kitayama and Michael C. Constantinou, April 14, 2018.

MCEER-19-0001 MCEER-19-0001 "Development and Validation of a Seismic Isolation System for Lightweight Residential Construction," by Huseyin Cisalar and Michael C. Constantinou, March 24, 2019.

MCEER-20-0001 "A Multiscale Study of Reinforced Concrete Shear Walls Subjected to Elevated Temperatures," by Alok Deshpande and Andrew S. Whittaker, June 26, 2020.

MCEER-20-0002 "Further Results on the Assessment of Performance of Seismically Isolated Electrical Transformers," by Shoma Kitayama and Michael C. Constantinou, June 30, 2020.

MCEER-20-0003 "Analytical and Numerical Studies of Seismic Fluid-Structure Interaction in Liquid-Filled Vessels," by Ching-Ching Yu and Andrew S. Whittaker, August 1, 2020.

MCEER-22-0001 "Modeling Triple Friction Pendulum Bearings in Program OpenSees Including Frictional Heating Effects," by Hyun-Myung Kim and Michael C. Constantinou, April 18, 2022.

MCEER-22-0002 "Physical and Numerical Simulations of Seismic Fluid-Structure Interaction in Advanced Nuclear Reactors," by Faizan Ul Haq Mir, Ching-Ching Yu, Andrew S. Whittaker and Michael C. Constantinou, July 8, 2022.

MCEER-22-0003 "Impedance-Matching Control Design for Shake-Table Testing and Model-in-the-Loop Simulations," by Sai Sharath Parsi, Mettupalayam V. Sivaselvan and Andrew S. Whittaker, September 30, 2022.

MCEER-22-0004 "Earthquake-Simulator Experiments of a Model of a Seismically-Isolated, Fluoride-Salt Cooled High-Temperature Reactor," by Faizan Ul Haq Mir, Kaivalya M. Lal, Benjamin D. Kosbab, Nam Nguyen, Brian Song, Matthew Clavelli, Kaniel Z. Tilow and Andrew S. Whittaker, October 24, 2022.

MCEER-23-0001 “Mid-height Seismic Isolation of Tall, Slender Equipment in Advanced Nuclear Power Plants,” by Kaivalya M. Lal, Andrew S. Whittaker and Michael C. Constantinou, February 4, 2023.

MCEER-23-0002 “Development of Performance-based Testing Specifications for Seismic Isolators,” by Hyun-Myung Kim and Michael C. Constantinou, August 18, 2023.

MCEER: Earthquake Engineering to Extreme Events

University at Buffalo, The State University of New York
133A Ketter Hall | Buffalo, NY 14260
mceer@buffalo.edu; buffalo.edu/mceer

ISSN 1520-295X